NISTIR 4347

ASSESSMENT OF THE FIRE PERFORMANCE OF SCHOOL BUS INTERIOR COMPONENTS

Emil Braun
Sanford Davis
John H. Klote
Barbara C. Levin
Maya Paabo

U.S. DEPARTMENT OF COMMERCE
National Institute of Standards
and Technology
Center for Fire Research
Gaithersburg, MD 20899

Sponsored by:
Office of Vehicle Safety Standards
National Highway Traffic Safety
Administration
Department of Transportation
Washington, DC 20590

U.S. DEPARTMENT OF COMMERCE
Robert A. Mosbacher, Secretary

NATIONAL INSTITUTE OF STANDARDS
AND TECHNOLOGY
John W. Lyons, Director

NIST

NISTIR 4347

ASSESSMENT OF THE FIRE PERFORMANCE OF SCHOOL BUS INTERIOR COMPONENTS

Emil Braun
Sanford Davis
John H. Klote
Barbara C. Levin
Maya Paabo

U.S. DEPARTMENT OF COMMERCE
National Institute of Standards and Technology
Center for Fire Research
Gaithersburg, MD 20899

July 1990

Final Report

Sponsored by:
Office of Vehicle Safety Standards
National Highway Traffic Safety Administration
Department of Transportation
Washington, DC 20590

U.S. DEPARTMENT OF COMMERCE
Robert A. Mosbacher, Secretary
NATIONAL INSTITUTE OF STANDARDS AND TECHNOLOGY
John W. Lyons, Director

ASSESSMENT OF THE FIRE PERFORMANCE OF SCHOOL BUS INTERIOR COMPONENTS

EXECUTIVE SUMMARY

INTRODUCTION

Nonmetallic interior materials, including seat assemblies, of all motor vehicles sold in the United States must meet Federal Motor Vehicle Safety Standard FMVSS No. 302. Since its inception in 1968, this standard has been applied to school buses as well as cars, trucks, and general purpose buses and passenger vehicles. Recently, the National Highway Transportation Safety Administration (NHTSA) began a review of the appropriateness of the test method defined in FMVSS No.302 as it specifically applies to school buses. Questions have been raised regarding the level of fire protection provided school bus occupants by the current version of this standard. If this level of fire protection proves inadequate, what suitable changes can be made to FMVSS No.302 to improve school bus occupant fire safety?

FMVSS No.302 uses a rectangular burn chamber in which a test specimen is mounted, with its exposed surface facing down, in a horizontal orientation. A small diffusion burner flame (flame height of 38 mm) is applied from below to one end of the exposed surface of a test specimen. The time of flame spread between two marked points on the specimen holder is used to calculate the flame spread rate. The maximum allowed flame spread rate of four inches per minute applies to all motor vehicle interior components exposed to the passenger compartment. This regulation has been applied to the interior components of school buses.

In January, 1989, NHTSA asked the Center for Fire Research (CFR) of the National Institute of Standards and Technology (NIST) to investigate the possibility of replacing the existing test method in FMVSS No. 302 with another test method or procedure that would improve the fire safety of school bus occupants beyond that currently provided by the existing test method.

A review of the interior finish of school buses has shown that, while there are several combustible components (e.g., rubber floor mats, electrical wiring, headliners, etc.) in a school bus interior, seat assemblies represent the single largest type of combustible fuel. CFR, therefore, developed a testing program that would provide data on the fire performance characteristics of seat assemblies used in school buses. The fire performance characteristics of seat assemblies were evaluated in small-scale (i.e., laboratory-scale) test methods as well as large-scale tests (i.e., open burning of fully assembled seats) and full-scale tests (i.e., seat assemblies placed in a simulated bus enclosure). Test results were used to assess material fire performance as it would impact on occupant tenability conditions inside of a simulated bus enclosure. Using the results of these studies, this report presents a procedure that could be used as a replacement for the existing test method defined in FMVSS No.302. The new test method combines a test protocol with a data analysis protocol to assess material performance in terms of occupant tenability.

TEST PLAN

Six school bus seat assemblies were purchased from a commercial manufacturer using currently available seating materials - cover fabrics and foam cushions. One seat assembly represented a typical seat assembly now found on existing school buses. The seating materials were shown to comply with FMVSS No.302. No attempt was made to design seat assemblies that would conform to other mandatory requirements, such as impact protection.

Small-scale tests (Cone Calorimeter and LIFT Apparatus) were used to evaluate each assembly's fire characteristics for:

- ignitability,
- flame spread,
- rate of heat release,
- yields of specific gaseous products, and
- smoke generation.

Also, a quick test version of the NBS Toxicity Protocol based on an N-Gas estimate of the LC_{50} was used to measure the toxic potency of individual components found in each seat assembly.

Large-scale tests were performed on fully assembled seats using the furniture calorimeter to determine the fire characteristics of each seat assembly when exposed to 50 kW and 100 kW ignition sources. Data was obtained on each seat assembly showing the:

- rate of heat release,
- mass loss rate, and
- yields of specific gaseous products (CO, CO_2, HCN, HCL).

Full-scale tests were performed on each seat assembly in a simulated school bus enclosure measuring *2.44* m wide by 2.13 m high by 8.23 m long. Three seat assemblies were placed in the rear corner of the enclosure. The seat assemblies were position on a load platform in a manner similar to that found in a real school bus. The seat assembly located in the comer was exposed to a 100 kW natural gas fire from a box burner having a surface area of 0.05 m^2. Measurements were made of the:

- rate of heat release,
- mass loss rate,
- specific gas species (CO, CO_2, O_2, HCN, HCL) concentrations and yields, and
- upper and lower layer compartment temperatures.

Computer simulations of the impact of varying the ignition source strength were also conducted in order to separate material performance from ignition source performance, *two* possible causes of the development of untenable conditions.

RESULTS

The computer simulations of the impact of the ignition source on the development of untenable conditions in the simulated bus enclosure demonstrated that an ignition source of about 500 kW could produce conditions in the enclosure that would lead to incapacitation of bus occupants. Ignition sources greater than 1000 kW could develop lethal conditions in an enclosure of

the size used in this study. The simulations also showed that temperature, possibly irradiance, and not smoke toxicity represent the most immediate threats to life safety.

Full-scale tests showed that the peak rate of heat release of the standard seat assembly, F_1/C_1, was an order of magnitude higher than the heat release rate of the other five seat assemblies. Seat to seat flame spread was observed with seat assembly F_1/C_1. As measured by tenability calculations, this seat assembly was the only one of the six tested that produced an atmosphere that represented a significant toxicoligical threat to bus occupants. Seat assemblies F_2/C_3 and F_3/C_3 also produced untenable conditions in the test enclosure. However, only a thermal limit was exceeded. These seat assemblies produced incapacitating and lethal conditions in the enclosure within 120 s to 170 s. The remaining three seat assemblies produced no untenable conditions when exposed to the ignition burner.

Large-scale testing produced similar results. However, the difference between seat assembly F_1/C_1 and the other seat assemblies was not as great. Also, the 50 kW and 100 kW box burner tests showed little difference between the remaining five seat assemblies, while the 50 kW line burner showed that seat assembly F_2/C_3 peak heat release rate between F_1/C_1 (505 kW) and the other seat assemblies (85 kW to 125 kW).

A comparison of small-scale test results shows that material ranking does not follow any consistent pattern from material to material. Also, the spread in the data for a given test method is not very large.

CONCLUSIONS

No one simple small-scale test should be used to measure the fire performance of a material when exposed to an ignition source, Since consideration must be given to a combination of factors, such as ease of ignition, flame spread, rate of heat release, generation of gaseous species, smoke development, and toxicity of the combustion products, examination individual results for each of the parameters considered for the development of hazardous conditions in a school bus enclosure reveals that similarities and differences depend on the exposure conditions and geometry of the enclosure. These additional parameters are not taken into account in small-scale testing and no simple method exists for translating these parameteric values into full-scale assessments of tenability or escape times.

Therefore, a full-scale test protocol that can form the basis for compliance testing of seat assemblies for use in school buses is outlined. This test protocol is based on seat assembly tests in a standardized room. The acceptance level is determined by calculating the tenability conditions in the enclosure and comparing these results to tenability limits. To ensure that unknown toxicants are not producing an unusually toxic atmosphere in the bus enclosure, it maybe necessary to perform animal toxicity testing.

TABLE OF CONTENTS

LIST OF TABLES

LIST OF FIGURES

ASSESSMENT OF THE FIRE PERFORMANCE OF SCHOOL BUS INTERIOR *COMPONENTS*

ABSTRACT

Since seat assemblies represent the single largest type of combustible fuel in a school bus interior, this study is limited to currently used and state-of-the-art material assemblies. Six different seat assemblies having a range of fire performance were examined. Small-scale tests (Cone Calorimeter, LIFT, and NBS Toxicity Protocol) were performed on these materials. Large-scale tests (Furniture Calorimeter) were conducted on single seat assemblies. Full-scale tests were performed using a simulated bus enclosure measuring 2.44 m wide by 2.13 m high by 8.23 m long and three seat assemblies. The impact of ignition source size was determined by computer simulation. It was found that a 500 kW ignition source could produce untenable thermal conditions in the simulated bus enclosure. Seat assemblies were exposed to 50 kw and 100 kw ignition sources in the large-scale tests and 100 kW ignition source in the full-scale tests. It was found that the small-scale tests were unable to provide a simple method for material selection that was consistent with the full-scale test results. At the present time, small-scale fire tests of materials cannot be depended upon to predict the fire behavior in the real world. Therefore, based on the full-scale test results, a generalized full-scale test protocol for seat assembly evaluation was developed that combines full-scale testing in an enclosure with an analysis protocol that determines the time-to-untenable conditions. The procedure defines the conditions under which toxicity testing would be necessary. Full-scale test instrumentation and material orientation are also described.

Keywords: Cone Calorimeter; fire performance; flame spread; foams; furniture calorimeter; combustion products; hazard; ignitability; rate of heat release; school buses; smoke; tenability; toxicity.

1. INTRODUCTION

Nonmetallic interior materials, including seat assemblies, of all motor vehicles sold in the United States must meet Federal Motor Vehicle Safety Standard FMVSS No. 302. Since its inception in 1968, this standard has been applied to school buses as well as cars, trucks, and general purpose buses and passenger vehicles. Recently, the National Highway Transportation Safety Administration (NHTSA) began a review of the appropriateness of the test method defined in FMVSS No.302 as it specifically applies to school buses. Questions have been raised regarding the level of fire protection provided school bus occupants by the current version of this standard. If this level of fire protection proves inadequate, what suitable changes can be made to FMVSS No.302 to improve school bus occupant fire safety?

In January, 1989, NHTSA asked the Center for Fire Research (CFR) of the National Institute of Standards and Technology (NIST) to investigate the possibility of replacing the existing test method in FMVSS No. 302 with another test method or procedure that would improve,the fire safety of school bus occupants beyond that currently provided by the existing test method.

While there are several combustible components (e.g., rubber floor mats, electrical wiring, headliners, etc.) in a school bus interior, seat assemblies represent the single largest type of combustible fuel. CFR, therefore, developed a testing program that would provide data on the fire performance characteristics of seat assemblies used in school buses. The fire performance characteristics of seat assemblies were evaluated in small-scale (i.e., laboratory-scale) test methods as well as large-scale tests(i.e., open burning of fully assembled seats) and full-scale tests (i.e., seat assemblies placed in a simulated bus enclosure). Test results were used to assess material fire performance as it would impact on occupant tenability conditions inside of a simulated bus enclosure. Using the results of these studies, this report presents a procedure that could be used as a replacement for the existing test method defined in FMVSS No.302. The new test method combines a test protocol with a data analysis protocol to assess material performance in terms of occupant tenability.

In order to establish the background for this project, it is first appropriate to review the history of the development of the current flammability standards for automotive and (similar) rail vehicles and to review other standards which are germane to the fire scenarios involved in this study. This discussion concludes with the 1988 accident in Carrollton, Kentucky, involving a former school bus, which gave a high degree of public attention to this fire safety issue.

1.1 HISTORY

In 1968, the IIT Research Institute under contract from the National Highway Safety Bureau (NHSB) of the Federal Highway Administration (U.S. Department of

Transportation) investigated the flammability characteristics of various passenger car and school bus interior materials; evaluated existing laboratory test methods; assembled fire prevention codes and fire statistics; and recommended to the NHSB a test procedure and a flammability performance standard for automotive vehicle interiors. Over 200 interior materials, representing both domestic and foreign makes of automobiles, were tested to determine their relative flame spread rates [1][1]. The highest burning rates were found for certain upholstery cover and headliner materials when tested as single layers. Based on the recommendations contained in that study, the NHSB published Federal Motor Vehicle Safety Standard FMVSS No. 302 entitled Flammability of Interior Materials - Passenger Cars, Multi-Purpose Passenger Vehicles, Trucks, and Buses [2]. In FMVSS No. 302, test specimens are mounted, with their exposed surfaces facing **down**, in a horizontal orientation in a rectangular burn chamber. A small diffusion burner flame is applied from below to one end of the exposed surface of the test specimen. The time of flame spread between two marked points on the specimen holder is used to calculate the flame spread rate. Based on IIT Research Institute work, NHSB specified a maximum flame spread rate of four inches per minute for all motor vehicle interior components exposed to the passenger compartment. This regulation has been applied to the interior components of school buses.

The Center for Fire Research at the National Bureau of Standards conducted a study of the fire safety of a transit bus supplied by the Washington (DC) Metropolitan Area Transit Authority (WMATA) in *1974.* They determined the minimum ignition source necessary to initiate a fire in the bus and the means by which a fire, once started, was most likely to grow and spread [3]. Tests showed that accidental ignition by a cigarette or dropped match was unlikely; however, the **seat** could be ignited with one or two matches, if applied at the proper location (e.g., by an arsonist). If ignited, fire growth and spread in the bus **was** primarily through involvement of the seat cushions. Fire then spread from seat to seat with little direct involvement of other interior materials. In a companion study of the **WMATA** Metrorail cars, it was concluded that the seat padding and covering (and the plastic wall lining) were also potential sources of fire hazard [4,5].

In 1976, the National Highway Traffic Safety Administration (NHTSA) issued a report prepared by the AMF Advanced Systems Laboratory entitled "Development of a Unitized School Bus" [6]. This report recommended the extensive use of padding for occupant protection in order to withstand frontal, rearward, and side impacts of 30 mph. This padding was in addition to the seat padding already in use. No specific recommendations were made for assessing the fire performance of these interior components and it was assumed that the FMVSS No. 302 applied.

A study carried out by Nelson et al. [7] on rail car assembly and transit bus interior assembly mock-ups demonstrated that polyurethane foam seats which met the requirements of the voluntary Urban Mass Transportation Administration (UMTA) guidelines [8] caused room flashover in 6 to 7 minutes. Using a different ignition source and compartment design, Peacock and Braun [9] showed

---

[1] Numbers in brackets refer to the literature references in Section 7.

that, in AMTRAK passenger rail vehicle mock-up fire experiments, a polyurethane foam seat assembly which met the UMTA guidelines performed well, while a conventional polyurethane foam seat assembly resulted in flashover conditions in eight minutes.

1.2 OTHER STANDARDS

Although we are not aware of any programs specifically conducted to determine the fire behavior of school bus interiors, there is applicable information available relating to materials for other modes of ground transportation. Following are examples of some attempts to test interior materials and evaluate design features to assess vehicle interior fire performance.

In November **1978,** a Downtown People Mover Workshop co-sponsored by the West Virginia University College of Engineering and the Urban Mass Transportation Administration (U.S. Department of Transportation) was held in Morgantown, WV. A presentation entitled "Fire Safety Guidelines for Vehicles in a Downtown People Mover System" [10] by R.D. Peacock of the National Bureau of Standards described the available test methods for evaluating the fire performance of vehicle components and provided guidance for material acceptance. A more detailed discussion is given in NBSIR 78-1586 [**11**].

Hathaway and Flores surveyed nine U.S. transit authorities to assess the overall fire threat in transit systems for the calendar year **1978** [12]. They used a fault tree analysis as a means of qualitatively presenting how minor incidents occur and how they may become major incidents. Their report showed how fault trees and scenarios allow for the identification of prospective countermeasures to eliminate the occurrence of an incident or to ensure that a minor incident does not develop further. In this study, only *0.4* percent of the incidents in rail rapid transit systems and **7.0** percent of the incidents in transit buses involved fires starting in the occupant compartment from arson or by cigarette ignition..

In **1983,** the National Fire Protection Association first published NFPA 130, Standard for Fixed Guideway Transit Systems (current edition published in **1988)** [**13**]. Chapter *4* (Vehicles) and Appendix D provide recommendations for testing the flammability and smoke characteristics of rail transit vehicle materials. These recommendations were based in part on the voluntary Urban Mass Transportation Administration Guidelines, which were ultimately published by the Department of Transportation in **1984** [**14**]. These guidelines represented an early attempt to control Compartment fire growth beyond the limited control imposed by FMVSS No.302.

An unpublished report prepared by The Ohio State University Engineering Experiment Station in 1984 for the Transit Development Corporation [15] assessed the fire performance of vehicle interiors through the use of rate of heat and smoke release. Using these data and a mathematical model, predictions of the course of a developing fire was described in that report. The results of these predicitions were never compared to actual full-scale fire performance.

In 1984, ASTM published a Proposed Test Method for Determining Fire Performance of Public Ground Transportation Seat Assemblies [16]. This test method is designed to simulate the fire exposure conditions that are experienced in the interior of public ground transportation vehicles where the seat assembly is directly involved; however, it is not intended to simulate fires that may develop from sources on the exterior of vehicles, such as electric arcs or fuel spills. The method, using full-scale seat assemblies installed in a 2.44 m wide by 3.66 m deep by 2.44 m high compartment having an open door, could be adapted to evaluate the fire behavior of seat assemblies when exposed to a gasoline fire.

1.3 RECENT PROBLEM

On May 14, 1988, a fiery crash took place in Carrollton, Kentucky, between a pickup truck traveling the wrong way on an Interstate highway and a 1977 former school bus returning from a church youth outing. Twenty-seven passengers on the bus were killed and, although burned beyond recognition, the victims were judged by the Kentucky Medical Director to have died by smoke inhalation. Survivors stated that the bus burst into flame almost immediately after the collision, presumably from a ruptured fuel tank. The vintage of the school bus was manufactured prior to the issuance of the National Highway Traffic Safety Administration (NHTSA) fuel system protection requirements (FMVSS No. 301 [17]) for fuel tank reinforcement and protection, but after the issuance of FMVSS No302. It can therefore be assumed that the seat assemblies in this bus met the maximum flame spread rate requirements of FMVSS No.302.

In November 1988, NHTSA issued a report which provided a summary and update of school bus safety activities conducted by NHTSA [18]. The report discusses NHTSA's actions to improve school bus safety. This includes programs affecting human behavior and motor vehicle safety performance, a study of the magnitude of school bus-related injuries and fatalities (with particular interest in the factors involved in the Carrollton, KY, crash), and current agency activities to make school bus transportation even safer. An Advance Notice of Proposed Rulemaking for the Flammability of Interior Materials, published in November 1988 [19], announced that NHTSA is considering the issuance of a proposal to upgrade FMVSS No. 302, Flammability of Interior Materials, as it applies to large buses (including school buses) over 10,000pounds gross vehicle weight.

In January 1989, the Center for Fire Research (CFR) at the National Institute of Standards and Technology was asked by NHTSA to assess the fire performance of school bus seat assemblies when exposed to internal and external fires and to develop a protocol which will evaluate the fire performance of materials used in school bus seats.

1.4 APPROACH

The largest source of combustible material in a school bus interior is the seat assembly. Thus, the NHTSA/NIST approach to limiting the rate of fire growth in school buses presumes that the solution to the problem is better material selection for this application. Given that ignition of seats will occur, efforts are aimed at selecting materials that will delay ignition and exhibit low flame spread rates and low heat release rates. In addition, smoke generation and the toxicity of the combustion products should be reduced to a level that would not result in hazardous conditions in the school bus.

The presumption is that a fire in a bus would result from a fuel spill in the bus (or from under the bus which has had its structural integrity breached). The fire behavior of materials in full-scale experiments approximating these fire conditions in a simulated bus compartment (using materials with a full range of fire performance) were conducted and analyzed to provide guidance for estimating the time available for escape. The results of these experiments were used to determine which fire parameters are most important and governed the strategy for the development of an improved method for assessing seat material fire performance.

Small-scale and large-scale laboratory tests were then used to measure the pertinent materials' fire properties so that comparisons could be made with full-scale fire performance. The parameters investigated were:

- ignitability,
- flame spread,
- rate of heat release,
- smoke generation, and
- toxicity of combustion products.

All of these fire characteristics can affect escape from a school bus involved in a fire.

State-of-the-art compartment fire modeling was used to assess the fire performance of seat assemblies in a full-scale bus simulation. These are zone models which assume that the compartment is divided into two distinct regions: the upper zone is a hot layer comprised of a potentially hazardous environment and the lower zone is a cool layer consisting of a relatively safe environment. To the extent that this is valid in real fires, these models provide a vehicle for studying the interaction of various fire phenomena and translating data obtained from one compartment size to another compartment size without the need for performing additional fire tests.

The materials used in this study as examples are all currently available. Thus, with the establishment of realistic fire performance criteria, it is expected that a desired level of fire safety can be achieved today, although perhaps at some additional cost.

2. EXPERIMENTAL PROCEDURES

2.1 MATERIALS

Six different typical seat assemblies were selected to represent a wide range of expected fire performance. The primary materials for each assembly were a single padding and a single cover fabric. Each assembly consisted of a tubular steel frame with back and bottom cushions attached (Figure 1). The seat back unit contained a 6 mm plywood insert and the seat cushion unit contained a 13 mm plywood insert. Assembled back and seat units were purchased from a major manufacturer of school buses (Thomas Built Buses, Inc.) and mounted on steel frames obtained from a school bus "graveyard." In addition, foam pads and cover materials (unassembled) were purchased for the small-scale tests. Each seat assembly was tested according to FMVSS No.302 and found to have a flame spread rate of less than 4 inches per minute (Appendix A). A summary of the materials and their physical measurements is given in Table 1. A description of each of the material combinations follows.

2.1.1 Standard Polyurethane Foam/Standard Vinyl Cover (F_1/C_1)

The standard foam for this study is a rebonded polyurethane having a density of 73 kg/m^3, typical of current production by the bus manufacturer; expanded polystyrene beads were distributed throughout the foam matrix. The cover material, also typical of current production, is a calendered vinyl bonded to a knitted polyester scrim with an overall areal density of 870 g/m^2.

2.1.2 Standard Polyurethane Foam/Standard Vinyl Cover with Kevlar[2] Backing (F_1/C_2)

The foam is the same as described in 2.1.1. The cover material is a calendered vinyl bonded to a loosely woven polyester scrim to which was applied a non-woven Kevlar backing; the overall areal density is 830 g/m^2.

2.1.3 Melamine-Treated Polyurethane Foam/UMTA-Type Vinyl Cover (F_2/C_3)

The foam is a melamine-treated polyurethane having a density of 85 kg/m^3. The cover material is a calendered vinyl bonded to a double-knit polyester fabric; the overall areal density is 770 g/m^2. The cover material was certified by

---

[2] Certain commercial products are identified in this report in order to adequately specify the materials and apparatus used. Such identification does not imply recommendation by the National Institute of Standards and Technology, nor does it imply that these products identified are the best available for the purpose.

the manufacturer to meet the UMTA guidelines [8] and is henceforth referred to as UMTA-type vinyl.

2.1.4 CMHR Polyurethane Foam/UMTA-Type Vinyl Cover (F_3/C_3)

The foam is a combustion-modified high-resiliency (CMHR) polyurethane having a density of 49 kg/m^3. The UMTA-type vinyl cover is the same as described in 2.1.3.

2.1.5 LS Neoprene[2] Foam/UMTA-Type Vinyl Cover (F_4/C_3)

The foam is a low smoke polychloroprene having a density of 145 kg/m^3. The UMTA-type vinyl cover is the same as described in 2.1.3.

2.1.6 IMPAK SR-10LS[2] Polyurethane Foam/UMTA-Type Vinyl Cover (F_5/C_3)

The foam is a rebonded flame retardant-treated polyurethane having a density of 90 kg/m^3. The UMTA-type vinyl cover is the same as described in 2.1.3.

2.2 METHODS OF INVESTIGATION

2.2.1 Full-scale Experiments

A total of six experiments were conducted to evaluate the fire performance of the six school bus seat assemblies. In each test, three seat rows (each with one seat assembly) were installed in one corner of a simulated school bus compartment as they would be in a real school bus (Figure 1). In this way, flame spread across a seat and from seat to seat could be observed. All three seats were mounted on a load cell to facilitate the measurement of total weight loss. Ignition was accomplished by a box burner located adjacent to the aisle edge of the rearmost seat assembly. The box burner had a surface area of 0.05 m^2. The burner was adjusted to produce a 100 kW natural gas flame. This energy release rate was used because it approximates the energy released by a gasoline spill of about the same surface area and did not contribute so much energy into the compartment as to mask the performance of the seat assemblies. In addition, a gas burner calibration test was performed to quantify the contribution of the ignition burner to the heat, smoke, and gas generation rates in the compartment.

In each test, gas temperatures, gas concentrations, and mass loss were recorded and used to determine the heat release rate, upper and lower layer temperatures, and gas concentrations in the upper layer. These data were used to assess tenability within the compartment, The six tests were also recorded on video tape for later viewing.

2.2.1.1 Room Configuration

The experimental arrangement is shown in Figure 2 and consisted of a single compartment measuring 2.44 m wide by 2.13 m high by 8.23 m long, lined with noncombustible materials. A doorway measuring 1.02 m wide by 1.83 m high provided the sole ventilation path into and out of the compartment. These dimensions approximate a full size school bus as determined by field inspection of actual school buses. The materials used in constructing the compartment and their thermal properties are listed in Table 2 [20].

2.2.1.2 Instrumentation

Table 3 lists all the instrumentation used in these experiments and the location of sampling points. Figure 2 shows the location of sampling points within the test compartment and the adjoining smoke collection hood. Vertical lines of eight thermocouples each were located in the corner and in the center of the compartment to determine the upper compartment temperature and the location of the hot upper layer interface. A thermocouple tree composed of seven thermocouples was located in the doorway together with a differential pressure transducer to measure mass flow in and out of the compartment. All thermocouples were exposed junction thermocouples made from 28 gauge wire. A heat flux meter was located in the wall opposite the ignition seat.

The three seat assemblies were placed on a load cell, approximately 100 mm above the floor, located in the far corner of the compartment (Figure 2). The load cell continuously monitored mass loss.

A collection hood was used ,to remove decomposition products exiting the burn compartment. A set of instruments installed in the collection hood was used to determine continuously heat release rate (by oxygen consumption calorimetry [21]), gas concentrations, and smoke concentration.

2.2.1.3 Combustion Gas Analysis

In order to sample the fire environment for toxic gas species, two gas probes were centered in the compartment 100 mm from the ceiling. One gas probe, a 19 mm diameter stainless steel pipe, was connected to non-dispersive infrared (NDIR) analyzers for continuous measurement of carbon monoxide and carbon dioxide; oxygen concentrations were measured continuously with a paramagnetic analyzer. The other gas probe, a 55 mm diameter glass tube, was connected to a blower motor to ensure that the sampling was performed on a time-resolved representative portion of the combustion products in the upper part of the compartment. Sample ports along this tube were provided for hydrogen chloride (HCl) and hydrogen bromide (HBr) impinger sampling and hydrogen cyanide (HCN) evacuated glass bulb sampling of the compartment environment. The gaseous products were collected in 250 mℓ glass impinger bottles containing approximately 125 mℓ of 5 mM potassium hydroxide (KOH). The flow of gases through the impinger was controlled by a mass flow controller. The ratio of gases collected to gases exhausted was nominally 1:1000; however, the exact value for each test was recorded and used in all subsequent computations.

After the collection period, the impingers were weighed and transferred to plastic containers. Prior to analysis, the filter containing the soot was placed into the impinger solution. The samples were analyzed for Cl^-, Br^-, and CN^- on a commercially available ion chromatograph (Waters Model ILC-1 Ion/Liquid Chromatograph[2]) equipped with a Waters *430* Total Conductivity Detector[2] and a Waters *460* Electrochemical Detector[2]. The electro-chemical detector (specifically for CN^-) was used with a glassy carbon electrode and a saturated KCl reference electrode; an anion column (ICPAK-A[2]) preceded by an Anion Guard-Pak Precolumn Module[2] was used. Chromatograms were recorded on a Spectra-Physics Model SP *4270* Integrator[2].

2.2.2 Large Scale-Experiments: Furniture Calorimeter

The furniture calorimeter [22] was designed to measure the heat release and mass loss rates of furniture items burning in the open air. Figure 3 is a schematic representation of the apparatus. The basic principle of the apparatus, oxygen consumption calorimetry, has previously been described by Huggett [21]. The heat release rate is computed from measurements of mass flow and oxygen concentration through the exhaust stack. The effective heat of combustion can readily be determined from the heat release rate and the corresponding measured mass loss rate of the sample. Carbon monoxide and CO_2 concentrations also were monitored during each test and used to correct the heat release rate calculations; detailed calculations for making these corrections are described by Parker [23].

Single school bus seat assemblies were tested in the furniture calorimeter. These assemblies consisted of a tubular steel frame with seat back and seat cushion attached. The seat assemblies were ignited by either a line burner placed in the cushion back crevice (simulating a fire on the seat) or a box burner similar to that used in the full-scale tests placed adjacent to the side edge of the seat assembly (simulating a fuel fire under the seat). Initial tests involved the box burner or line burner adjusted to produce a 50 kW flame. In all cases, the seat assemblies were exposed to flames from the burners for *200* seconds. Follow-up tests on seat assemblies that did not propagate a flame across the cushion or back surface at 50 kW were performed with the box burner adjusted to 100 kW.

2.2.3 Small-Scale Experiments

In order to measure the fire properties needed for input into a model for assessing the performance of materials for bus seats, a series of small-scale tests were carried out on assemblies and materials. The Cone Calorimeter provides data for ignitability, rate of heat release, smoke generation, and *gas* yields; with the exception of ignitability, these data can be related to the full-scale test data. The flame spread data from the Lateral Ignition and Flame Spread Test (LIFT) can be compared only qualitatively to the full-scale test results; again, ignitability data can only be related to the scenarios involved and provides information as to the ease of ignition. The toxicity test results provide a means for estimating the toxic potency of the materials

used in seat assemblies based on yields of known toxic species; toxicity can only be determined by a full toxic hazard assessment.

2.2.3.1 Cone Calorimeter

The NBS Cone Calorimeter (Figure 4) has been previously described by Babrauskas [24] and is currently pending as an ASTM standard test method [25]. Briefly, this is a bench-scale instrument from which heat release rate is determined by measurement of oxygen depletion in the gas flow stream of combustion products and air. An external radiant flux of up to 100 kW/m^2 may be imposed on the specimen by a temperature-controlled electric heater. Since the heater operates at a moderate temperature (up to 1000 °C) and behaves very nearly as a black body, the effective spectral distribution is likely to be very close to that expected from compartment fires [26].

Changes in sample mass during an experiment were measured continuously by a load cell. Smoke obscuration and decomposition products also were measured continuously. Smoke obscuration was determined by measuring the extinction of light from a helium-neon laser located in the exhaust duct downstream of the burning sample. A gas sampling arrangement in the exhaust duct provided appropriate gas samples to a flame ionization analyzer for total hydrocarbon measurements, a paramagnetic O_2 analyzer for oxygen consumption, and a pair of non-dispersive infrared analyzers for the determination of CO and CO_2. To analyze the combustion products for acid gases (HCl, HBr, and HCN), batch samples were taken and analyzed by ion chromatography. For one sample at each irradiance level, a portion of the gaseous products and soot in the main exhaust duct were collected by replacing the soot collection filter with a batch sampling apparatus (as described in 2.2.1.3).

Composite specimens (foam and cover) were tested only in the horizontal position to avoid the problems associated with materials that melt and drip, and because a prior correlation had been successful for upholstered furniture [27]. The samples were exposed to a preset external irradiance with a spark igniter mounted above the center of the sample to ignite the pyrolysis products. Sparking was initiated at the beginning of the exposure and continued until sustained burning developed across the sample surface. Tests were terminated when flaming on the sample extinguished. Three replicates of each assembly were tested at each of three external irradiances: 35, 50, and 75 kW/m^2.

2.2.3.2 Flame Spread (LIFT)

The LIFT apparatus [28,29] is a bench-scale device used to determine ignition and flame spread properties of a broad class of combustible materials and is currently being promulgated as a standard through ASTM [30]. A schematic of the apparatus is shown in Figure 5. It consists of a (pre-mixed natural gas-air) radiant heat source, a sample holder, and a pilot flame to promote ignition. The sample is backed by an inert insulating material. A steel plate is positioned above the sample to extend the sample surface and provide for the development of a boundary Layer containing pyrolyzed gases and

entrained room air. An acetylene-air pilot flame is positioned above the sample adjacent to the steel plate such that it interrupts the escaping gaseous mixture containing the pyrolyzed gases generated at the sample surface. The external irradiance distribution at the sample surface, normalized to its value at 50 mm, is shown in Figure 6.

For both the ignition and flame spread tests, foam samples were cut to a thickness of 38 mm. Foam samples were overwrapped with the appropriate cover fabric. The sides and back of each sample were covered with aluminum foil, and a backing board of 13 mm thick mineral board was used.

Ignition tests were conducted by exposing the composites to an external irradiance that varied from 10 to 65 kW/m^2 and recording the time-to-ignition. The minimum external irradiance necessary for ignition is experimentally determined as the limit at which no ignition occurs. The minimum external irradiance necessary for ignition (as determined by this method) was obtained only for seat assembly F_1/C_2. The other seat assemblies had minimum external irradiance values below the minimum operating temperature of the radiant panel. The ignition/external irradiance data for these seat assemblies were obtained from the Cone Calorimeter. In the data analysis, the Cone Calorimeter times-to-ignition vs. external irradiance were treated as if they were obtained on the LIFT apparatus.

Flame spread tests were conducted as described by Quintiere and Harkleroad [28] with sample sizes of 150 X 800 mm. The specimens were exposed at the 50 mm position to external irradiances that were approximately 10% higher than the minimum external irradiance required for ignition. The samples were exposed to this resulting irradiance profile until a state of thermal equilibrium was achieved based on an analysis of the time-to-ignition data. Seat assemblies F_1/C_1 and F_1/C_2 were preheated to equilibrium, while the UMTA-type vinyl (C_3) covered foams were preheated for only 45 to 60 seconds in order to prevent random self-ignition.

2.2.3.3 Toxicity

The acute inhalation toxicity of the combustion products of the five foams and three cover materials was assessed individually by the N-Gas model [31] using the NBS Toxicity Test Method apparatus [32]. The N-Gas model is an approach for estimating smoke toxicity, (i.e., primary toxic gases are identified and quantified to allow prediction of the toxic potency of the mixed gases) and to determine if unusual toxicants exist. An unusual toxicant exists if the predicted toxicity is not explained by the contributions of the primary toxicants examined. Animal tests are used to verify these predictions.

The calibration gases for the CO, CO_2, and HCN measurements were commercially supplied in specified concentrations in nitrogen. The concentration of HCN in the commercially supplied cylinders was routinely checked by silver nitrate ($AgNO_3$) titration [33], since it is known that the concentration of HCN stored under these conditions will decrease with time. All chemicals used in the ion chromatographic procedure were of reagent-grade quality. The water was deionized to 18 megohm-cm resistivity.

Fischer *344* male rats, weighing 200 to 300 grams, were obtained from Taconic Farms (Germantown, NY)[2]. Animal care and maintenance were performed in accordance with the procedures outlined in the National Institutes of Health's "Guide for the Care and Use of Laboratory Animals." Each rat was housed individually in suspended stainless steel cages and provided with food (Ralston Purina Rat Chow 5012[2]) and water ad libitum. Twelve hours of fluorescent lighting per day were provided using an automatic timer. The rats were allowed to acclimate to laboratory conditions for at least seven days prior to experimentation.

2.2.3.3.1 Toxicity Test System

The animal exposures were conducted using the combustion system, the chemical analysis system, and the animal exposure system that were designed for the NBS Toxicity Test Method [32]. A schematic of the experimental arrangement is illustrated in Figure 7. The NBS Toxicity Test apparatus is a closed system in which all the gases and smoke are kept in a 200 liter rectangular animal exposure chamber for the duration of the exposure.

The individual samples were decomposed in a cup furnace located directly below the animal exposure chamber such that all the combustion products from the test material flowed directly into the chamber. The samples were examined under flaming conditions which were achieved by setting the furnace 25°C above the predetermined autoignition temperature of each material. During the experiments, an electric spark igniter above the cup furnace or 1 ml ethanol added to the sample, was used to assure immediate flaming.

The combustion products were analyzed for CO, CO_2, O_2, HCN, HBr, and HCl (as described in 2.2.1.3). The CO, CO_2, and O_2 data (millivolts) were recorded by an on-line computer every 15 seconds. All combustion products and gases that were removed for continuous analysis were returned to the chamber. The presence of HCN in the combustion products was determined by gas chromatography (GC) and by ion chromatography (IC). Syringe samples (100 $\mu\ell$) of the chamber atmosphere were analyzed for HCN approximately every three minutes with a gas chromatograph equipped with a thermionic detector [34]. In addition, HCl and HBr were analyzed by IC. Impinger samples (collected by bubbling gases from the animal exposure box at the nose level near animal port No. 1 through 25 ml of 5 mM KOH) were analyzed for HCl, HBr, and HCN by using an ion chromatograph equipped with two different detectors, a conductivity detector for HCl and HBr and an electrochemical detector for HCN. The apparatus is diagrammed in Figure 8. All concentrations of CO, CO_2, O_2, and HCN (by GC) are the average 30 minute exposure values which were calculated by integrating the area under the instrument response curve and dividing by the exposure time. The acid gas concentrations of HCl, HBr, and HCN (by IC) are the average exposure values which were calculated from the ionic impinger concentrations and the gas flow and exposure time.

Six rats were exposed in each experiment. Each animal was placed in a restrainer and inserted into one of six portholes located along the front of the exposure chamber such that only the head of each animal was exposed. Animal exposures started when the sample was dropped into the preheated cup,

and lasted for 30 minutes. The toxicological endpoint was death, either during the 30 minute exposure or during the 30 minute exposure plus post-exposure period. (The post-exposure period was usually 14 days. However, if some animals were still losing weight on day 14, they were kept until they either recovered or died. The animals were considered to have recovered when they gained weight over a three day period.) All animals (including the unexposed controls) were weighed daily from the day of arrival until the end of the post-exposure observation period.

2.2.3.3.2 N-Gas Model Prediction

The toxic potency of each material was approximated using the N-Gas model and, in addition, an LC_{50} was determined for the cover designated as the UMTA-type vinyl (C,) The current N-gas model is based on the studies of the toxicological interactions of four gases - CO, CO,, HCN, and reduced O, - and is used to estimate the amount of material necessary to produce an LC,, for the 30 minute exposure [31,35,36]. The model prediction is based on the empirical mathematical relationship

$$\frac{m[CO]}{[CO_2] - b} + \frac{[HCN]}{d} + \frac{21-[O_2]}{21 - LC_{50}O_2} \approx 1 . \qquad \text{(Eq. 1)}$$

The numbers in brackets are average concentrations during a 30 minute exposure period. The parameters m and b are the slope and intercept values (-18 and 122000, respectively, when CO, is less than or equal to 50000 ppm), d is the LC,, concentration of HCN (160 ppm for 30 minute exposures), and $LC_{50}O_2$ is the percent O, that causes 50 percent of the animals to die in 30 minutes (5.4 percent).

To include the post-exposure deaths, the following assumptions were made:

1. At the levels examined here and normally produced in real fires, HCl and HBr only cause post-exposure deaths.

2. The toxic interaction of HCl and HBr with the other gases are additive.

The formula now becomes:

$$\frac{m[CO]}{[CO_2] - b} + \frac{[HCN]}{d} + \frac{21 - [O_2]}{21 - LC_{50}O_2} + \frac{[HBr]}{3000} + \frac{[HCl]}{3700} \approx 1 \qquad \text{(Eq. 2)}$$

where all values are same as in Eq. 1, except d now equals 110 ppm and the HBr and HCl LC,, values for 30 minute exposures plus post-exposure deaths are 3000 and 3700 ppm, respectively.

Ideally, when this equation is unity, 50 percent of the animals should die. Based on previous studies with pure gases, the mean N-Gas value for these

gases was calculated as 1.1 ± 0.2. Since the concentration-response curves for animal lethalities from smoke are very steep, it is assumed that if some percentage (not 0 nor 100 percent) of animals die, the experimental loading is close to the predicted $LC_{,,}$ value.

2.2.3.3.3 $LC_{,,}$ Determination

When results of tests based on the N-Gas model do not approximate 1 as shown in Eq. 2, indicating the presence of an unusual toxicant, a more precise $LC_{,,}$ determination is required. In the experiments conducted to determine the $LC_{,,}$ values, the percentage of animals dying at each smoke concentration was plotted to produce a concentration-response curve from which the $LC_{,,}$ value was calculated for the 30 minute exposures and for the 30 minutes plus post-exposure observation period. The $LC_{,,}$ in this case is defined as the amount of material placed in the furnace divided by the exposure chamber volume (mg/ℓ) which caused 50 percent of the animals to die within-exposure or during the within-exposure plus the post-exposure observation period. The $LC_{,,}$ values and the 95 percent confidence limit were calculated by the statistical method of Litchfield and Wilcoxon [37]. In this study, a full $LC_{,,}$ determination was only needed for the UMTA-type vinyl (C_3).

2.2.4 Fire Modeling

Computer fire modeling was used to evaluate the development of hazardous conditions in a compartment. HAZARD I [38], which includes a two zone fire model, is composed of an ensemble of programs designed to estimate the consequences of specified fire in a compartment(s). HAZARD I is a sequence of procedures implemented in computer software to calculate the development of hazardous conditions over time, to calculate the time needed by building occupants to escape under those conditions, and to estimate the resulting loss of life based on assumed occupant behavior and tenability criteria. These calculations are performed for a specified enclosure and set of fire scenarios of concern. It was used in this work to assess:

- the changes in a compartment environment caused by the presence of an ignition source and the resulting tenability times of temperature, irradiance, and toxicity for ignition sources of varying strength;
- the relative importance of the causes of hazard (i.e., temperature, irradiance, and toxicity).

Also, the tenability portion of HAZARD I was used to determine times to incapacitation and lethality for temperature, irradiance, and toxicity in the full-scale tests of the six seat assemblies. As will be seen in *4.2*, this tool is used to determine an upper limit for the ignition source such that the ignition source does not become the limiting factor affecting time to escape from a burning school bus.

3. RESULTS

3.1 FULL-SCALE EXPERIMENTS

These tests were designed not only to determine when hazardous conditions would develop in the compartment, but to determine the likelihood of flame propagation from seat-to-seat. However, it should be recognized that the actual numerical values obtained in these full-scale tests depend on the size and shape of the compartment and the doorway opening. For the same size door opening and fire size, smaller compartments could be expected to achieve untenable conditions sooner. Also, it should be noted that unlike a "real bus fire", air flow in and out of the compartment was restricted to the doorway opening. The presence of windows that could break open could dramatically alter the development of untenable conditions in the compartment.

3.1.1 Gas Burner

A preliminary full-scale test was conducted with only the ignition burner in the compartment. The burner was placed in the same location it would occupy when seat assemblies were in position on the load platform. This test was performed to verify the operation of all instruments in the test facility and to determine the threat represented by the burner to occupants in the bus simulation independent of the seat assemblies under test. The threat posed by the ignition burner was assessed by the depth and temperature of the upper layer of hot gases in the compartment, the gas concentrations of CO, CO_2, and O_2 and the irradiance level received by two targets. One target was located on the wall opposite the ignition burner. The second was located at the mid-point of the floor of the bus simulation. The irradiance level at the latter location was calculated from measurements of the upper gas temperature and location of the interface. The average upper gas temperature was taken as the bulk ceiling temperature. The ceiling emissivity was assumed to be 1; this assumption would lead to an overestimate of the critical irradiance levels.

3.1.1.1 Rate of Heat Release

Figure 9 shows the heat release rate (HRR) for the ignition burner alone. It can be seen that approximately 90 s was required to achieve a steady-state heat release rate. The average heat release rate during steady-state burning was 100 ± 9 kW. A compartment of this size would require an energy release rate of approximately 1600 kW before flashover (complete compartment fire involvement) could be expected to occur.

3.1.1.2 Temperature and Location of Upper Layer

The temperatures of the upper and lower gas layers are shown in Figure 10. During the period of steady-state rate of heat release from the gas burner, the temperatures of the upper and lower gas layers were about 125°C and 33°C,

respectively. Figure 11 shows the location of the interface between the upper hot gases and lower cool gases (according to the method described by Cooper et al. [39]) at the center of the bus simulation. The presence in these tests of a separation between the upper hot gases and lower cool gases is consistent with the basic assumption of zone models and encourages their use in assessing fire growth in a compartment. The lowest level of the interface at the center of the compartment was approximately 1.18 m from the floor.

3.1.1.3 Gas Concentrations (CO, CO_2, O_2)

Figure 12 shows the CO, CO_2, and O_2 concentrations at the center of the compartment near the ceiling. The average gas concentration for CO, CO_2, and O_2 during steady-state burning was 91 ± 30 ppm, *1.43 ± 0.04* percent, and 19.03 ± *0.04* percent, respectively. Peak CO and CO_2 readings were 193 ppm and 1.52 percent and minimum O_2 was 18.95 percent.

3.1.1.4 Target Irradiance

Two targets were defined for these tests. One target was a heat flux sensor located on the compartment side wall opposite the ignition source. The other was a hypothetical point, not actually measured, on the floor centered in the compartment. The irradiance impinging on this latter target was calculated based on the distance between the interface and the floor and the temperature of the gases above the interface. It was assumed that both the hot gases and the compartment ceiling radiated uniformly at the average temperature of the hot gases with a total emissivity near 1. While this assumption is not strictly correct for the upper gas layer in the bum tests (i.e., the upper gas layer in the burner tests was optically thin and the bulk of the radiant energy came from the ceiling), it is appropriate for the particulate laden upper gas layer in subsequent tests that included school bus seat assemblies. The view factor for this geometric arrangement was recalculated as the floor-to-interface distance varied. Figure 13 shows the results for the ignition burner. The side wall irradiance never achieved a steady-state value. Ninety seconds after ignition of the burner the side wall irradiance was 1.1 kW/m^2. This value increased to 1.7 kW/m^2 just prior to flame extinguishment. The floor irradiance also increased throughout the exposure from 0.011 to 0.014 kW/m^2.

3.1.2 Seat Assembly Tests

Single tests of the six seat assemblies were performed in the simulated bus enclosure, Table *4* lists the initial weight of the three-seat configuration for each seat assembly and the percentage weight loss (based on foam, cover fabric, and plywood insert weight) at the conclusion of the test.

Material combination F_1/C_1 not only ignited and burned the entire width of the first seat assembly but also propagated the flames from seat-to-seat. Four minutes after ignition of the burner, all three seat assemblies for material combination F_1/C_1 were actively burning.

Material combination F_2/C_3 exhibited flame spread along the entire exposed seat assembly and ignition, but limited flame spread, on the back of the second seat assembly.

During four seat assembly tests (F_1/C_2, F_3/C_3, F_4/C_3, and F_5/C_3), for which behavior was similar; burning and flame spread were limited to a portion (less than 50 percent of the surface area) of the seat assembly first exposed to the ignition burner. There was some thermal degradation observed on the back of the second seat but flames did not spread along the length of the first seat assembly nor from seat-to-seat. The seat back forward of the ignition seat assembly for test F_3/C_3 also thermally degraded without igniting and spreading the fire from seat-to-seat. Approximately 45 minutes after the termination of the test, seat assembly F_4/C_3 re-ignited in the rearmost seat. Flames did not spread throughout the seat assembly nor did they spread to the adjacent seat assemblies. Re-ignition was caused by in-depth charring of the plywood insert used as a stiffener in the seat back cushion.

3.1.2.1 Rate of Heat Release

Figures 14 through 16 show the heat release rate (HRR) data from the simulated bus compartment. These values were calculated based on measurements of the exhaust gases exiting the simulated bus compartment. (Note: scales are different for each figure in order to maximize resolution.) Table 5 summarizes the HRR data in terms of the peak HRR and the 60 s average about the peak HRR. The time to peak HRR is also tabulated. The highest peak and average HRR values were obtained with the F_1/C_1 seat assembly, 3045 kW and 2780 kW, respectively. This was followed by seat assemblies F_2/C_3, with a peak HRR of 255 kW and an average HRR of 190 kW, and F_3/C_3, with a peak HRR of 205 kW and an average HRR of 170 kW - an order of magnitude below seat assembly F_1/C_1. Three seat assemblies, F_1/C_2, F_4/C_3, and F_5/C_3, had HRR values, peak and average, which were 50 percent below the values obtained from seat assemblies F_2/C_3 and F_3/C_3.

3.1.2.2 Compartment Temperature and Location of Interface

Figures 17 through 22 show the location of the gas layer interface in the center of the compartment for each test and the temperatures above and below the interface. Tables 6 and 7 summarize the results of these tests by tabulating the location of the interface in the center of the compartment at the time of maximum upper compartment temperature as well as the temperature below the interface. At maximum upper compartment temperature, the interface height was approximately 1.2 m except for test F_1/C_1, when the comparmtrnent was at flashover conditions (i.e., upper compartment temperature above 600°C). Also, the upper and lower compartment temperatures at the time of the minimum interface location are tabulated. In all cases, the time for the minimum location of the interface occurred after the peak HRR. This was due to the extinguishment of the flames (burner or burning material) in the rear of the bus simulation. Without the presence of a large heat source, the bouyancy forces induced by the combustion of the burner or seat assembly disappeared,

allowing the smoke layer to descend to the floor. These results show that at the maximum upper compartment temperature, only seat assembly F_1/C_1 had an interface location below 1 m and a lower compartment temperature above the upper compartment temperature of the 100 kW gas burner test. For the other seat assemblies, the location of the interface at this time was approximately the same as observed with only the gas burner.

3.1.2.3 Mass Loss

The rate of mass loss is a key parameter in determining the impact the seat assembly will have on the toxicity and fire growth in a compartment. Figure 23 shows the cumulative mass loss for each seat assembly tested. The initial mass and percentage mass loss are listed in Table 4. The time dependent data represents a more realistic picture of the contribution that a given seat assembly will have on the development of fire conditions in a compartment. Table 8 summarizes the mass loss rate at the time of maximum HRR, $\dot{m}_q$, and at the time of peak mass loss rate, $\dot{m}_p$. It is unclear why the times to peak mass loss and peak heat release rate differ in a manner that is not consistent with instrument delay times or ventilation conditions. For both tabulated mass loss rates, seat assembly F_1/C_1 had the highest, by an order of magnitude or more, mass loss rate. The other seat assemblies had approximately the same $\dot{m}_p$, while the $\dot{m}_q$ values varied somewhat for these seat assemblies.

3.1.2.4 Gas Concentrations (CO, CO_2, O_2, HCN, HCl, and HBr)

Carbon monoxide, CO_2, and O_2 were measured continuously in the large-scale bus simulation fire tests. Gases used for the determination of HCl and HBr were collected in a 5 mM KOH liquid filled impinger. Each impinger sampled the compartment atmosphere over a period of five minutes. Evacuated bulbs were also filled with samples of the compartment atmosphere during these tests for HCN analysis. These grab samples were analyzed after each test. Figures 24 through 29 show the various gas concentrations during each test.

Table 9 summarizes these results at the peak HRR. It can be seen that only seat assembly F_3/C_3 produced any detectable amounts of HBr. Seat assemblies F_4/C_3 and F_5/C_3 also produced no detectable amounts of HCN. (Note: Very little of these seat assemblies burned. If, however, a larger ignition source were used, HCN would be an expected decomposition product based on the results of toxicity and Cone Calorimeter tests.) Because of the presence of the vinyl cover fabrics, HCl was detected in each test. Seat assemblies F_1/C_2, F_4/C_3, and F_5/C_3 produced, at the peak HRR, about the same amounts of HCl. These three seat assemblies burned approximately the same amount. Burning was somewhat more extensive for seat assembly F_3/C_3 and it had a higher HCl concentration at the peak HRR. Seat assembly F_2/C_3 burned one complete seat with an HCl concentration of 155 ppm. Seat assembly F_1/C_1 generated an order of magnitude more HCl than the other seat assemblies, about 1700 ppm.

The overall gas yields for CO, CO_2, HCN, HCl, and HBr are summarized in Table 10 for each seat assembly test. The data show that comparable CO and CO_2 yields were obtained for all tests except for F_1/C_2, which produced less CO per

unit mass of material burned. This seat assembly had the highest HCl yield. This may be due to the presence of a Kevlar backing on the cover fabric which tended to protect the foam substrate. HCN yield was highest for the standard seat assembly, F_1/C_1.

3.2 LARGE-SCALE EXPERIMENTS: FURNITURE CALORIMETER

3.2.1 Heat Release Rate

The heat release rate of the ignition sources were measured in the furniture calorimeter. Figure 30 shows the heat release rate of the three ignition sources as a function of time. It was found that the line burner, in free air, had a steady-state average heat release rate of 50 ± 3 kW. The box burner, in free air, had a steady-state average heat release rate of 50 ± 5 kW and 100 ± 16 kW. The seat assemblies were exposed to the flames from these burners for 200 seconds. The line burner was located in the crevice formed by the seat and back cushions. The box burner was located on the outside edge of the seat assembly.

Based on observed burning behavior, the seat assemblies can be divided into two distinct groups. Assemblies F_1/C_1 and F_2/C_3 continued to burn after the removal of the ignition source. The remaining four seat assemblies extinguished or continued to burn with a weak, localized flame shortly after the removal of the ignition source. For assemblies F_1/C_1 and F_2/C_3, tabulated values were taken after the removal of the ignition source and represent material performance data independent of an ignition source. For the other seat assemblies, the tabulated values represent the burning seat assembly plus the ignition source. Seat assemblies F_1/C_1 and F_2/C_3 were not subjected to the 100 kW exposure.

Figures 31 and 32 show the heat release rates for the six seat assemblies. Care should be taken in interpreting these graphs because of scale differences used to resolve the data. The average and peak heat release rates for the six seat assemblies tested are summarized in Table 11. The tabulated average values are based on the 60 second intervals about each peak heat release rate. For the 50 kW line burner, the average rate of heat release was 330 kW and 200 kW for F_1/C_1 and F_2/C_3, respectively. These values represent data obtained after the removal of the ignition source. The remaining four materials had heat release rates of 60 kW to 80 kW, including the heat release rate of the ignition source. With the 50 kW box burner, the average rate of heat release was 330 kW for assembly F_1/C_1 and 50 kW for assembly F_2/C_3. The other assemblies varied from 35 kW to 80 kW. Peak heat release rates varied from 81 kW to 577 kW for both 50 kW exposures.

Some differences were observed between the 50 kW line burner and the 50 kW box burner. The line burner produced higher average and peak heat release rates than the box burner. These differences were attributed to the larger area involved in a shorter time period during the line burner exposures than the box burner exposures. The most dramatic difference was observed with the

F_2/C_3 seat assembly. It had an average heat release rate of 200 kW following the line burner exposure but had only an average 50 kW heat release rate following the 50 kW box burner exposure. Seat assemblies F_3/C_3 and F_5/C_3 had average heat release rates during the 50 kW box burner exposures that were less than the heat release rate of the box burner alone. The results were somewhat erratic, as reflected in a 50 percent coefficient of variation, but the low heat release rate appears to be indicative of an interaction between the decomposition products produced from these two seat assemblies and the box burner. This was not observed with the line burner.

Box burner tests at 100 kW were performed only on the four seat assemblies that did not propagate a flame. In these tests the seat assemblies also extinguished shortly after the removal of the ignition source. In all cases the average rate of heat release was always in excess of the ignition source varying from 130 to 200 kW. Peak heat release rates varied from 152 to 245 kW.

3.2.2 Target Irradiance

As a measure of the impact a burning seat assembly would have on other seat assemblies and items in close proximity, a heat flux sensor was placed 0.5 m from the front edge of the seat cushion of the seat assembly. Background tests (burner calibration tests without seat assemblies) showed that the irradiance level measured by the target sensor was 0.5, 1.0, and 1.6 kW/m^2 for the 50 kW line burner, the 50 kW box burner, and the 100 kW box burner, respectively. The average and peak irradiance values to this target sensor from burning seat assemblies are listed in Table 12; these values have not been corrected for the contribution of the ignition burners. Except for the F_1/C_1 seat assembly, the other seat assemblies produced average irradiance levels for all exposure conditions that were less than twice the background level. Assembly F_1/C_1 had average irradiances of 9.3 and 7.7 kW/m^2 for the two 50 kW burners. Peak values for this seat assembly were 12.8 kW/m^2 for the line burner and 18.4 kW/m^2 for the 50 kW box burner. These latter values indicate that this seat assembly could be expected to ignite "easily ignitable" target fuels (40).

3.2.3 Mass Loss

The mass of each seat assembly (not including the seat frame) is listed in Table 13 along with the total amount of material consumed by each of the burner exposures. Approximately 90 percent of seat assembly F_1/C_1 and 35 to 45 percent of seat assembly F_2/C_3 were consumed in the two 50 kW tests. The other four seat assemblies had lost from 0.2 percent (F_4/C_3 assembly exposed to the 50 kW box burner) to 3.8 percent (F_3/C_3 assembly exposed to the 100 kW box burner) of their total mass during the three exposure conditions. For assembly F_1/C_2, the exposure condition did not appear to effect the amount of material consumed. The fabric cover of this seat assembly never cracked or parted. Post-test observations showed that the foam cushion beneath the fabric melted and charred but did not appear to have been burned beyond the area of scorched fabric. The UMTA-type vinyl melted and partially burned exposing all of the foam cushions to the ignition burners.

Table 14 is a summary of the average and peak mass loss rates for the six seat assemblies. Assemblies F_1/C_1 and F_2/C_3 had an order of magnitude higher mass loss rate than the other four seat assemblies exposed to the 50 kW line burner. The average mass loss rate of seat assembly F_2/C_3 during a 50 kW box burner exposure was reduced to 2.8 g/s from 10.5 g/s with the 50 kW line burner. The average mass loss rate for the other four seat assemblies was approximately constant for the three burner exposures. Peak mass loss rates for these seat assemblies varied according to the burner exposure condition.

3.2.4 Gas and Smoke Yields

The ignition burners produced approximately 4.8 g/s of CO_2 at 50 kW and 9.4 g/s at 100 kW. The CO_2 yield values reported in this section have been corrected for the presence of the ignition burner. No correction was necessary for the CO yield since the ignition burners alone produced no detectable concentrations of CO. The average smoke specific extinction area values for the ignition burners were less than I percent of the average specific extinction area of any seat assembly and the mass flow rate through the exhaust stack for all tests varied by less than 15 percent. Therefore, specific extinction area was not corrected for the presence of the ignition burner.

Table 15 lists the CO_2 and CO yields (kg/kg) of the six seat assemblies. The CO_2 and CO yields varied according to the ignition burner in use. However, the CO/CO_2 ratio appears to be more consistent. Assemblies F_1/C_1 and F_2/C_3 have CO/CO_2 ratios for both 50 kW burners of 0.03 and 0.06, respectively. With the exception of seat assembly F_1/C_2 exposed to the 50 kW line burner, the other seat assemblies have comparable (same order of magnitude) CO/CO_2 ratios, which vary from 0.12 to 0.83.

The average specific extinction areas are tabulated in Table 16. These data are based on a 60 second time period measured 30 seconds on each side of the peak. Because of the large fluctuations in readings resulting in high standard deviations, all six seat assemblies were judged to have approximately the same smoke extinction area. The overall average specific extinction area was found to be 330 ± 90 m^2/kg. The individual average values varied from 190 to 520 m^2/kg.

3.3 SMALL-SCALE EXPERIMENTS

3.3.1 Cone Calorimeter

3.3.1.1 Time-to-Ignition

Table 17 is a listing of the average times-to-ignition and, where multiple tests were performed, their standard deviation. Times-to-ignition were

determined for both the specified external irradiances (i.e., 35, 50, and 75 kW/m²) used to determine the heat release rate and for external irradiances near the minimum external irradiance needed for piloted ignition. As expected, the data show that as the external irradiance increases, the time-to-ignition decreases. At high external irradiances, the time-to-ignition varied from 1.0 to 2.5 s at 75 kW/m² and 2.0 to 5.0 s at 50 kW/m². The times-to-ignition at low irradiances varied from 48.6 to 83.4 s at 10 kW/m². Below 10 kW/m², F_1/C_1 and F_1/C_2[3] would not ignite and below 3.5 kW/m², the foams covered with the UMTA-type vinyl (C_3) would not ignite. Except at 75 kW/m², the time-to-ignition appears to be primarily controlled by the cover and is independent of the padding. At an external irradiance of 75 kW/m², the distinction among the cover materials appears to disappear. However, the differences between average values of the UMTA-type vinyl covered foams increases.

Brown et al. [41] reviewed some of the literature on time-to-ignition of various materials. In general, they found that the time-to-ignition, t_{ig}, is proportional to $1/\dot{q}''^n$, where $\dot{q}''$ is the external irradiance and n is either 1 or 2. If the material is thermally thin (i.e., the thermal wave reaches the back surface before ignition occurs), n will equal 1. If, however, the material is thermally thick, n will equal 2. Figures 33 and 34 are plots of the time-to-ignition as a function of external irradiance. Table 18 summarizes the results of a linear regression analysis based on $t_{ig} \propto 1/\dot{q}''^n$ for each seat composite tested. The values of n varied from -1.71 to -1.79 for the standard foam (F_1) covered with standard vinyl with and without a Kevlar backing, and from -1.96 to -2.05 for the foams covered with the UMTA-type vinyl. This indicates that the seat composites tend to behave as thermally thick materials.

3.3.1.2 Heat Release Rate

In general, the rate of heat release data for common materials and composites obtained in the Cone Calorimeter display a curve with a single peak heat release rate [42]. In some cases, composite materials have been shown to produce multiple heat release rate peaks [41,43]. In the present case, the bus seat composites exhibited mixed behavior. Figures 35 through 40 show typical heat release rate curves for the six seat composites at three external irradiances - 35, 50, and 75 kW/m². The standard vinyl, without a Kevlar backing, over standard foam, F_1/C_1, (Figure 35) produced two heat release rate peaks and the standard vinyl with a Kevlar backing over standard foam, F_1/C_2, (Figure 36) produced three heat release rate peaks. In contrast, the UMTA-type vinyl covered foams produced single peak heat release rates (Figures 37 through 40). In all cases, the initial peak heat release rate occurred within 25 seconds of sample ignition. Figure 41 shows the heat release rate curves for composite F_1/C_2 with a 90 mm diagonal cut through the cover material.

---

[3] F_1/C_2 composite time-to-ignition data below 35 kW/m² were obtained on the LIFT apparatus and not the Cone Calorimeter. In the past, these data have been found to be comparable.

Like the uncut sample, this sample also produced three peak heat release rates.

Table 19 summarizes the average peak heat release rate data. As expected, the maximum average heat release rate for any one composite increased with increasing external irradiance. All of the UMTA-type vinyl covered foams had approximately the same maximum heat release rate for a given external irradiance. For example, the average heat release rate for the UMTA-type vinyl covered foams was approximately 320, 370, and 400 kW/m^2 at external irradiances of 35, 50, and 75 kW/m^2, respectively. The results for the standard foam covered composites varied depending upon the nature and integrity of the cover material. For any given external irradiance, the highest maximum rate of heat release was obtained with the F_1/C_1 composite. The lowest heat release rate was obtained with the F_1/C_2 composite. The F_1/C_2 composite with a diagonal cut across the surface of the cover material had a lower maximum heat release rate for the 35 and 50 kW/m^2 external irradiances than the UMTA-type vinyl covered foam assemblies. At 75 kW/m^2, all of the standard foam covered composites had higher heat release rates than the UMTA-type vinyl covered foam assemblies.

Multiple heat release rate peaks listed in Table 19 are associated with standard foam assemblies. Also listed in the table are the times between the first and last peak heat release rates. As expected, this also decreases with increasing external irradiance for a given composite. For a given irradiance, the F_1/C_1 composite had the shortest time between heat release rate peaks and the F_1/C_2 composite had the longest observed time interval. The F_1/C_2 cut composite had intermediate times.

Babrauskas and Krasny [27] have demonstrated that the rate of heat release averaged over the first 180 s after ignition could best be used to predict the fire performance of upholstered furnishings in full-size furniture calorimeter tests. Kanury and Martin [41] also have used average values for deducing physicochemical properties of essentially homogenous materials in fire environments. Table 20 lists the expanding average rate of heat release. (The rate of heat release was averaged over fixed periods of time during the burning process beginning with ignition. This procedure allowed for the determination of the suitability of the use of an average heat release rate over 180 s as well as other averaging periods.) This procedure retained the essential form of the original data and smoothed the heat release rate data for use in determining material thermal response characteristics. Table 20 includes the time to peak heat release rate. As noted previously, the rate of heat release increases with increasing external irradiance.

3.3.1.3 Mass Loss Rate and Effective Heat of Combustion

Table 21 summarizes the effective heat of combustion, ΔH_{eff}, the overall average mass loss rate, $\dot{m}_a$ and the mass loss rate, m, during maxima in the heat release rate curves. The ΔH_{eff} was determined by taking the ratio of total heat released divided by total mass loss. The ΔH_{eff} values for the standard foam composites all appear to be approximately 20 MJ/kg. The other composites varied from 16.5 MJ/kg for composite F_2/C_3 to 8.3 MJ/kg for seat

assembly F_4/C_3. In Cone Calorimeter testing of these seat assemblies, the ΔH_{eff} appears to be a function of the foam and not the cover.

The overall average mass loss rates, $\dot{m}_a$, listed in Table 21 showed that, as expected, the average mass loss rate for a given composite was found to be a function of the external irradiance. Composite F_1/C_1, at any given external irradiance, had the highest average mass loss rate; composite F_5/C_3 had the lowest. For those composites exhibiting multiple peaks, the mass loss rate, $\dot{m}$, during the first peak heat release rate was the same or higher than the mass loss rate during subsequent peak heat release rates. The Kevlar covered composite (F_1/C_2) had a lower mass loss rate than the F_1/C_1 composite without the Kevlar backing.

Table 22 lists the total heat released and the mass lost by each sample assembly from ignition to the peak heat release rate and from ignition to the end of the test. Up to the peak heat release rate, samples using the standard foam (F_1) generated 15 to 30 times more heat than the other foam assemblies with an order of magnitude greater weight loss. In terms of the total heat released over the entire test, foam F_1 produced the largest quantity of heat at any exposure level and foam F_4 the least amount of heat at any exposure level. With the exception of foam F_1, the total heat released varied by no more than a factor of three for small changes in mass loss. Figure 42 shows a plot of the data in Table 22. Also shown in this figure, for each set of data, are the least square fits (solid line). The linear fit of the peak heat release data has a slope of 17 MJ/kg with a correlation coefficient of 0.997 and a $y = 0$ intercept passing nearly through $x = 0$. While there is a large gap between the data at opposite ends of the line, the data suggest that, independent of the peak rate of heat release, all of the materials tested have approximately the same effective heat of combustion up to the peak heat release rate. The linear fit of the heat release data over an entire test has a slope of 22 MJ/kg with a correlation coefficient of 0.932. The intercept for this regression is approximately 1 when $y = 0$. Table 20 and the plot of the heat release over an entire test shows that the effective heat of combustion is a function of the chemical makeup of the composite. The difference between these two sets of data implies that, after the peak heat release rate has occurred, the material decomposing and/or combustion mechanism is changing.

3.3.1.4 Yields of Specific Gaseous Products

The concentrations of CO and CO_2 were determined by continuous gas sampling of the effluent gas stream, while HCl, HBr, and HCN were determined from impinger samples collected during the combustion process and analyzed with an LC/ion chromatograph. The sampling and analysis procedure for acid gas determination followed the procedure previously described for the large-scale tests. Three replicates were used in the determination of CO and CO_2 yields and, because the same sampling port was used for either acid gas or soot determination, only a single value was reported for acid gas analysis. The values reported in Table 23 are the overall yield values normalized by the mass consumed from the test specimen during the gas sampling period. The gaseous product yields for a given composite appear to be independent of external irradiance. Even

where there are discrepancies (e.g., HBr yields for composite F_3/C_3), they differ by only about a factor of two.

The actual CO and CO_2 yields were dependent on the sample (foam/cover composite) being tested. Composite F_1/C_1 had the lowest CO yield, 0.062 kg/kg, and highest CO_2 yields, 1.29 kg/kg, while composite F_3/C_3 had the highest CO yield, 0.120 kg/kg, and composite F_4/C_3 had the lowest CO_2 yield, 0.39 kg/kg.
Because of the presence of vinyl cover materials in all composites tested, HCl was present in all cases. Composite F_4/C_3 had the highest HCl yield, 0.061 kg/kg, and F_1/C_1 had the lowest HCl yield, 0.024 kg/kg. The yields of HCl for the other composites were about the same, 0.039 kg/kg.

HCN was not detected in the decomposition products produced by composite F_4/C_3. HCN yield was relatively constant at 0.003 kg/kg for all composites tested except for F_1/C_2. Because of the presence of the Kevlar backing to the vinyl cover material, composite F_1/C_2 never exposed the foam to direct irradiation from either the cone heater or the flame. The continued presence of the Kevlar backing forced the foam decomposition products to pass through a layer of charred material. The charred layer may have been at a higher surface temperature, resulting in a nearly four-fold increase in the yield of HCN, 0.011 kg/kg.

HBr was detected only in the decomposition gases of composite F_3/C_3. HBr yields varied from 0.007 to 0.015 kg/kg.

3.3.1.5 Soot and Smoke Production

Smoke yield was measured by the extent of smoke obscuration of a monochromatic beam of light traversing a cross-section of the exhaust stack. Instantaneous readings were averaged in the same manner as the rate of heat release. The soot yield was determined by measuring the amount of particulates collected on a filter during the entire testing period. Soot yield determinations were made for each composite and external irradiance. The means of these values are reported.

Table *24* summarizes the average soot yield and specific extinction area for 60 second time intervals based on an expanding average. The average soot yield appeared to be independent of external irradiance and a function only of the foam/cover combination. The specific extinction area was only moderately affected by external irradiance. While there was a general trend towards decreasing smoke yield with increasing time, the smoke yield can be taken as being constant, except for composite F_5/C_3.

3.3.2 Flame Spread (LIFT)

Some problems were encountered in using the LIFT apparatus for the determination of material thermal properties based on ignition data and flame spread. The vinyl cover materials used in these tests exhibited a tendency to expand towards the external radiant source. This resulted in a degree of

uncertainty in the distance between the material surface and the external radiant source. An uncertainty in this distance causes uncertainty in the actual external irradiance applied to the material surface at ignition. This behavior affects calculations of the ignition temperature, T_{ig}, heat transfer coefficient, h_e, and effective thermal inertia, kpc. This tendency to move closer to the external radiant source was most pronounced for the UMTA-type vinyl covered foam composites. Also, because of the behavior of the UMTA-type vinyl cover material, these composites could not be preheated to thermal equilibrium. With the exception of the F_1/C_1 composite, time-to-ignition data from the Cone Calorimeter were used for the ignition analysis,

The standard analysis followed in this report assumes that flame spread results were obtained after the sample had achieved thermal equilibrium. During the flame spread tests, the standard vinyl, with and without the Kevlar backing material, over standard foam (F_1/C_1 and F_1/C_2) were preheated to thermal equilibrium. The UMTA-type vinyl cover material rapidly melted, burned, and exposed the foam substrate before thermal equilibrium could be achieved. Results associated with this cover material were obtained after a preheat time of only 45 to 60 seconds. The F_2/C_3 composite burned in two distinct parts. First, the vinyl cover material burned and extinguished. The foam, which was burning slower than the cover material, reached the position of the extinguished cover material and re-ignited it. Both materials continued to burn together. The computed flame spread rate was a combination of the burn rates of both materials. The other three UMTA-type vinyl covered composites behaved similarly.

3.3.2.1 Determination of Thermal Properties

The important properties of a material are thermal conductivity, k, density, ρ, and specific heat, c. Ignition analysis is based on a steady-state energy balance which holds for long heating times. The minimum energy for ignition, $q''_{o,ig}$, is given by

$$q''_{o,ig} = h_e (T_{ig} - T_\infty) , \qquad \text{(Eq. 3)}$$

where

T_{ig} = ignition temperature,
T_∞ = ambient temperature, and
h_e = heat transfer coefficient.

It has been shown that the ignition data can be used to determine an effective material $k\rho c$ from the expression

$$k\rho c = 4/\pi(h_e/b)^2 , \qquad \text{(Eq. 4)}$$

where

b = ignition parameter determined by the ratio of the minimum ignition energy and the external irradiance.

Table 25 lists the thermal property data calculated from the ignition data. It was found that the minimum ignition energies for the UMTA-type vinyl covered foam composites were lower than the minimum ignition energies for the standard vinyl with and without the Kevlar backing. This may have been in part due to the behavior of the UMTA-type vinyl, as previously explained. The uncertainty in the minimum energy necessary for ignition is reflected in the apparently low surface temperature at ignition for the UMTA-type vinyl, 139°C, compared to F_1/C_1 and F_1/C_2, with surface temperatures of 284 and 349°C, respectively.

3.3.2.2 Determination of Flame Spread Properties

Flame spread can be represented by either a thermal equilibrium model given by

$$V^{-\frac{1}{2}} = C[\dot{q}''_{o,ig} - \dot{q}''_{\bullet}F(t)] \quad \text{(Eq. 5)}$$

for $$\dot{q}''_{o,s} \leq \dot{q}''_{\bullet}F(t) \leq \dot{q}''_{ig} ,$$

or a general flame spread model given by

$$V = \frac{\Phi}{k\rho c(T_{ig} - T_s)^2} , \quad \text{(Eq. 6)}$$

where Φ is a material flame spread parameter defined as

$$\Phi = \frac{4}{\pi} / (Cb)^2 . \quad \text{(Eq. 7)}$$

Φ is a general purpose term that includes gas phase properties, flame temperature, and chemical kinetics.

Table 26 lists the flame spread properties of the six composites tested in the LIFT apparatus. Composite F_1/C_1 was preheated to equilibrium; the foam and vinyl cover burned together. The F_1/C_2 composite also was preheated to equilibrium. The cover material for this composite charred, but did not burn away to expose the foam. The F_2/C_3 composite, preheated for only 45 to 60 seconds, burned in two stages, which accounts for the anomalous values listed in Table 26. The initial flame spread was due to the vinyl cover material, which burned and extinguished itself. The foam burned at a lower flame spread rate until the point of cover material extinguishment and then re-ignited the cover. The foam/cover composite continued burning with one flame front. The remaining three composites behaved in a similar manner, except that these foams charred.

3.3.3 Toxicity

3.3.3.1 Autoignition Temperature

The lowest temperature of the cup furnace which caused the samples to flame (without the spark igniter or ethanol) within 30 minutes was determined for all eight materials. The autoignition temperatures for the foams and the cover materials are given in Tables 27 and 28, respectively. The three vinyl cover materials and the CMHR foam (F_1) exhibited intermittent flaming behavior; the four remaining foams burned with a continuous flame for various lengths of time.

3.3.3.2 Chemical and Toxicological Data

The chemical and toxicological data for the eight bus seat materials are presented in Tables 27 through 29. Kost of the eight materials showed considerable residue after the 30 minute decomposition periods. The residual amounts ranged from a low of 8 percent for the standard foam (F_1) and melamine-treated foam (F_2) to a high of 49 percent for the LS Neoprene foam (F_4). The average amount of CO generated from a 40 mg/l loading of the eight materials over the 30 minute exposures without animals ranged from 1160 ppm (F_2) to 4730 ppm (C_2); the levels of **HCN** generated by a 40 mg/l loading of the five foams ranged from **65** ppm (F_1) to 645 ppm (the melamine-treated foam being the highest **HCN** producer). Only the Kevlar-backed vinyl material (C_1) produced significant amounts of HCN as a degradation product. The HCN concentrations as determined by gas chromatography **(GC)** generally tended to be slightly **lower** than those determined by ion chromatography (IC). This might be caused by the fact that during GC analysis only gaseous HCN is being measured but during IC analysis soot and aerosols also are collected in the impingers and any adsorbed **HCN** will contribute to the total ionic concentration. The average HCl Concentrations for the three vinyl materials at a 40 mg/l loading ranged from 240 ppm (C_3) to 1070 ppm (C_1). The HCl levels in the combustion products of the **foams** tested were an order of magnitude less. Hydrogen bromide was detected only in the combustion products of the CMHR foam (F_3). Graphic representations and least squares linear regression analyses of the generation of CO, HCN, and HCl versus mass loading of the various materials are shown in Figures 43 through 45.

Each material was tested first at two loadings (20 and 40 mg/l) without any animals being present. Based on the concentrations of CO, CO_2, O_2, HCN, HCl, and HBr, N-Gas values for each material at its respective test loadings were determined and are listed in Tables 27 and 28. These analytical gas data then were used to predict the value of the LC_{50}. The eight materials were tested with animals in the flaming mode at mass loadings equivalent to the predicted LC_{50}'s. From the animal results at the predicted LC_{50}, an approximate LC_{50} could be estimated. If the approximate LC_{50} indicated that the toxic potency was greater than that indicated by the predicted LC_{50} (i.e., there is an unusual toxicant present), a more precise LC_{50} was determined through a series of additional experiments (see 2.2.3.3.3).

The standard foam (F_1), when decomposed in the flaming mode at 40 mg/ℓ mass loading, produced an N-Gas value of 1.03 for within-exposure and 1.22 for within- plus post-exposure. At this loading, only one death occurred during the 30 minute exposure; no additional deaths occurred post-exposure. However, no animals died when .exposed to higher loadings up to 45 mg/ℓ with N-Gas values of 1.12 and 1.30 for within- and within- plus post-exposure, respectively. Therefore, the approximate LC_{50} value appears to be higher than 45 mg/ℓ and higher than that predicted by the N-Gas formula. This may be the result of a gas which interacts with the other major gaseous products in an antagonistic fashion. There were no post-exposure deaths noted with this material. The graphs of the post-exposure weights of the animals indicate that following an initial weight loss (as high as 45 grams), the animals appeared to recover and gain weight (Figures 46 through 48).

At the 20 and 40 mg/ℓ loadings, the N-Gas values for melamine-treated foam (F_3) were much higher (2.06 and 4.51 for within-exposure, respectively) than the LC_{50} prediction value of 1.1. Therefore, the animals were exposed to a mass loading of 10 mg/ℓ which was expected to produce an N-Gas value close to 1.0. Two animals died within the exposure and one animal died within 24 hours, indicating that the LC_{50} for this foam is approximately 10 mg/ℓ or, in terms of the N-Gas model, 1.19 for within-exposure and 1.68 for within- plus post-exposure. The melamine-treated foam is an extremely high HCN producer and appears to have a higher toxic potency than the other materials tested in this study (Table 29). Following an initial weight loss as high as 30 grams, the surviving animals appeared to gain weight normally (Figure 49).

The CMHR foam (F_3) burned inconsistently, even though the spark igniter was left on continuously. This resulted in some scatter in the combustion product concentrations and the calculated N-Gas values. At the 20 mg/ℓ loading, the N-Gas value was 0.73 for the within- and 0.91 for the within- plus post-exposure. At the 40 mg/ℓ loading without animals, the N-gas value was 1.71 for the within- and 2.11 for the within- plus post-exposure. Consequently, the material loading was adjusted such that the N-Gas prediction value was close to 1.1. Because of the inconsistent flaming, the N-Gas values at 21 and 26 mg/ℓ loadings were practically the same as for 20 mg/ℓ loading. At 21 mg/ℓ loading, two animals died during post-exposure [on day 6 following weight losses of as much as 60 grams (Figure 50)] and no animals died at 26 mg/ℓ loading [with weight losses of approximately 30 grams (Figure 51)]. At a higher loading of 30 mg/ℓ, (N-Gas values of 1.03 and 1.15 for within- and within- plus post-exposure, respectively), two animals died during post-exposure [on days 8 and 13 with weight losses of 80 and 130 grams (Figure 52)]. At the highest loading tested, 40 mg/ℓ (N-Gas values of 1.31 and 1.55 for within- and within- plus post-exposure, respectively), all animals died during the 30 minute exposure. The CMHR foam produced both HCl and HBr, irritant gases which may be causing the post-exposure deaths. The CMHR foam has a higher toxic potency than the standard foam when compared at the same loading (Table 29).

The LS Neoprene foam (F_4), when decomposed at mass loadings of 20 and 40 mg/ℓ, left about 50 percent residue and, therefore, produced low amounts of the monitored gases. The N-Gas values for the 40 mg/ℓ loading were 0.58 and 0.67

for within- and within- plus post-exposure, respectively, and no animals died when exposed to this loading [they lost approximately 30 grams before assuming a more normal growth pattern (Figure 53)]. Doubling of the loading (80 mg/ℓ) such that the N-Gas value was approximately 1 (the experimental values were 1.03 and 1.16 for the within- and within- plus post-exposure, respectively), resulted in one death during the 30 minute exposure. The animals lost 30 to *40* grams following the exposure and then resumed normal growth (Figure *54*). At *85* mg/ℓ loading (the N-Gas values were 1.21 and 1.38 for the within- and within- plus post-exposure, respectively), *5/6* animals died during the 30 minute exposure. The post-exposure growth was similar to that seen at 80 mg/ℓ (Figure 55). Based on these results, the approximate LC_{50} value is between 80 and 85 mg/ℓ. Since the N-Gas value is between 1.03 and 1.20, this foam is not considered unusually toxic and the measured gases alone may be considered responsible for the observed toxicity.

When 20 mg/ℓ of the IMPAK SR-10LS foam (F_5) was decomposed in the flaming mode, the N-Gas values were 0.60 and 0.76 for the within- and within- plus post-exposure, respectively. At *40* mg/ℓ loading, the N-Gas values were 1.67 and 1.97. The mass loadings used for animal exposures were such that the N-Gas prediction value was about 1, a value at which deaths of some animals would be expected. At 28 mg/ℓ loading (N-Gas values of 0.98 and 1.23 for the within- and within- plus post-exposure, respectively), no animals died within the 30 minute exposure and one animal died within five hours following the exposure. At 33 mg/ℓ loading (N-Gas values of 1.06 and 1.35 for the within- and within- plus post-exposure, respectively) one animal died during the 30 minute exposure, one animal died within *24* hours after the exposure, and one animal lost 70 grams before recovering (Figure 56). Therefore, the approximate LC_{50} value is about 33 mg/ℓ and the toxicity of the flaming combustion products of this foam would not be considered extremely toxic. Since the N-Gas value is approximately 1.0 at the approximate within-exposure LC_{50}, the toxicity of the measured gases alone may be considered responsible for the observed deaths.

The standard vinyl cover (C_7), when decomposed in the flaming mode at the 20 mg/ℓ loading, resulted in N-Gas values of 0.33 and 0.36 for the within- and within- plus post-exposure, respectively. Because of the tendency to flame in an inconsistent manner, the spark igniter was left on until all flaming subsided (2 to *4* minutes). At the *40* mg/ℓ loading, the N-Gas values increased to 0.72 and 0.79. At these N-Gas values, no deaths would be expected to occur. When the loading was increased to 56 mg/ℓ to produce a within- plus post-exposure N-Gas value close to 1.1 (i.e., the experimental values were 1.10 and 1.17 for the within- and within- plus post-exposure, respectively), *3/6* animals died during the 30 minute exposure and two more animals died within the next *24* hours. The remaining animal lost about 50 grams before starting to regain weight (Figure *57*). This indicates that the approximate LC_{50} value is close to *56* mg/ℓ. Since the N-Gas value at this LC_{50} is close to 1.1, the toxicity of these combustion products may be attributed to those gases that were monitored.

When the Kevlar-backed vinyl (C_7) was decomposed at 20 and *40* mg/ℓ loadings in the flaming mode, the N-Gas values ranged from *0.92* to 1.67 for the within- exposure and from 1.19 to 2.07 for the within- plus post-exposure. Similar to

the standard vinyl cover, the spark igniter needed to be left on during the flaming period to maintain flaming. The analytical results indicated that the predicted LC_{50} value would be between 19 and 26 mg/ℓ. A test at 22 mg/ℓ produced no deaths. However, at 25 mg/ℓ (Table 28), two out of the six animals died during the 30 minute exposure and the N-Gas value was 1.12. Therefore, the toxicity of this material may be attributed to the measured gases. The surviving animals lost about 35 grams before recovering (Figure 58). The Kevlar-backed vinyl has about twice toxic potency as the standard vinyl.

The UMTA-type vinyl (C,) burned in a very inconsistent manner, regardless of whether ethanol or the spark igniter was used. The flaming subsided in about one minute with ethanol and in about three minutes with the spark igniter. When 20 mg/ℓ and 40 mg/ℓ loadings were decomposed in the flaming mode, the N-Gas prediction values were 0.16 and 0.43, respectively, for within-exposure and 0.21 and 0.72, for the within- plus post-exposure. Since the material produced HCl, post-exposure deaths were expected. Therefore, the material loading for the animal test was based on results of the initial 40 mg/ℓ test without animals. In other words, if 40 mg/ℓ produced an N-Gas value of 0.72, then approximately 60 mg/ℓ should generate an N-Gas value of 1.1. Therefore, the animals were exposed to a loading of 59.9 mg/ℓ. The N-Gas value at this loading was 0.55 and 0.73 for the within- and within- plus post-exposure, respectively. Two animals died within the 30 minute exposure and four died within three hours following the exposure. Unless other gases that were not monitored were contributing to the toxicity, no deaths would be expected at these N-Gas values. The animal exposure was repeated at a lower loading of 40 mg/ℓ and, while no animals died during the exposure, five died within the first 24 hours of the post-exposure period and the sixth animal lost 55 grams and died by day 4 (Figure 59). The N-Gas value for the within- plus post-exposure was 0.45.

Since deaths were occurring at N-Gas values significantly less than 1, additional experiments were conducted to determine the more precise LC,, of the UMTA-type vinyl material. The 30 minute within-exposure LC_{50} was 65 mg/ℓ with 95 percent confidence limits of 62 to 68 mg/ℓ. The LC,, for the 30 minute exposure and 14 day post-exposure observation period was 35 mg/ℓ with 95 percent confidence limits of 30 to 40 mg/ℓ. Examination of Table 28 shows that the N-Gas value for the within-exposure LC,,, 65 mg/ℓ, (no HCl included in the N-Gas calculation) is 1.20 and indicates that the toxic interaction of the four gases used in this calculation are most likely responsible for the deaths. However, the N-Gas value for the within- plus post-exposure LC,, value, 35 mg/ℓ, (including HCl) is only 0.60 and indicates that the toxic interaction of the gases only accounts for 60 percent of the toxicity. Therefore, either one or more unanalyzed gases are contributing to the toxic combustion atmospheres or some synergistic effect of the toxic gases is occurring.

3.3.3.3 Yields of Specific Gases (CO, CO,, O,, HCN, HCl, and HBr)

Table 30 summarizes the gaseous yields of CO, CO_2, O_2, HCN, HCI, and HBr. These values are based on the amount of material consumed and the average gas

concentrations at the end of the 30 minute testing period. The CO and CO_2 yields were relatively constant for all materials, with an average CO yield of 0.13 kg/kg and an average CO_2 yield of 1.4 kg/kg except for the standard foam (F_1) and the melamine foam (F_3) which had CO yields of 0.04 and 0.03, respectively, and CO_2 yields of 2.0 for both. Only the CMHR foam (F_2) produced any HBr, with a yield of 7.2×10^{-3} kg/kg. The standard vinyl (C_1) had an HCl yield of 1.1×10^{-2} kg/kg, while the Kevlar-backed vinyl (C_2) and the UMTA-type vinyl (C_3) produced approximately the same yield of HCl which was twice that of C_1. The foams had higher HCN yields than the cover fabrics, except for the Kevlar-backed vinyl (C_2), which produced approximately the same yield of HCN as the foams. This can be attributed to the presence of the Kevlar backing.

4. USE OF INDIVIDUAL *SMALL-SCALE* METHODS

4.1 COMPARISON OF TEST PARAMETERS

Test methods are designed to provide material fire performance data under a well defined set of thermal, environmental, and geometric conditions. If fundamental knowledge is available that correlates a given measured property with those factors controlling decomposition chemistry, meaningful predictions can be made based on the results of small-scale laboratory tests. Lacking detailed chemical decomposition models, care must be exercised in translating small-scale test data to full-scale results. In any material evaluation procedure that uses data from multiple test methods, the ability to use data from these different test methods with varying exposure conditions depends on the degree of similarity in the decomposition chemistry of a material. Factors affecting the decomposition rate of a material are heating rate (external irradiance and heat losses), enclosure geometry (ventilation conditions and flame air entrainment), and material configuration (panel, chair, table, etc.). While the decomposition rate may vary with test conditions, comparable decomposition chemistry would allow for data comparisons to be made among different test conditions. A comparison will be presented of the yields of specific gases, toxic potency, and heat release rates from the individual test methods and the full-scale tests. It will be seen that results from the individual test methods can not be used to evaluate full-scale performance.

4.1.1 Yields of Specific Gases

In comparing gas yield test results from the various experimental conditions used in this program, absolute gas concentrations become meaningless among test methods because of the different thermal and ventilation conditions. The primary characteristics that can be used as an indicator of comparable decomposition chemistry are the yields of specific gases.

The overall yields of specific gaseous products provide a more reliable means for comparing the data to full-scale test data. From a toxicological perspective, the critical gases involved, based on applications of the N-Gas model to the NBS Toxicity Test Method, were found to be CO, CO_2, reduced O_2, HCN, HCl, and HBr. Overall yields of CO, CO_2, HCN, HCl, and HBr were determined for the full-scale, Cone Calorimeter, and NBS Toxicity Test Method tests. Overall yields of CO and CO_2 were also determined for the large-scale tests in the furniture calorimeter.

4.1.1.1 CO and CO_2

The CO and CO_2 data are summarized in Table 31. Yield values for the full-scale, large-scale, and Cone Calorimeter tests are for the combustion of the composite seat assembly, while the yield values for the NBS Toxicity Test Method are for the individual components.

The CO yields for all composite seat assemblies were similar across the test procedures to within about a factor of 2. A comparison of the CO_2 yields showed that the full-scale tests produced the highest CO_2 yields for all tested seat assemblies. The largest yields obtained in the full-scale tests of seat assemblies F_4/C_3 and F_5/C_3 were 3.0 and 2.9 kg/kg, respectively. Two possible uncertainties may have combined to produce these large yield values, First, fluctuations in the burner fuel feed rate (**i.e.** heat release rate) could introduce an unknown quantity of CO_2 into the compartment. Since the CO_2 values were corrected for the presence of the gas burner in both the full-scale and large-scale tests, an error in the assumed CO_2 mass production rate of the gas burner could cause large CO_2 yields to be attributed to the test material. Second, since only about one percent of the total mass available for combustion in the full-scale tests were actually burned for these two seat assemblies, the mass loss data were near the resolution limit of the load cell; this would increase the uncertainty in the mass loss data. While direct comparisons cannot be made between the individual material gas yield data in the NBS Toxicity Test Method and the seat assembly tests, the variation in CO and CO_2 yields for the individual materials did not vary over a wide range. The CO yields varied from 0.04 to 0.19 kg/kg and the CO_2 yields varied from 1.0 to 2.0 kg/kg. These values were found to be similar to the range of composite yield values obtained in the other test procedures.

The CO/CO_2 ratio is an indicator of the ventilation conditions and tendency to flame during the combustion of a material. Table 32 summarizes the CO/CO_2 yield ratio for all four test conditions. Although there were some test-to-test variations for a given material or composite, the data show that, within a factor of 2 to 3, similar ventilation conditions were observed in all four tests for all materials, except for seat assembly F_4/C_3 which showed a factor of 30 difference in ventilation conditions across the three seat assembly tests. It was observed that flaming on this seat assembly quickly extinguished beyond the contact area of the ignition burner and was replaced by active smoldering of the foam cushion.

4.1.1.2 HCN, HCl, and HBr

Table 33 summarizes the yield data for HCN, HCl, and HBr for the full-scale, Cone Calorimeter, and NBS Toxicity Test Method tests. In addition to CO and reduced O_2, these gases account for the toxic potency associated with the decomposition of these materials. Except for seat assemblies F_5/C_3 and F_1/C_1, yields of these gases for a given seat assembly were similar for all test conditions. Seat assembly F_5/C_3 produced an order of magnitude less HCN and F_1/C_1 produced an order of magnitude less HCl in the full-scale tests than was observed in the other composite seat assembly tests. Seat assembly F_3/C_3 was the only one detected to produce HBr. Based on the NBS Toxicity Test Method, HBr resulted from the combustion of the foam component of this seat assembly.

In general, the CO/CO_2 yield ratios indicate that all tests were performed under similar ventilation conditions, within a factor of 3. As expected from the results of the NBS Toxicity Test Method, HCN, HCl, and HBr (where present) were detected in the decomposition gases under all test conditions. The gas yields for a given seat assembly were within a factor of 2 for the full-scale and Cone Calorimeter, except in the full-scale tests for seat assemblies F_5/C_3 where the HCN differed by a factor of 10, and F_1/C_1 where the HCl yield also differed by a factor of 10.

4.1.2 Toxic Potency

The NBS Toxicity Test Method, as applied in this work, evaluates the toxic potency of the decomposition products of individual materials tested under flaming conditions, i.e., 25°C above the material's autoignition temperature. End-use applications, however, involve a combination of materials. In the case of **bus** seats, each seat is a combination of cover and **foam,** plus any additional materials needed to provide good mechanical performance (i.e., wood, nonwoven fabrics, etc.). It is recognized that the decomposition products at any given time in an open or closed compartment depend on the specific materials burning at that time and the residence time of the decomposition products in the compartment. Since a seat assembly is composed of a thin cover and a foam component, the toxic potency of the resulting atmosphere in these tests can be approximated by assuming concurrent burning of all materials in the assembly. Assuming no interactions between the burning chemistry of the components that would alter the decomposition products, the toxic potency of these decomposition products would be the mass fraction weighted sum of the LC_{50} for the individual components. The $LC_{50}(m)$ of the material assembly is

$$LC_{50}(m) = \sum_{i}^{n} M_f(i)\ LC_{50}\ (i) \quad (mg/\ell)\ , \qquad \text{(Eq. 8)}$$

where

i = 1 to n components,
$M_f(i)$ = the mass fraction of the i^{th} component in the assembly, and
$LC_{50}(i)$ = the LC_{50} of the i^{th} component in the assembly.

This can be applied to the data from the seat assemblies investigated in this study. Table 4 lists the mass fraction of cover and foam for each seat assembly. The approximate or determined LC_{γ} values are taken for the within-exposure condition from Table 29 for each component. Using these data with Eq.8, an effective $LC_{50}(m)$ is calculated for each seat assembly (Table 34). These values will be used later in section 5.1. The effective $LC_{50}(m)$ for a given assembly varied by no more than a factor of 3 from the LC_{γ} values of the individual components, The ability of most toxicological tests to distinguish among differences in the toxic potency of materials is limited to a resolution of about a factor of 3. This indicates that, over the range of materials tested in this program, toxicologically only small differences exist among these materials.

4.1.3 Heat Release Rate

Babrauskas and Krasny [27] have shown that an empirical correlation could be developed for upholstery furniture based on the 180 s after-ignition average heat release rate at an external irradiance of 25 kW/m^2 in the Cone Calorimeter, plus a series of shape and material factors. The product of these terms and an empirically determined constant produced a reasonable estimate of the peak heat release rate in large-scale tests. This correlation proved to be unable to predict full-scale performance from the results of the Cone Calorimeter data in this study. Lack of correlation was probably due to the fact that 35 kW/m^2 external irradiance data were used and the seat assemblies that were used were somewhat more resistant to burning than those investigated in their work.

Several additional correlations were attempted of the heat release rate from the full-scale tests with either the Cone Calorimeter results or the large-scale test results. In the discussion that follows, it should be noted that the Cone Calorimeter and large-scale test represent single seat assembly values. Only the full-scale test of seat assembly F_1/C_1 spread to the adjacent seat assemblies. Therefore, in order to compare heat release rate data from these three test procedures for seat assembly F_1/C_1, one-third of the full-scale test values for this seat assembly were used in the correlation analysis. Figure 60 shows a comparison of the large-scale test results (Table 11) and the full-scale test results (Table 5) with the solid line representing a linear least squares fit of all six data points. The data appear to correlate reasonably well with a calculated correlation coefficient of 0.90. However, deleting the data point representing test F_1/C_1 from the analysis results in the linear least squares calculation producing a negative slope for the correlation line (not shown). This indicates a lack of a physically meaningful correlation.

A comparison of the Cone Calorimeter 60 s average rate of heat release (Table 20) and the average rate of heat release from the full-scale tests (Table 5), Figure 61, shows a correlation (solid line) that also appears reasonable with a correlation coefficient of 0.87 excluding test data from seat assembly F_1/C_1. This represents an uncertainty of about a factor of 2. The regression line has a slope of about 2. Including data from seat assembly F_1/C_1 in the

linear least squares analysis reduces the correlation coefficient to only 0.6 or a factor of 3 uncertainty, but does not alter the general trend of the regression line. This indicates that a correlation maybe possible between the Cone Calorimeter and the full-scale tests for this specific scenario and seat assembly design.

4.2 **MATERIAL EVALUATION**

Acceptable end-use material fire performance depends on the tolerance level for material failure. It is easy to say that materials shall not burn, but this has to be translated into quantifiable measurements based on material performance, often somewhat removed from end-use conditions. For any organic material, thermal conditions can be found that will cause the material to burn Reasonable questions to ask regarding a material's suitability for a specific application are (1) how the material will affect the development of hazardous fire conditions in a given enclosure and (2) what level of hazard is acceptable? Two questions need to be considered in this type of evaluation:

- How much thermal energy is needed to ignite the material?
- How rapidly will the material, once ignited, burn and affect the time to evacuate the enclosure?

The first question deals with the size of the ignition source needed to cause material ignition and subsequent flame spread. The second question deals with the interaction of people with the fire environment in a given enclosure and the environment which results from the products of combustion.

Tenability criteria are determined by human response to a fire environment. These criteria are used to determine, in an idealized sense, when one can reasonably assume that escape from the fire environment becomes impossible. Escape is defined as the ability to vacate an enclosure or to find a safe haven within the enclosure. These tenability criteria deal with human response limits to:

- Temperature (convective heat transfer to the body);
- Irradiance (radiant heat transfer to the body);
- Smoke density (impairment of visibility); and
- Smoke toxicity.

Tenability limits are time-integrated functions of the intensity of exposure. Therefore, no single set of limit values can be defined for incapacitation or lethality due to temperature, irradiance, and toxicity. It also is assumed that an occupant's ability to move about a smoke-filled space controls the exposure time for the other three parameters. For a detailed discussion of these tenability limits and the formulas used to calculate these limits, the reader is directed to the HAZARD I manuals [38].

4.2.1 Impact of Ignition Source

Since various ignition sources can be encountered in the day-to-day operation of a school bus, it is necessary to determine the impact of the strength of the ignition source on the habitability and egress potential from the bus interior, excluding the presence of any interior furnishings. This will provide a basis for the Selection of seat materials based on acceptable fire performance. Ideally, for a given ignition source strength (i.e., rate of heat release), material performance should not significantly decrease the available time for escape as estimated from the ignition source alone. While the determination of acceptable egress times for a school bus enclosure is beyond the scope of this report, it must include the physical state of the occupants, the physical state of the school bus (e.g., upright or overturned), the availability and accessability of exit paths, and the availability of external assistance (police, rescue, and fire services personnel).

Using HAZARD I [38], a series of computer simulations, based on the school bus configuration employed in the full-scale experiments, were performed varying the strength (i.e., heat release rate) of the ignition source. Heat release rates were varied from 100 kW, that used in these experiments, to 1000 kW. In these test cases, it was assumed that approximately 20 seconds was required to achieve a full-power steady-state heat release rate. In the actual burner experiments, time to steady-state heat release varied *from* 30 to 90 seconds. Most of this variation was due to operator adjustments to the flow control valve. Figure *62* shows the rate of heat release for four test cases. Figure 63 shows the resulting upper and lower compartment temperatures for the same four test cases. If we assume compartment flashover to be defined as an upper layer temperature of approximately 600°C [44], then a heat release rate of about 1000 kW will cause compartment flashover in approximately *400* seconds. The approximations of Thomas [45], however, suggest a value of 1600 kW before the initiation of flashover. The lower compartment temperature at this time is calculated to be expected to be 110°C, which is a problem in itself. Table 35 summarizes these results. While the upper layer of the compartment in every computer simulation developed untenable conditions (for both incapacitation and lethality), the lower layer first requires a 250 kW ignition source to became incapacitating and a 1000 kW ignition source to become lethal. Because of the anticipated human response to the elevated temperatures in the upper layer (i.e., individuals will drop to the floor when the upper layer temperature exceeds 50°C), tenability is judged based on conditions in the lower layer, For the given geometric conditions and doorway opening, the model in no case predicted the height of the lower layer to be less than 1 m from the floor. This would provide an escape path of relatively clean air for occupants leaving an upright burning school bus with an open door. If the ignition source is greater than 500 kW, the ignition source controls the rate of fire growth and the development of untenable conditions. Therefore, the type of seat assembly installed in the school bus does not markedly affect the time to develop an incapacitating or lethal environment.

Based on the results of the Cone Calorimeter tests, an external irradiance of 35 kW/m^2 would have ignited all of the tested seat assemblies in less than 10 seconds. How large a source fire would be necessary to produce this incident irradiance? A technique described by Modak [46] can be used to estimate the

size of the fire source, Q_o, necessary to produce a given external irradiance on the surface of a seat assembly.

$$Q_o = 4\pi \dot{q}''_e R^2 / \chi_R \quad \text{(Eq. 9)}$$

where

$\dot{q}''_e$ = external irradiance impinging on the target (kW/m^2),
R = the radial distance between the center of the fire and the target material (m), and
χ_R = the fraction of the total heat released by the source that is radiation. This value can range from *0.2* for non-luminous clean burning fuels to *0.45* for soot-producing fuels.

While this equation ignores any contribution of the hot gas layer in the upper part of a compartment to the total incident irradiance, it can be assumed that the hot gas layer is not well developed within the first 10 to *20* seconds of exposure. (A sooty fire, such as from burning gasoline, has a large radiation component.) Figure 64 shows the required size of the ignition source as a function of radial distance between the source and target and χ_R for an incident irradiance of 35 kW/m^2. For any significant distances (>0.5 m) between the ignition source and target seat assembly, the total rate of heat release will be in excess of that necessary to produce untenable thermal conditions in the lower portion of the compartment and, at a distance of 1 m, the ignition source strength would have to be such that thermal conditions in the compartment would approach flashover. Therefore, non-contact ignition will only occur from large fires.

4.2.2 Impact of a Gasoline Pool Fire

Burgess et al. [47] have measured the mass burning rates of liquid pool fires. Their study has shown that the burning rate is a function of pool diameter and reaches a maximum mass burning rate for large pools. Included in their investigation were the burning characteristics of gasoline fuels. The total heat release rate of a pool fire can be simply described as

$$\dot{q} = \dot{m}_{max} \Delta H_c A \quad \text{(Eq. 10)}$$

where

$\dot{m}_{max}$ = the maximum burning rate ($g/m^2 \cdot s$),
ΔH_c = the heat of combustion (kJ/g), and
A = the surface area of the pool (m^2).

For a 1 m^2 pool of gasoline with a ΔH_c equal to *48* kJ/g and a maximum burning rate of *45* $g/m^2 \cdot s$, the maximum heat release would be approximately 2000 kW. The computer simulations of the gas burner discussed in section *4.2.1* provide a means of assessing the impact of this type of fire on the interior of the bus. If all of the heat is released in the bus, this is well in excess of what is needed to develop untenable conditions in both the upper and lower layers of a full-size school bus, Fuel-fed fires represent a source of energy that can negate the advantages of seat assemblies with otherwise excellent fire performance properties.

4.2.3 Tenability

Applying the tenability criteria used in HAZARD I (Table 36) to the full-scale test data shows that three of the seat assemblies generated an enclosure environment that would have resulted in incapacitation or death to the occupants of the enclosure within a two to three minute time period (Table 37). Complete evacuation of the enclosure under these test conditions would need to have been accomplished within this time period to ensure that occupants would not be exposed to lethal conditions. With the ignition source used in these simulations (100 kW), the other three seat assemblies did not develop a debilitating atmosphere within the enclosure during the duration of the test. Larger fires would have resulted in the development of untenable conditions in the enclosure without requiring the involvement of the seat assemblies.

Based on HAZARD I estimates of the impact of the ignition source on tenability, the incapacitation time in the lower layer of the enclosure for a 500 kW ignition source would be 450 seconds. This ignores any contribution of radiation and toxic potency associated with the decomposition products. It is assumed that the CO yield for the ignition source is low and that temperature is the primary cause of incapacitation or death. The large-scale test results show that the peak heat release rate of seat assemblies F_1/C_2, F_4/C_3, and F_5/C_3 - these seat assemblies did not produce untenable conditions in the full-scale tests with a 100 kW ignition source - appear to be approximately 1.5 to 2.5 times the ignition source strength. Assuming that the peak heat release rate for these seat assemblies was twice the ignition source strength in the full-scale tests, an extrapolation to a 500 kW ignition source would result in a total heat release rate of approximately 1000 kW. This would result in an escape time of about only 70 seconds.

HAZARD I was also used to determine the relative importance of the measures of the development of untenable conditions. It was observed (Figure 31) that the fire duration of individual seats fall into two distinct groups: about 300 seconds and 1000 seconds. Thus two generalized heat release rate curves were used for this portion of the analysis (Figure 65).

Table 38 lists the minimum fire sizes needed to reach specific tenability limits. The steady heat release rate listed in each line of table 38 is the smallest value (within 1 kW) that will cause a specific tenability limit to be exceeded. For example, a 300 second duration fire with a steady heat release rate of 49 kW will activate the FLUX tenability indicator. This indicator is not activated at 48 kW. For the seat assemblies evaluated in this report, the heat of combustion varied from 8 to 21 MJ/kg. The calculations listed in table 38 assume a heat of combustion value of 21 MJ/kg. The effect of different values of heat of combustion is discussed later. For these computer fire simulations, the upper layer temperatures and interface heights between the layers are shown in figures 66 through 69.

Incapacitation due to irradiance are for steady heat release rates of 11 and 49 kW at 1000 and 300 seconds, respectively. At these heat release rates, the upper layer gas temperatures are only 80°C and 130°C as shown in figures 66 and 68. The irradiance tenability limit is based on exposed skin. This is not an appropriate measure for school bus occupants who genrally wear some clothing.

This clothing will tend to increase the irradiance necessary to cause untenabile conditions. Further study of the effects of irradiance on clothed individuals is necessary.

Of the two criteria for incapacitation due to temperature, TEMP1 occurs at a smaller fire size: 323 and 347 kW for the **1000** and 300 secods fires. Thus it seems that the only appropriate acceptance tenability limit for the hazard due to temperature. It therefore follows that a fire that reaches 350 kW in the standard room is about the largest that can be tolerated by people, on a purely thermal basis.

An indication of the effect of toxic gases can be obtained by calculating an LC_{50} of the gases in the standard room and comparing this to the animal toxicity data. For this comparison to be rigorous, the combustion chemistry needs to be the same for the room fire and the small-scale toxicity test. It is believed that this is the case for early fire development in the standard room.

HAZARD I calculates the time exposure Ct value, where C is the material concentration (mg/ℓ or g/m^3) in the upper layer and t is the exposure time (minutes). If the exposure is just sufficient to produce lethal results in half the exposed population, the Ct value can be divided by an exposure time to obtain an LC_{50}. In order to allow for comparison to the small-scale toxicity test, a 30 minute exposure time is used. Therefore,

$$LC_{50} = \frac{(Ct)_\ell}{30} \quad , \qquad \text{(Eq. 11)}$$

where $(Ct)_\ell$ is the time-integrated exposure of mass concentration to cause lethality to 50% of those exposed. However, incapacitation is of more interest in this application than lethality. It has been suggested [38] that values of 1/3 to 1/2 of the lethal values of $(Ct)_\ell$ be used as an incapacitation indicator. Using 1/3 as a conservative estimate of incapacitation, then the lethal exposure $(Ct)_\ell = 3\ (Ct)_i$. Substituting this into the above equation gives

$$LC_{50} = \frac{(Ct)_i}{10} \quad . \qquad \text{(Eq. 12)}$$

Calculated values of LC_{50} are listed in table 39 for heat of combustion values of 8 MJ/kg and of 21 MJ/kg. The LC_{50} values are much larger for the smaller heat of combustion. At a lower heat of combustion, more material must be burned to produce the same heat release rate. This results in a higher concentration of lost fuel in the gases in the room. These higher concentrations increase the calculated values of Ct.

The fires that are of particular interest are the smallest ones for which the TEMP1 limit indicated incapacitation (table 38). These are the 347 kW fire at 300 second duration and the **323** kW fire at **1000** second duration. The calculated LC_{50} values for these two fires ranged from about 1 to 7 mg/ℓ. All of the bus seat materials (table 29), except for melamine-treated polyurethane foam, had much higher LC_{50} values. Melamine-treated polyurethane foam had an LC_{50} of 10 mg/ℓ.

While it is extremely unlikely that a bus seat assembly will be developed that will have an LC_{50} value near 1 mg/ℓ, and also unlikely that an assembly will be developed with a value as low as 7 mg/ℓ, an assembly with a value as low as 7 mg/ℓ would mean that about the same fire size would result in incapacitation due to both toxicity and elevated temperature (TEMP1).

4.3 SMALL-SCALE TEST METHODS SUMMARY

Table 40 is a tabulation of the ranking order of performance for the seat assemblies according to each test procedure. These rankings are compared to the ranking order of performance in the full-scale tests based on the time to reach untenable conditions in the enclosure. No single test appears to assess and rank these seat assemblies adequately with respect to end-use tenability conditions. It appears that full-scale testing of multiple seat assemblies may provide the only means for accurately assessing the fire performance of a seat assembly design.

5. APPROACHES TO MATERIAL QUALIFICATION PROCEDURES

Seat assemblies used in school buses represent complex structures that are composed of multiple materials in varying orientations. This complexity is a result of the need to meet comfort, flammability, and impact protection requirements, This complexity, however, also increases the difficulty in assessing the impact of changes in seating design on fire safety. For example, the introduction of a fire barrier in a seat assembly (F_1/C_2) greatly improved the fire performance of the standard seat assembly without substantially altering the fuel load in the bus enclosure. However, while the effect of vandalism on fire performance was not investigated in any rigorous manner, extensive acts of vandalism could be expected to compromise the effectiveness of the barrier material, as seen in the increased rate of heat release from Cone Calorimeter tests performed on seat assembly F_1/C_2 when this seat assembly was tested with a clean cut in the cover material.

It is currently within the grasp of fire technology to extrapolate single compartment test data from one enclosure size to another enclosure size and to assess the impact of changes in seat design on escape potential. HAZARD I provides the computer software implementation to accomplish this translation. Such an approach would allow for different seat assembly performance requirements to be applied to buses of varying sizes and to assess fire safety from one set of test results. However, the use of full-scale testing to evaluate small changes in seat design can be costly. Manufacturers will have to develop cost-effective procedures to screen material assemblies prior to submission for full-scale evaluation.

It should first be noted that the results presented here demonstrate that the time available to evacuate a school bus is a function of both the strength of

the external fire source and the fire performance of the seat assembly. It can be expected that an external fire source that releases energy at the rate of approximately 500 kW or more of into the bus interior will quickly develop untenable conditions in the compartment independent of the composition of the seat assembly. Therefore, simulations should concentrate on safety in the face of smaller ignition sources.

5.1 PROCEDURE FOR FULL-SCALE MATERIAL ASSESSMENT

Full-scale compartment evaluations of finished assemblies have only recently matured to the point were standard test procedures have been developed. The state of California has adopted a full-scale compartment test procedure, California Bulletin 133 [48], for qualifying upholstered furniture for high risk occupancies in buildings. ASTM has proposed a standard room fire test procedure for general evaluation of wall and ceiling materials [49]. Both of these procedures recognize the importance of defining the enclosure and ventilation conditions to ensure repeatable and relevant results. They take into account the interaction of the burning item(s) with the enclosure and the hot gases collected in the upper layer of the compartment. They also provide the data necessary to determine escape potential given a set of tenability criteria. The use of one of these test procedures, combined with a HAZARD I type of analysis, would provide a means for the assessment of relative hazard of seat assemblies intended for use in school buses.

While California Bulletin 133 defines an ignition source, the ASTM room fire test does not specify an ignition source for use with seat assemblies. At this point in time, additional work is necessary to determine the acceptability of the California Bulletin 133 ignition source or alternatively to develop a new ignition source consistent with the anticipated end-use application.

To best use the results of the work reported here, full-scale testing should be based on full-size bus enclosures of the type used in the current work. The test conditions would use:

- a compartment measuring 2.44 m wide by 2.13 m high by 8.23 m long;
- three seat assemblies installed in one corner of the compartment so that the essence of fire growth is captured (i.e., seat-to-seat, as well as laterally across a seat);
- a gas burner ignition source with a heat release rate of 100 kW applied to the inside edge of the rear most seat assembly.

Since the time available for evacuation is a critical parameter, measurements need to be made that allow for the determination of the time to reach untenable conditions. Furthermore, these measurements need to be sufficient to allow for an assessment of hazard for other enclosure volumes through the use of such tools as HAZARD I. Therefore, minimal instrumentation for a full-scale test would be:

- a load platform;
- two thermocouple trees (8 to 10 thermocouples per tree) - one located in the center of the compartment and one located in the diagonal corner opposite the three seat assemblies;
- a heat flux meter located on the floor in the center of the compartment;
- a gas sampling port(s) located near the ceiling (within 150 mm of the ceiling) in the center of the compartment (gas analysis would have to include CO, CO, , O, and any other gas species assumed to affect material toxic potency);
- instrumented exhaust hood for the determination of heat release rate and yields of gaseous products of combustion (temperature, flow, CO, CO_2, O, and any other gas species assumed to affect material toxic potency).

5.2 PROCEDURE FOR SCHOOL BUS SEAT ASSEMBLY ACCEPTANCE TESTING

Based on full-scale test results, the preceding section defined a full-scale test procedure for determining the tenability limits associated with a given bus size. This test procedure was enclosure size dependent. It could not assure the end-user that a passing seat assembly in a full size bus simulation like that used in this report would not cause untenable conditions in a bus of smaller size. Furthermore, the test procedure requires that a specflized test enclosure be constructed. It is possible, however, to generalize the data from these tests and develop a full-scale test protocol that would be applicable to all bus sizes. The results of performing test evaluations with a smaller compartment size would be tenability assessments that were more conservative than those based on seat assembly tests performed on a full size bus compartment. In addition, the selection of a standardized compartment geometry would enable testing laboratories to follow the test protocol without the need for constructing a specialized compartment for bus seat assembly evaluations.

The Test Protocol would require the use of full size seat assemblies tested in a well defined enclosure with a well defined doorway opening and evaluating the results by computer calculations of tenability limits. The use of computer fire modeling would further allow for the assessment of the interaction of seat assembly fire performance and bus size. The test protocol is divided into three parts:

- enclosure and doorway dimensions and instrumentation;
- fuel geometry and ignition mode;
- assessment tools.

The compartment would have the same dimensions and doorway opening as the standard ASTM Room [49] (i.e., *2.44* m wide by 3.66 long by *2.44* m high). The instrumentation for the standard ASTM Room fire test would be approximately the same as that previously listed for the full-scale test procedure described in section 5.1. Namely:

- a load platform;
- two thermocouple trees (8 to 10 thermocouples per tree) - one Located in the center of the compartment and one located in the diagonal corner opposite the seat assemblies;
- a heat flux meter located on the floor in the center of the compartment;
- a gas sampling port(s) located near the ceiling (within 150 mm of the ceiling) in the center of the compartment (gas analysis would have to include CO, CO_2, O, and any other gas species assumed to affect material toxic potency);
- instrumented exhaust hood for the determination of heat release rate and yields of gaseous products of combustion (temperature, flow, CO, CO,, O, and any other gas species assumed to affect material toxic potency).

This test protocol is primarily interested in assessing tenability conditions and the spread of the fire from the first seat exposed to the ignition source to adjacent seat assemblies. Therefore, the test protocol can be limited to:

- two seat assemblies installed in one corner of the compartment so that the essence of fire growth is captured (i.e., seat-to-seat, as well as laterally across a seat);
- a gas burner ignition source with a heat release rate of 100 kW to 300 kW applied to the inside edge of the rear most seat assembly.

The data from the test procedure would be used to determine thermal and toxicological impact on bus occupants. The Time-to-Untenable conditions will be determined for the standard room using TENAB, a program contained in HAZARD I. HAZARD I could also be used to assess the impact of seat fire performance on other bus enclosure sizes.

This testing sequence has three possible outcomes:

- untenable conditions develop in the enclosure (the seat assembly design could be rejected);
- time-to-untenable conditions is greater than the evacuation time (perform quick-check toxicity test to verify normal toxicity);
- conditions in the enclosure remain tenable for the duration of the test (perform quick-check toxicity test to verify normal toxicity).

For the last two possible outcomes, toxicity testing is necessary to verify that the materials under evaluation do not produce decomposition gases that result in the material having an LC,, value of much less than 10 mg/ℓ.

6. SUMMARY AND CONCLUSIONS

The fire assessment of materials suitable for use in the interiors of school buses needs to be judged on the basis of the materials' potential for causing the development of life-threatening conditions in the event of a deliberate or accidental fire.

- No one simple small-scale test should be used to measure the fire performance of a material when exposed to an ignition source. Therefore, consideration must be given to a combination of factors, such as ease of ignition, flame spread, rate of heat release, generation of gaseous species, smoke development, and toxicity of the combustion products. Examination of the results for each of the parameters considered for the development of hazardous conditions in a school bus geometry reveals some similarities and some differences depending on the exposure conditions or the material used.

  Ignitability
  - Ignition is controlled by the cover material.
  - At 50 kW or below, the ratio of the times-to-ignition for the standard vinyl/UMTA-type vinyl is 2/1.
  - At 75 kW, the times-to-ignition for all the tested composites are approximately equivalent.
  - The ignition sensitivity as defined by the exponent n in $1/\dot{q}''^{n}$ slope (regression slope of ln time-to-ignition vs. ln external irradiance) was comparable for all seat composites. The value of n was found to be approximately 2.

  Flame Spread
  - Minimum irradiance necessary for lateral flame spread ($q''_{o,s}$) was lowest for the standard foam and standard vinyl combination (highest flame spread rate).
  - Minimum irradiance necessary for lateral flame spread was about the same for the UMTA-type vinyl covered foams.
  - Minimum irradiance necessary for lateral flame spread was highest for the standard foam covered with the Kevlar-backed vinyl (lowest flame spread rate).

  Rate of Heat Release
  - In the full-scale bus simulation, the standard foam and standard vinyl combination produced the highest peak and average rates of heat release (more than an order of magnitude higher than the others.
  - In the furniture calorimeter, the standard foam and standard vinyl combination also produced the highest heat release rates, although the spread amongst all the assemblies was not as great.
  - As expected, heat release rates increased with increasing external irradiance in the Cone Calorimeter. Only the composites containing the standard foam exhibited multiple peaks, the one

with the standard vinyl being the highest. There was no distinction amongst the other foams.

Generation of Gaseous Species

- In the Cone Calorimeter, the CO/CO_2 ratios were independent of external irradiance. Overall, the ratios varied no more than by a factor of four.
- Hydrogen cyanide yields were highest for the standard foam and standard vinyl in the full-scale bus simulation, while in the Cone Calorimeter and the toxicity tests, the melamine-treated foam produced the highest HCN yield. On the other hand, the melamine-treated foam produced the lowest CO yield in the toxicity tests.

Smoke Development

- Little distinction in average specific extinction area could be made among the six seat assemblies evaluated in the furniture calorimeter or in the Cone Calorimeter.
- Average soot yields were independent of external irradiance; however, average soot yields ranged from *0.044* for the standard foam covered with the Kevlar-backed vinyl to 0.103 for the neoprene foam covered with the UMTA-type vinyl.

Toxicity

- Of the five foams, the melamine-treated foam had the highest toxic potency and the neoprene foam had the lowest.
- The Kevlar-backed vinyl cover had a higher toxic potency than the other two cover materials, which were similar.
- UMTA-type vinyl had a higher LC_{50} value than predicted by the N-Gas model.

- HAZARD I analysis was used to determine the impact on tenability of different ignition sources in a large school bus enclosure. It was found that for the compartment size used in this study:
  - incapacitating conditions developed between 250 kW and 500 kW;
  - lethal conditions developed at about 1000kW.

- HAZARD I analysis was also used to determine minimum measurement requirements. This analysis showed that:
  - exposure to temperatures of 65°C or more (TEMP1) was the most stringent tenability criteria;
  - toxicity would incapacitate people no sooner than would temperature.

- Tenability analysis of the full-scale test data showed that:
  - three seat assemblies produced incapacitating conditions (F_1/C_1, F_2/C_3, and F_3/C_3) in the bus enclosure;
  - one seat assembly (F_1/C_1) produced lethal conditions in the bus enclosure;
  - three seat assemblies did not produce an incapacitating or lethal environment in the bus enclosure.

- Full-scale test protocol is outlined that can form the basis for compliance testing of seat assemblies for use in school buses. This test protocol is based on seat assembly tests in a standardized room. The acceptance level is determined by calculating the tenability conditions in the enclosure and comparing these results to tenability limits. To ensure that unknowrr toxicants are not producing an unusually toxic atmosphere in the bus enclosure, it maybe necessary to perform animal toxicity testing.

7. REFERENCES

[1] Goldsmith, A., Flammability Characteristics of Vehicle Interior Materials, Final Technical Report, Project 56152, IIT Research Institute, Chicago, IL (May 1969).

[2] Flammability of Interior Materials - Passenger Cars, Multi-Purpose Passenger Vehicles, Trucks, and Buses, Title 49, Transportation, Code of Federal Regulations, Part 571.302.

[3] Braun, E., Report of Fire Test on an AM General Metro Bus, Nat. Bur. Stand. (U.S.), NBSIR 75-718 (1975).

[4] Braun, E., A Fire Hazard Evaluation of the Interior of WMATA Metrorail Cars, Nat. Bur. Stand. (U.S.), NBSIR 75-971 (1975).

[5] Birky, M.M., et al, Measurements and Observations of the Toxicological Hazard of Fire in a Metrorail Interior Mock-up, Nat. Bur. Stand. (U.S.), NBSIR 75-966, (1976).

[6] Adams, L., et al, Development of a Unitized School Bus, Vol. II - Technical Report, DOT HS-802 005, AMF Advanced Systems Laboratory, Goleta, CA (August 1976).

[7] Nelson, G.L., et al, Material Performance in Transportation Vehicle Assemblies, J. of Fire and Flammability, 8, 262 (1977).

[8] Litant, I., Guidelines for Flammability and Smoke Emission Specifications - TSC-76-US-6, Department of Transportation (July 1976).

[9] Peacock, R.D., and Braun, E., Fire Tests of Amtrak Rail Vehicle Interiors, Nat. Bur. Stand. (U.S.), NBS Tech Note 1193 (1984).

[10] Proceedings of Third Downtown People Mover Workshop, System Operation and Maintenance, Morgantown, WV (November 8-10, 1978).

[11] Peacock, R.D., Fire Safety Guidelines for Vehicles in a Downtown People Mover System, Nat. Bur. Stand. (U.S.), NBSIR 78-1586 (1979).

[12] Hathaway, W.T., and Flores, A.L., Identification of the Fire Threat in Urban Transit Vehicles, Transportation Systems Center (DOT), UMTA-MA-06-0051-80-1 (1980).

[13] NFPA 130, Fixed Guideway Transit Systems, National Fire Protection Association, Quincy, MA (1988).

[14] Recommended Fire Safety Practices for Rail Transit Material Selection, Federal Register, 49, No. 158, 32482 (August 14, 1984).

[15] Smith, E.E., Fire Safety Evaluation of Rapid Transit Systems, Report to the Transit Development Corporation, Washington, DC, unpublished (1984).

[16] American Society for Testing and Materials, 1984 Annual Book of ASTM Standards, "Proposed Test Method for Determining Fire Performance of Public Ground Transportation Seat Assemblies," E-5 Proposal P 108, Section 4, Vol. 04.07, Philadelphia, PA, p. 1092 (1984).

[17] Fuel System Integrity, Title 49, Transportation, Code of Federal Regulations, Part 571.301.

[18] School Bus Safety, National Highway Traffic Safety Administration, Department of Transportation (November 1988).

[19] Flammability of Interior Materials; Advance Notice of Proposed Rulemaking, Federal. Register, 53, No. 214, 44827 (November 4, 1988).

[20] Peacock, R.D., Davis, S., and Lee, B.T., An Experimental Data Set for the Accuracy Assessment of Room Fire Models, Nat. Bur. Stand. (U.S.), NBSIR 88-3752 (1988).

[21] Huggett, C., Estimation of the Rate of Heat Release by Means of Oxygen Consumption Measurements, Fire and Materials, 8, 61 (1980).

[22] Babrauskas, V., Lawson, J.R., Walton, W.D., and Twilley, W.H., Upholstered Furniture Heat Release Rates Measured with a Furniture Calorimeter, Nat. Bur. Stand. (U.S.), NBSIR 82-2604 (1982).

[23] Parker, W.J., Calculations of the Heat Release Rate by Oxygen Consumption for Various Applications, Nat. Bur. Stand. (U.S.), NBSIR 81-2427 (1982).

[24] Babrauskas, V., Development of the Cone Calorimeter · A Bench-Scale Heat Release Apparatus Based on Oxygen Consumption, J. Fire Sci., 8, 81 (1984).

[25] American Society for Testing and Materials, 1990 Annual Book of ASTM Standards, Standard Test Method for Heat and Visible Smoke Release Rates for Materials and Products Using an Oxygen Consumption Calorimeter, ASTM E 1354, Section 4, Vol. 04.07, Philadelphia, PA, (1990).

[26] Babrauskas, V., and Parker, W.J., Ignitability with the Cone Calorimeter, Nat. Bur. Stand. (U.S.), NBSIR 86-3445, (1986).

[27] Babrauskas, V., and Krasny, J.F., Predictions of Upholstered Chair Heat Release Rates from Bench-Scale Measurements, Fire Safety: Sci. & Eng., ASTM STP 882, Harmathy, T., Ed., Philadelphia, PA, p. 268 (1985).

[28] Quintiere, J.G., and Harkleroad, M., New Concepts for Measuring Flame Spread Properties, Fire Safety: Sci. & Eng., ASTM STP 882, Harmathy, T., Ed., Philadelphia, PA, p. 239 (1985).

[29] Quintiere, J.G., The Application of Flame Spread Theory to Predict Material Performance, J. Nat. Bur. Stand., 93, 61 (1988).

[30] American Society for Testing and Materials, 1990 Annual Book of ASTM Standards, Standard Method for Determining Material Ignition and Flame Spread Properties, ASTM E 1321-90, Section 4, Vol. 04.07, Philadelphia, PA (1990).

[31] Babrauskas, V., Levin, B.C., and Gann, R.G., A New Approach to Fire Toxicity for Hazard Evaluation, Fire J., 81, 2 (1987).

[32] Levin, B.C., Fowell, A.J., Birky, M.M., Paabo, M., Stolte, A., and Malek, D., Further Development of a Test Method for the Assessment of the Acute Inhalation Toxicity of Combustion Products, Nat. Bur. Stand. (U.S.), NBSIR 82-2532 (1982).

[33] Kolthoff, I.M., and Sandell, E.B., Textbook of Quantitative Inorganic Analysis, 2nd Ed., p. 546, MacMillan Co., New York, NY (1953).

[34] Paabo, M., Birky, M.M., and Womble, S.E., Analysis of Hydrogen Cyanide in Fire Environments, J. Comb. Tox., 6, 99 (1979).

[35] Levin, B.C., Paabo, M., Gurman, J.L., and Harris, S.E., Effects of Exposure to Single or Multiple Combinations of the Predominant Toxic Gases and Low Oxygen Atmospheres Produced in Fires, Fund. Appl. Tox., 9, 236 (1987).

[36] Levin, B.C., Paabo, M., Gurrnan, J.L., Harris, S.E., and Braun, E., Toxicological Interactions Between Carbon Monoxide and Carbon Dioxide, Toxicology, 47, 135 (1987).

[37] Litchfield, J.T., and Wilcoxon, F., A Simplified Method of Evaluating Dose-Effect Experiments, J. Pharmacol. and Exp. Therapeutics., 96, 99 *(1949).*

[38] Bukowski, R.W., Peacock, R.D., Jones, W.W., and Forney, C.L., Technical Reference Guide for the Hazard I Fire Hazard Assessment Method, Nat. Inst. Stand. & Tech. (U.S.), NIST Handbook 146, Vol. II (1989).

[39] Cooper, L.Y., Harkleroad, M., Quintiere, J.G., and Rinkinen, W.J., An Experimental Study of Upper Hot Layer Stratification in Full-scale Multi-Room Fire Scenarios, J. Heat Trans., 104, *741* (1982).

[40] Babrauskas, V., Will the Second Item Ignite?, Nat. Bur. Stand. (U.S.), NBSIR 81-2271 (1981).

[41] Brown, J.E., Braun, E., and Twilley, W.H., Cone Calorimeter Evaluation of the Flammability of Composite Materials, Nat. Bur. Stand. (U.S.), **NBSIR** 88-3733 (1988).

[42] Kanury, A.M., and Martin, B.M., A Profile of the Heat Release Rate Calorimeter, International Symposium on Fire Safety of Combustible Materials, Univ. of Edinburgh (UK) (1975).

[43] Braun, E., Shields, J.R., and Harris, R.H., Flammability Characteristics of Electrical Cables Using the Cone Calorimeter, Nat. Inst. Stand. & Tech. (U.S.), NISTIR *88-4003 (1989).*

[44] Babrauskas, V., Upholstered Furniture Room Fires - Measurements, Comparison with Furniture Calorimeter Data, and Flashover Predictions, J. Fire Sci., 2, 5 *(1984).*

[45] Thomas, P.H., Testing Products and Materials for Their Contribution to Flashover in Rooms, Fire and Materials, 5, *103 (1981).*

[46] **Modak,** A.T., Thermal Radiation from Pool Fires, Combustion and Flame, 29, *177 (1977).*

[47] Burgess, D.S., Grumer, J., and Wolfhard, H.G., Burning Rates of Liquid Fuels in Large and Small Open Trays, International Symposium on the Use of Models in Fire Research, Publication *786,* Nat. Acad. Sci. (November 1959).

[48] Technical Bulletin *133,* Flammability Test Procedure for Seating Furniture for Use in Public Occupancies, California Department of Consumer Affairs, Bureau of Home Furnishings **and** Thermal Insulation, North Highlands, CA (April *1988).*

[49] American Society for Testing and Materials, 1983 Annual **Book** of ASTM Standards, "Proposed Method for Room Fire Test of Wall and Ceiling Materials and Assemblies," E-5 Proposal, Section 4, Vol. *04.07,* Philadelphia, PA, p. *958 (1983).*

8. ACKNOWLEDGEMENTS

The authors would like to acknowledge our sponsor, the National Highway Traffic Safety Administration, and, in particular, Messrs. R. Hitchcock, C. Gauthier, E. Jettner, and R. Strombotne, without whose support this project would not have been conducted.

We want to thank Dr. R. Gann for helpful discussions in the formulative and interpretative stages of this project.

Our thanks also to Messrs. R. Zile, R. McLane, and G. Roadarmel, who built the full-scale test facility for the bus simulation and assisted in implementing the full-scale experiments and the furniture calorimeter experiments; Ms. I. Rivera, who assisted in implementing the full-scale experiments; and Mrs. P. Martin, who reduced the full-scale and large-scale test data. We appreciate the efforts of Mr. J. R. Shields in performing the Cone Calorimeter tests, and Messrs. S. Dolan and A. Perez, who performed the flame Spread tests.

We would like to thank Mr. R. Harris, who performed the ion chromatography analyses, and Miss N. Eller and Mr. R. McCombs, who assisted in performing the toxicology experiments.

Table 1. Physical Measurements of School Bus Seat Materials

Material Designation	Foams	Density kg/m³	Density lb/ft³
F_1	Rebonded PUR	73	4.6
F_2	Melamine-treated PUR	85	5.3
F_3	CMHR PUR	49	3.1
F_4	Polychloroprene	145	9.0
F_5	Rebonded FR PUR	90	5.6

	Cover Materials	Areal Density g/m²	Areal Density oz/yd²	Thickness mm	Thickness in
C_1	Standard	870	25.6	0.76	0.030
C_2	Kevlar-backed	830	24.6	1.2	0.047
C_3	UMTA-type	770	22.6	1.1	0.043

Table 2. Materials Used in the Construction of the Full-scale Bus Simulation

Location	Material	Thickness mm	Density kg/m^3	Specific Heat kJ/kg-K	Thermal Conductivity W/m-K	Emissivity
Ceiling and Walls (Substrate)	Gypsum Board	12.7	930	1.09	0.17	----
Ceiling and Walls (Interior Finish)	Calcium Silicate	12.7	720	1.25 @ 200°C 1.33 @ 300°C 1.55 @ 600°C	0.118 @ 200°C 0.114 @ 300°C 0.124 @ 600°C	0.83
Floor (Substrate)	Concrete	102	2280	1.04	1.82	----
Floor (Interior Finish)	Gypsum Board	12.7	930	1.09	0.17	----

Table 3. Location of Instrumentation in tho Full-Scale Bus Simulation

Load Cell

Load Platform 1.22 m by 1.83 m, 0.10 m from floor (SE corner).

Thermocouple Trees

Tree 1 - Northeast corner (0.61 m from the north and east walls)
8 thermocouples; 0.36, 0.76, 1.17, 1.58, 1.88, 2.03, 2.08, 2.13 m from the floor.

Tree 2 - Center of compartment (4.12 m from east wall and 1.22 m from north wall)
8 thermocouples; 0.36, 0.76, 1.17, 1.58, 1.88, 2.03, 2.08, 2.13 m from tho floor.

Treo 3 - Northwort corner (0.61 m from tho north and wost walls)
8 thermocouples; 0.36, 0.76, 1.17, 1.58, 1.88, 2.03, 2.08, 2.13 m from tho floor.

Tree 4 - Exit Doorway (vertical centerline)
7 thermocouples; 0.25, 0.41, 1.02, 1.17, 1.32, 1.63 m from tho floor.

Exhaust Hood - 10 thermocouples equally distributed along tho cross sectional area of the exhaust hood.

Smoke Meters

Compartment - 1 vortical smoke motor (1.22 m from tho north and wort walls).

Compartment - 1 horizontal smoke motor (1.52 m from wost wall) 1.98 m from floor.

Exhaust hood - 1 smoke motor.

Static Pressure Probes

Compartment - west wall - 1 probo 0.10 m from tho floor.

Exhaust Hood - 9 probes equally distributed along the cross sectional area of tho exhaust hood.

Gas Probes

Compartment - CO, CO_2, O_2
1 probo 0.10 m from ceiling (4.12 m fran east wall and 1.22 m fran north wall).
- HCN, HCl, HBr
1 probe 0.10 m from ceiling (4.12 m fran east wall and 0.91 m fran north wall).

Exhaust Hood - CO, CO_2, O_2
1 probo centerline of exhaust hood.

Heat Flux Meter

Compartment - 1 totalhoat flux motor on north wall (1.07 m fran east wall and 0.46 m from floor).

Table 4. Initial Mass and Percentage Mass Loss for the Three Seat Configuration Used in the Full-Scale Bus Simulation

Seat Assembly	Initial Mass[a] kg	Mass Loss[a] %	Fraction[b]	
			Fabric	Foam
F_1/C_1	36.0	99	0.25	0.75
F_1/C_2	34.6	2	0.23	0.77
F_2/C_3	29.6	15	0.20	0.80
F_3/C_3	37.7	10	0.30	0.70
F_4/C_3	49.1	1	0.13	0.87
F_5/C_3	51.8	1	0.19	0.81

[a] Includes cover, foam, and plywood.
[b] Excludes the mass of wood used in seat bottom and seat back.

Table 5. Peak Heat Release Rate, Time to Peak Heat Release Rate, and 60 s Average about the Peak Heat Release Rate for Seat Assemblies in the Full-scale Bus Simulation

Seat Assembly	Peak HRR[a] kW	Average HRR[b] kW	Time of Peak HRR s
F_1/C_1	3045	2780 ± 200	380
F_1/C_2	105	95 ± 8	290
F_2/C_3	255	190 ± 45	140
F_3/C_3	205	170 ± 30	200
F_4/C_3	105	85 ± 15	470
F_5/C_3	125	85 ± 20	120

[a] Heat Release Rate.
[b] 60 second average about the peak HRR.

Table 6. Height of the Interface above the **Floor** at the Time of Maximum Upper Layer Temperature in Simulated **Bus**

Seat Assembly	at Maximum Upper Layer Temperature			
	Height m	Time s	Upper Layer °C	Lower Layer °C
F_1/C_1	0.22	337	668	133
F_1/C_2	1.20	267	136	36
F_2/C_3	1.19	107	183	37
F_3/C_3	**1.18**	147	173	37
F_4/C_3	1.20	467	141	37
F_5/C_3	1.22	77	138	30

Table 7. Height of the Interface Above the **Floor** at the Time of Minimum Interface Location in Simulated **Bus**

Seat Assembly	at Minimum Interface			
	Height m	Time s	Upper Layer °C	Lower Layer °C
F_1/C_1	0.19	477	546	229
F_1/C_2	1.18	417	133	37
F_2/C_3	0.80	827	64	30
F_3/C_3	0.81	777	44	28
F_4/C_3	0.84	687	42	29
F_5/C_3	1.20	277	127	33

Table 8. Summary of Mass Loss Rates During Peak Heat Release Rate and Peak Mass Loss in Simulated Bus

Seat Assembly	at Peak HRR		at Peak Mass Loss	
	Time s	$\dot{m}_q$ g/s	Time s	$\dot{m}_p$ g/s
F_1/C_1	377	102	307	158
F_1/C_2	287	2	337	11
F_2/C_3	137	6	97	17
F_3/C_3	197	5	137	14
F_4/C_3	467	4	487	14
F_5/C_3	117	1	397	11

Table 9. Gas Concentrations During **Peak** Heat Release Rate in the Simulated Bus Compartment

Seat Assembly	Time to Peak HRR[a] s	Gas Concentrations CO_2 %	CO ppm	O_2 %	HCl[b] ppm	HCN[c] ppm	HBr ppm
F_1/C_1	377	12.6	14000	5.6	1720	700	ND[d]
F_1/C_2	287	1.1	30	19.0	80	5	ND[d]
F_2/C_3	137	2.1	2900	17.7	155	70	ND[d]
F_3/C_3	197	1.5	2600	17.9	120	10	20
F_4/C_3	467	1.1	20	19.0	75	ND[e]	ND[d]
F_5/C_3	117	1.3	1000	18.6	80	ND[e]	ND[d]

[a] Heat Release Rate.
[b] Values of impinger bottle around the time of peak HRR.
[c] Interpolated values.
[d] Not detected, < 0.1 ppm.
[e] Not detected, < 1.0 ppb.

Table 10 Gas Yields of CO, CO_2, HCN, HCl, and HBr in Bus Simulation

Seat Assembly	Gas Yields (kg/kg)				
	CO	CO_2	HCN x 10^{-3}	HCl x 10^{-2}	HBr x 10^{-2}
F_1/C_1	0.10	1.9	8.3	0.18	--[b]
F_1/C_2	0.04	2.5	2.2	5.2	--[b]
F_2/C_3	0.08	1.9	2.9	1.4	--[b]
F_3/C_3	0.11	2.0	1.8	2.5	1.3
F_4/C_3	0.10	3.0	--[a]	3.1	--[b]
F_5/C_3	0.17	2.9	0.16	2.4	--[b]

[a] Not detected, < 1.0 ppb.
[b] Not detected, < 0.1 ppm.

Table 11. Average and Peak Heat Release Rates for Seat Assemblies Tested in the Furniture Calorimeter

Seat Assembly	Average Heat Release Rate (kW)		
	50 kW Line Burner	50 kW Box Burner	100 kW Box Burner
F_1/C_1	330 ± 100[b]	330 ± 20	---[c]
F_1/C_2[a]	80 ± 20	80 ± 20	130 ± 20
F_2/C_3	200 ± 70	50 ± 20	---[c]
F_3/C_3[a]	80 ± 30	45 ± 25	140 ± 10
F_4/C_3[a]	60 ± 35	60 ± 25	165 ± 25
F_5/C_3[a]	70 ± 10	35 ± 20	200 ± 25

Seat Assembly	Peak Heat Release Rate (kW)		
	50 kW Line Burner	50 kW Box Burner	100 kW Box Burner
F_1/C_1	505	575	---[c]
F_1/C_2[a]	110	110	165
F_2/C_3	330	100	---[c]
F_3/C_3[a]	125	80	150
F_4/C_3[a]	115	95	210
F_5/C_3[a]	85	75	245

[a] Values determined during ignition burner exposure (not corrected for the heat release rate of the ignition burner).
[b] Represents ± one standard deviation.
[c] Not tested under this condition.

Table 12. Average and Peak Irradiance (kW/m^2) of a Target Exposed to Seat Assemblies Tested in the Furniture Calorimeter

Seat Assembly	50 kW Line Burner		50 kW Box Burner		100 kW Box Burner	
	Average	Peak	Average	Peak	Average	Peak
F_1/C_1	9.3 ± 2.3	12.8	7.7 ± 0.8	18.4	--[a]	--[a]
F_1/C_2	1.4 ± 0.1	1.6	0.5 ± 0.1	0.6	1.2 ± 0.1	1.3
F_2/C_3	2.6 ± 1.0	4.3	1.0 ± 0.1	1.1	--[a]	--[a]
F_3/C_3	1.8 ± 0.3	2.4	0.7 ± 0.1	0.9	1.8 ± 0.2	2.0
F_4/C_3	1.6 ± 0.2	1.7	0.5 ± 0.1	0.7	1.5 ± 0.3	2.0
F_5/C_3	2.0 ± 0.2	2.3	0.5 ± 0.1	0.9	1.6 ± 0.3	2.0

[a] Not tested under this condition.

Table 13. Initial Weight and Total Mass Consumed for Seat Assemblies Tested in the Furniture Calorimeter

Seat Assembly	Initial Weight kg	Total Mass Consumed (kg)		
		Line Burner 50 kW	Box Burner 50 kW	Box Burner 100 kW
F_1/C_1	11.8	11.34	10.39	--[a]
F_1/C_2	11.8	0.16	0.13	0.12
F_2/C_3	9.6	4.53	3.40	--[a]
F_3/C_3	12.7	0.33	0.13	0.48
F_4/C_3	15.9	0.22	0.03	0.15
F_5/C_3	17.0	0.26	0.08	0.36

a) Not tested under this condition.

Table 14. Average and Peak Mass Loss Rates for Seat Assemblies Tested in the Furniture Calorimeter

Seat Assembly	Average Mass Loss Rate (g/s)		
	50 kW Line Burner	50 kW Box Burner	100 kW Box Burner
F_1/C_1	19.0 ± 4.9[b]	15.9 ± 1.6	---[c]
F_1/C_2[a]	1.0 ± 0.3	0.6 ± 0.3	0.4 ± 0.3
F_2/C_3	10.5 ± 3.4	2.8 ± 0.9	---[c]
F_3/C_3[a]	1.9 ± 0.6	0.7 ± 0.7	0.6 ± 0.4
F_4/C_3[a]	2.0 ± 0.6	0.1 ± 0.02	1.5 ± 0.2
F_5/C_3[a]	1.6 ± 0.5	0.6 ± 0.3	2.3 ± 0.5

Seat Assembly	Peak Mass Loss Rate (g/s)		
	50 kW Line Burner	50 kW Box Burner	100 kW Box Burner
F_1/C_1	25.7	28.0	---[c]
F_1/C_2[a]	1.3	0.9	1.2
F_2/C_3	14.6	4.2	---[c]
F_3/C_3[a]	2.6	1.8	1.0
F_4/C_3[a]	2.5	0.4	1.8
F_5/C_3[a]	2.1	1.0	2.9

[a] Values determined during ignition burner exposure.
[b] Represents ± one standard deviation.
[c] Not tested under this condition.

Table 15. Gaseous Yields of CO and CO_2 for Three Ignition Conditions as Determined in the Furniture Calorimeter

Seat Assembly	50 kW Line Burner			50 kW Box Burner			100 kW Box Burner		
	CO_2 kg/kg	CO kg/kg	CO/CO_2 -	CO_2 kg/kg	CO kg/kg	CO/CO_2 -	CO_2 kg/kg	CO kg/kg	CO/CO_2 -
F_1/C_1	1.54 ± 0.13	0.05 ± 0.01	0.03	1.69 ± 0.18	0.05 ± 0.01	0.03	[illegible]	[illegible][a]	[illegible]
F_1/C_2	1.74 ± 0.15	0.04 ± 0.01	0.02	2.01 ± 0.60	0.36 ± 0.05	0.18	0.33 ± 0.07	0.[illegible] ± 0.04	0.42
F_2/C_3	1.39 ± 0.28	0.08 ± 0.03	0.06	1.78 ± 0.45	0.1 ± 0.04	0.06	[illegible]	[illegible]	[illegible][a]
F_3/C_3	1.7 ± 0.19	0.28 ± 0.04	0.[illegible]	1.50 ± 0.38	0.[illegible]2 ± 0.[illegible]	0.28	0.[illegible] ± 0.08	0.13 ± 0.04	0.32
F_4/C_3	0.23 ± 0.02	0.12 ± 0.02	0.52	0.61 0.10	0.26 ± 0.[illegible]	0.43	0.2[illegible] ± 0.03	0.2[illegible] ± 0.0[illegible]	0.83
$F_{[illegible]}C_3$	0.7[illegible] ± 0.08	0.27 ± 0.04	0.35	2.26 ± 0.78	0.26 ± 0.09	0.12	0.[illegible]3 ± 0.11	0.[illegible] ± 0.0[illegible]	0.[illegible]4

[a] Not tested under this condition.

Table 16. Average Specific Extinction Area for Seat Assemblies Tested in the Furniture Calorimeter

Seat Assembly	Average Specific Extinction Area (m^2/kg)		
	50 kW Line Burner	50 kW Box Burner	100 kW Box Burner
F_1/C_1	320 ± 50	290 ± 60	---[a]
F_1/C_2	300 ± 280	190 ± 110	290 ± 90
F_2/C_3	310 ± 80	410 ± 130	---[a]
F_3/C_3	400 ± 480	520 ± 270	---[b]
F_4/C_3	260 ± 180	240 ± 190	320 ± 160
F_5/C_3	390 ± 230	450 ± 230	290 ± 230

[a] Not tested under this condition.
[b] Erratic results.

Table 17. Time-to-Ignition and, Where Applicable, Standard Deviation[a] for Seat Composites Tested in the Cone Calorimeter

seconds

Composite Designation	External Irradiance (kW/m²)								
	2.5	3.5	5	7.5	10	15	35	50	75
F_1/C_1	---[b]	---[b]	NI[c]	NI	83 4[a]	35 2[a]	8 5 ± 0 2	5 0 ± 0 6	2 5 ± 0 3
F_1/C_2	---[b]	---[b]	---[b]	---[b]	99 0[a]	42 5[a]	8 2 ± 0 6	4 3 ± 0 3	2 1 ± 0 3
F_1/C_2 (cover)[d]	---[b]	---[b]	---[b]	---[b]	---[b]	---[b]	8 1[a]	4 1[a]	2 2[a]
F_2/C_3	NI	462[a]	174[a]	---[b]	48 6[a]	21 8[a]	4 0 ± 1 2	2 1 ± 0 4	2 1 ± 0 3
F_3/C_3	NI	736[a]	260[a]	---[b]	50 4[a]	21 8[a]	4 1 ± 0 4	2 0 ± 0 2	1 7 ± 0 5
F_4/C_3	NI	546[a]	233[a]	---[b]	48 8[a]	---[b]	4 0 ± 0 6	2 2 ± 0 1	1 0 ± 0 1
F_5/C_3	NI	510[a]	208[a]	---[b]	49 2[a]	22 1[a]	3 8 ± 0 2	2 2 ± 0 2	1 4 ± 0 4

[a] Single value, otherwise three replicates.
[b] Not tested under this condition.
[c] No Ignition.
[d] Sample surface had a diagonal cut through the cover fabric. Foam was not visibly exposed to the external irradiance.

Table 18. Determination of Regression Slope of Time-to-Ignition vs. External Irradiance for Seat Composites Tested in the Cone Calorimeter

Composite Designation	Regression Slope
F_1/C_1	-1.72
F_1/C_2	-1.79
F_1/C_2 (cut)	-1.71
F_2/C_3	-1.99
F_3/C_3	-2.03
F_4/C_3	-2.05
F_5/C_3	-1.96

[a] Sample surface had a diagonal cut through the cover fabric. Foam was not visibly exposed to the external irradiance.

Table 19. Summary of Peak Heat Release Rates and Times between Multiple Peaks for Seat Assemblies Tested in the Cone Calorimeter

Composite Designation	External Irradiance								
	[illegible]			50 kw/m^2			[illegible] 2		
	1st Peak kW/m^2	Last Peak kW/m^2	Interval s	1st Peak kW/m^2	Last Peak kW/m^2	Interval s	1st Peak kW/m^2	Last Peak kW/m^2	Interval s
F_1/C_1	80 ± 10	00 ± 30	25	320 ± 10	50 ± 25	20	410 ± 5	00 ± 40	30
F_1/C_2[a]	80	190	55	20	20	410	30	40	20
F_1/C_2 (c t)[b]	90	20	41	240	35	35	29	50	25
F_2/C_3	30 ± 10			20 ± 5			410 ± 10		
F_3/C_3	20 ± 5			80 ± 10			90 ± 5		
F_4/C_3	20 ± 20			20 ± 5			80 ± 5		
F_5/C_3	20 ± 30			30 ± 10			0 ± 10		

[a] Single test sample included in analysis.
[b] Single sample tested.

Table 20. Expanding Average Rate of Heat Release for Seat Composites Tested in the Cone Calorimeter

Composite Designation	External Irradiance kW/m^2	Time to Peak HRR[a] s	Rate of Heat Release (kW/m^2) Average from time of ignition plus								
			6 s	12 s	180 s	24 s	3 s	3 s	6 s	9 s	
F_1/C_1	35	300 ± 25	200 ± 5	195 ± 5	185 ± 10	195 ± 15	220 ± 20	235 ± 15			
	50	250 ± 20	240 ± 15	225 ± 15	235 ± 15	270 ± 20	295 ± 5	270 ± 15			
	75	205 ± 10	305 ± 5	305 ± 10	355 ± 15	415 ± 0	360 ± 5	310 ± 5			
F_1/C_2	35	510	120 ± 25	120 ± 15	95 ± 10	75 ± 10	75	80	80	90	100
	50	430 ± 30	160 ± 5	135 ± 5	120 ± 5	110 ± 5	110 ± 0	110 ± 5	130 ± 10	145 ± 5	
	75	335 ± 40	215 ± 5	170 ± 5	155 ± 10	185 ± 25	215 ± 15				
F_1/C_2 (cut)	35[b]	440	140	135	105	90	90	95	10	10	
	50[b]	325	190	150	125	130	150	180			
	75[b]	260	255	200	190	220	265	260			
F_2/C_3	35	20 ± 5	210 ± 10	225 ± 5	215 ± 5	210 ± 5	200 ± 5	190 ± 5			
	50	15 ± 0	245 ± 10	245 ± 10	235 ± 5	225 ± 5	215 ± 5	190 ± 5			
	75	15 ± 0	320 ± 10	300 ± 10	285 ± 10	270 ± 10	230 ± 5	200 ± 5			
F_3/C_3	35	15 ± 5	165 ± 5	155 ± 0	150 ± 0	130 ± 0	110 ± 0	100			
	50	15 ± 0	210 ± 5	195 ± 5	180 ± 5	160 ± 5	160 ± 5	150 ± 5			
	75	10 ± 5	275 ± 5	245 ± 5	220 ± 5	200 ± 0	180 ± 0	170 ± 0			
F_4/C_3	35	15 ± 0	115 ± 5	65 ± 5							
	50	15 ± 0	130 ± 5	75 ± 0							
	75	10 ± 0	150 ± 5	90 ± 5							
F_5/C_3	35	15 ± 5	170 ± 10	140 ± 5	120 ± 5	115 ± 10	110 ± 10	105 ± 10			
	50	15 ± 0	200 ± 5	165 ± 5	150 ± 5	140 ± 5	130 ± 5	125 ± 5			
	75	15 ± 5	265 ± 0	215 ± 5	195 ± 10	175 ± 5	160 ± 5	150 ± 5			

[a] Heat Release Rate.
[b] Single sample tested.

Table 21. Summary of Mass Loss Rate and Effective Heat of Combustion of Seat Composites Tested in the Cone Calorimeter

Composite Description	External Irradiance kW/m^2	ΔH_{eff} MJ/kg	Avg Rate of Mass Loss $g/s\text{-}m^2$	Mass Loss Rate ($g/s\text{-}m^2$) during periods of peak rate of heat release		
				1st Peak	2nd Peak	3rd Peak
F_1/C_1	35	19.3 ± 0.6	13.0 ± 1.1	16.1 ± 0.3	13.6 ± 0.8	
	50	19.1 ± 0.5	16.3 ± 0.8	19.3 ± 1.0	16.7 ± 0.3	
	75	19.5 ± 0.4	21.4 ± 0.6	22.7 ± 0.6	23.0 ± 1.2	
F_1/C_2	35	19.4	6.0	11.7	8.7	6.1
	50	20.0 ± 0.1	8.1 ± 0.2	12.8 ± 0.6	9.0 ± 0.5	8.0 ± 0.1
	75	20.1 ± 0.8	10.7 ± 0.7	15.4 ± 0.2	11.5 ± 0.4	12.2 ± 0.5
F_1/C_2 (cut)	35[a]	21.1	7.2	10.1	7.9	7.0
	50[a]	21.0	9.1	13.3	8.7	9.9
	75[a]	20.8	11.8	17.4	12.8	14.2
F_2/C_3	35	17.3 ± 0.1	11.1 ± 0.3	17.2 ± 0.6		
	50	16.2 ± 0.3	13.4 ± 0.6	21.6 ± 0.6		
	75	16.0 ± 0.4	15.9 ± 0.7	28.4 ± 0.3		
F_3/C_3	35	11.0 ± 0.4	10.9 ± 0.6	15.1 ± 0.1		
	50	13.3 ± 1.0	11.7 ± 0.7	19.8 ± 0.4		
	75	13.8 ± 0.4	13.4 ± 0.3	25.5 ± 0.6		
F_4/C_3	35	8.9 ± 0.3	9.9 ± 0.5	10.1 ± 0.6		
	50	8.0 ± 0.3	10.8 ± 0.3	12.4 ± 0.1		
	75	7.9 ± 0.1	12.1 ± 0.4	14.4 ± 1.1		
F_5/C_3	35	13.6 ± 0.2	6.9 ± 0.3	14.2 ± 0.8		
	50	14.8 ± 0.7	7.6 ± 0.1	17.5 ± 0.3		
	75	15.1 ± 0.1	9.7 ± 0.3	21.7 ± 0.4		

[a] Single sample tested.

Table 22. Summary of Total Heat Release and Mass Loss in the Cone Calorimeter

Composite Designation	External Irradiance					
	35 kW/m²		50 kW/m²		75 kW/m²	
	THR[a] MJ/m²	Mass Loss kg/m²	THR MJ/m²	Mass Loss kg/m²	THR MJ/m²	Mass Loss kg/m²
From Ignition to Peak Heat Release Rate						
F_1/C_1	63	3.9	70	4.3	80	4.5
F_1/C_2	48	3.0	59	3.4	69	3.9
F_1/C_2 (cut)	51	2.9	54	3.0	62	3.4
F_2/C_3	3	0.3	3	0.3	4	0.3
F_3/C_3	2	0.3	3	0.3	3	0.2
F_4/C_3	2	0.2	3	0.2	2	0.1
F_5/C_3	3	0.3	3	0.2	4	0.2
From Ignition to the End of Combustion						
F_1/C_1	102	5.3	103	5.4	112	5.7
F_1/C_2	91	4.7	103	5.1	112	5.6
F_1/C_2 (cut)	106	4.9	103	5.0	107	5.2
F_2/C_3	75	4.3	73	4.9	71	4.5
F_3/C_3	35	3.2	64	4.8	67	4.8
F_4/C_3	8	0.9	9	1.2	12	1.5
F_5/C_3	57	4.2	72	4.9	75	5.0

[a] Total Heat Released.

Table 23. Average Gas Yields for Seat Composites Tested in the Cone Calorimeter

Composite Designation	Irradiance kW/m^2	Average Gas Yields CO[a] kg/kg	CO_2[a] kg/kg	CO/CO_2 -	HCl[b] kg/kg	HBr[b] kg/kg	HCN[b] kg/kg
F_1/C_1	35	0.062 ± 0.001	1.28 ± 0.06	0.048	0.026	-	0.003
	50	0.063 ± 0.004	1.26 ± 0.01	0.050	0.025	-	0.004
	75	0.060 ± 0.004	1.33 ± 0.06	0.045	0.021	-	0.003
F_1/C_2	35	0.060 ± 0.006	0.90 ± 0.21	0.067	0.049	-	0.005
	50	0.065 ± 0.001	1.25 ± 0.06	0.043	0.033	-	0.003
	75	0.066 ± 0.002	1.28 ± 0.09	0.052	0.035	-	0.003
F_2/C_3	35	0.081 ± 0.002	0.9[illegible] ± 0.01	0.084	0.049	-	0.011
	50	0.083 ± 0.001	0.9[illegible] ± 0.01	0.092	0.041	-	0.010
	75	0.069 ± 0.001	0.9[illegible] ± 0.02	0.077	0.032	-	0.012
F_3/C_3	35	0.107 ± 0.0[illegible]	0.60 ± 0.02	0.178	0.047	0.015	0.003
	50	0.133 ± 0.0[illegible]	0.70 ± 0.08	0.190	0.027	0.007	0.002
	75	0.121 ± 0.0[illegible]	0.70 ± 0.02	0.173	0.037	0.014	0.003
F_4/C_3	35	0.074 ± 0.005	0.44 ± 0.04	0.168	0.054[c]	-	-
	50	0.071 ± 0.001	0.38 ± 0.03	0.187	0.065[c]	-	-
	75	0.074 ± 0.002	0.35 ± 0.01	0.211	0.063[c]	-	-
F_5/C_3	35	0.[illegible]8 ± .0001	0.[illegible]1 ± 0.05	0.096	.0038	-	0.002
	50	0.[illegible]0 ± .0003	0.[illegible]8 ± 0.04	0.091	.0041	-	0.002
	75	0.[illegible]8 ± .0002	0.[illegible]3 ± 0.02	0.094	.0040	-	0.002

[a] Average of three specimens.
[b] Single values.
[c] Bubbling continued for 120 seconds after flame went out.

Table 24. Average Soot and Specific Extinction Area (average for times after ignition) for Seat Composites Tested in the Cone Calorimeter

Average of three specimens

Composite Designation	Irradiance kW/m2	Average Soot Yield[a] kg/kg	Specific Extinction Area m^2/kg					
			6 s	1[illegible] s	1[illegible] s	[illegible]0 s	30 s	[illegible]0 s
[illegible]$_1/C_1$	3[illegible]	0.061 ± 0.000	685 ± 10	690 ± 0	680 ± 10	685 ± 1[illegible]	640 ± 20	620 ± 1[illegible]
	5[illegible]	0.066 ± 0.001	645 ± 35	675 ± 30	665 ± 25	625 ± 2[illegible]	600 ± 15	605 ± 1[illegible]
	7[illegible]	0.057 ± 0.003	675 ± 35	690 ± 30	635 ± 25	595 ± 3[illegible]	600 ± 30	585 ± 3[illegible]
[illegible]$_1/C_2$	3[illegible]	0.122 ± 0.046	57[illegible] ± 1[illegible]	52[illegible] ± 5	46[illegible] ± 5	48[illegible] ± 70	-	-
	5[illegible]	0.049 ± 0.000	59[illegible] ± 1[illegible]	51[illegible] ± 5	44[illegible] ± 5	40[illegible] ± 5	[illegible]5 ± 0	[illegible]0 ± 10
	7[illegible]	0.049 ± 0.002	65[illegible] ± 4[illegible]	59[illegible] ± 45	57[illegible] ± 50	59[illegible] ± 55	[illegible]0 ± 20	[illegible]0 ± 40
F_1/C_2 (c[illegible])	3[illegible]	0.042[b]	620[b]	595[b]	570[b]	555[b]	53[illegible][b]	52[illegible][b]
	5[illegible]	0.043[b]	620[b]	585[b]	545[b]	530[b]	53[illegible][b]	51[illegible][b]
	7[illegible]	0.046[b]	645[b]	600[b]	585[b]	560[b]	53[illegible][b]	55[illegible][b]
F_2/C_3	3[illegible]	0.082 ± 0.000	470 ± 3[illegible]	480 ± 2[illegible]	50[illegible] ± 20	500 ± [illegible]	490 ± 20	475 ± 1[illegible]
	5[illegible]	0.101 ± 0.006	535 ± 3[illegible]	590 ± 2[illegible]	59[illegible] ± 15	570 ± [illegible]	550 ± 15	545 ± 1[illegible]
	7[illegible]	0.095 ± 0.002	575 ± 2[illegible]	605 ± 2[illegible]	58[illegible] ± 20	565 ± [illegible]	565 ± 25	570 ± 5[illegible]
[illegible]$_3$[illegible]$_3$	3[illegible]	0.088 ± 0.00[illegible]	430 ± [illegible]	41[illegible] ± 0	3[illegible] ± 5	[illegible]70 ± 5	[illegible]85 ± 0	[illegible]85[b]
	5[illegible]	0.081 ± 0.01[illegible]	525 ± 2[illegible]	52[illegible] ± 20	5[illegible] ± 1[illegible]	[illegible]70 ± 10	[illegible]55 ± 15	[illegible]40 ± 1[illegible]
	7[illegible]	0.073 ± 0.00[illegible]	580 ± 2[illegible]	59[illegible] ± 25	5[illegible] ± 1[illegible]	[illegible]50 ± 15	[illegible]35 ± 15	[illegible]30 ± 1[illegible]
$F_{[illegible]}/C_{[illegible]}$	3[illegible]	0.0[illegible]5 ± 0.011	470 ± 2[illegible]	4[illegible] ± 2	-	-	-	-
	5[illegible]	0.1[illegible]8 ± 0.007	555 ± 1[illegible]	5[illegible] ± 1	-	-	-	-
	7[illegible]	0.1[illegible]5 ± 0.001	625 ± 2[illegible]	5[illegible] ± 3	-	-	-	-
F_5[illegible]$_3$	35	0.047 ± 0.001	41[illegible] ± [illegible]	[illegible] ± 5	2[illegible]0 ± 10	270 ± 20	260 ± [illegible]	24[illegible] ± [illegible]
	50	0.048 ± 0.002	48[illegible] ± 3[illegible]	[illegible] ± [illegible]	4[illegible]0 ± 15	380 ± 10	360 ± [illegible]	35[illegible] ± [illegible]
	75	0.057 ± 0.000	52[illegible] ± [illegible]	[illegible] ± 0	5[illegible]0 ± 5	485 ± 5	465 ± [illegible]	45[illegible] ± [illegible]

[a] Average of two values.
[b] Single value.

Table 25. Material Thermal Properties of Seat Composites Based on Time-to-Ignition and External Irradiance Tested in the LIFT Apparatus

Composite Designation	Minimum Ignition Energy $q''_{o,ig}$ kW/m^2	Surface Temperature T_{ig} °C	Thermal Inertia $k\rho c$ (kW/m^2-K)^{2}s	Heat Transfer Coefficient h_e W/m^2-K	Ignition Parameter b $s^{-½}$
F_1/C_1	9.0	284	0.188	34.1	0.089
F_1/C_2	13.0	349	0.690	39.5	0.054
F_2/C_3	3.0	139	0.482	25.2	0.041
F_3/C_3	3.0	139	0,706	25.2	0.034
F_4/C_3	3.0	139	0.569	25.2	0.038
F_5/C_3	3.0	139	0.530	25.2	0.039

Table 26. Material Flame Spread Properties *for* Seat Composites Tested in the LIFT Apparatus

Composite Designation	Minimum External Irradiance For Flame Spread $q''_{o,s}$ kW/m^2	Flame Spread Correlation Factor C (m^2 s^{½})/(kW mm^{½})	Flame Beating Parameter Φ kW^2/m^3	Minimum Temperature Flame Spread °C
F_1/C_1	0.64	0.123	10.67	38
F_1/C_2	7.04	0.165	16.20	198
F_2/C_3	1.97	0.095	84.38	99
F_3/C_3	1.68	0.849	1.54	86
F_4/C_3	2.06	0.498	3.61	102
F_5/C_3	2.12	0.634	2.07	104

Table 27. Chemical and Toxicological Results from Decomposition of Seat Foam Materials[a]

Material Designation	AIT[c] °C	Initial Furnace Temp. °C	Mass/Chamber Vol. Loaded mg/ℓ	Mass/Chamber Vol. Consumed mg/ℓ	Time-Weighted Average Gas Concentrations[b] CO ppm	CO_2 %	O_2 %	HCN GC[d] ppm	HCN IC[e] ppm	HCl ppm	HBr ppm	N-Gas Prediction[f] WE[g]	N-Gas Prediction[f] WE + PE[h]	No. Died/No. Tested WE	No. Died/No. Tested WE + PE	Latest Day of Death
F_1	475	449	20.0	18.3	650	1.8	18.6	35	NM[i]	ND[j]	ND[k]	0.5	0.6	NM	NM	-
		448	40.0	36.8	1260	3.9	15.9	65	NM	ND	ND	1.0	1.2	NM	NM	-
		449	40.0	36.9	1120	4.0	15.9	65	NM	NM	NM	1.0	1.2	1/6	1/6	-
		449	42.0	38.6	1270	4.2	15.6	60	NM	NM	NM	1.0	1.2	0/6	0/6	-
		450	45.0	41.3	1470	4.2	15.5	65	NM	NM	NM	1.1	1.3	0/6	0/6	-
F_2	475	502	10.0	9.1	250	1.1	19.6	170	NM	NM	NM	1.2	1.7	2/6	3/6	1
		502	20.0	18.4	480	1.5	18.9	295	NM	NM	NM	2.1	2.9	NM	NM	-
		502	40.0	37.2	1160	2.9	17.0	645	NM	NM	NM	4.5	6.4	NM	NM	-
F_3	475	499	20.0	13.1	2040	0.6	20.0	55	60	35	30	0.7	0.9	NM	NM	-
		500	21.0	13.4	2130	0.7	20.0	55	50	35	50	0.8	0.9	0/6	2/6	6
		501	26.0	17.4	2150	1.1	19.4	55	60	10	15	0.8	0.9	0/6	0/6	-
		498	30.0	19.4	3140	0.9	19.6	70	85	10	30	1.0	1.2	0/6	2/6	13
		500	40.0	26.6	4100	1.4	19.0	80	125	10	50	1.3	1.6	6/6	6/6	-
		501	40.0	NM	4650	1.1	19.3	85	120	25	45	1.7	2.1	NM	NM	-
F_4	475	774	20.0	10.6	750	0.7	20.1	10	NM	NM	NM	0.3	0.3	NM	NM	-
		776	40.0	20.5	1550	1.3	19.3	35	NM	NM	NM	0.6	0.7	NM	NM	-
		776	40.0	21.3	1750	1.5	19.0	20	35	35	ND	0.6	0.6	0/6	0/6	-
		773	80.0	42.4	2950	2.5	17.8	45	50	25	ND	1.0	1.2	1/6	1/6	-
		774	85.0	45.6	3230	2.6	17.5	60	NM	NM	NM	1.2	NM	5/6	5/6	-
F_5	475	598	20.0	13.5	1030	1.0	19.7	55	70	5	ND	0.6	0.8	NM	NM	-
		600	28.0	18.8	1620	1.5	19.0	90	100	10	ND	1.0	1.2	0/6	1/6	0
		602	33.0	22.2	1690	1.6	19.0	100	105	15	ND	1.1	1.4	1/6	2/6	1
		600	40.0	27.0	2590	1.7	18.6	170	145	10	ND	1.7	2.0	NM	NM	-

[a] Materials decomposed in flaming mode; spark used to initiate ignition.
[b] Average gas concentrations over 30 minute exposure.
[c] Auto-ignition temperature.
[d] By gas chromatographic technique.
[e] By ion chromatographic technique.
[f] N-Gas prediction value based on equations (1) and (2).
[g] Within-exposure.
[h] Within-exposure + post-exposure.
[i] Not measured.
[j] Not detected, < 25 ppm.
[k] Not detected, < 1.0 ppb.

Table 28. Chemical and Toxicological Results from Decomposition of Seat Cover Materials[a]

Material Designation	AIT[c] °C	Initial Furnace Temp. °C	Mass/Chamber Vol. Loaded mg/ℓ	Mass/Chamber Vol. Consumed mg/ℓ	Average Gas Concentrations[b] CO ppm	CO_2 %	O_2 %	HCN GC[d] ppm	HCN IC[e] ppm	HCl ppm	HBr ppm	N-Gas Prediction[f] WE[g]	N-Gas Prediction[f] WE + PE[h]	No. Died/No. Tested WE	No. Died/No. Tested WE + PE	Latest Day of Death
C_1	500	524	19.9	16.5	1390	1.2	19.5	NM[i]	ND[j]	110	ND_k	0.3	0.4	NM	NM	-
		524	39.9	26.8	2960	2.2	18.2	2	ND	240	ND	0.7	0.8	NM	NM	-
		523	55.9	46.2	4130	3.2	16.9	2	ND	250	ND	1.1	1.2	3/6	5/6	1
C_2	50	526	19.8	15.9	2380	1.1	19.4	65	90	305	ND	0.9	1.2	NM	NM	-
		525	22.1	17.6	2590	1.3	19.1	65	80	275	ND	1.0	1.2	0/6	0/6	-
		523	25.1	19.8	2930	1.5	18.9	75	95	120	ND	1.1	1.4	2/6	2/6	-
		525	39.9	31.6	4730	1.8	18.4	105	50	355	ND	1.7	2.1	NM	NM	-
C_3	425	449[l]	10.1	8.0	570	0.5	20.3	NM	ND	160	ND	0.1	0.2	0/6	0/6	-
		451[l]	19.8	14.9	910	0.8	19.9	NM	ND	205	ND	0.2	0.3	0/6	0/6	-
		450[l]	19.9	17.6	710	0.5	20.3	NM	ND	185	ND	0.2	0.2	NM	NM	-
		450	30.1	23.7	2050	1.4	19.2	NM	5	325	ND	0.5	0.6	0/6	2/6	1
		453	34.9	27.8	2370	1.6	18.9	NM	10	200	ND	0.6	0.6	0/6	4/6	1
		453[m]	39.8	32.5	2110	0.9	19.6	ND	ND	1070	ND	0.4	0.7	NM	NM	-
		452	39.9	29.6	2400	1.5	19.0	NM	ND	330	ND	0.5	0.6	0/6	3/6	1
		452[l]	40.0	33.0	1120	1.1	19.6	NM	ND	620	ND	0.3	0.5	0/6	6/6	4
		451	40.2	30.5	2580	1.5	19.0	NM	ND	300	ND	0.6	0.7	1/6	5/6	3
		450	55.0	44.2	3290	2.2	18.0	5	5	525	ND	0.8	0.9	1/6	6/6	1
		452[l]	59.9	48.6	2430	1.5	18.9	NM	ND	655	ND	0.6	0.7	2/6	6/6	0
		448	60.2	47.4	3660	2.3	17.9	NM	10	1130	ND	0.9	1.2	0/6	6/6	1
		453	60.9	49.6	4030	2.5	17.6	NM	10	610	ND	1.0	1.2	1/6	6/6	0
		448	61.8	48.9	3750	2.5	17.5	NM	10	815	ND	0.9	1.2	1/6	6/6	0
		449	65.0	54.1	4740	2.9	17.0	NM	5	490	ND	1.2	1.3	6/6	6/6	0
		448	70.1	56.4	5160	2.9	17.1	NM	10	660	ND	1.3	1.5	6/6	6/6	0
		449	80.0	59.6	NM	NM	NM	NM	15	1200	ND	NM	NM	6/6	6/6	0

[a] Materials decomposed in flaming mode; spark used to initiate ignition.
[b] Average gas concentrations over 30 minute exposure.
[c] Auto-ignition temperature.
[d] By gas chromatographic technique.
[e] By ion chromatographic technique.
[f] N-Gas prediction based on equations (1) and (2).
[g] Within-exposure.
[h] Within-exposure + post-exposure.
[i] Not measured.
[j] Not detected, < 1.0 ppb.
[k] Not detected, < 0.1 ppm.
[l] Ethanol used to initiate ignition.
[m] Spontaneous ignition.

Table 29. Predicted, Approximate, and Determined LC_{50} Values

Material Designation	Predicted[a] LC_{50}, mg/l		Approximate[b] LC_{50}, mg/l		Determined[c] LC_{50}, mg/l	
	WE[d]	WE + PE[e]	WE	WE + PE	WE	WE + PE
F_1	40	40	>45	>45	ND[f]	ND
F_2	10	8	10	10	ND	ND
F_3	26-30	21-24	30-40	21-30	ND	ND
F_4	76-88	65-80	80-85	80-85	ND	ND
F_5	26-37	22-29	33	33	ND	ND
C_1	61-67	56-61	56	56	ND	ND
C_2	24-26	19-21	25	25	ND	ND
C_3	100-140	60-100	60	<60	65 (62-68)[g]	35 (30-40)[g]

[a] Predicted LC_{50} values from N-Gas values of analytical experiments without animals.
[b] Approximate LC_{50} values from animal experiments conducted at predicted LC_{50} values.
[c] Determined LC_{50} values from statistical analysis of animal tests [33].
[d] Within-exposure.
[e] Within- + post-exposure.
[f] Not determined.
[g] 95 percent confidence limits.

Table 30. Gas Yields of CO, CO_2, HCN, HCl, and HBr in the NBS Toxicity Test Method

Material Designation	Gas Yields (kg/kg)				
	CO	CO_2	HCN x 10^{-3}	HCl x 10^{-3}	HBr x 10^{-3}
F_1	0.04	2.0	2.1	--[a]	--[a]
F_2	0.03	2.0	21	--[a]	--[a]
F_3	0.19	1.1	5.0	2.0	7.2
F_4	0.09	1.4	1.6	1.8	--[a]
F_5	0.11	1.5	6.5	0.78	--[a]
C_1	0.12	1.6	0.07	11	--[a]
C_2	0.19	1.5	5.9	21	--[a]
C_3	0.09	1.0	0.21	22	--[a]

[a] Not detected.

Table 31. Gas Yields (kg/kg) of CO and CO_2 for the Full-Scale, Large-Scale, Cone Calorimeter, and NBS Toxicity Test Method

Seat Assembly	Seat Assembly Tests				Composite Designation	Cone Calorimeter		Material Designation	NBS Toxicity Test Method	
	Full-Scale		Large-Scale							
	CO	CO_2	CO	CO_2		CO	CO_2		CO	CO_2
F_1/C_1	0.10	1.9	0.05	1.5	F_1/C_1	0.05	1.3	F1	0.4	2.0
F_1/C_2	0.04	2.5	0.1	1.6	F_1/C_2	0.07	1.2	F2	0.5	2.0
F_2/C_3	0.08	1.9	0.1	1.0	F_2/C_3	0.8	0.9	F3	0.9	1.1
F_3/C_3	0.1	2.0	0.13	1.3	F_3/C_3	0.12	0.7	F4	0.8	1.4
F_4/C_3	0.10	3.0	0.20	0.2	F_4/C_3	0.07	0.4	F5	0.1	1.5
F_5/C_3	0.1	2.9	0.3	0.5	F_5/C_3	0.08	0.8	C_1	0.1	1.6
								C2	0.19	1.5
								C3	0.8	1.0

Table 32. CO/CO_2 Yield Ratios for the Full-Scale, Large-Scale, Cone Calorimeter, and NBS Toxicity Test Method

Seat Assembly	Seat Assembly Tests		Composite Designation	Cone Calorimeter	Material Designation	NBS Toxicity Test Method
	Full-Scale CO/CO_2	Large-Scale CO/CO_2		CO/CO_2		CO/CO_2
F_1/C_1	0 [illegible]	0 [illegible]9	F_1/C_1	0 0[illegible]6	F_1	0 [illegible]
F_1/C_2	0 0[illegible]5	0 [illegible]8	F_1/C_2	0 [illegible]8	F_2	0 0[illegible]
F_2/C_3	0 [illegible]2	0 [illegible]1	F_2/C_3	0 [illegible]9	F_3	0 13
F_3/C_3	0 0[illegible]5	0 [illegible]0	F_3/C_3	0 [illegible]1	F_4	0.0[illegible]4
F_4/C_3	0 [illegible]3	1 0	F_4/C_3	0 [illegible]5	F_5	0 0[illegible]
F_5/C_3	0 [illegible]9	0 [illegible]6	F_5/C_3	0 [illegible]0	C_1	0 0[illegible]
					C_2	0 12[illegible]
					C_3	0 [illegible]0

Table 33. Gas Yields (kg/kg) of HCN, HCl, and HBr for the Full-Scale, Cone Calorimeter, and NBS Toxicity Test Method

Seat Assembly	Full-Scale			Composite Designation	Cone Calorimeter			Material Designation	NBS Toxicity Test Method		
	HN x 1[illegible]-3	HCl x 10^{-2}	HBr = 10^{-2}		HCN x 10^{-3}	HCl x 10^{-2}	HBr x 10^{-2}		HCN x 10^{-3}	HCl x 10^{-3}	HBr x 10^{-3}
F_1/C_1	8 3	0 18	[illegible]-a	F_1/C_1	[illegible]3.0	2.0	-a	F_1	2 1	-a	-a
F_1/C_2	[illegible].2	[illegible] z	-a	F_1/C_2	[illegible]3	4.0	- a	F_2	[illegible]1	-a	- 4
F_2/C_3	[illegible].9	1 4	- a	F_2/C_3	1.0	4.0	-4	F_3	5 0	2.0	7.2
F_3/C_3	1 8	[illegible] [illegible]	1 3	F_3/C_3	3.0	4.0	1.0	F_4	1.6	1.8	- a
F_4/C_3	-a	[illegible] [illegible]	-a	F_4/C_3	- a	6.0	-a	F_5	6 5	0 8	- 6
F_5/C_3	0 16	2 4	- a	F_5/C_3	[illegible].0	4.0	- a	C_2	0 0	1	- a
								[illegible]	5.9	[illegible]1	-a
								C_3	0.21	2	- 6

[a] Not detected.

Table 34. Determination of an Effective LC_{50}(m) for Each Seat Assembly

Composite Designation	Fraction		LC_{50}		Effective LC_{50}(m)
	Fabric	Foam	Fabric	Foam	
F_1/C_1	0.25	0.75	56	>45	48
F_1/C_2	0.23	0.77	25	>45	40
F_2/C_3	0.20	0.80	65	10	22
F_3/C_3	0.30	0.70	65	30	40
F_4/C_3	0.13	0.87	65	80	78
F_5/C_3	0.19	0.81	65	33	39

Table 35. Upper and Lower Canpartmont Temperatures for Several Ignition Sources as Calculated by the HAZARD I Method for an Exposure Fire of 500 s in Duration

Strength of Ignition Source kW	Upper Layer Time to 600°C s	Lower Layer Temperature °C	Time to Incaoacitatiog Upper s	Time to Incaoacitatiog Lower s	Time to Lethality Upper s	Time to Lethality Lower s	Maximum Temperature at 500 s Upper °C	Maximum Temperature at 500 s Lower °C
100	---[a]	---	<5	---	<5	---	158	35
250	---[a]	---	<5	500	<5	---	310	60
500	---[a]	---	<<5	450	<<5	---	350	60
1000	400	110	<<5	70	<<5	240	615	125

[a] Did not reach 600°C.

Table 36. Results for Tenability Criteria from Full-Scale Tests

Seat Assembly	Time to Incaoacitation (s) Temperature	Time to Incaoacitation (s) Irradiance	Time to Incaoacitation (s) FED[a]	Time to Death (s) Temperature	Time to Death (s) Irradiance	Time to Death (s) FED[a]
F_1/C_1	167	237	367	167	---[b]	427
F_1/C_2	---[b]	---[b]	---[b]	---[b]	---[b]	---[b]
F_2/C_3	117	---[b]	---[b]	117	---[b]	---[b]
F_3/C_3	147	---[b]	---[b]	147	---[b]	---[b]
F_4/C_3	---[b]	---[b]	---[b]	---[b]	---[b]	---[b]
F_5/C_3	---[b]	---[b]	---[b]	---[b]	---[b]	---[b]

[a] Fractional Effective Dose.
[b] Did not exceed tonability Limits.

Table 37. Tenability[a] Limits Used in HAZARD I

Cause	Symbol used in HAZARD I	Incapacitation Level	Lethal Level
Temperature (from HAZARD Beta test)	TEMP1	65°C	100°C
Temperature (FED[b] due to convective heat)	TEMP2	1	NA[c]
Heat Flux (irradiance)	FLUX	NV[d]	NA
Toxic Gases (FED due to CO, CO_2, HCN, & O_2, from HAZARD Beta test)	FED1	0.5	1
Toxic Gases (FED-Purser's model due to CO, CO_2, HCN, & O_2,)	FED2	1	NA
Toxic Gases (Concentration-Time product)	CT	450 g-min/m^3	900 g-min/m^3

[a] Default tenability limits from reference [2].
[b] Fractional Effective Dose.
[c] Not Applicable.
[d] No single value because incapacitation due to heat flux depends on exposure history.

Table 38. Minimum Fire to Reach Specific Tenability Limits'

Fire Duration (s)	Steady Heat Release Rate (kW)	Incapacitation due to:	Lethality due to:
300	49	FLUX	-
300	347	TEMP1	-
300	568	TEMP2	-
300	568	-	TEMPl
1000	11	FLUX	-
1000	323	TEMP1	
1000	548		TEMPl
1000	560	TEMP2	

a) Calculations were made with the heat of combustion of 21 MJ/kg.

Table 39. Estimated $LC_{,,}$ of Combustion Gases that Would Cause Incapacitation

		Heat of Combustion of 21 MJ/kg		Heat of Combustion of 8 MJ/kg	
Fire Duration (s)	Peak Heat Release Rate (kW)	Ct[a] g-min/ℓ	LC_{50} to Reach Incapacitation[b] g/ℓ	Ct g-min/ℓ	LC_{50} to Reach Incapacitation g/ℓ
300	49	3	0.3	6	0.6
300	347	10	1	30	3
300	568	20	2	50	5
1000	11	2	0.2	5	0.5
1000	323	30	3	70	7
1000	548	50	5	100	10
1000	560	60	6	200	20

a) The concentration-time integrals, Ct, were calculated by HAZARD I.
b) This is 1/3 of the Lethal $LC_{,,}$.

Table 40. Fire Performance Ranking[a] of Materials Based on Results of Small- and Large-Scale Tests and Tenability Ranking Based on Full-scale Test Results

Composite Designation	Cone Calorimeter[b] Peak HRR[d]	LIFT[b] $q_{o,s}$	NBS Toxicity Test Method[c] LC_{50}[e]	Large-Scale[b] Peak HRR[g]	Full-Scale[b] Tenability[h]
F_1/C_1	4	6	2/2[f]	6[i]	4
F_1/C_2	1	1	2/3	2	1
F_2/C_3	3	4	5/1	5[i]	2
F_3/C_3	2	5	3/1	1	3
F_4/C_3	2	3	1/1	3	1
F_5/C_3	2	2	4/1	4	1

[a] Best performance represented by 1.
[b] Rank order based on total of 6 samples.
[c] Rank order based on total of 8 samples.
[d] Peak heat release rate at 35 kW/m^2 external irradiance.
[e] Based on within exposure $LC_{,,}$.
[f] Represents rank order of foam/cover.
[g] Peak heat release rate at 100 kW exposure.
[h] Based on full scale test results for first parameter to become untenable.
[i] Extrapolated from 50 kW results.

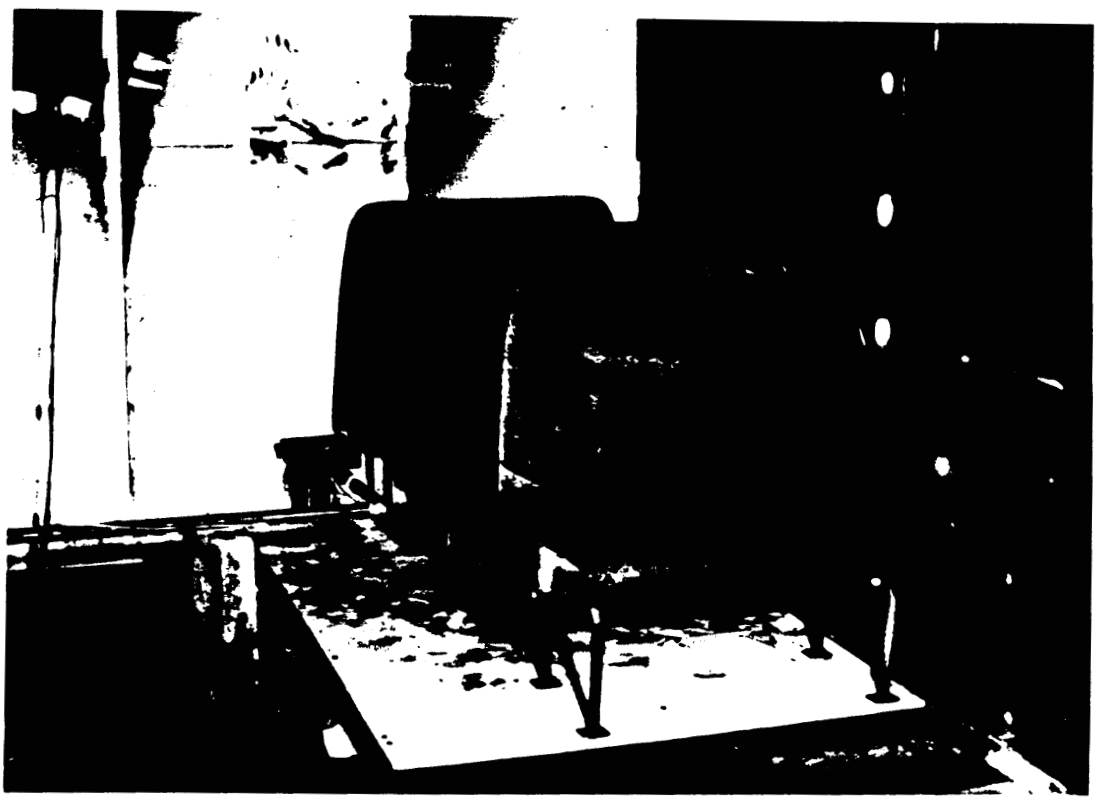

Figure 1. Photograph showing location of the three test seat assemblies and ignition burner

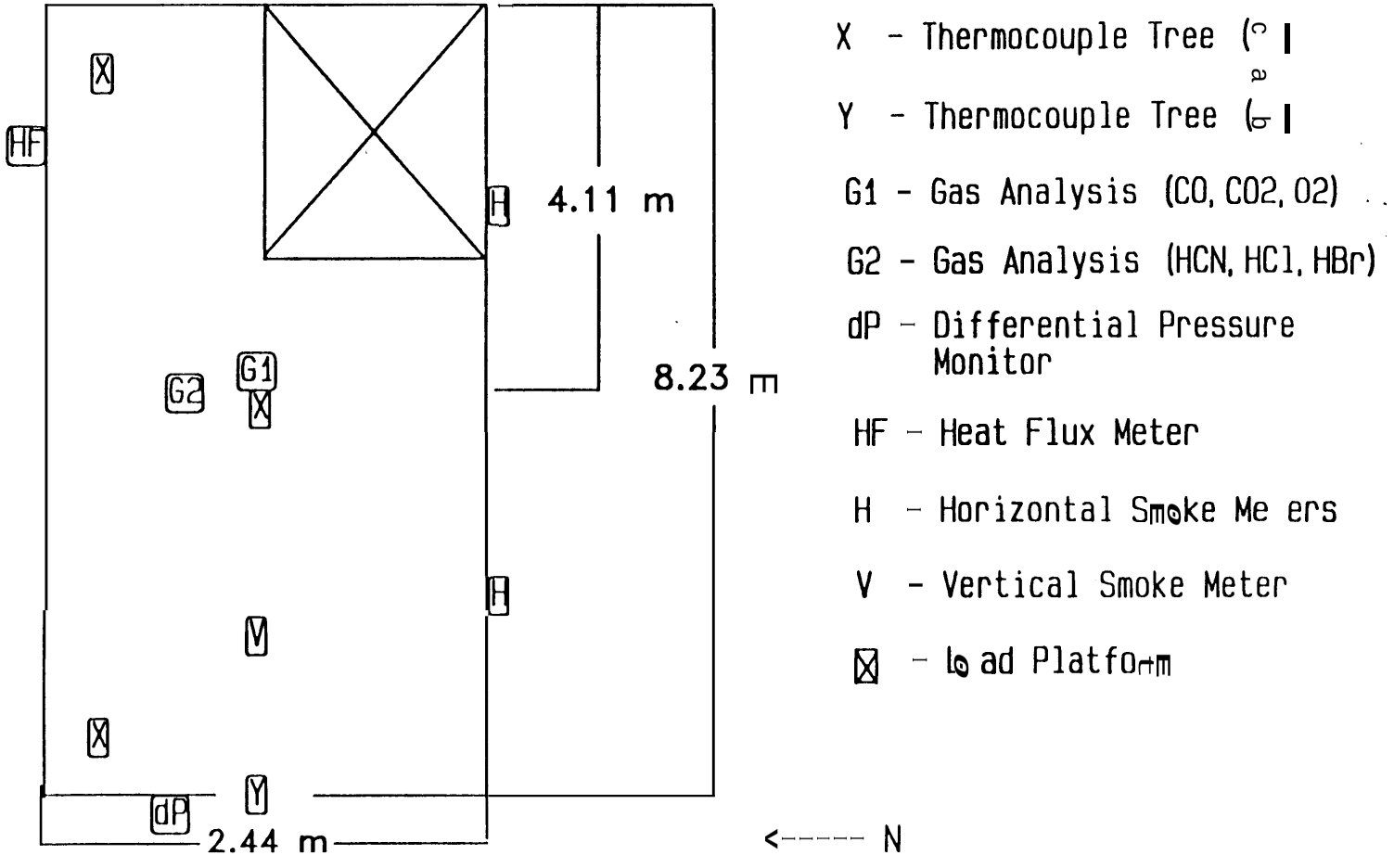

Figure 2. Schematic showing the floor plan of the bus simulation and instrument placement

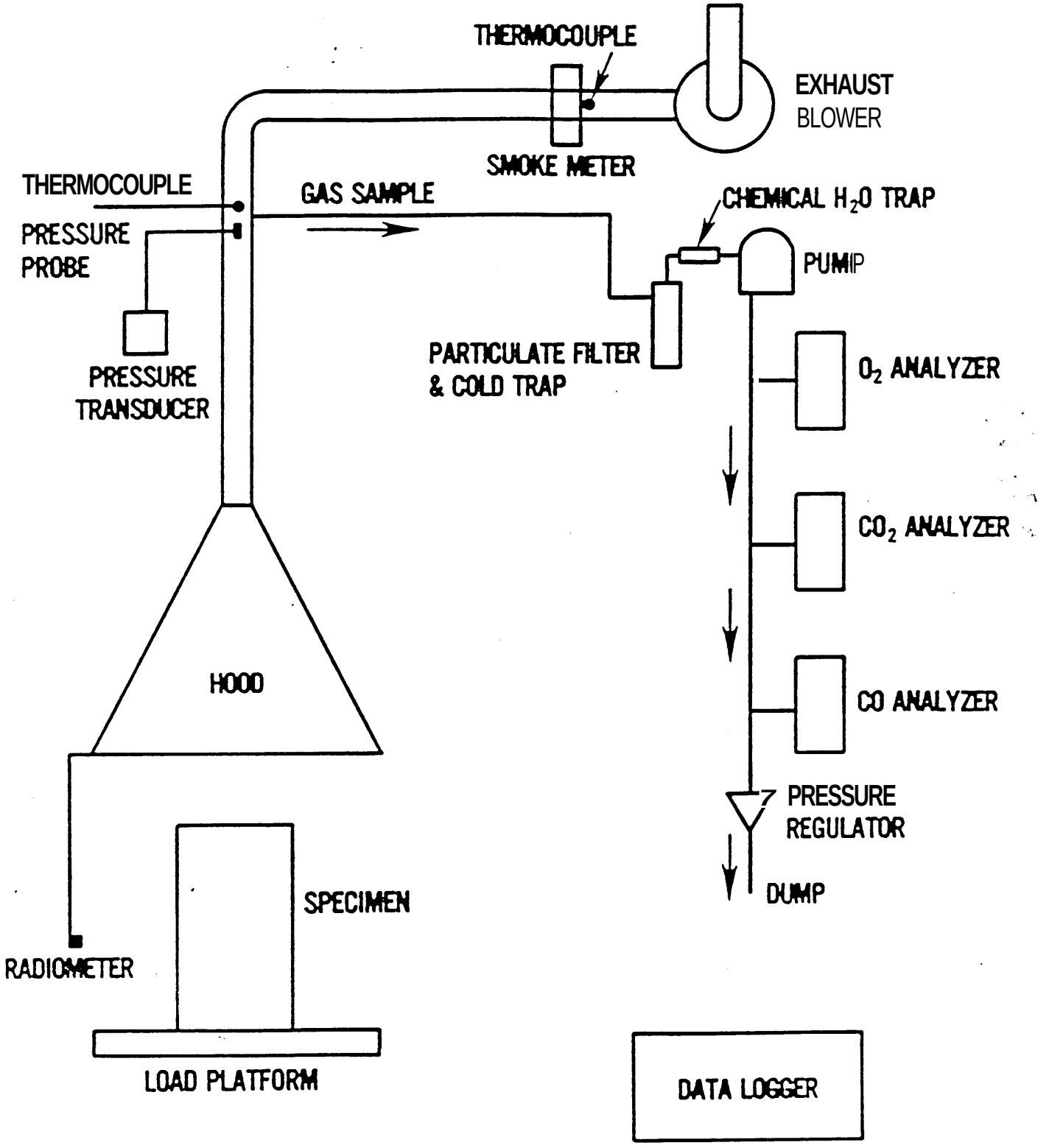

Figure 3. Furniture calorimeter, schematic of flow and instrumentation

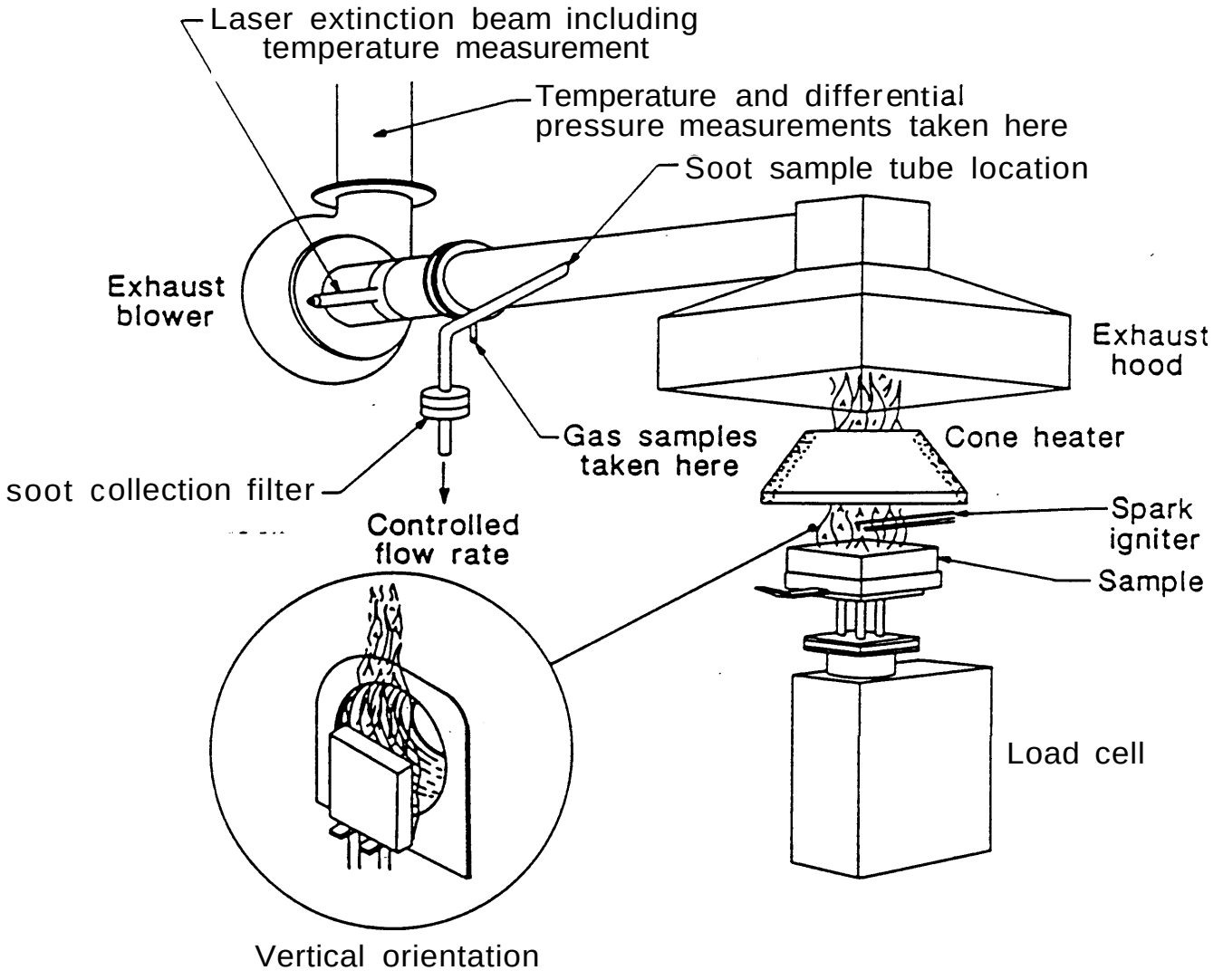

Figure 4. Schematic representation of cone calorimeter

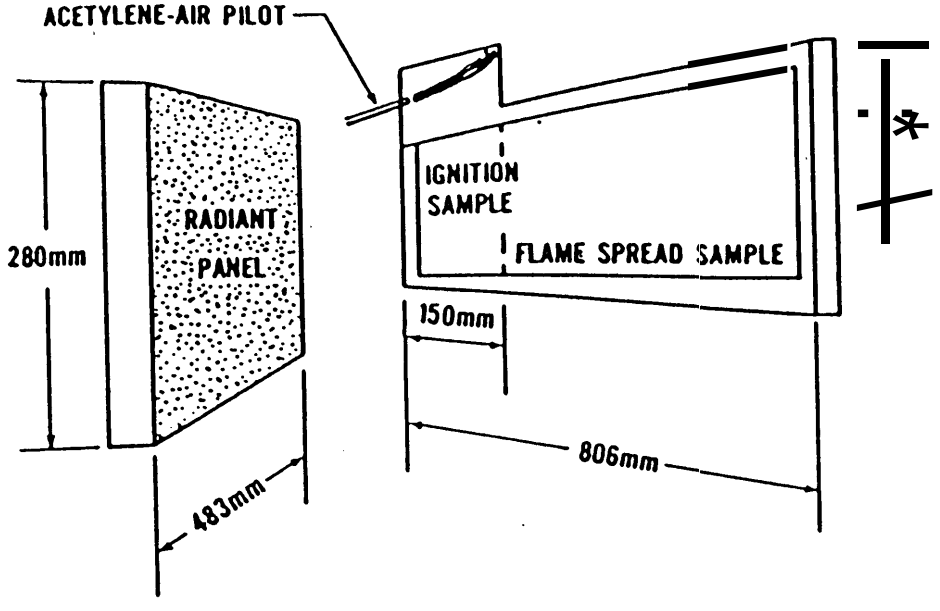

Figure 5. Schematic of ignition and flame spread apparatus (LIFT)

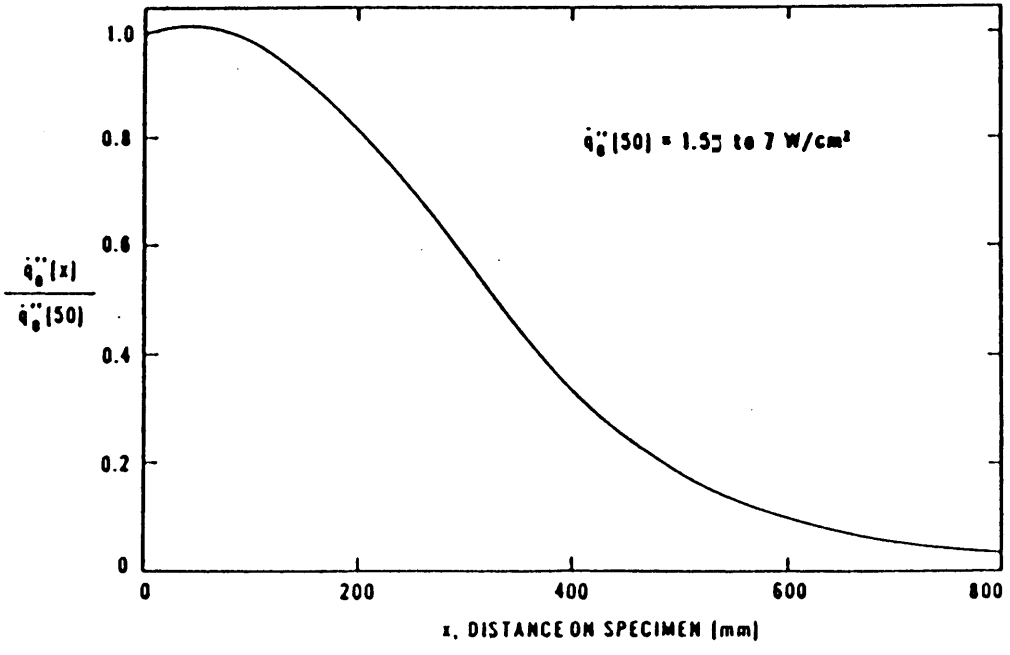

Figure 6. Normalized irradiance over the specimen

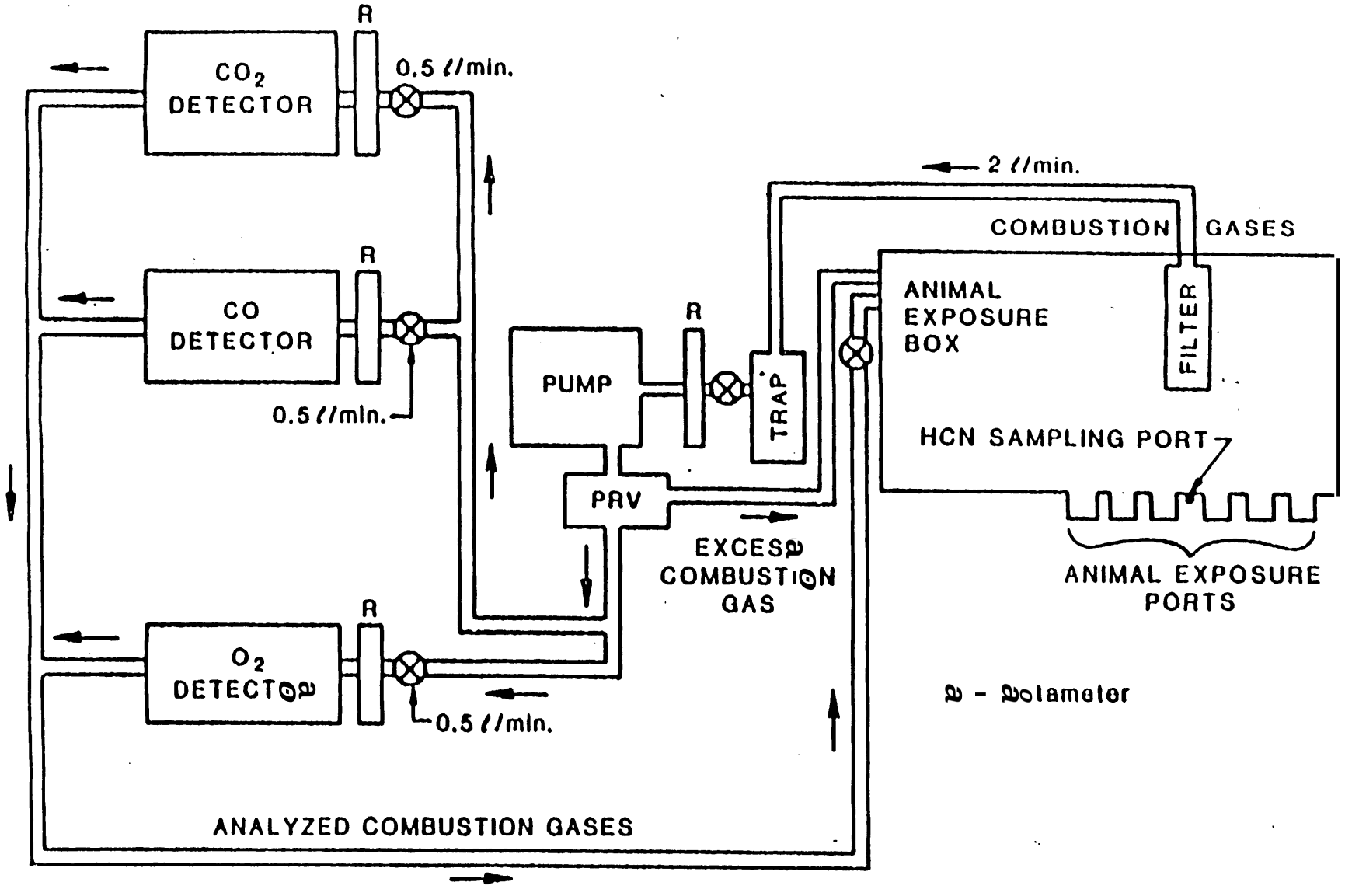

Figure 7. Schematic of NBS animal exposure and gas analysis system

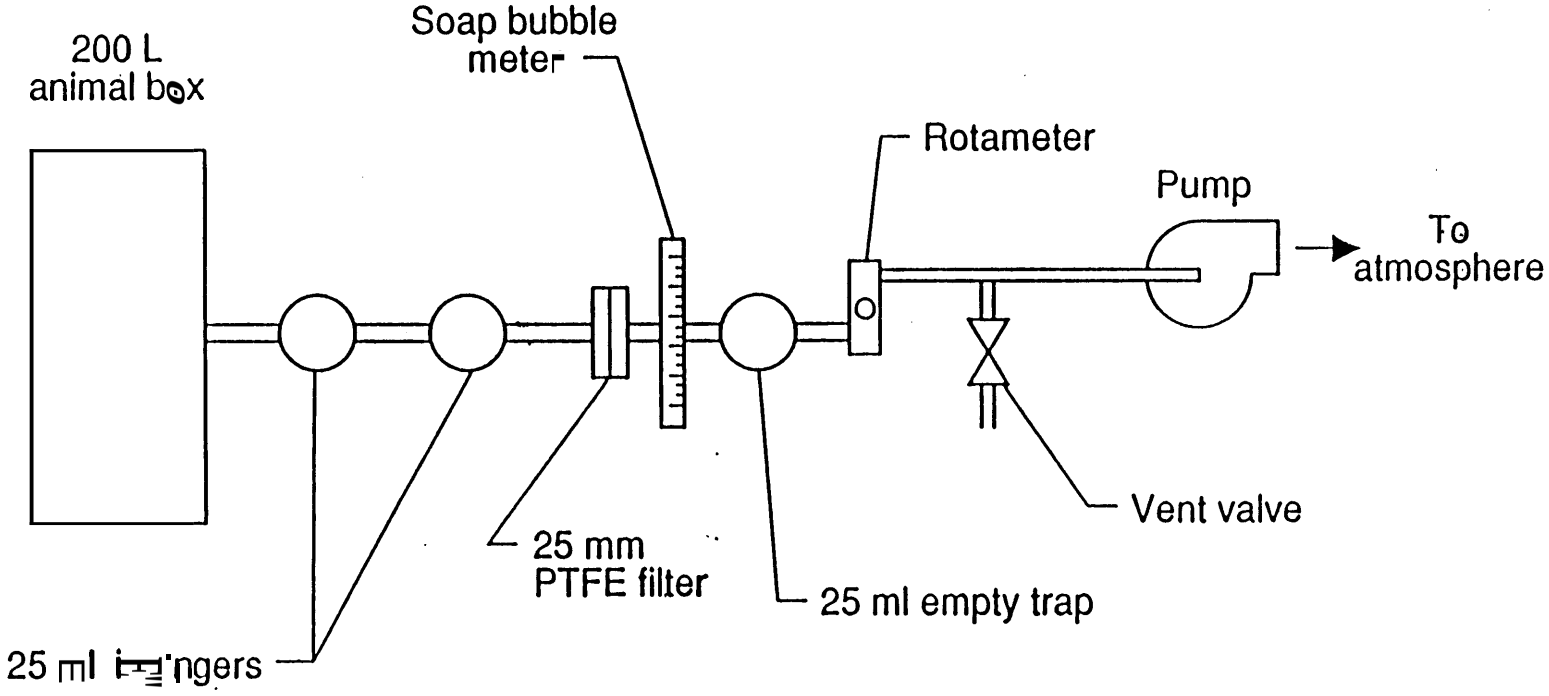

Figure 8 Impinger gas sampling in the small-scale toxicity test

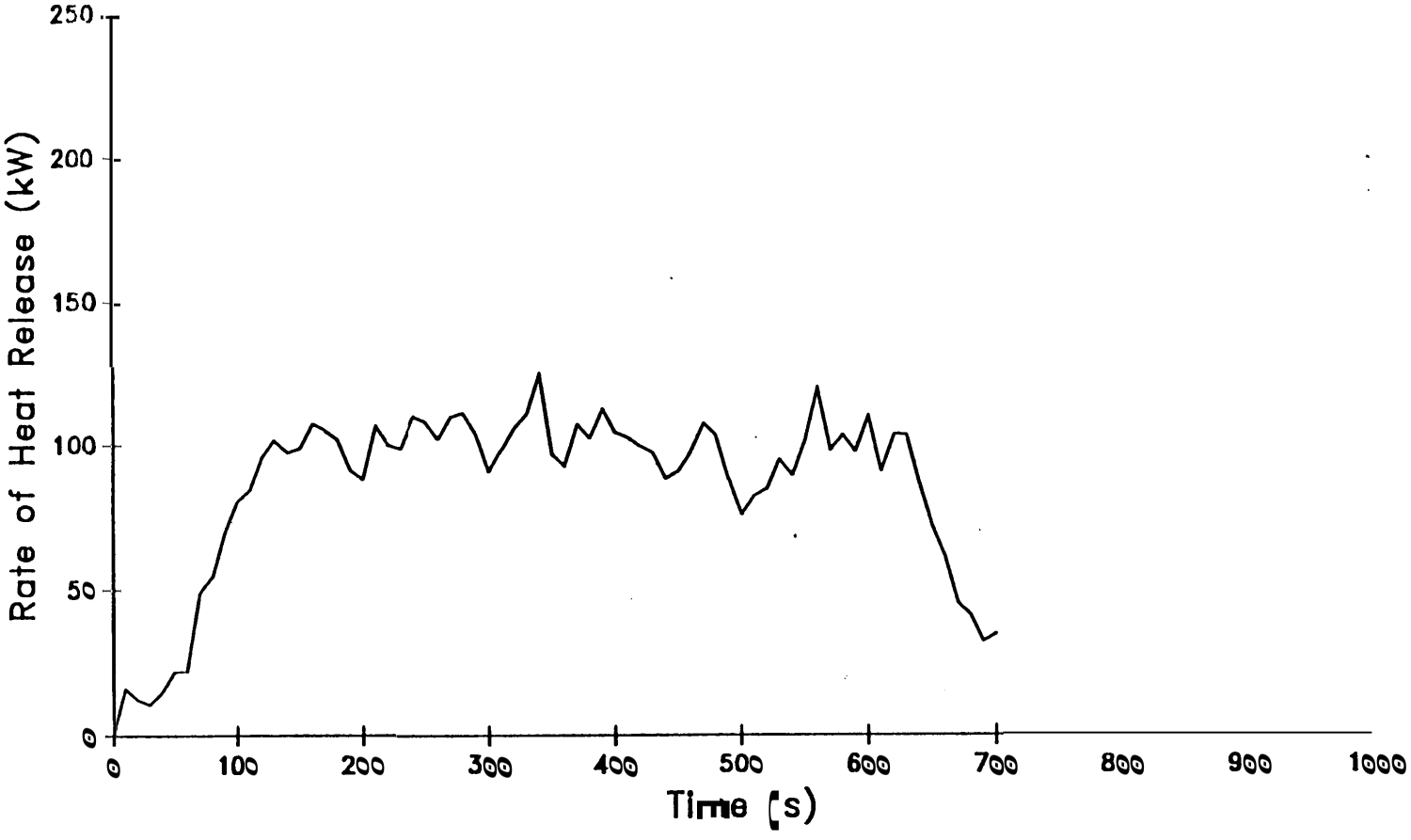

Figure 9. Actual rate of heat release from the ignition burner set at 100 kW in the bus simulation

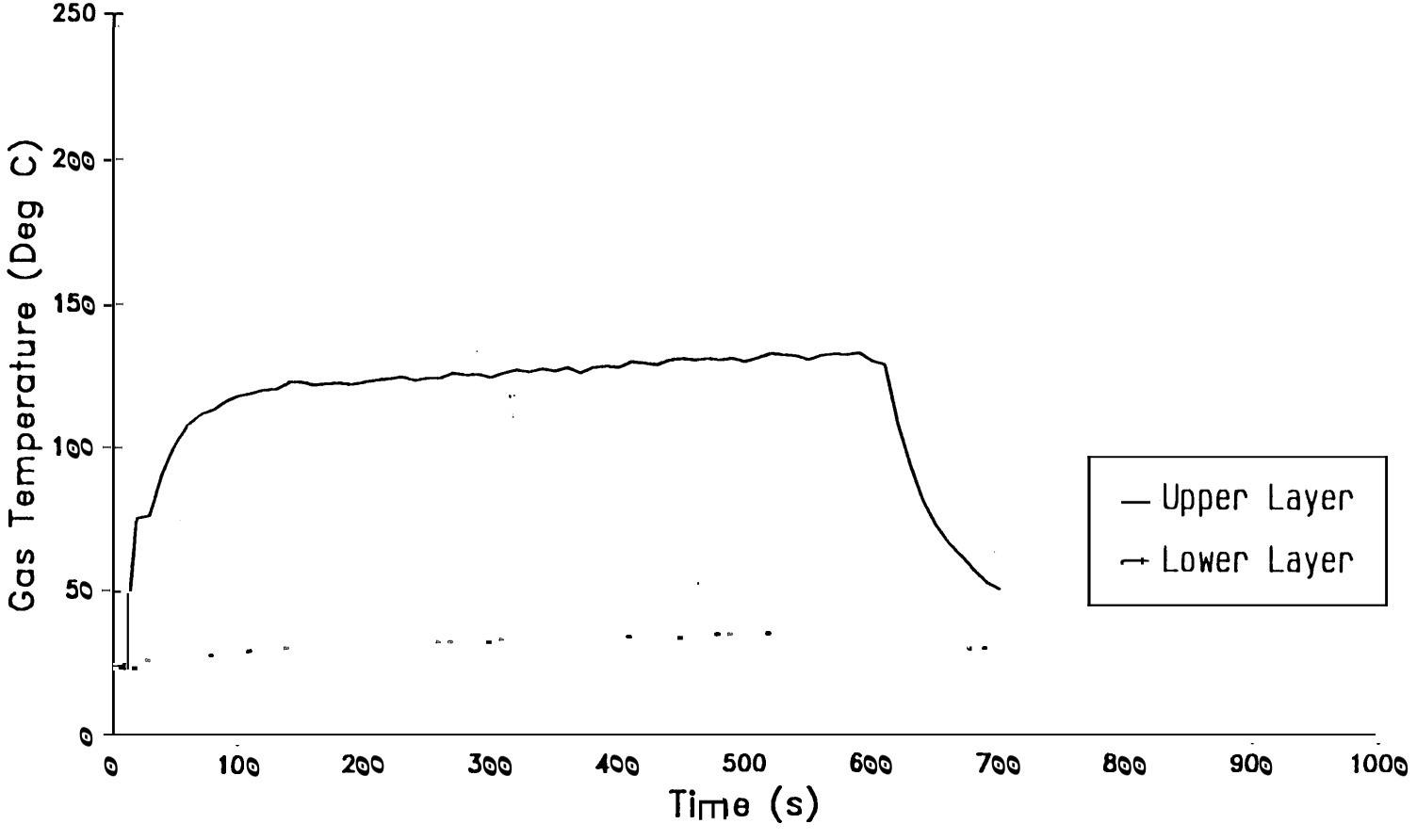

Figure 10. Gas temperatures of the upper and lower layers in the bus simulation caused by the 100 kW ignition burner

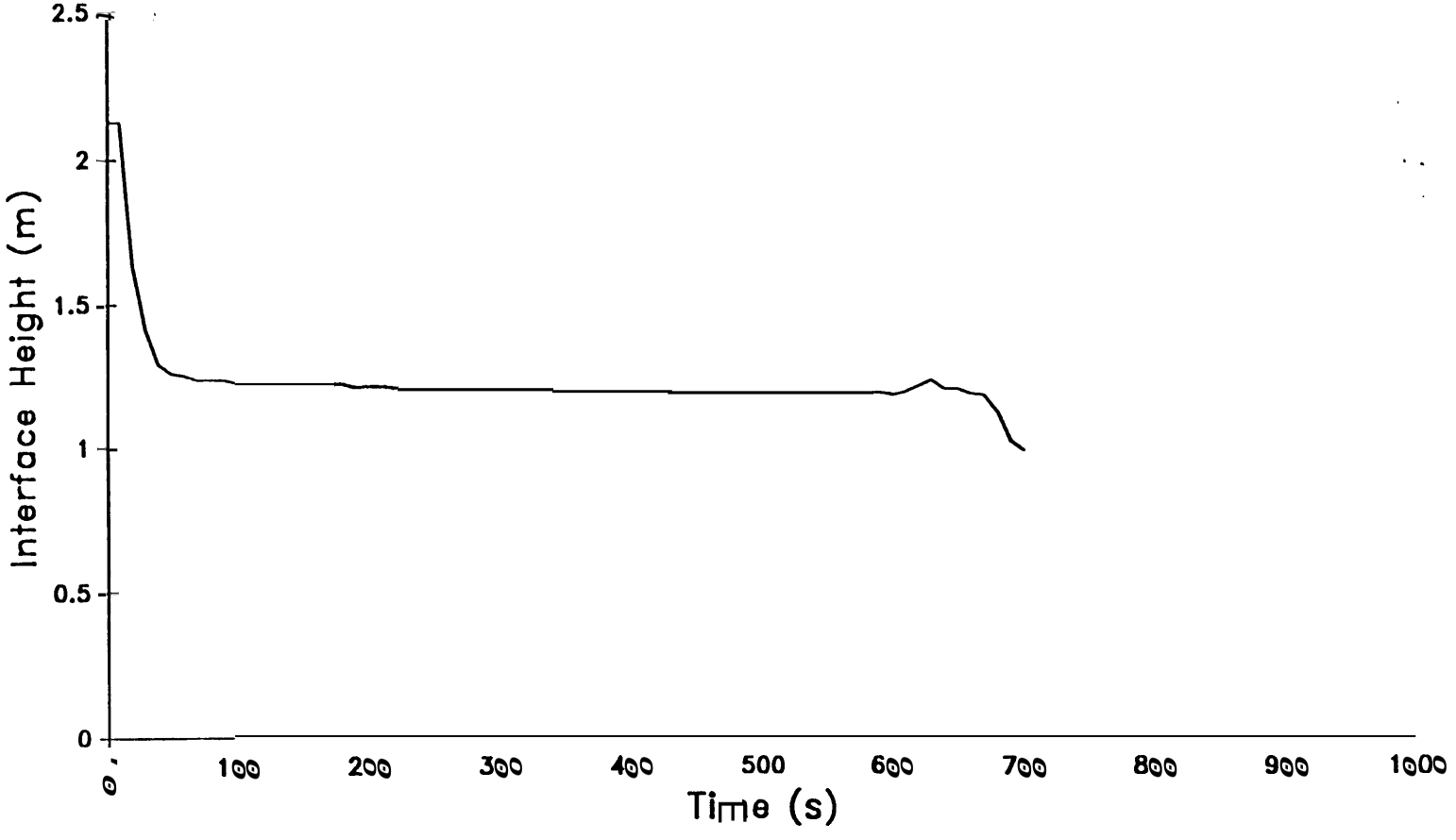

Figure 11. Interface height resulting from the 100 kW ignition burner in the bus simulation

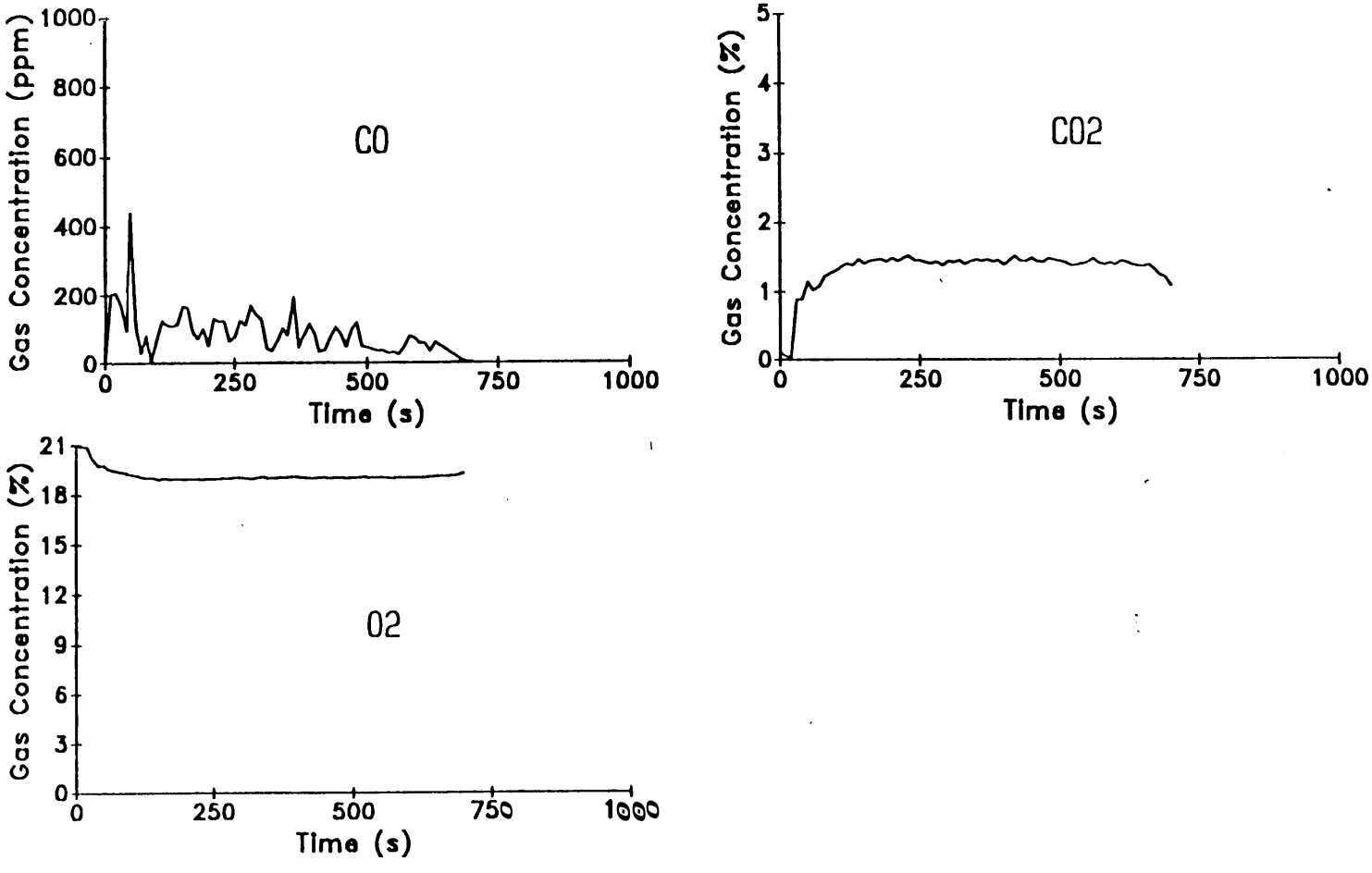

Figure 12. CO, CO_2, and O_2 gas concentrations in the upper layer of the bus simulation caused by the 100 kW ignition burner

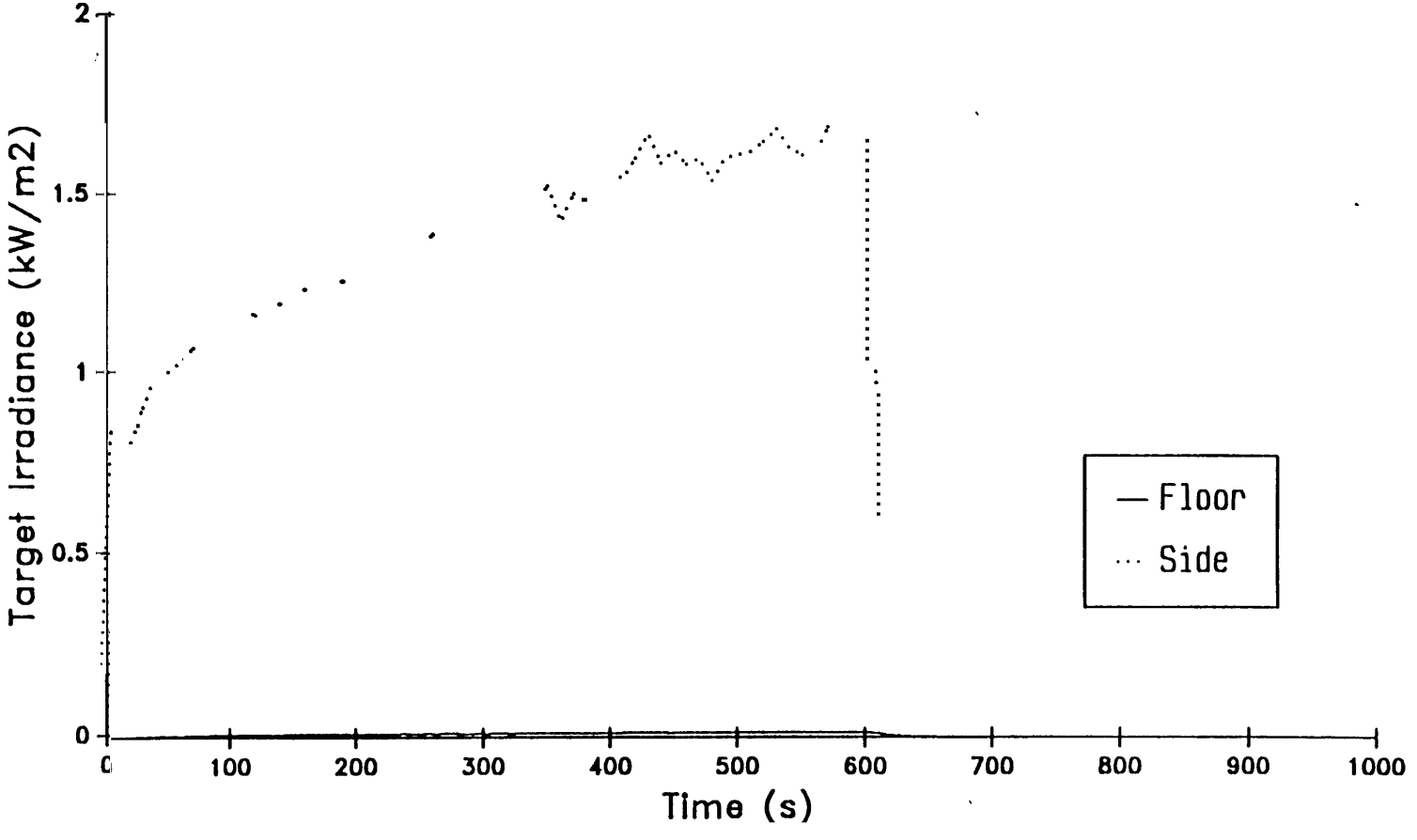

Figure 13. Irradiance levels calculated at the floor and measured at the side wall targets caused by the 100 kW ignition burner in the bus simulation

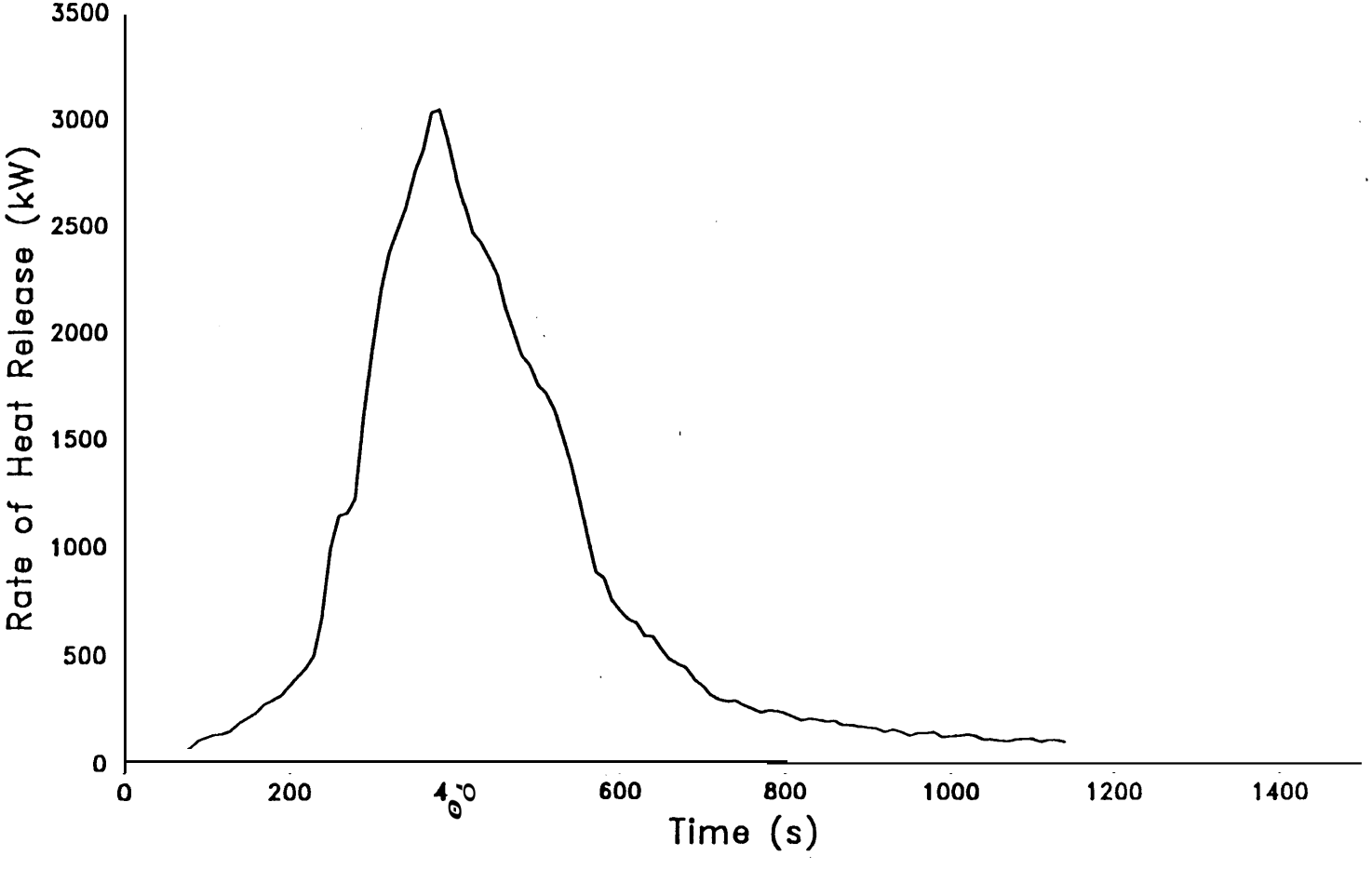

Figure 14 Rate of heat release for seat assembly F_1/C_1 tested in the bus simulation

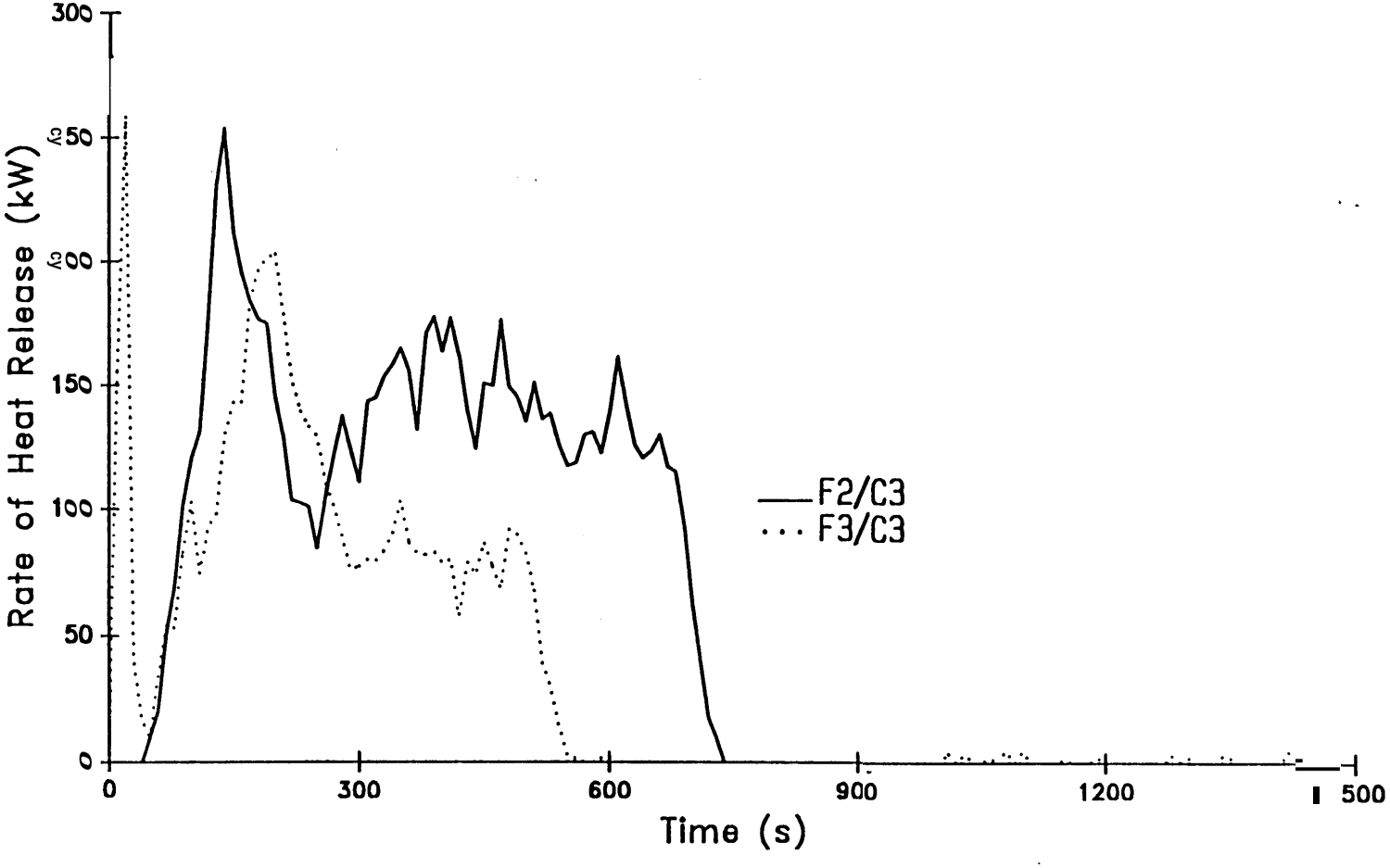

Figure 15. Rate of heat release for seat assemblies F_2/C_3 and F_3/C_3 tested in the bus simulation .

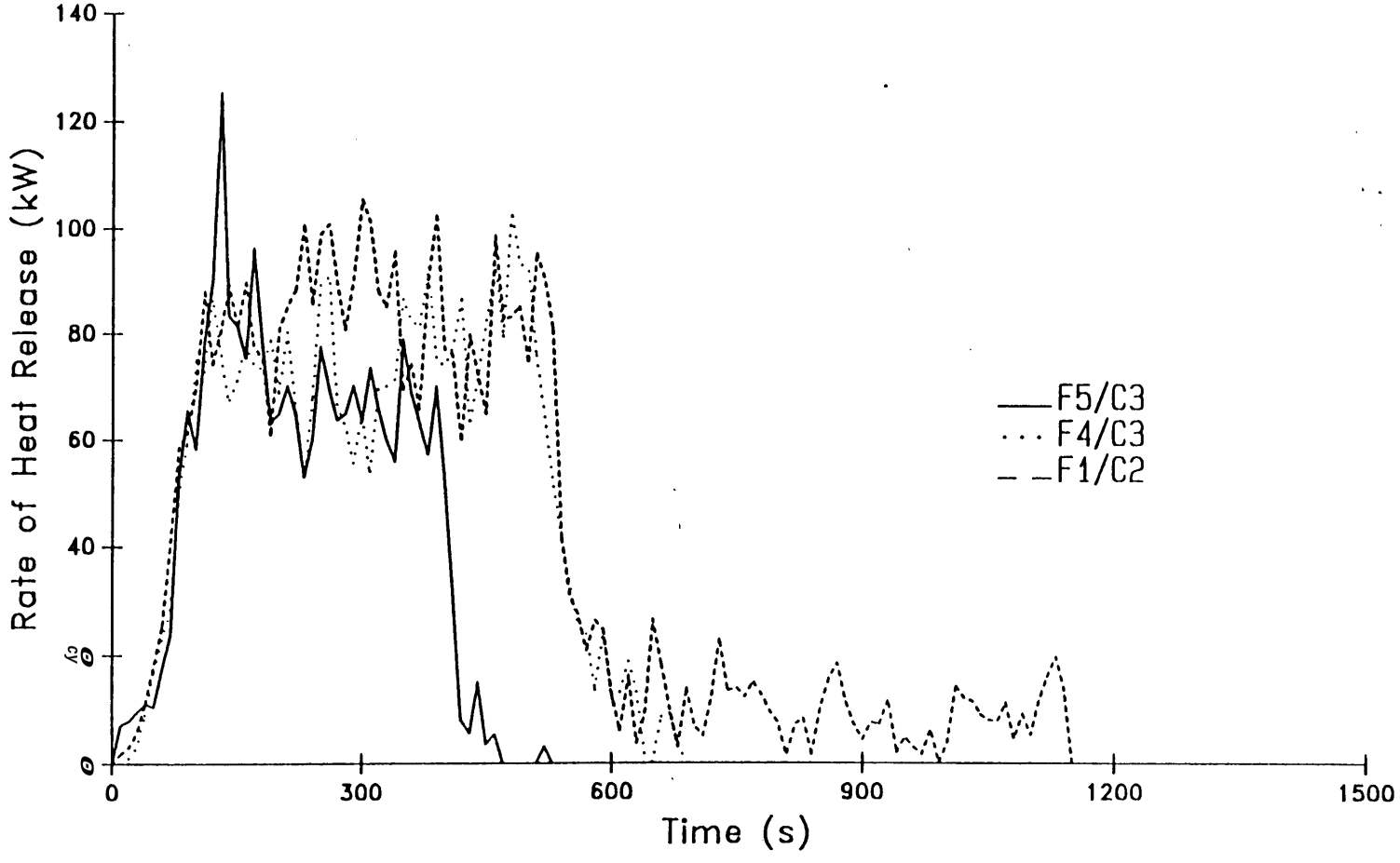

Figure 16. Rate of heat release for seat assemblies F_1/C_2, F_4/C_3, and F_5/C_3 tested in the bus simulation

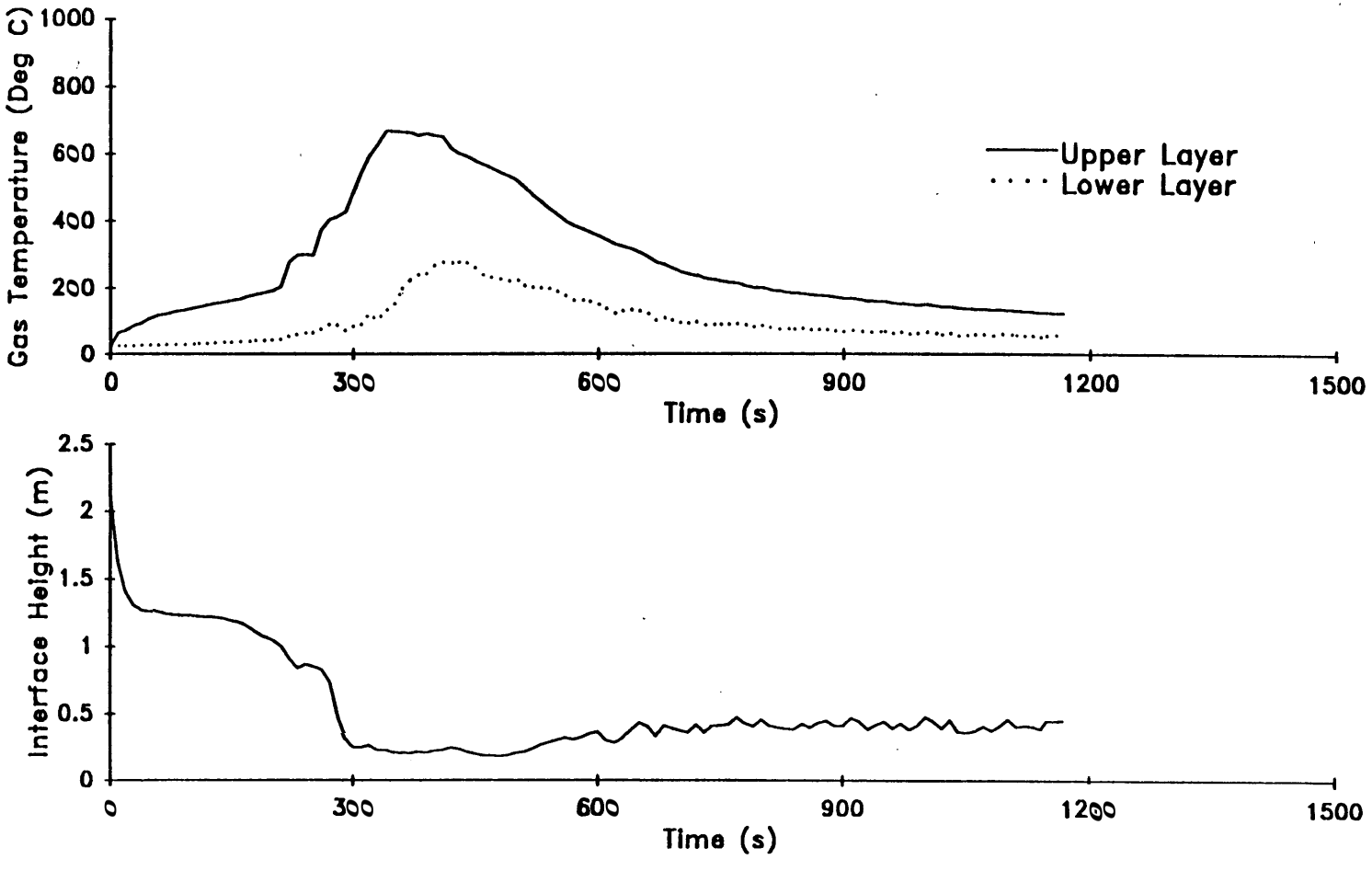

Figure 17. Upper and lower gas temperatures and interface height for seat assembly F_1/C_1 tested in the bus simulation

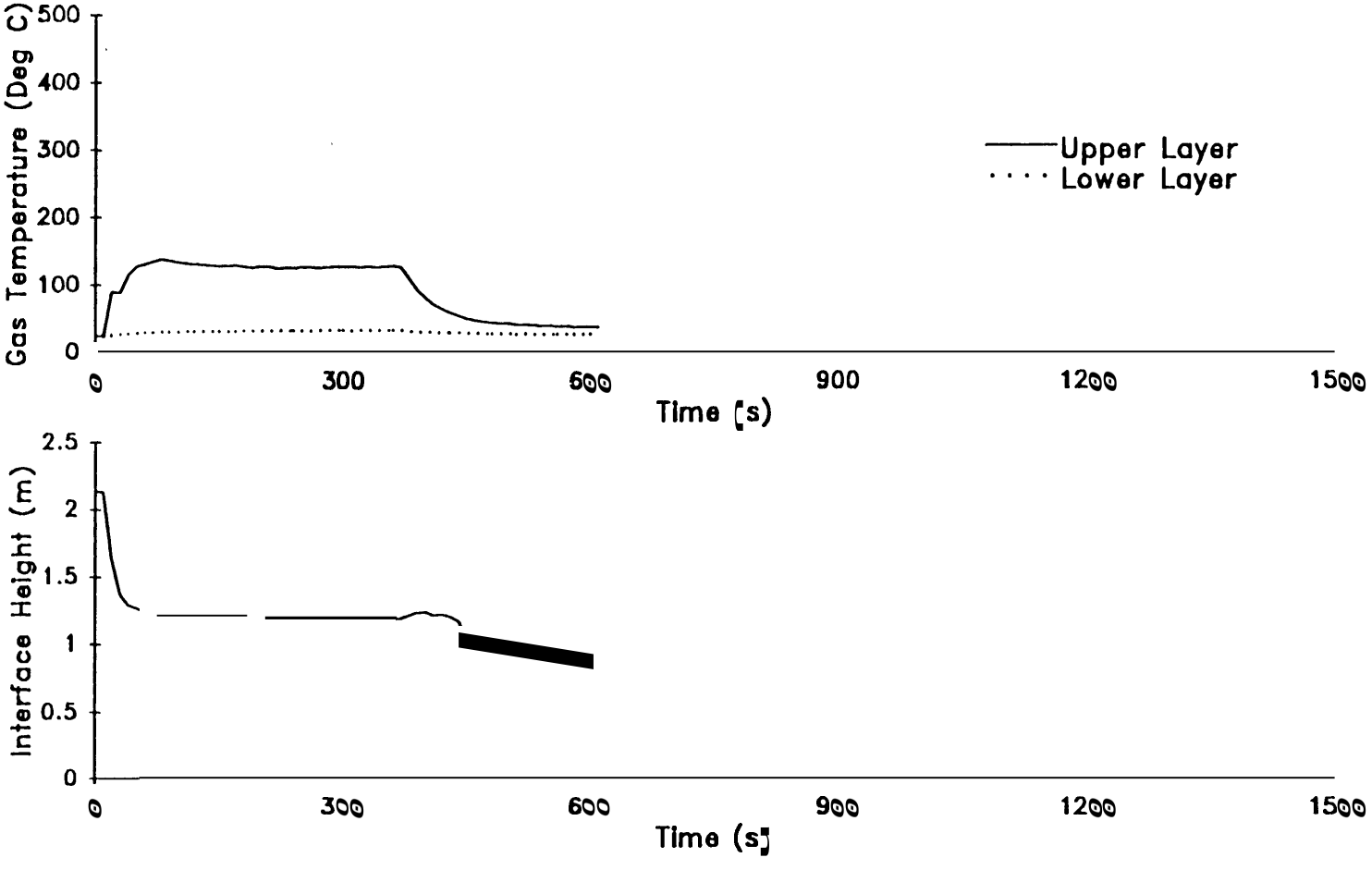

Figure 18 Upper and lower gas temperatures and interface height for seat assembly F_1/C_2 tested in the bws simulation

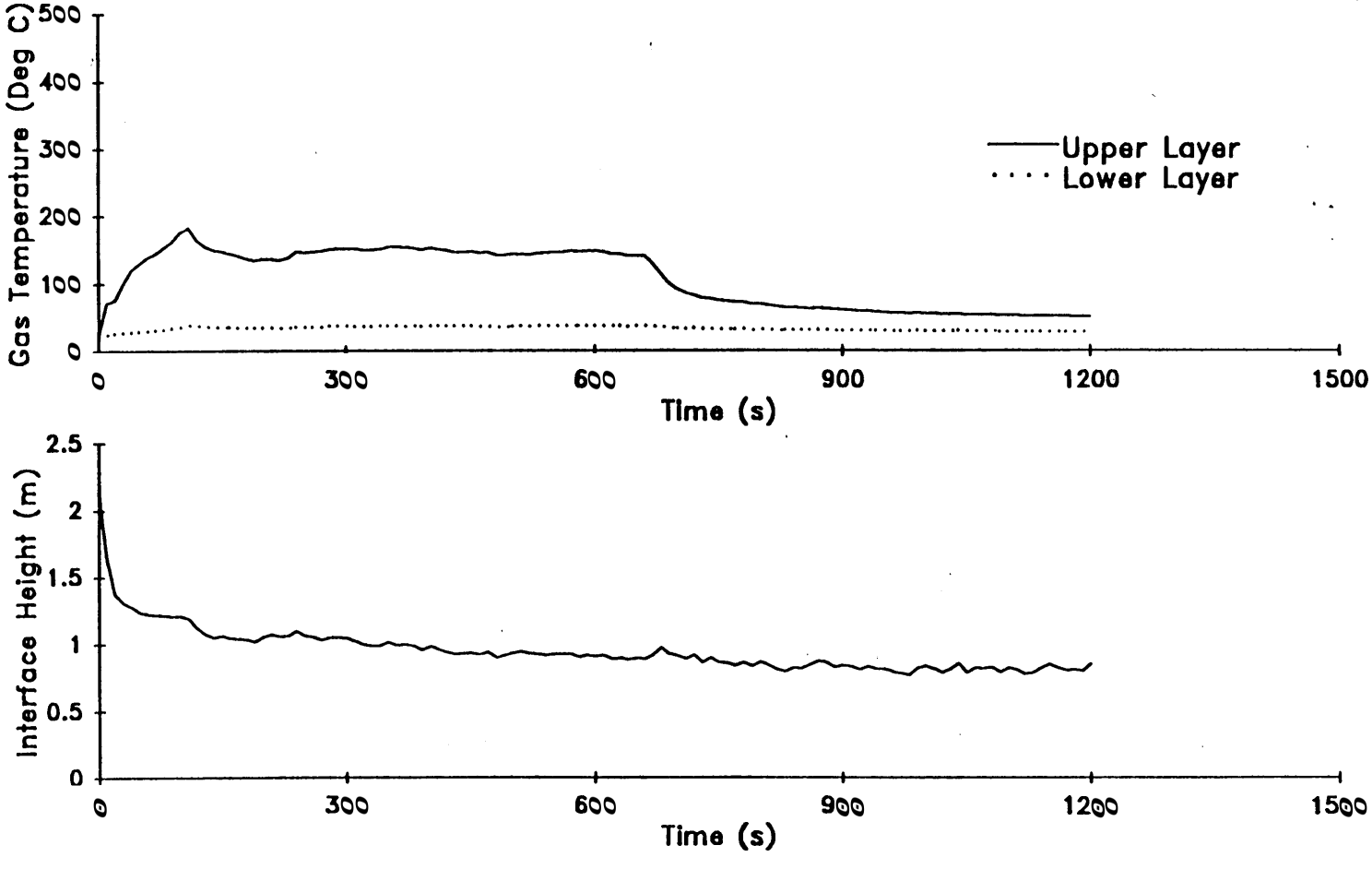

Figure 19. Upper and lower gas temperatures and interface height for heat assembly F_2/C_3 computed in the bus simulation

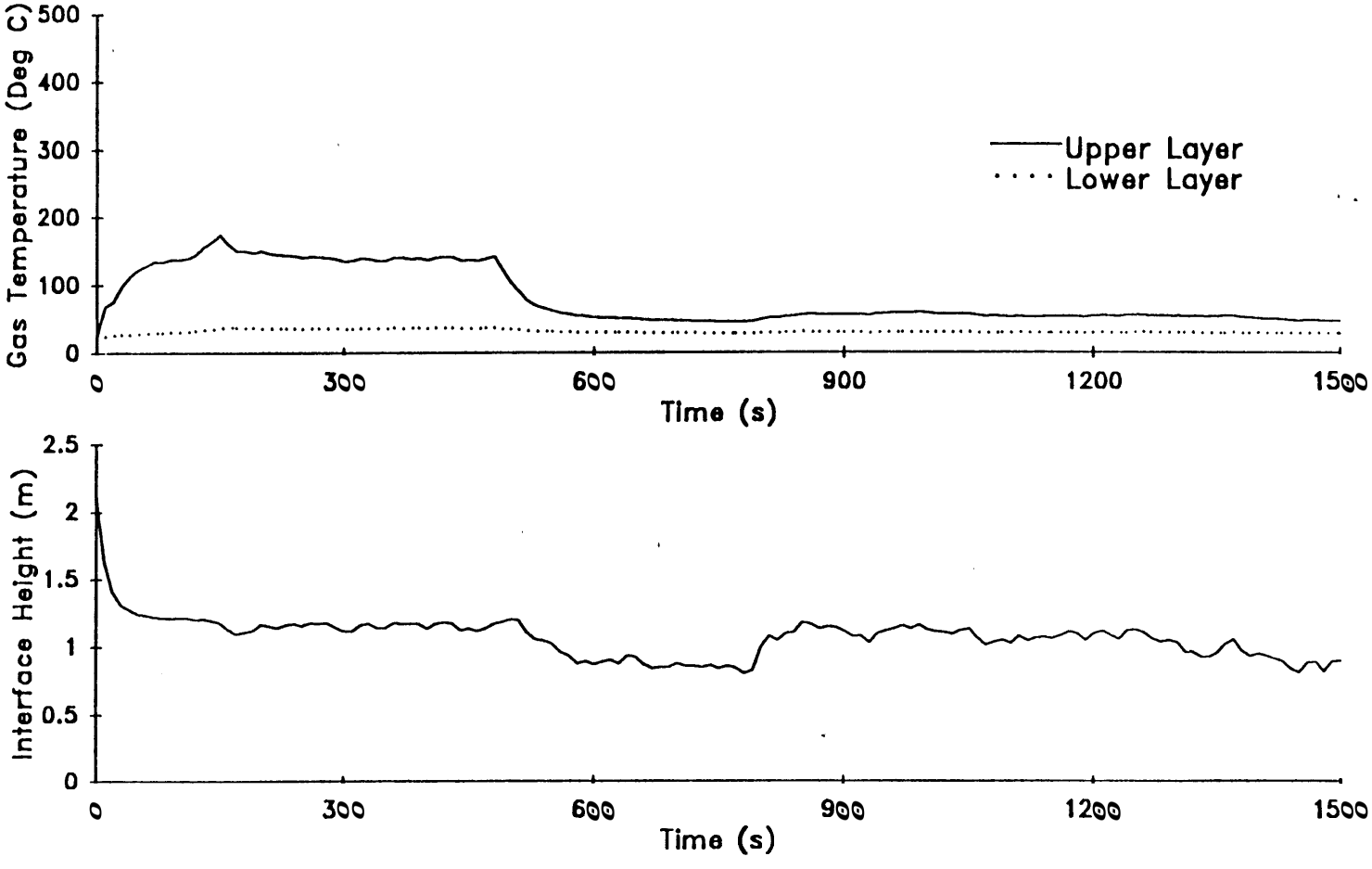

Figure 20 Upper and lower gas temperatures and interface height for seat assembly F_3/C_3 tested in the bus simulation

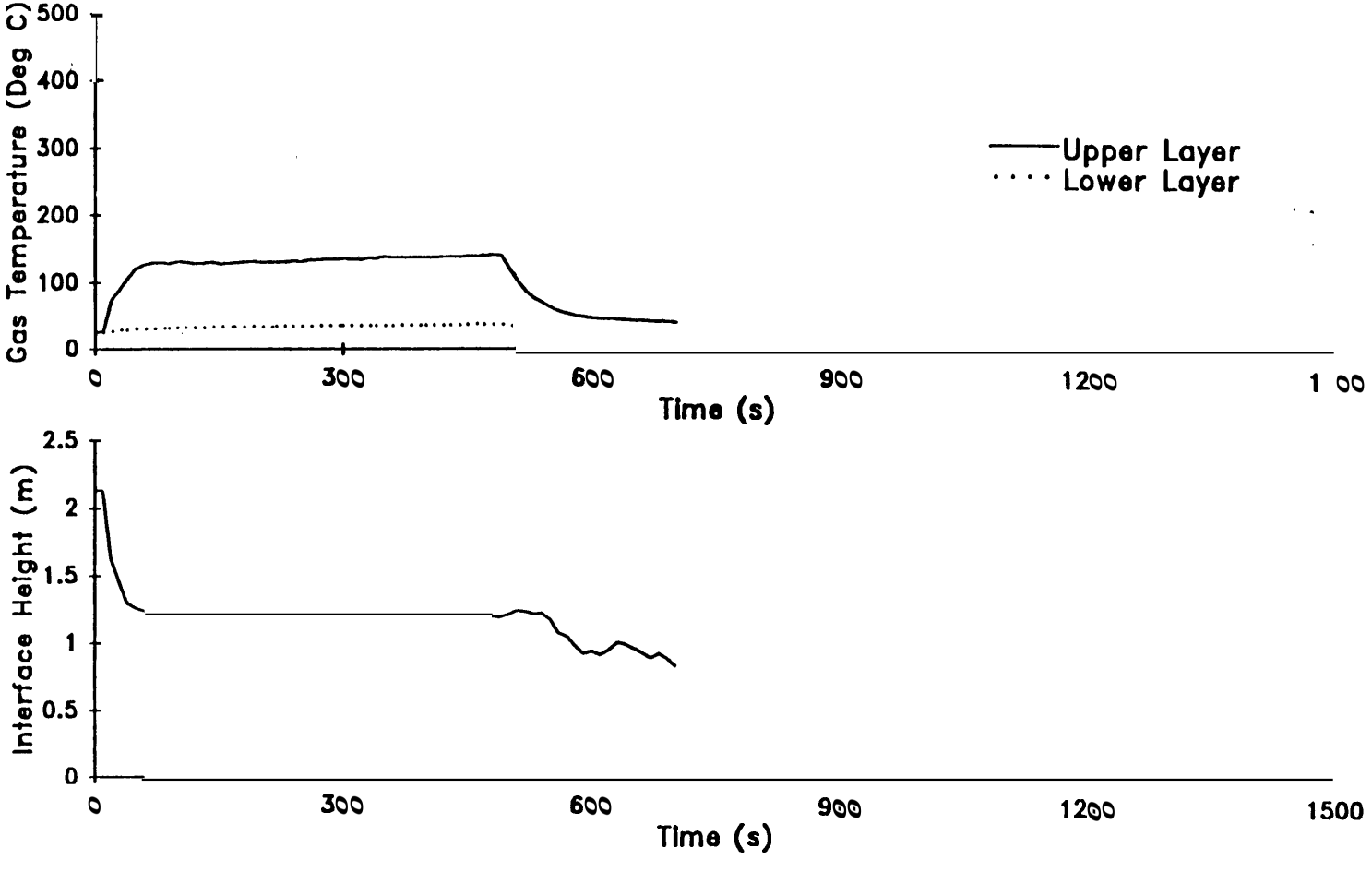

Figure 21. Upper and lower gas temperatures and interface height for seat assembly F_4/C_3 tested in the bus simulation

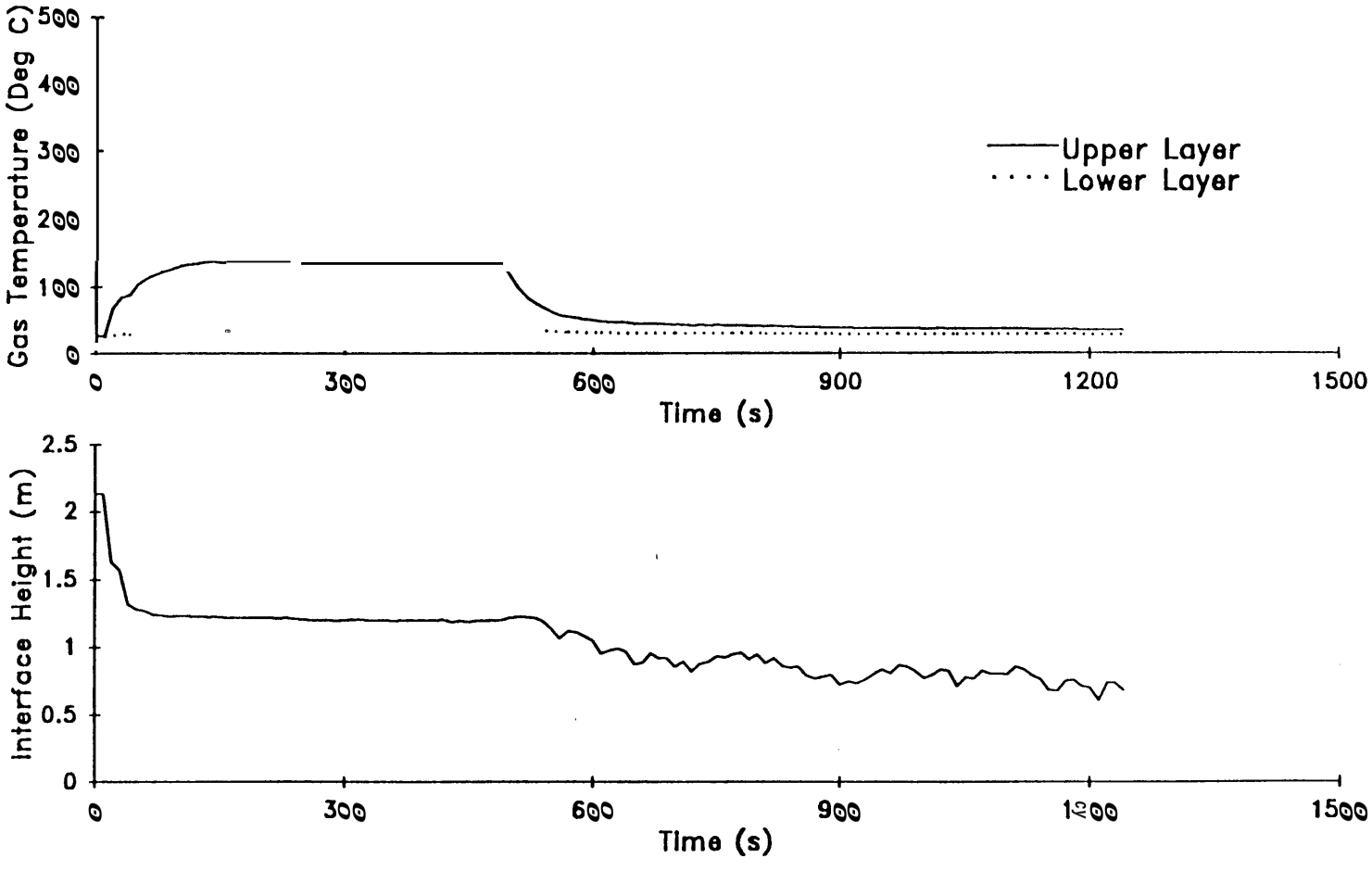

Figure 22. Upper and lower gas temperatures and interface height for seat assembly F_5/C_3 tested in the bus simulation

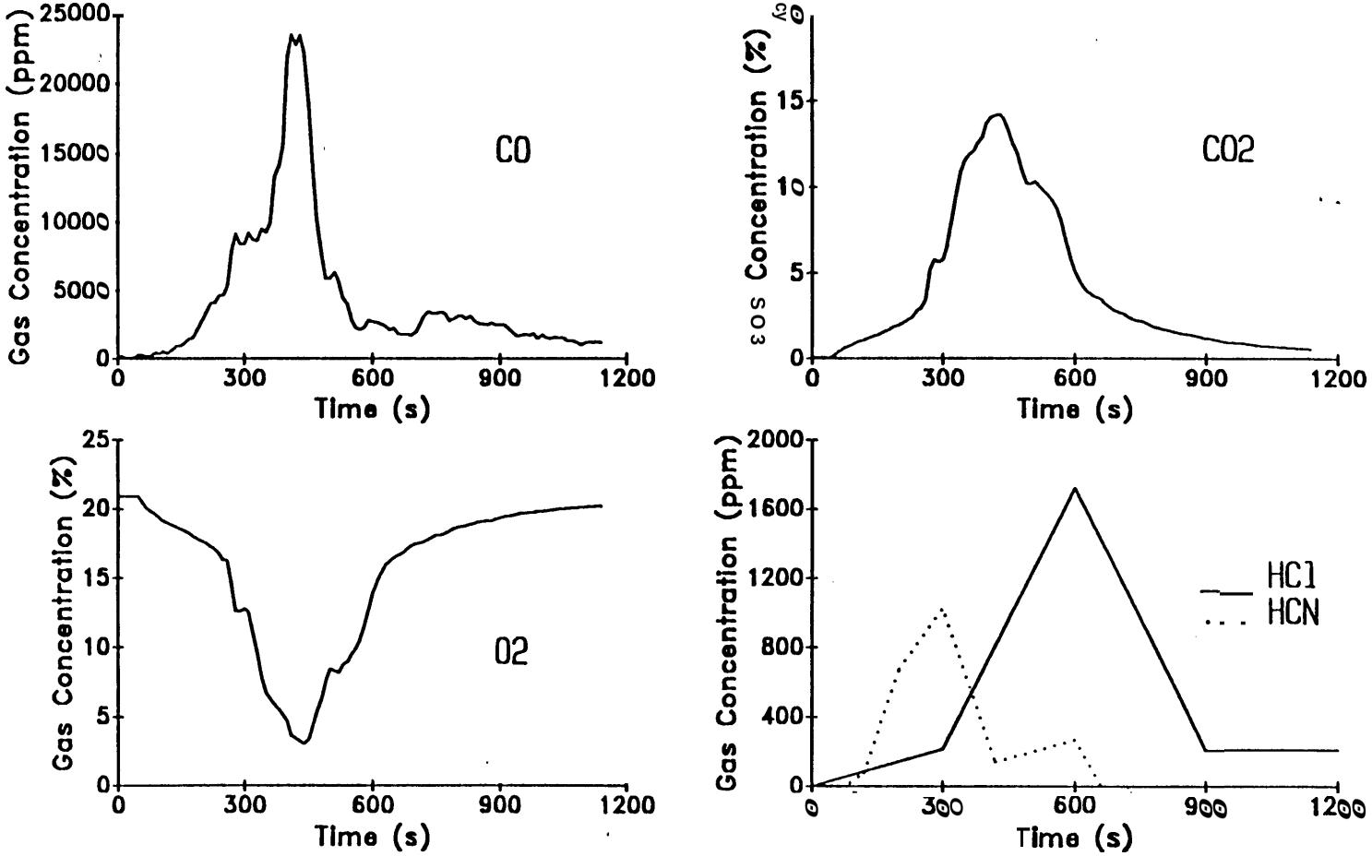

Figure 23. Gas concentrations (CO, CO_2, O_2, HCl, and HCN) for seat assembly F_1 tested in the bus simulation

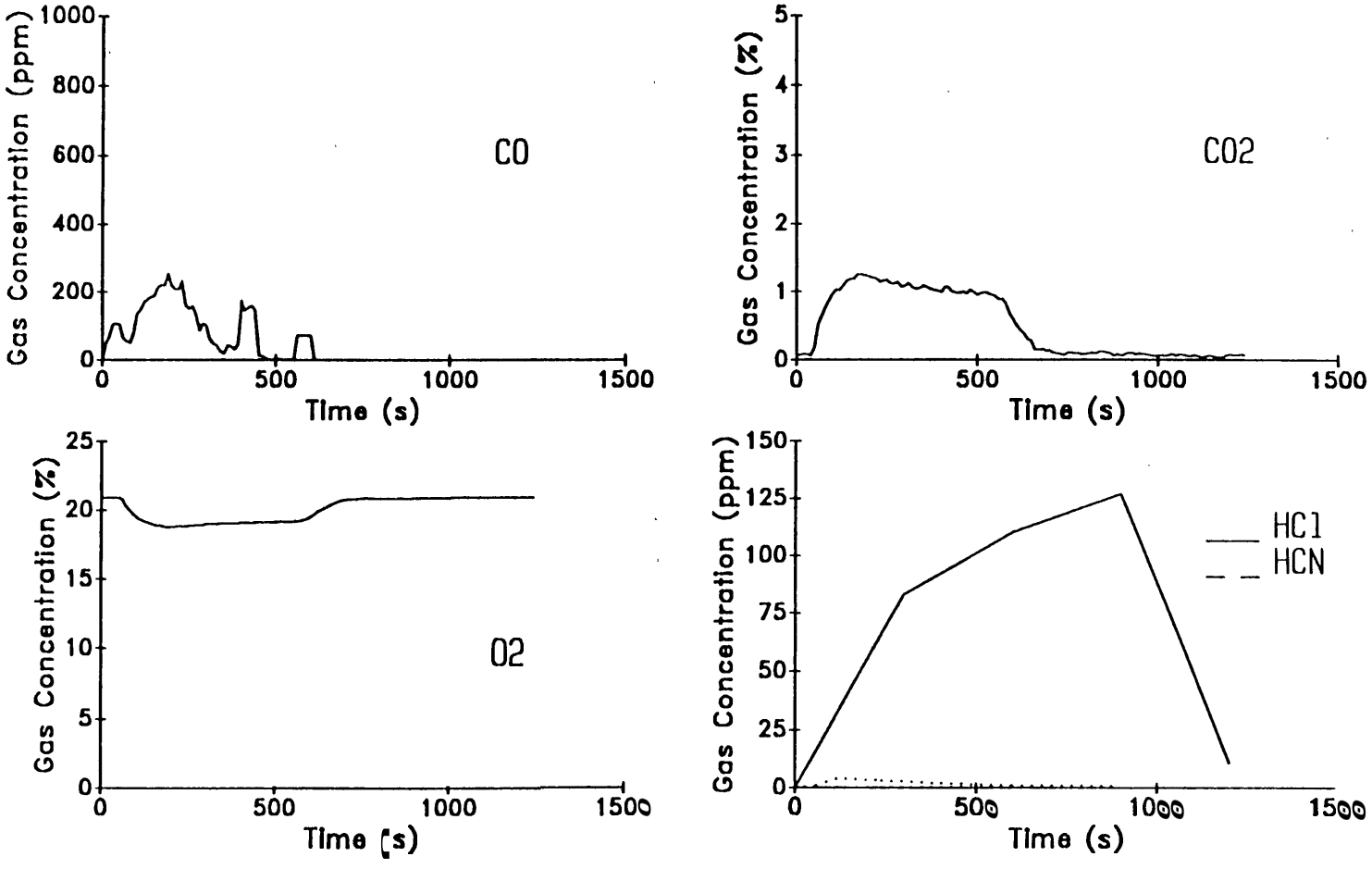

Figure 24. Gas concentrations (CO, CO_2, O_2, HCl and HCN) for seat assembly F_1/C_1 tested in the bus simulation

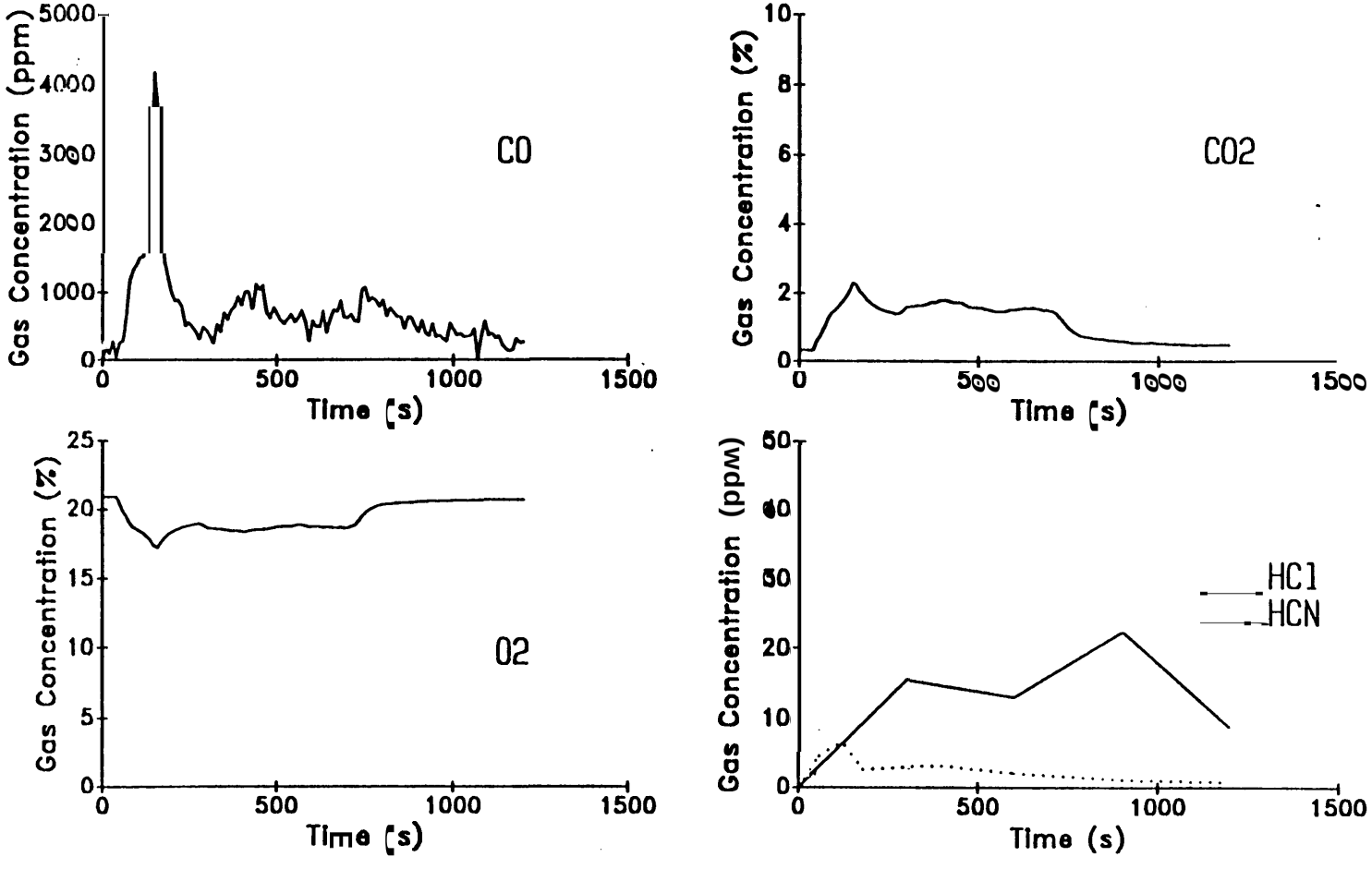

Figure 25. Gas concentrations (CO, CO_2, O_2 HCl, and HCN) for seat assembly F_2/C_3 tested in the bus simulation

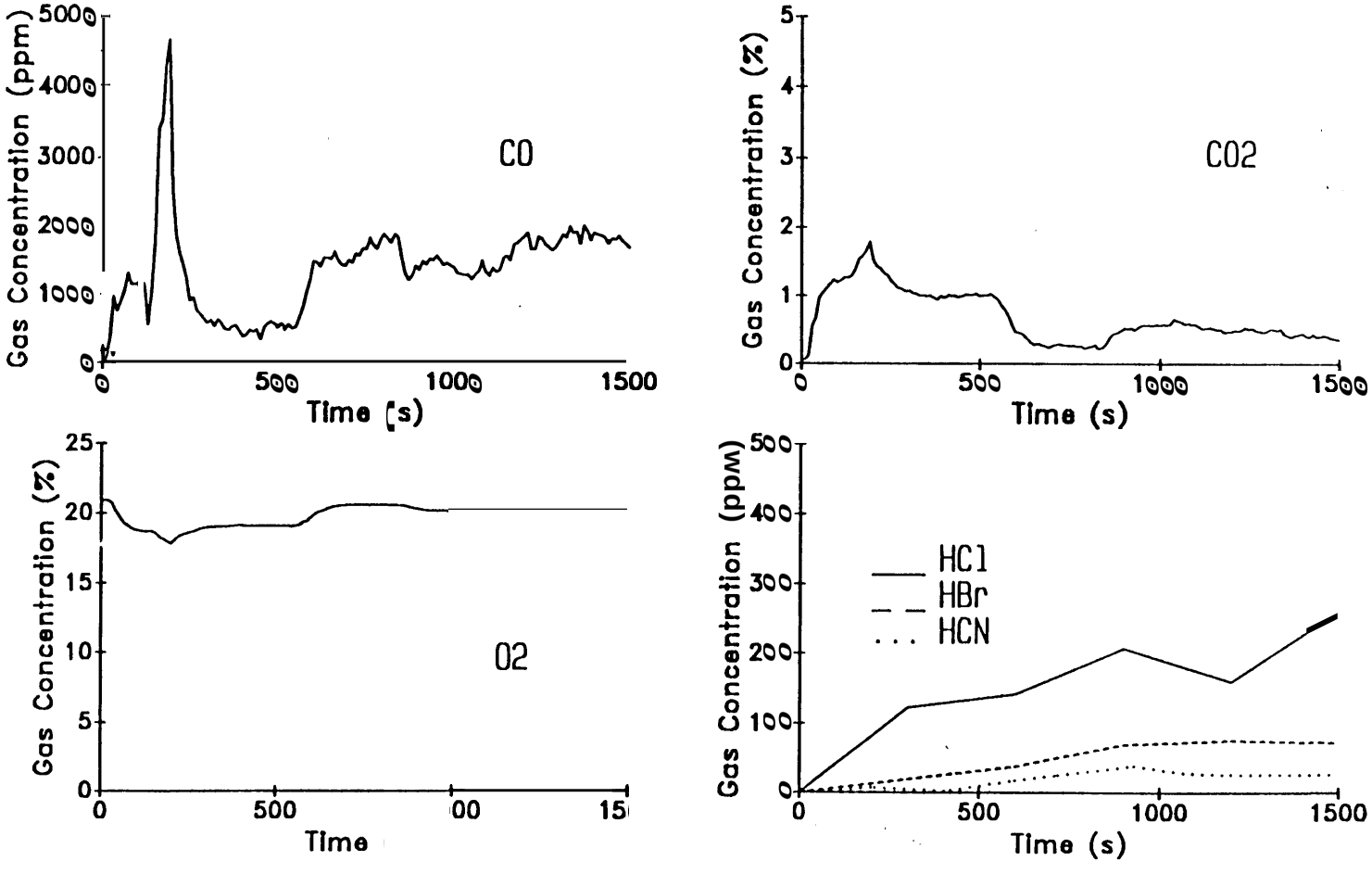

Figure 26. Gas concentrations (CO, CO_2, O_2, HCl, HBr, and HCN) for seat assembly F_3/C_3 tested in the bus simulation

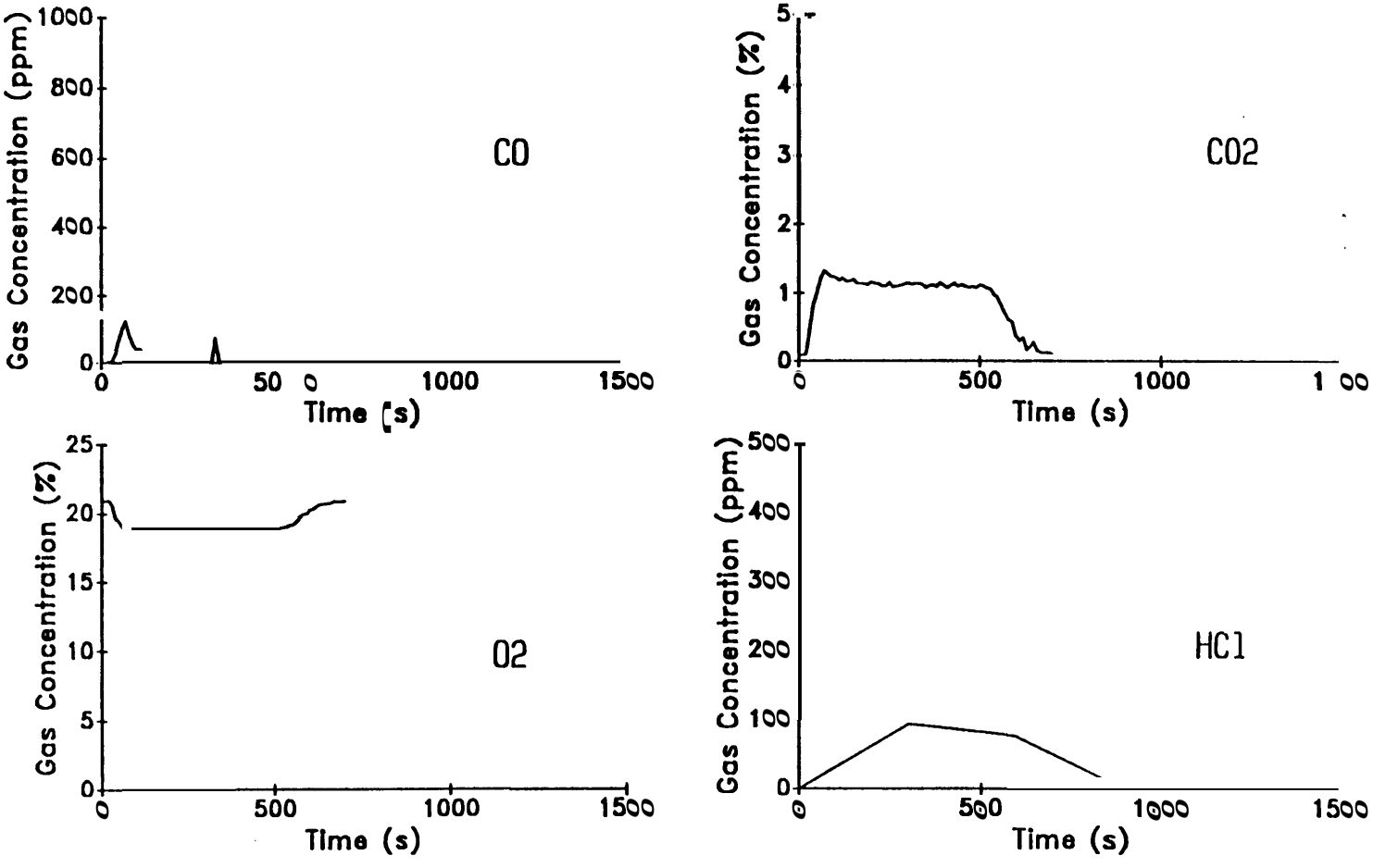

Figure 27. Gas concentrations (CO, CO_2, O_2, and HCl) for seat assembly F_4/C_3 tested in the bus simulation

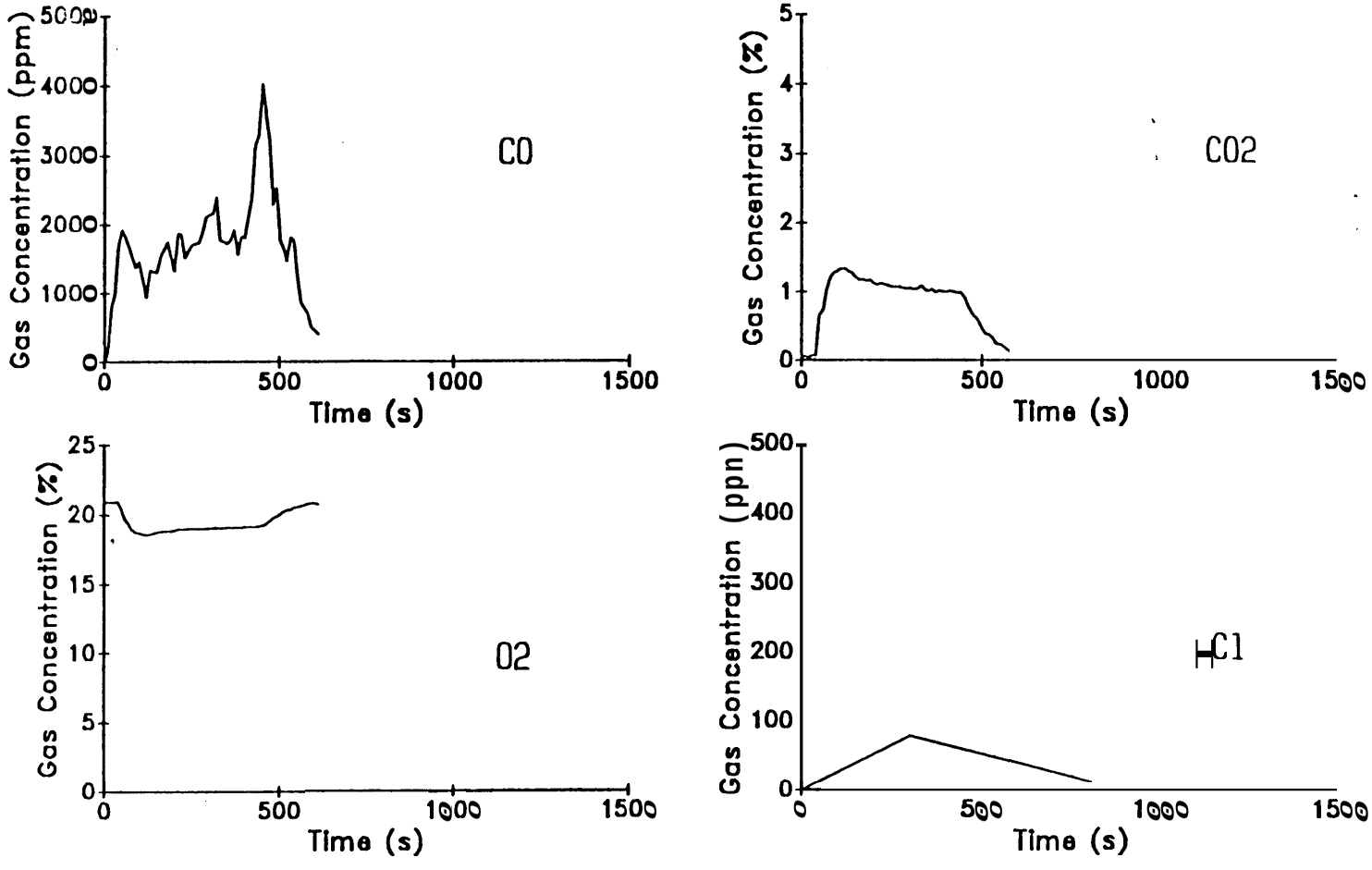

Figure 28. Gas concentrations (CO, CO_2, O_2, and HCl) for seat assembly F_5/C_3 tested in the bus simulation

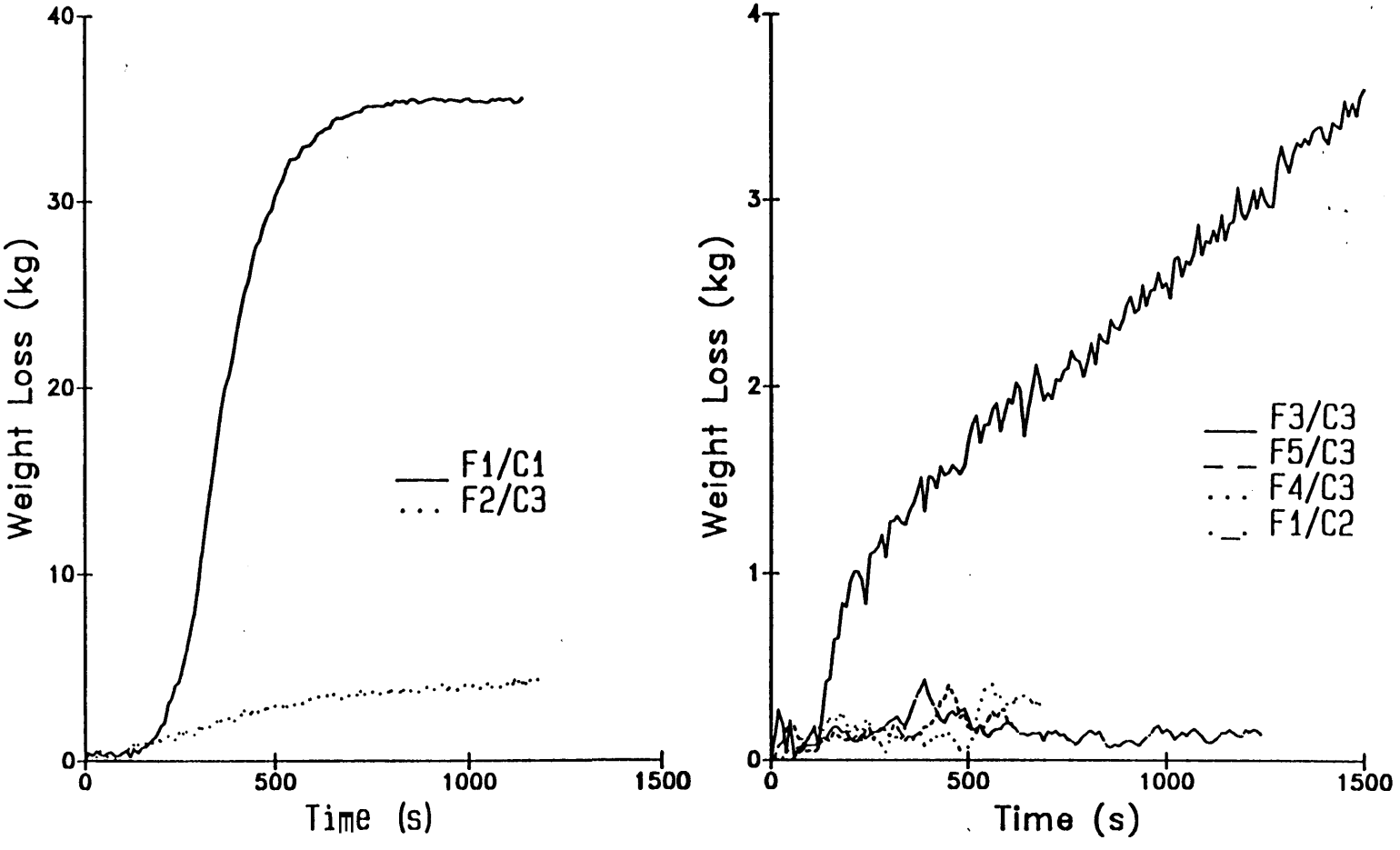

Figure 29. Weight loss of seat assemblies tested in the bus simulation

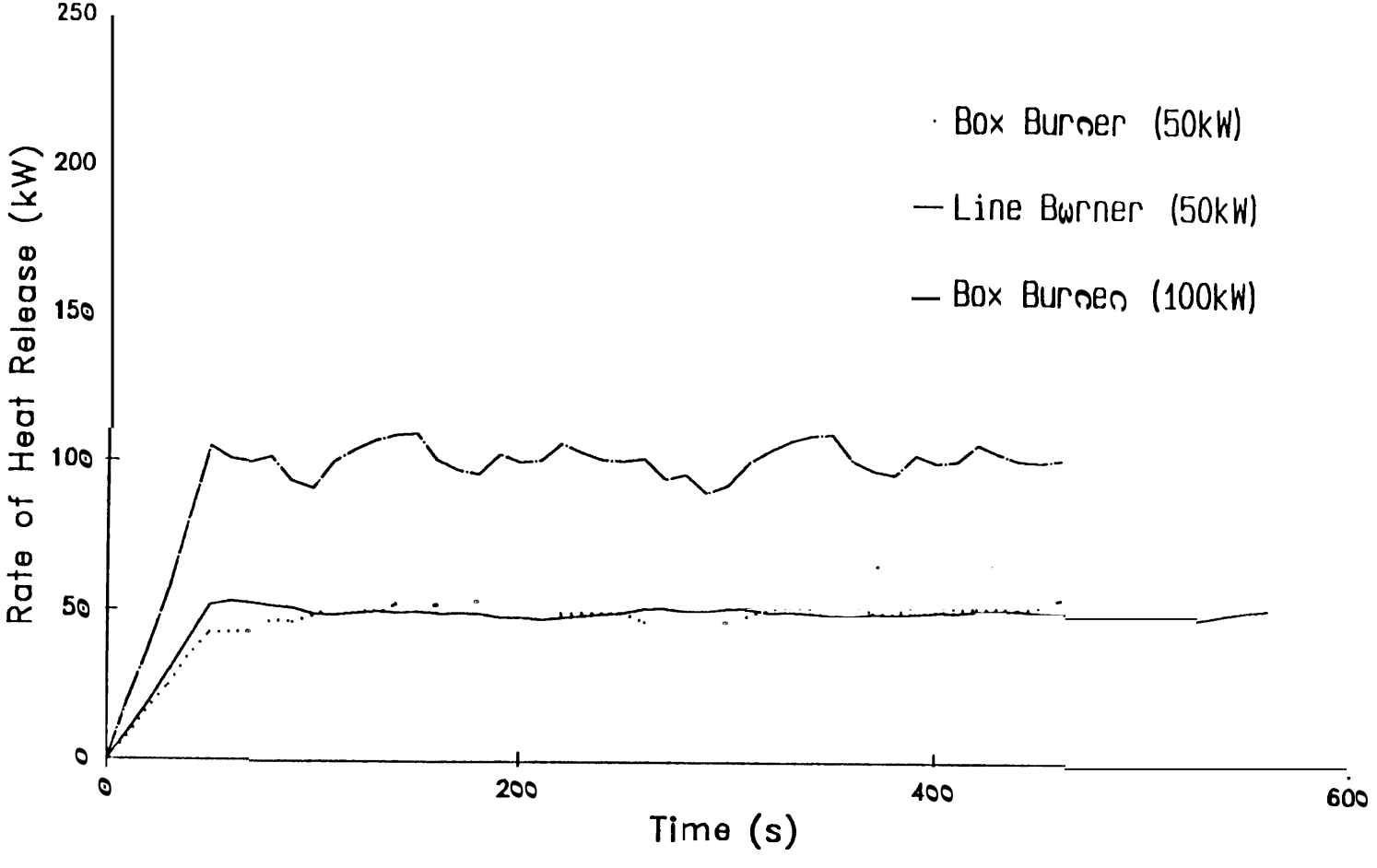

Figure 30. Heat release rates of three ignition sources used in the furniture calorimeter tests

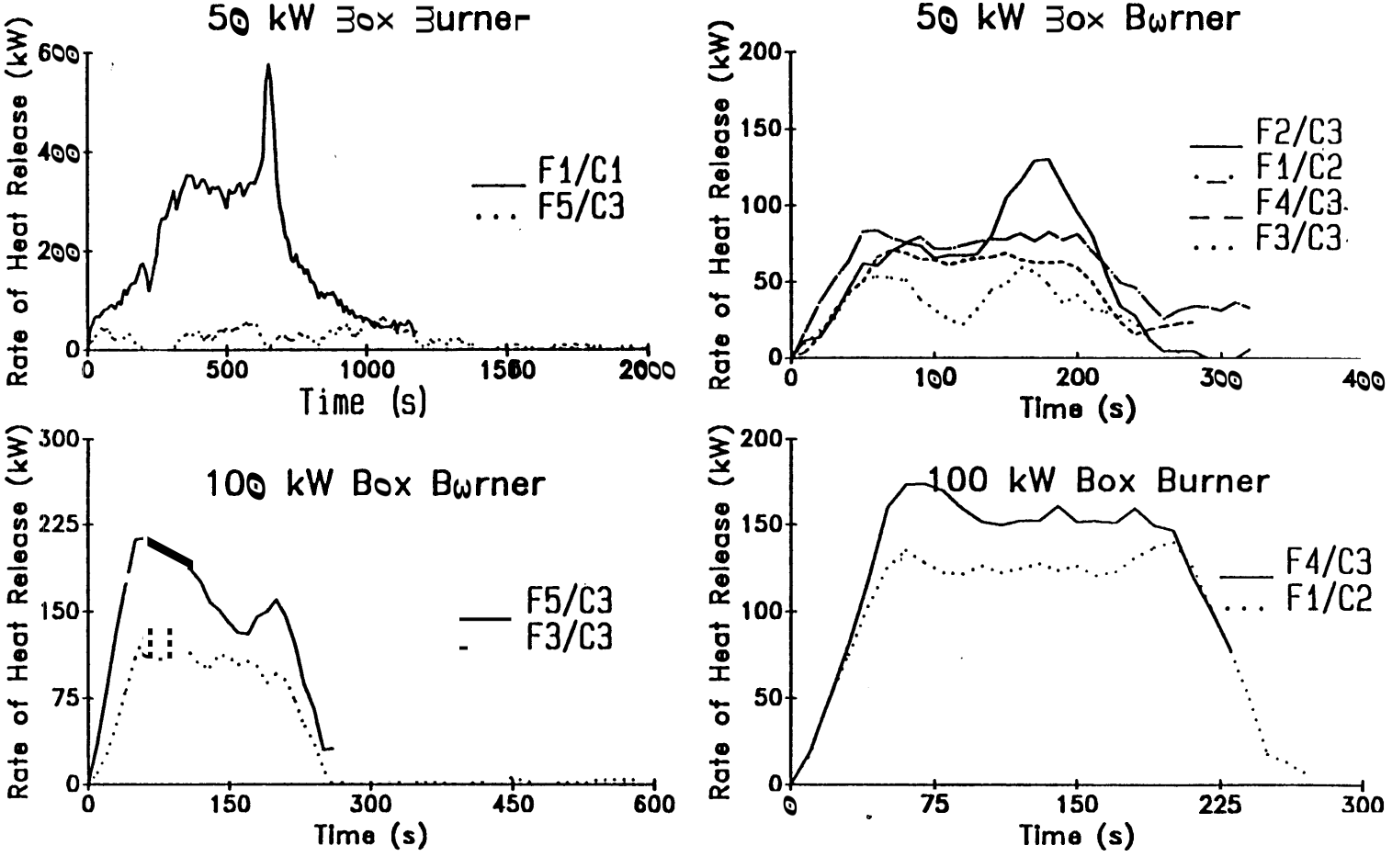

Figure 31. Heat release rates of seat assemblies exposed to 50 kW and 100 kW box burners in the furniture calorimeter tests

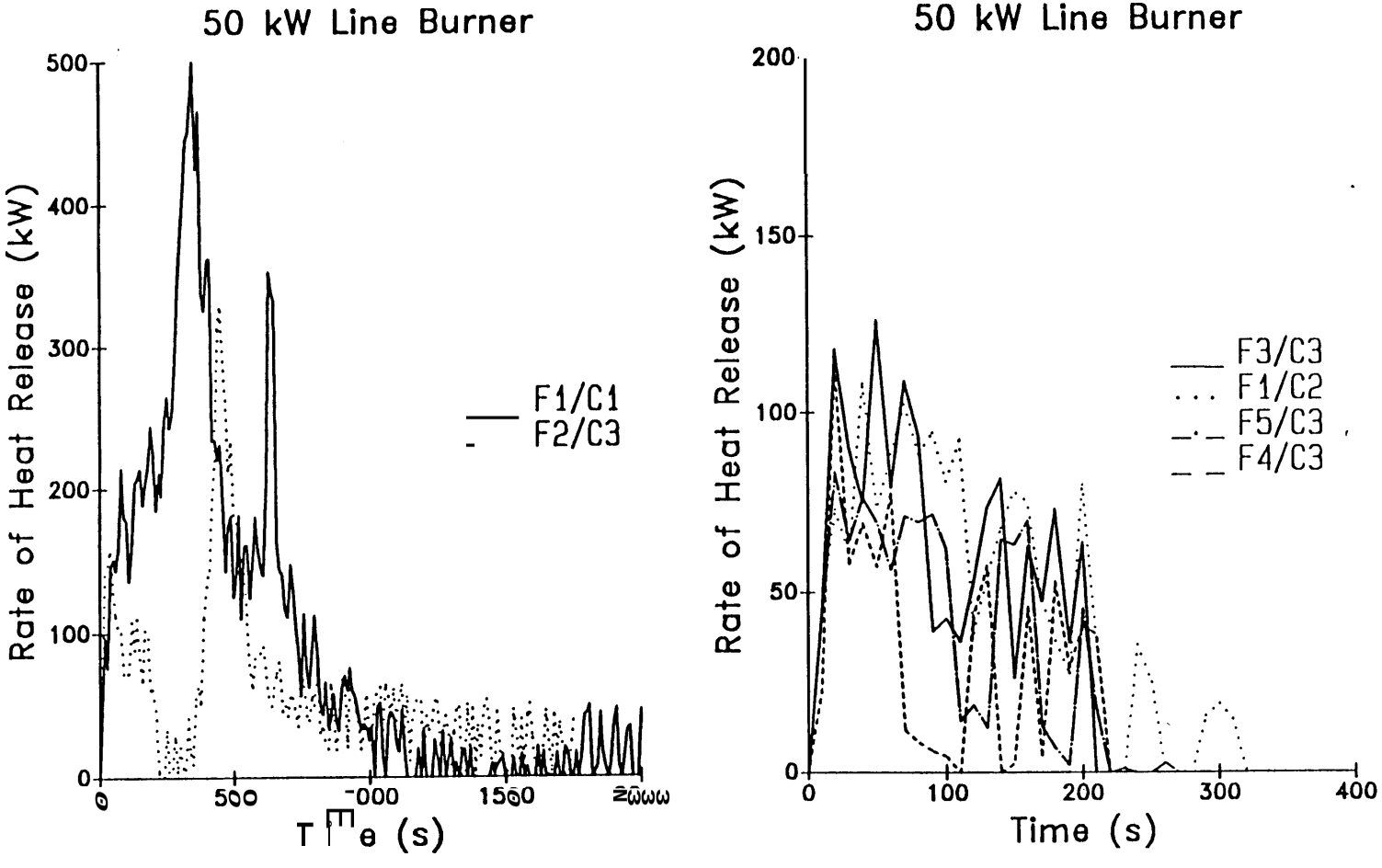

Figure 32. Heat release rates of seat assemblies exposed to the 50 kw line burner in the furniture calorimeter tests

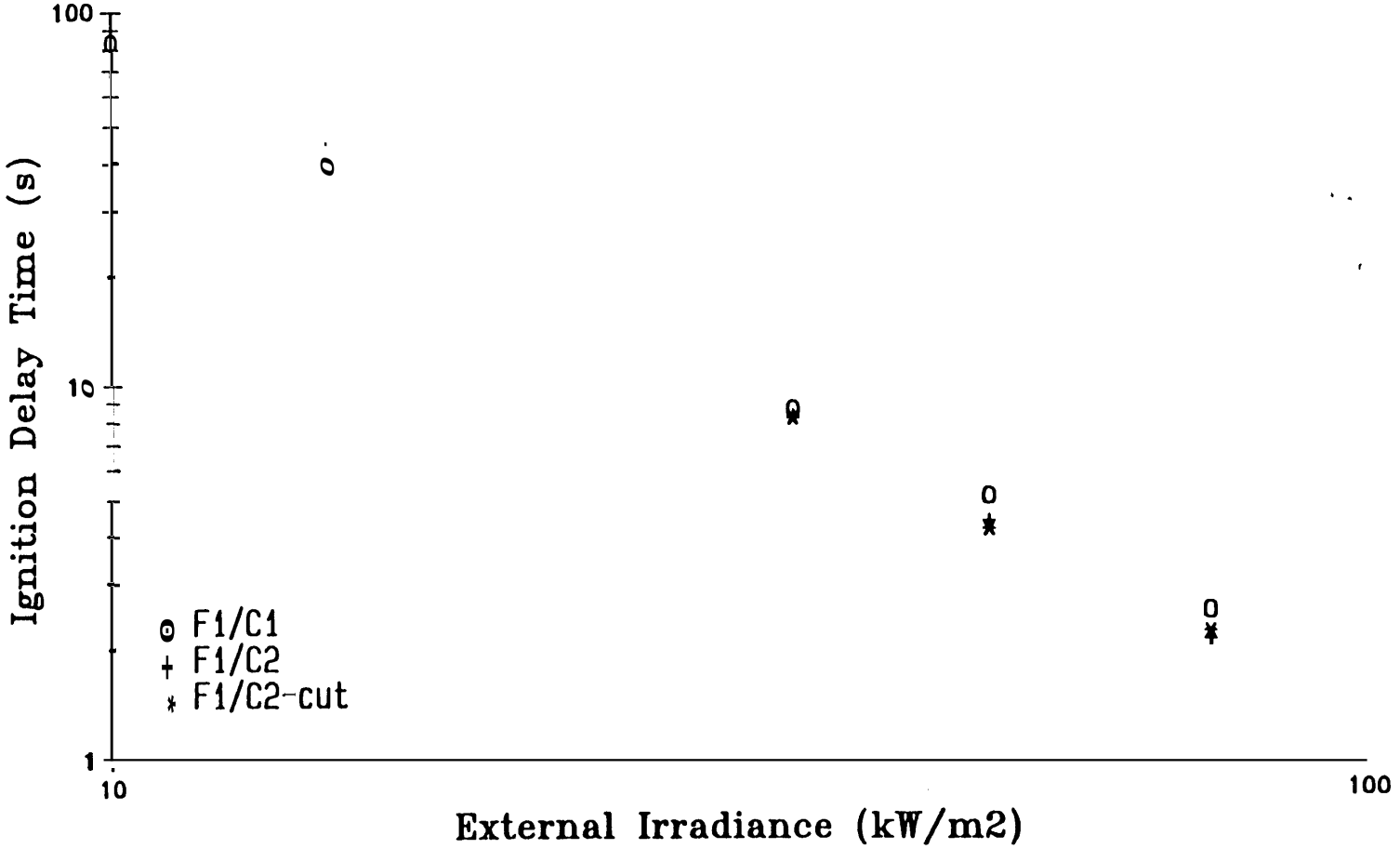

Figure 33. Times-to-ignition for composites F_1/C_1 and F_1/C_2 under varying external irradiances

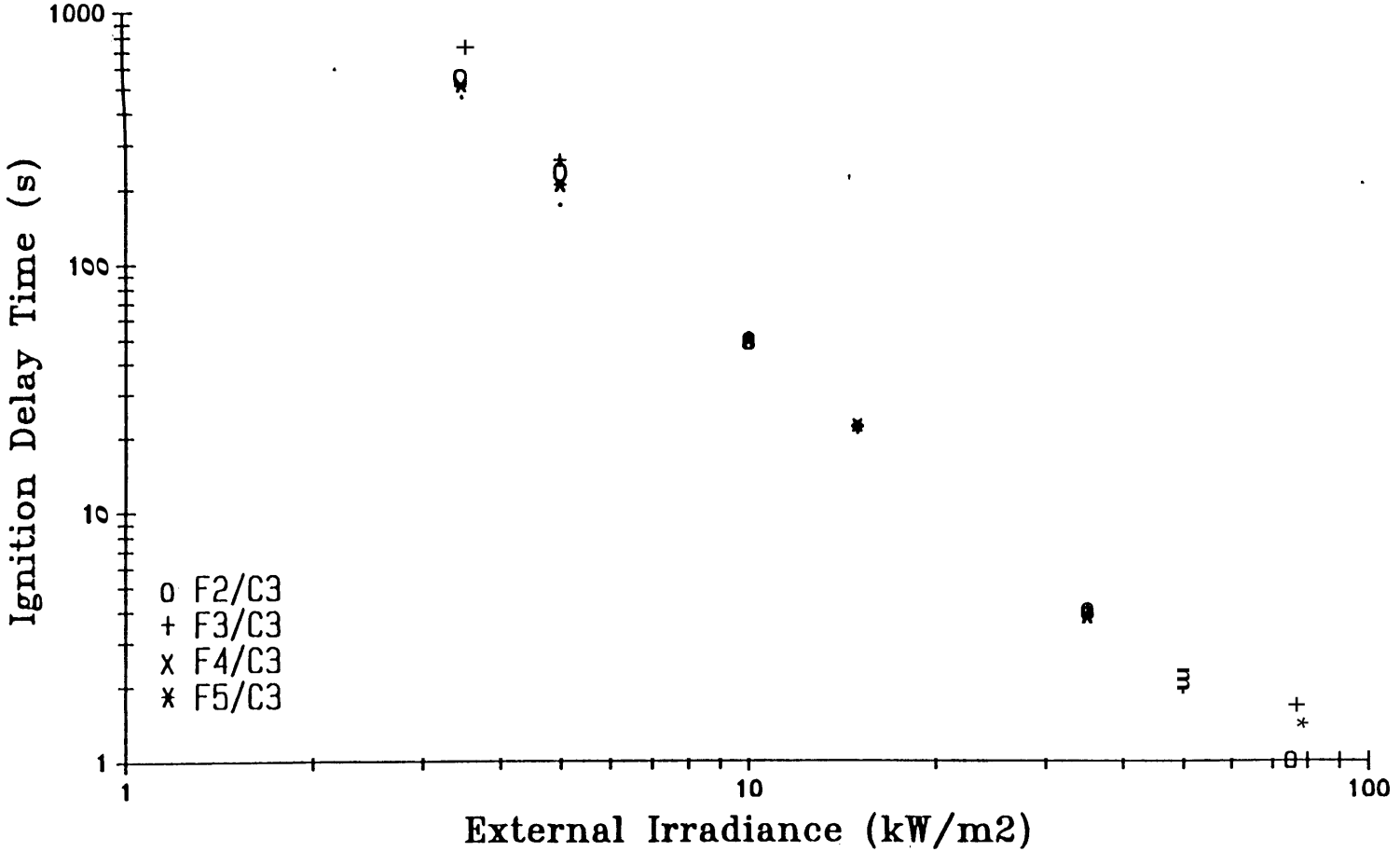

Figure 34. Times-to-ignition for composites F_2/C_3, F_3/C_3, F_4/C_3, and F_5/C_3 under varying external irradiances

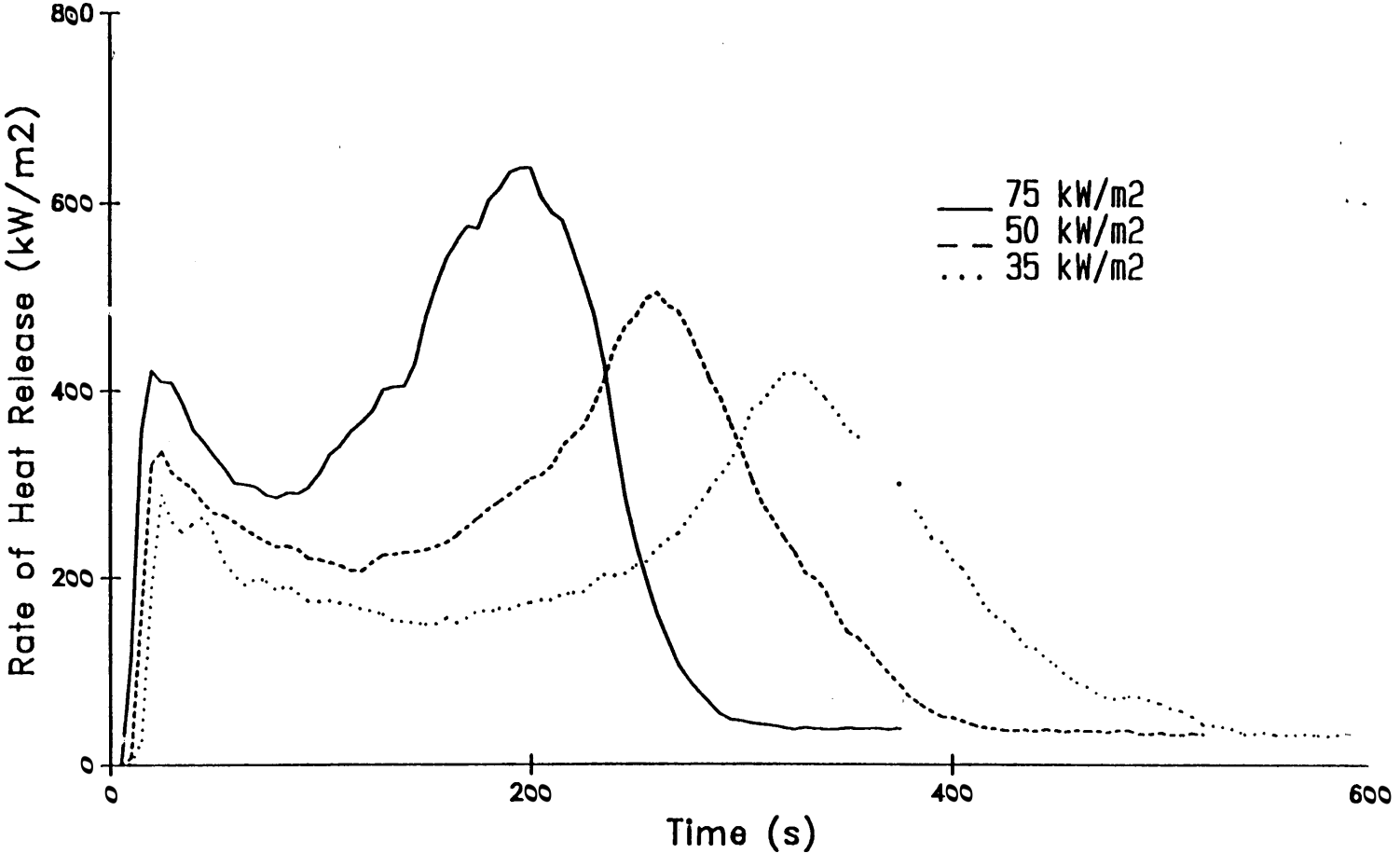

Figure 35. Rate of heat release of composite F_1/C_1 in the cone calorimeter at three external irradiances

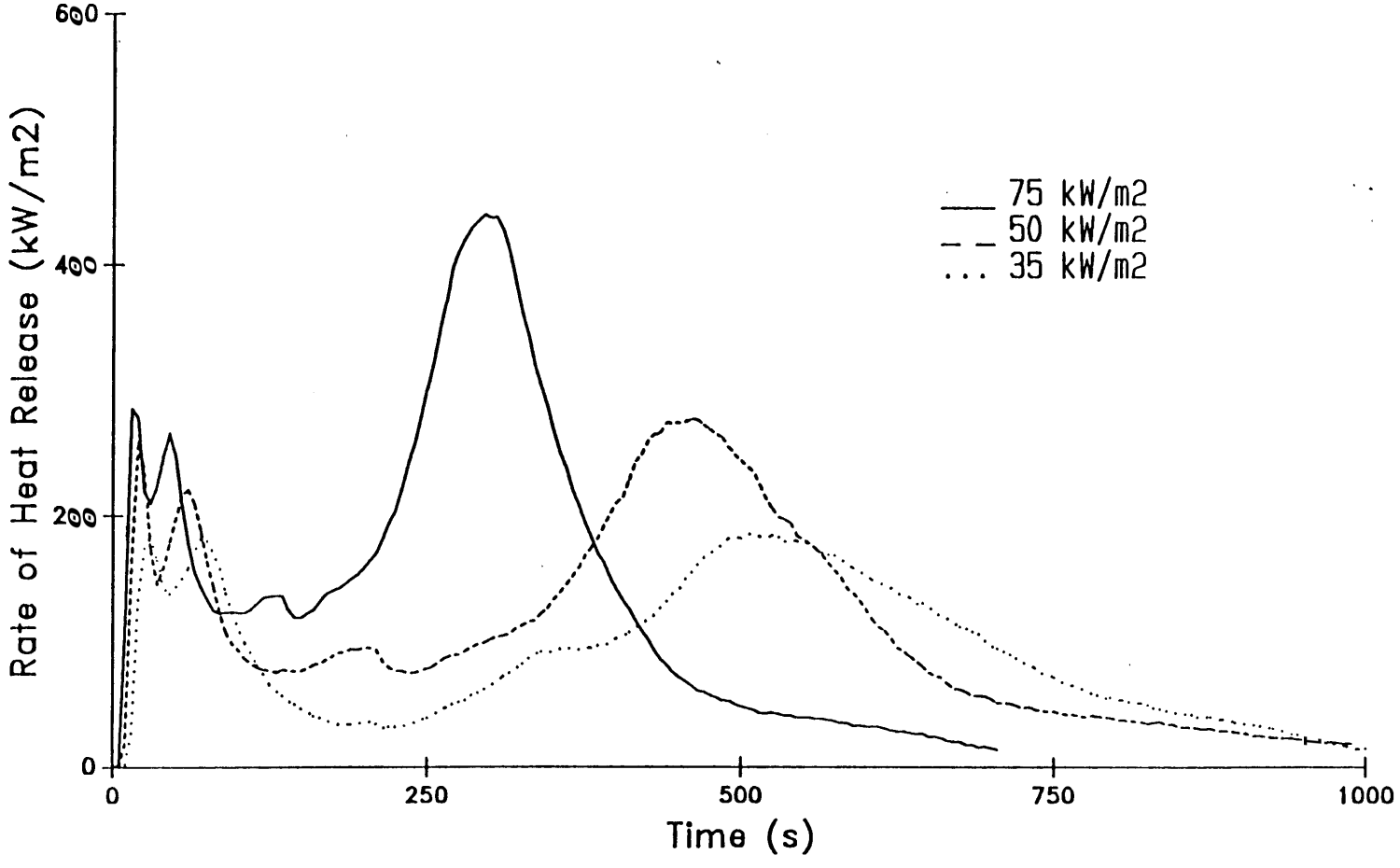

Figure 36. Rate of heat release of composite F_1/C_2 in the cone calorimeter at three external irradiances

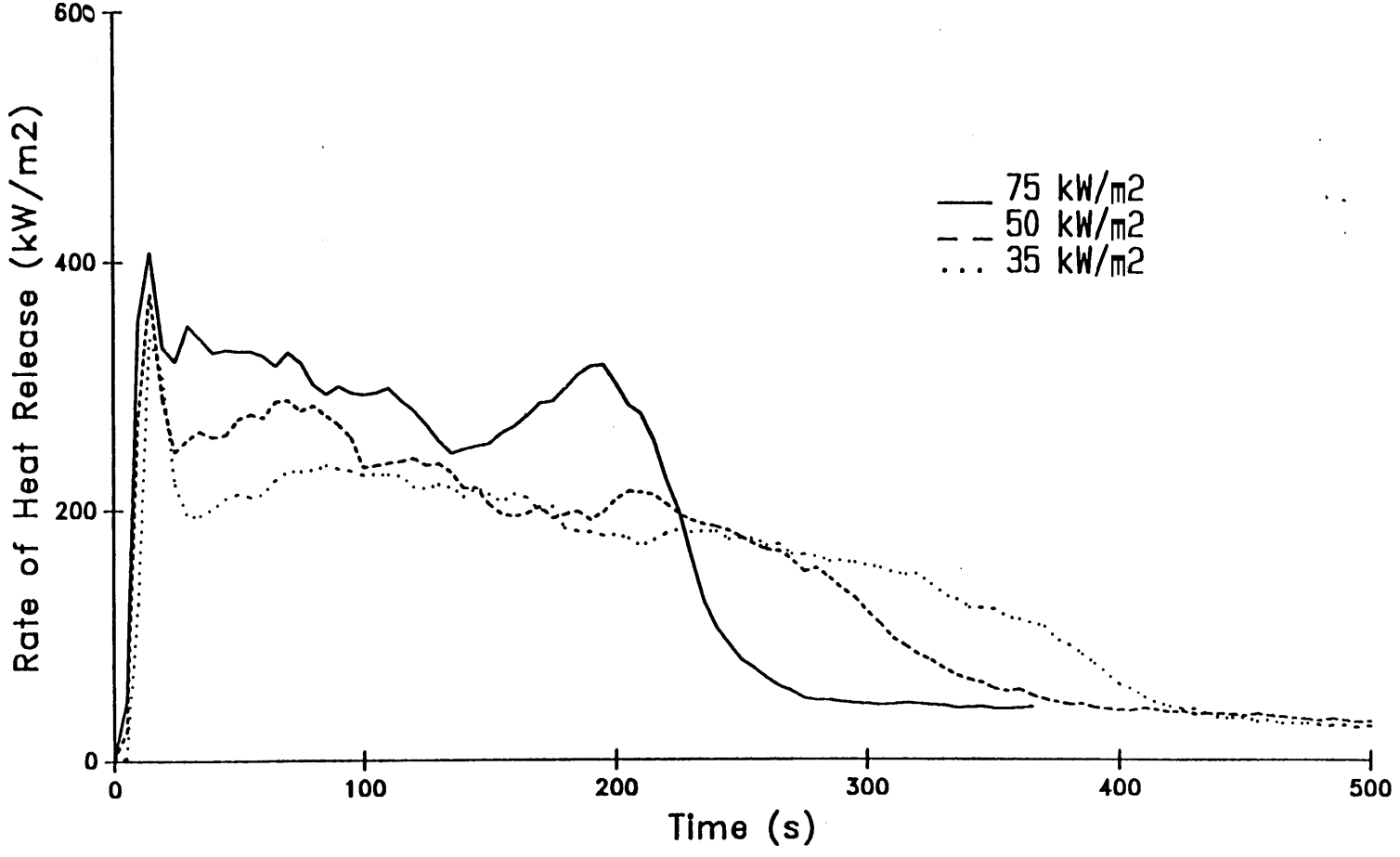

Figure 37. Rate of heat release of composite F_2/C_3 in the cone calorimeter at three external irradiances

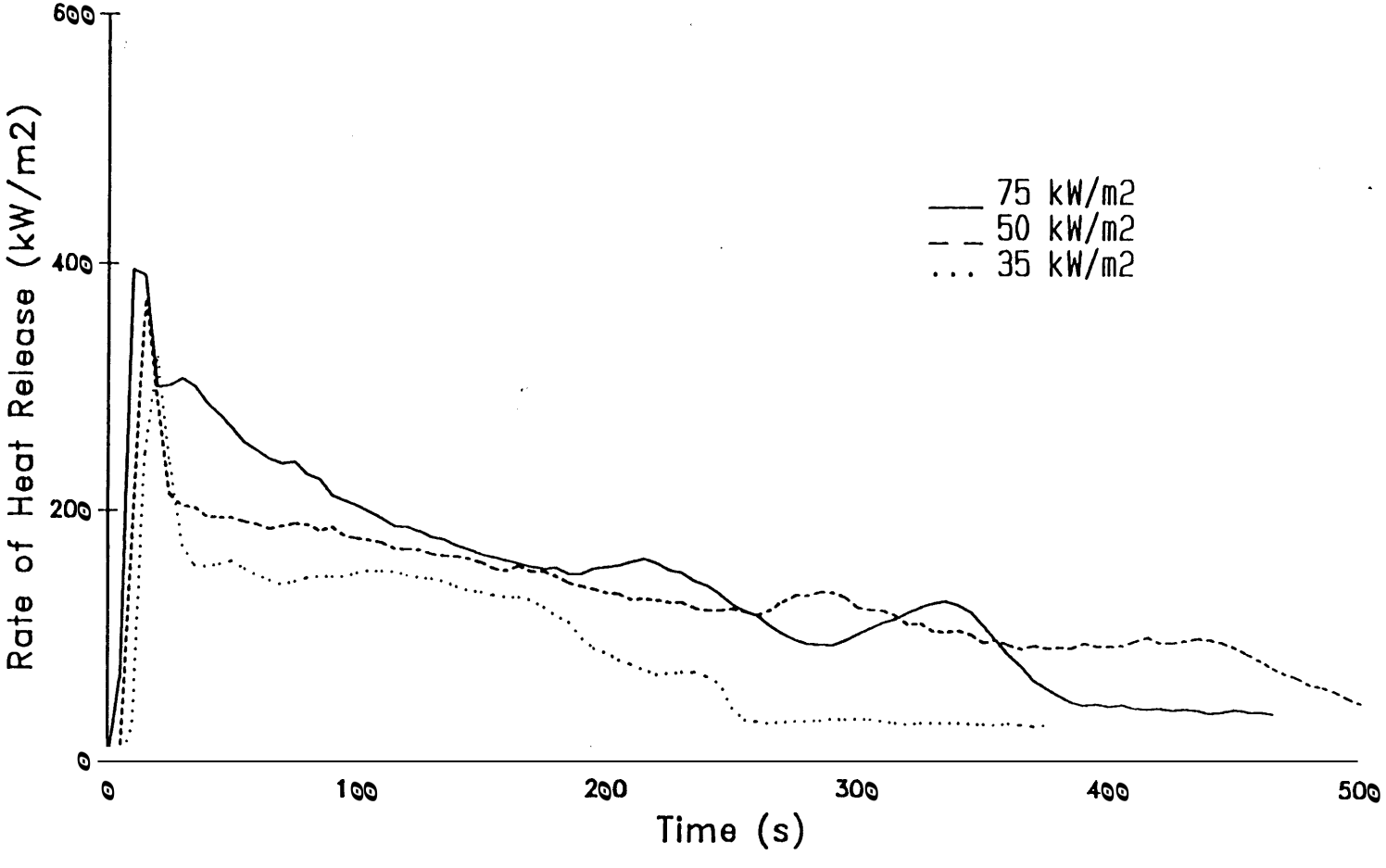

Figure 38. Rate of heat release of composite F_3/C_3 in the cone calorimeter at three external irradiances

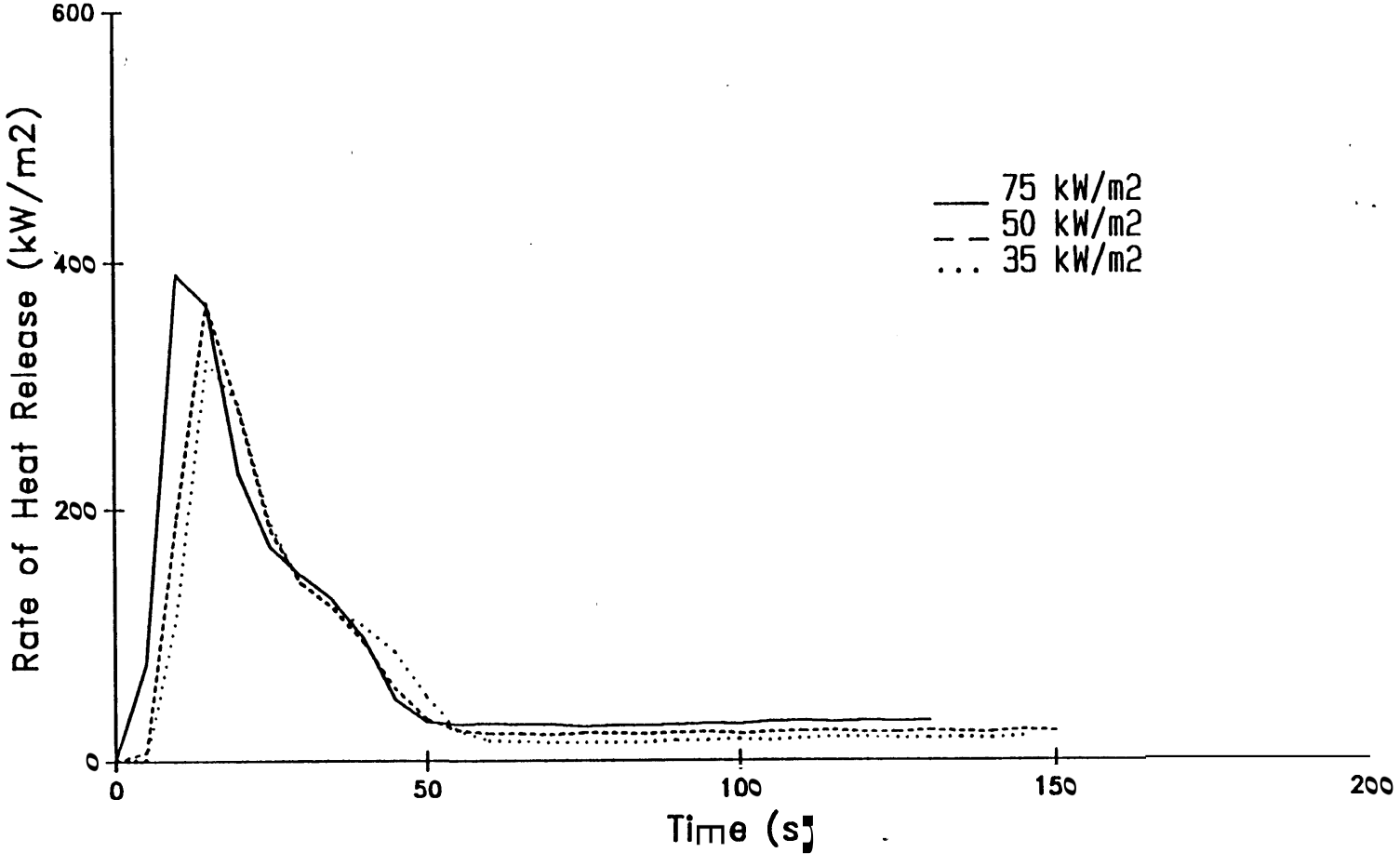

Figure 39. Rate of heat release of composite F_4/C_3 in the cone calorimeter at three external irradiances

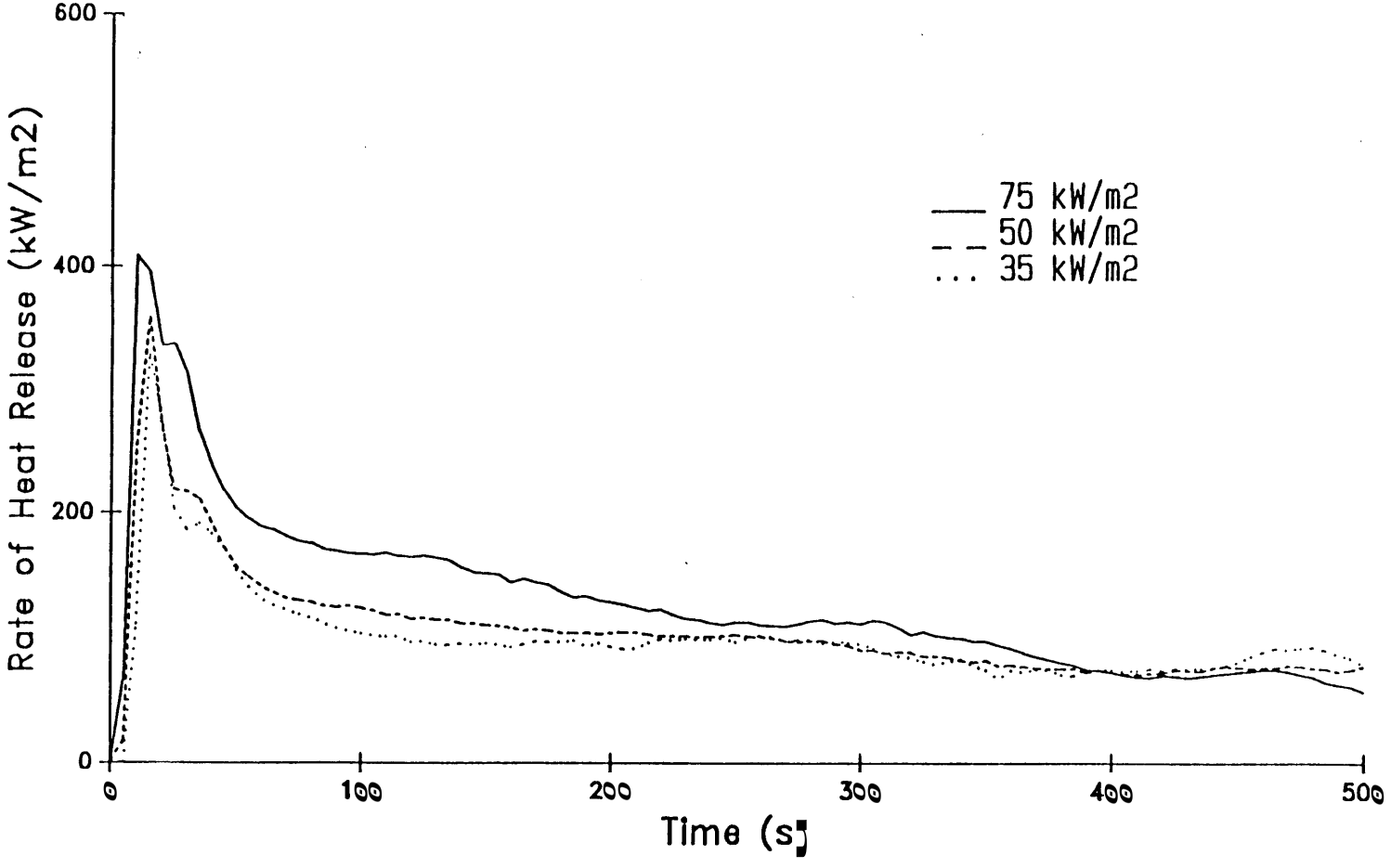

Figure 40. Rate of heat release of composite F_5/C_3 in the cone calorimeter at three external irradiances

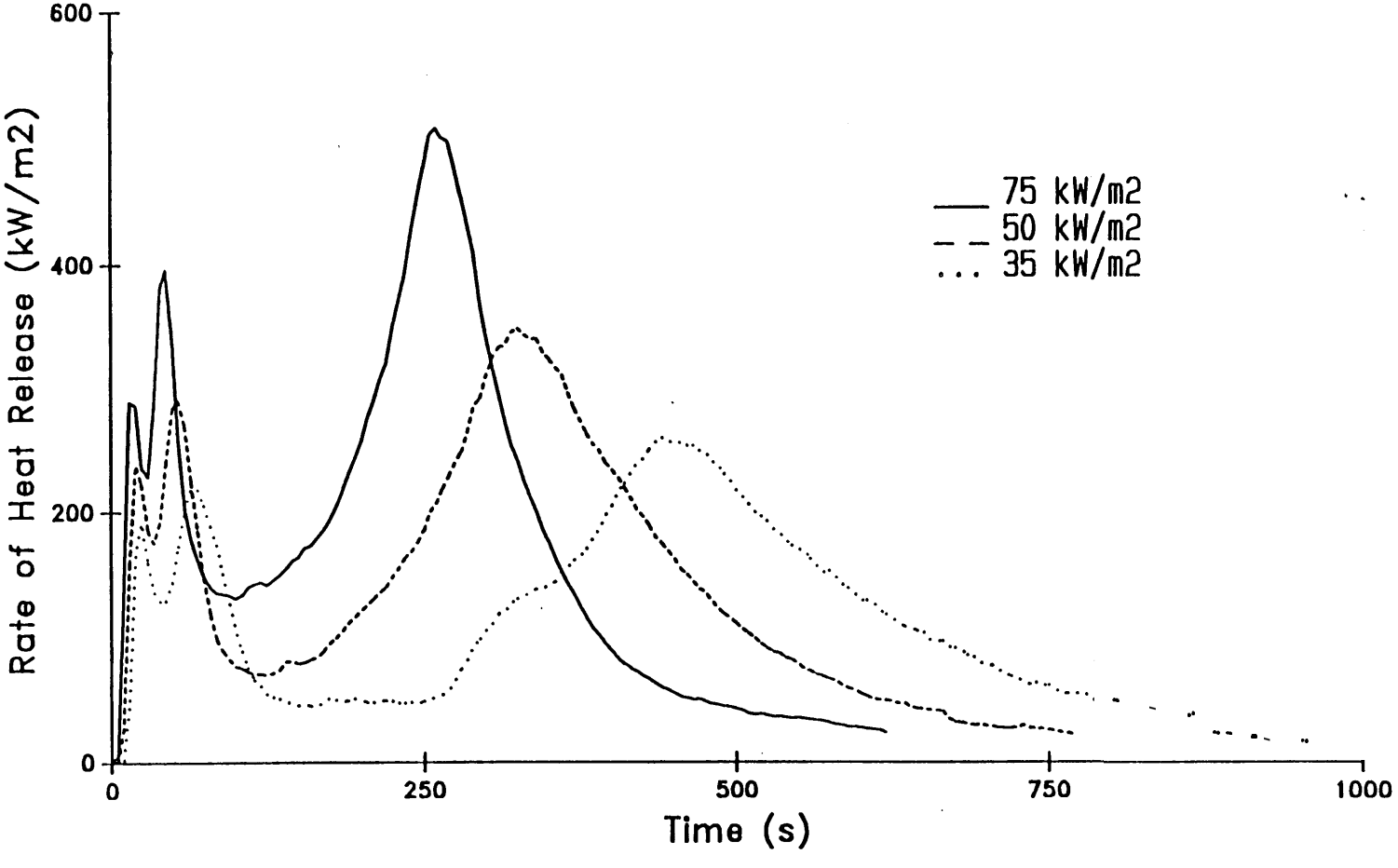

Figure 41. Rate of heat release of composite F_1/C_2 (cut) in the cone calorimeter at three external irradiances

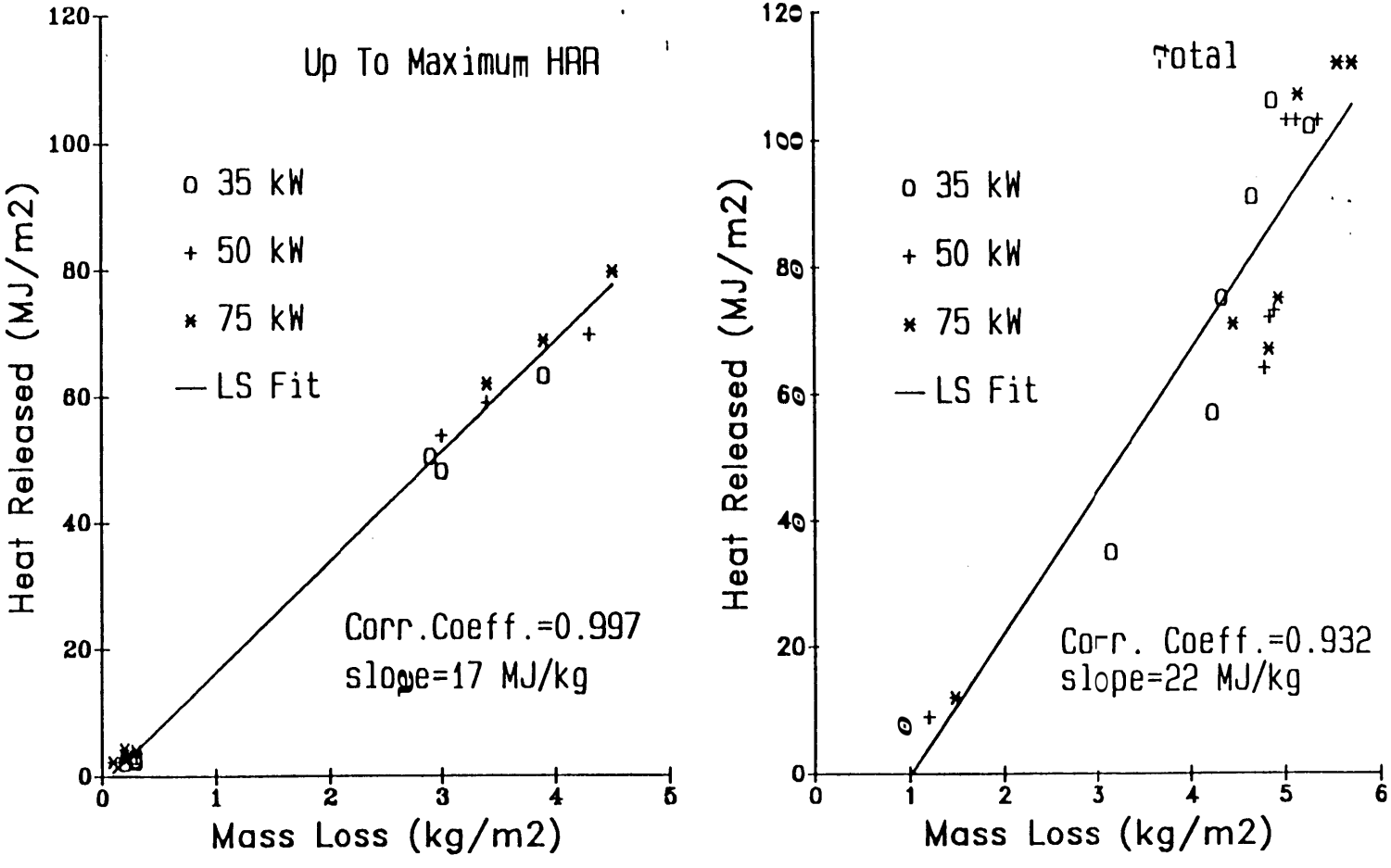

Figure 42. Total heat released and total mass loss for composites at three irradiance levels

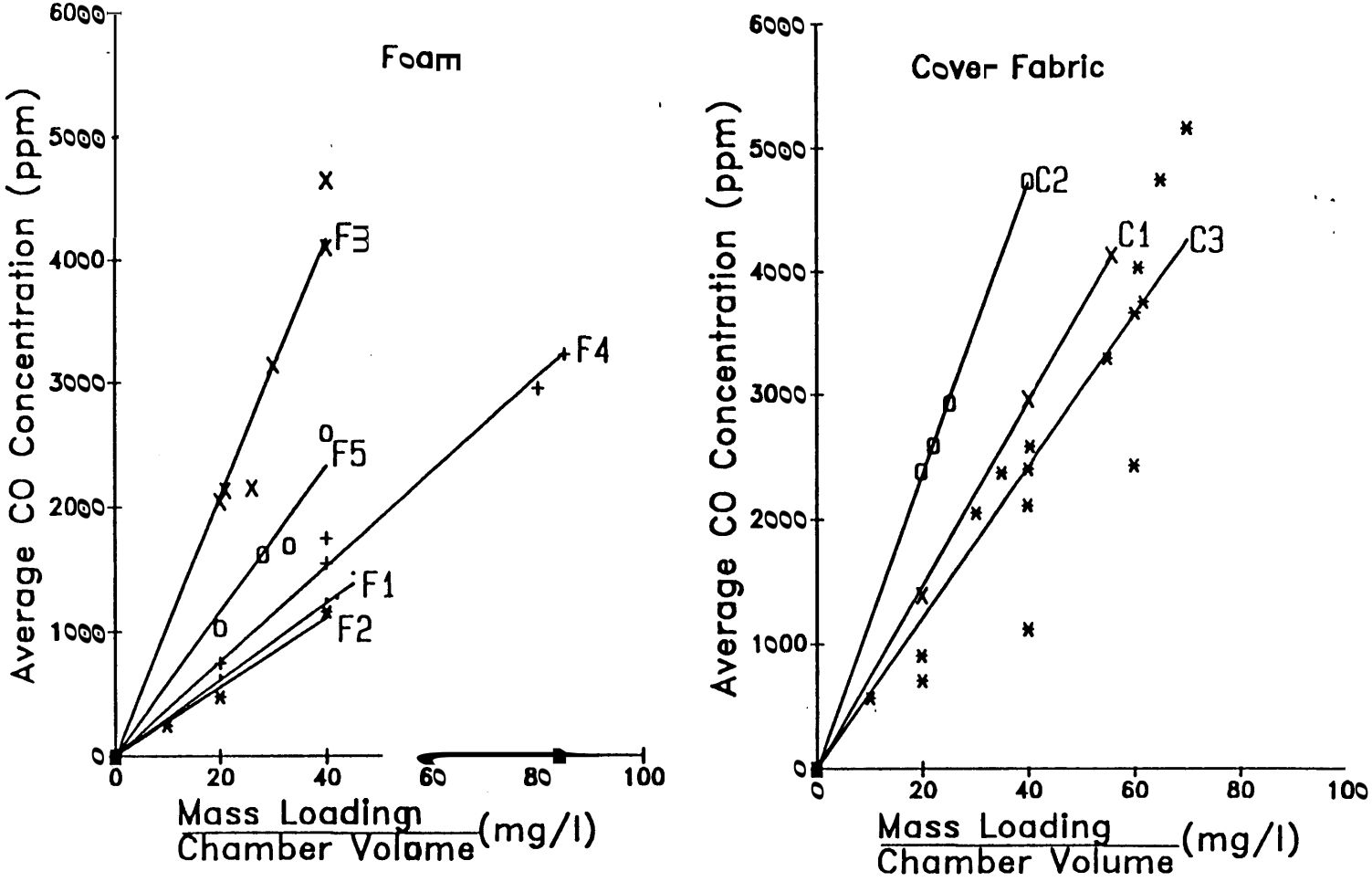

Figure 43. CO generation at various mass loadings for seat materials in the small-scale-toxicity test

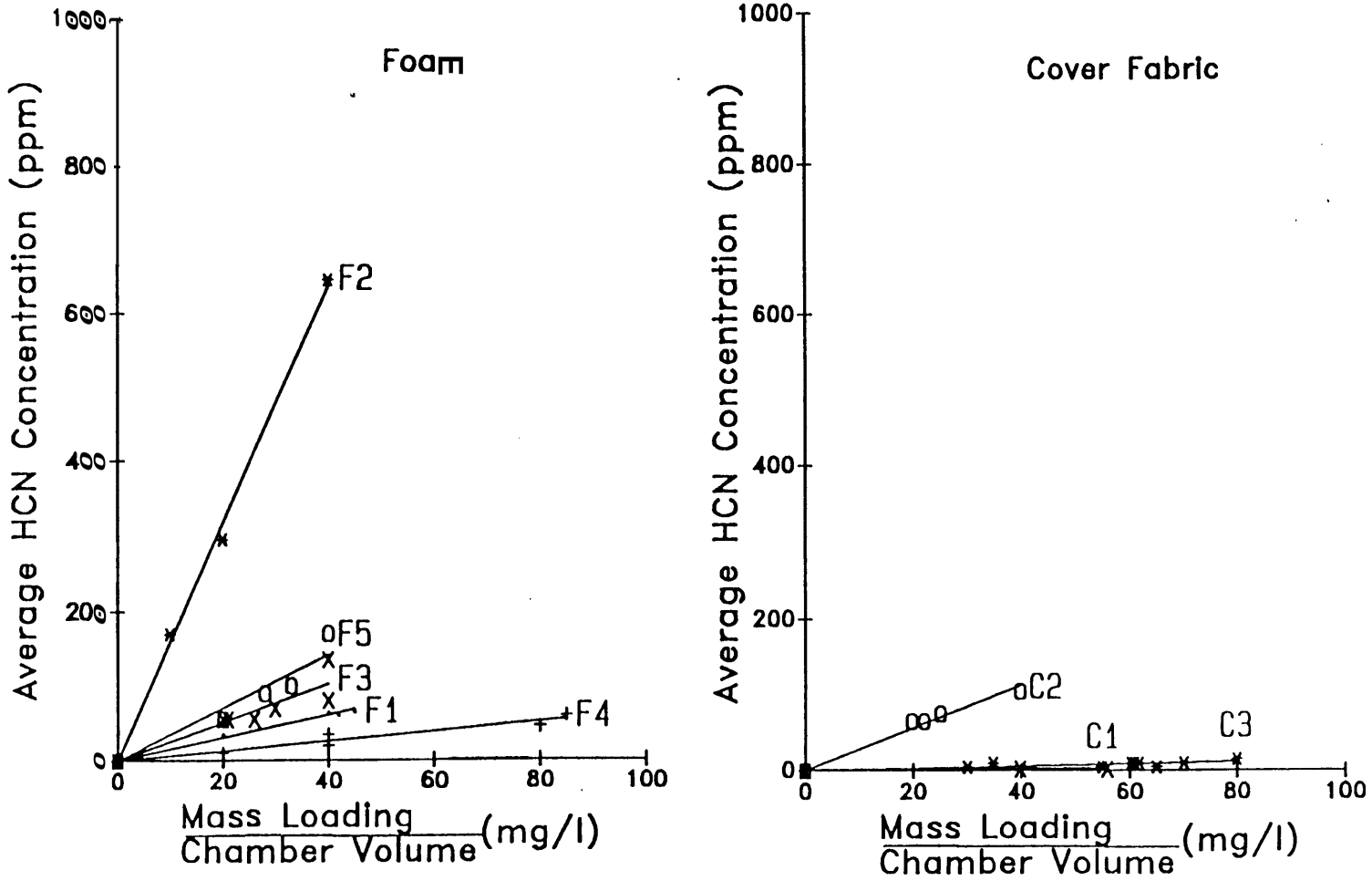

Figure 44. HCN generation at various mass loadings for seat materials in the small-scale toxicity test

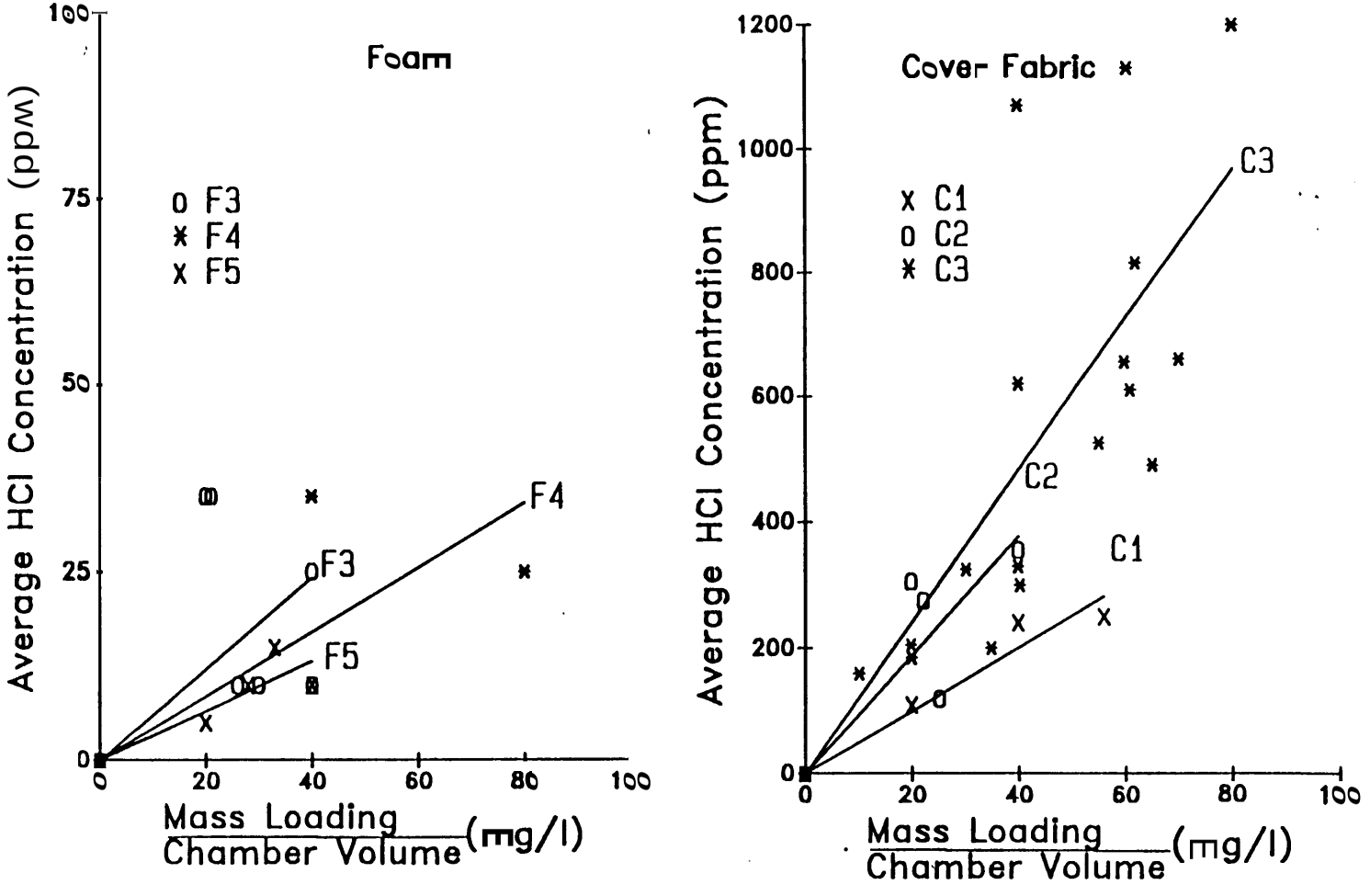

Figure 45. HCl generation at various mass loadings for seat materials in the small-scale toxicity test

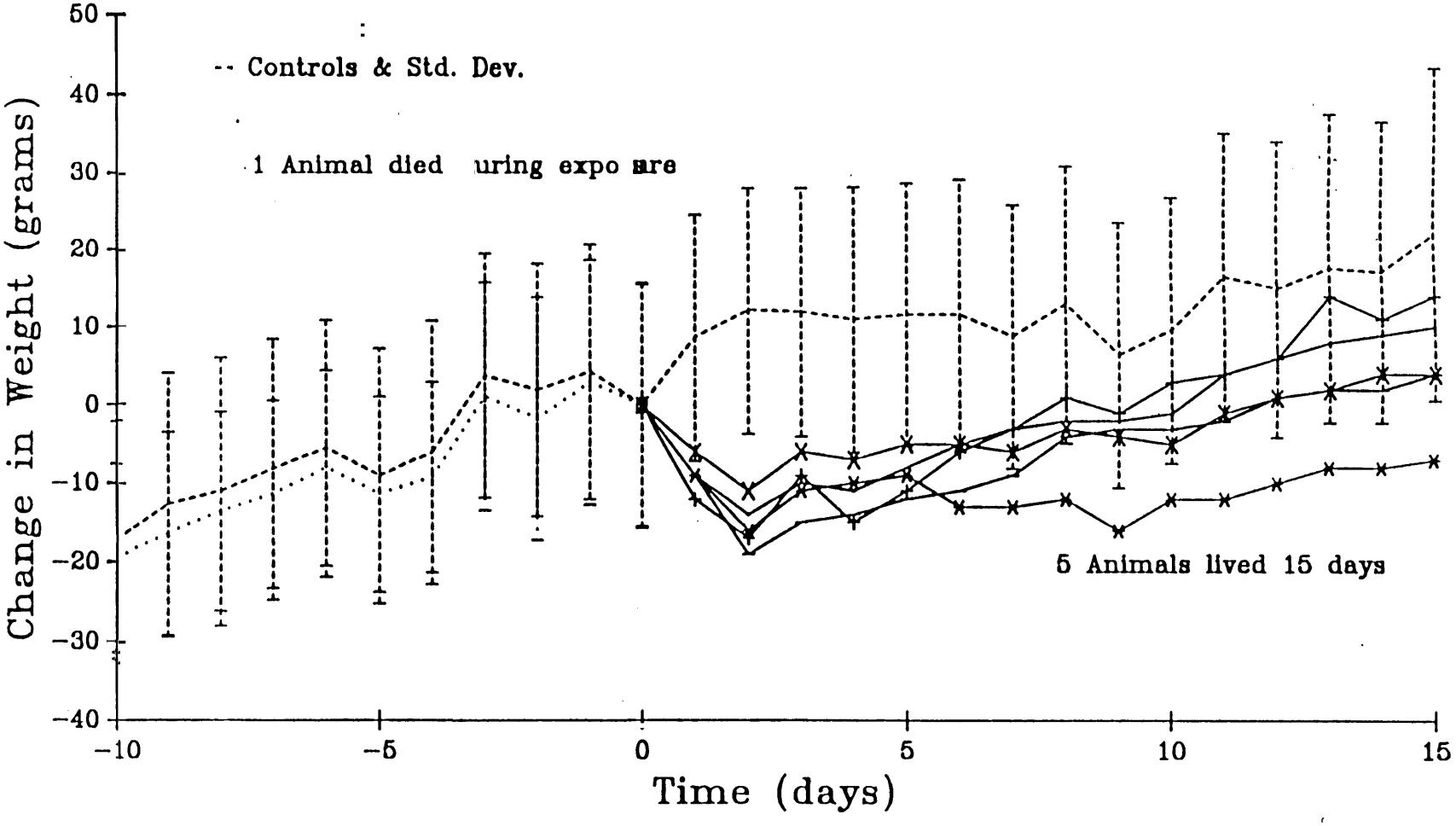

Figure 46. Individual animal weights following 30 minute exposure to 40 mg/ℓ Standard Foam (F_1)

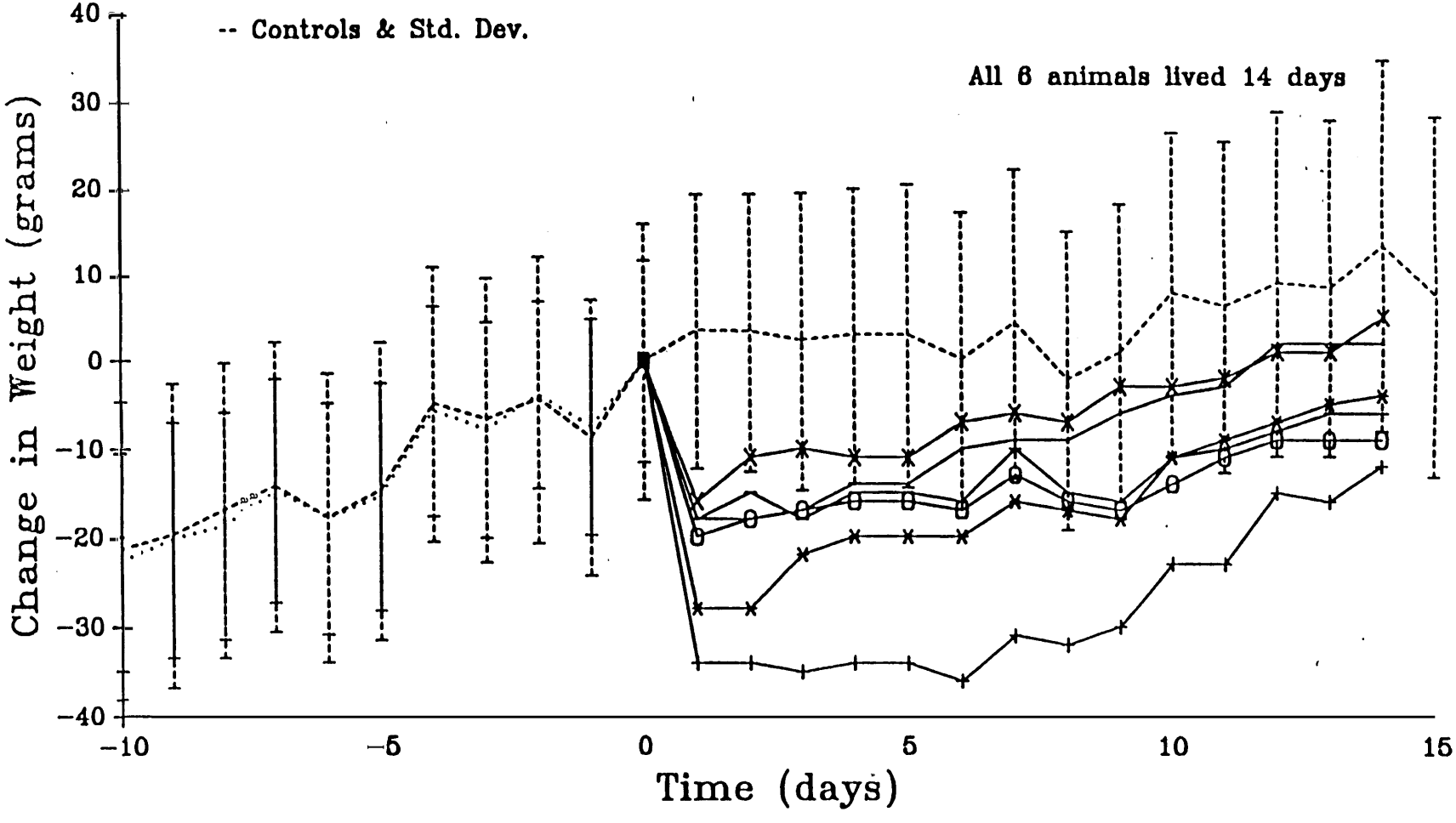

Figure 47. Individual animal weights following 30 minute exposure to 42 mg/ℓ Standard Foam (F_1)

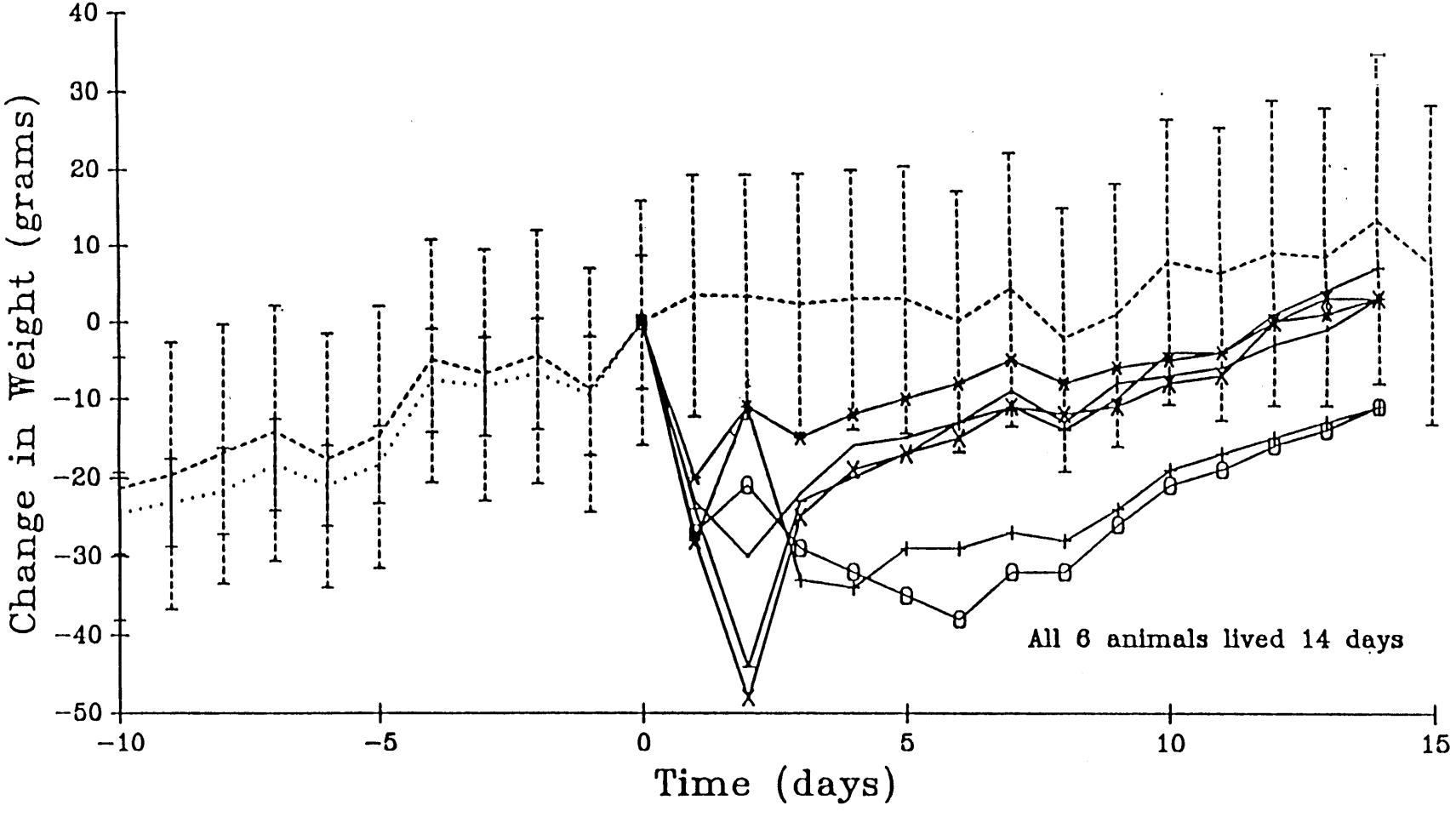

Figure 48. Individual animal weights following 30 minute exposure to 45 mg/ℓ Standard Foam (F_1)

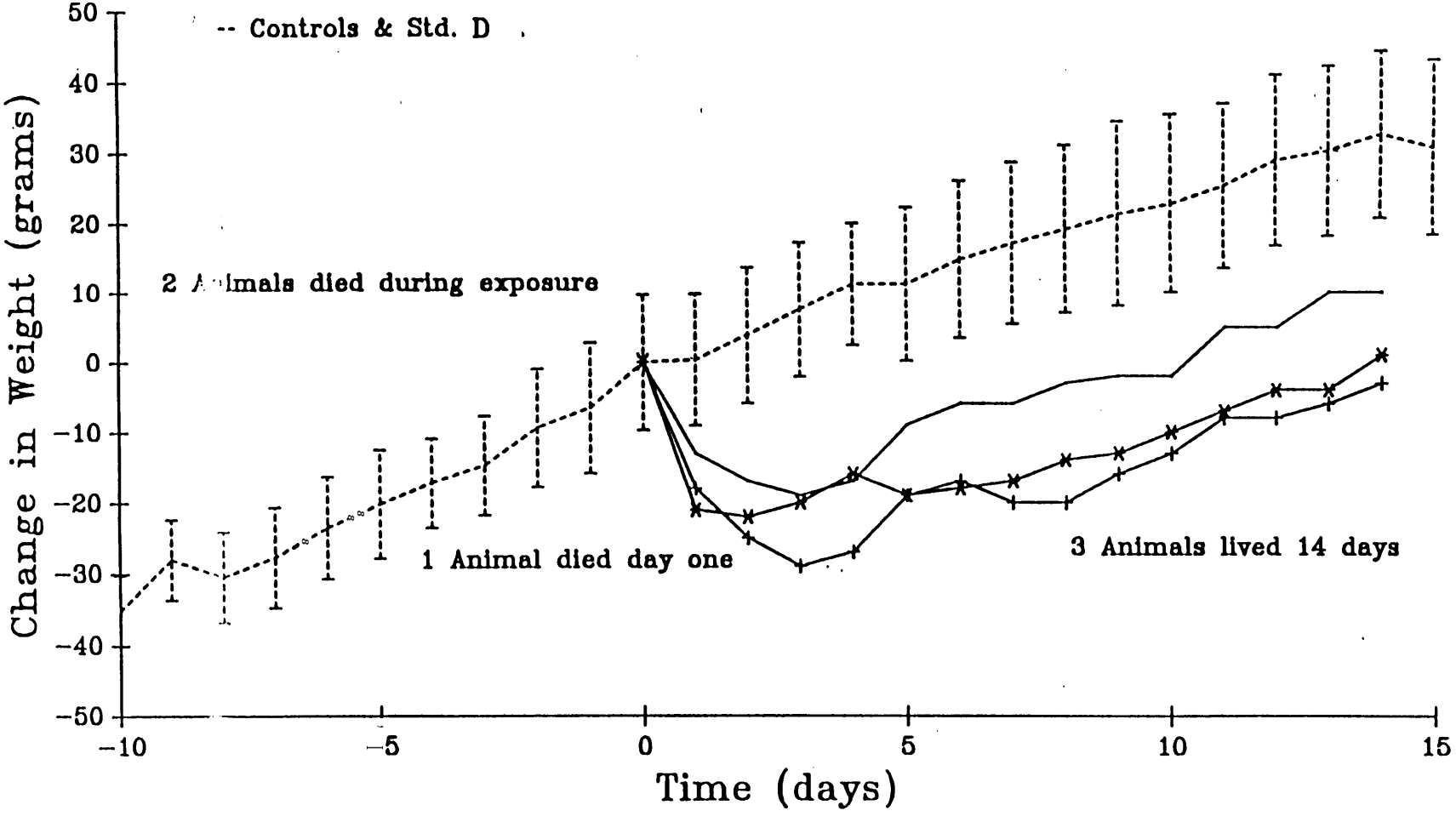

Figure 49. Individual animal weights following 30 minute exposure to 10 mg/ℓ Melamine-Treated Foam (F_2)

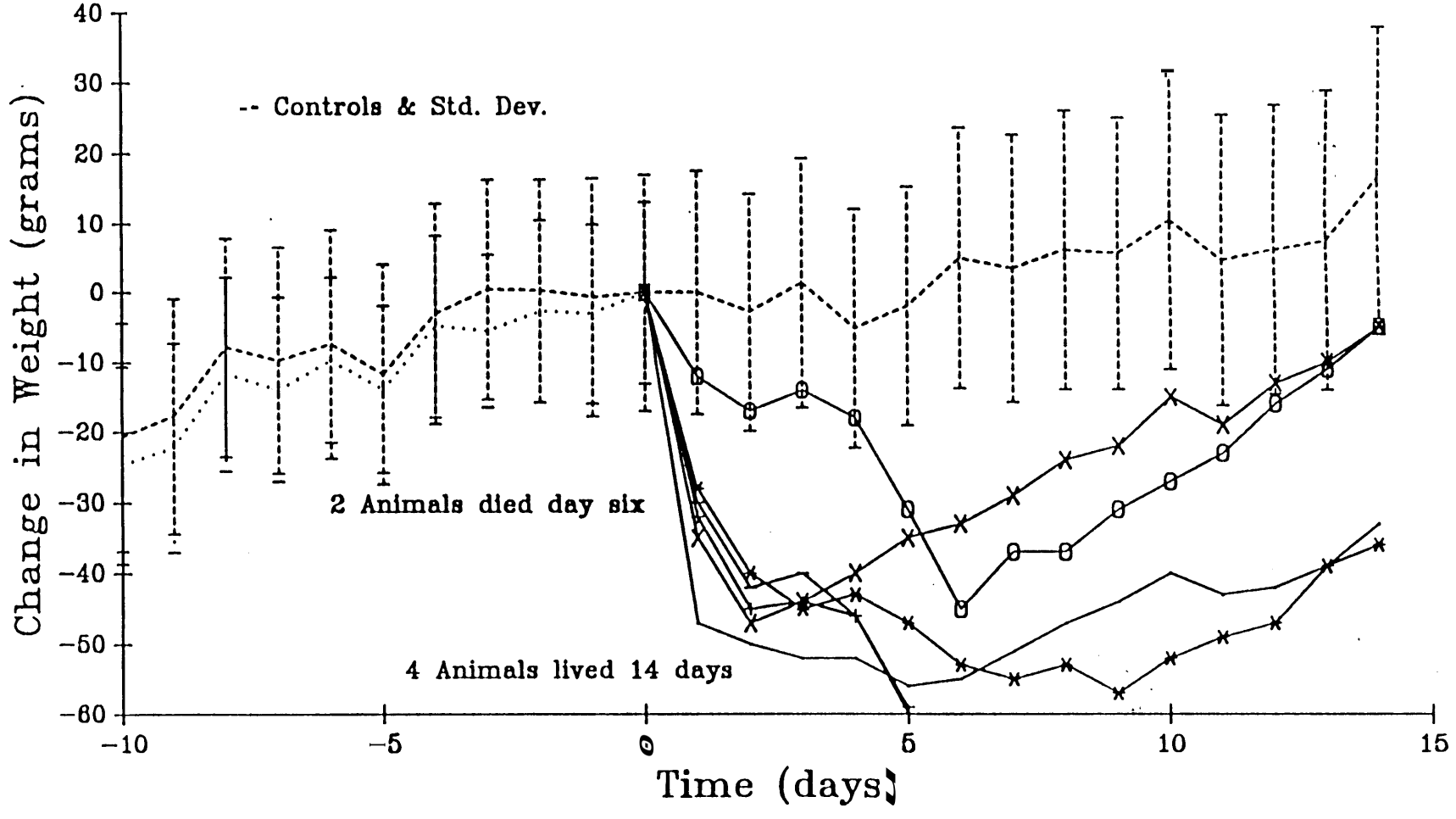

Figure 50 Individual animal weights following 30 minute exposure to 21 mg/ℓ CMHR Foam (F_3)

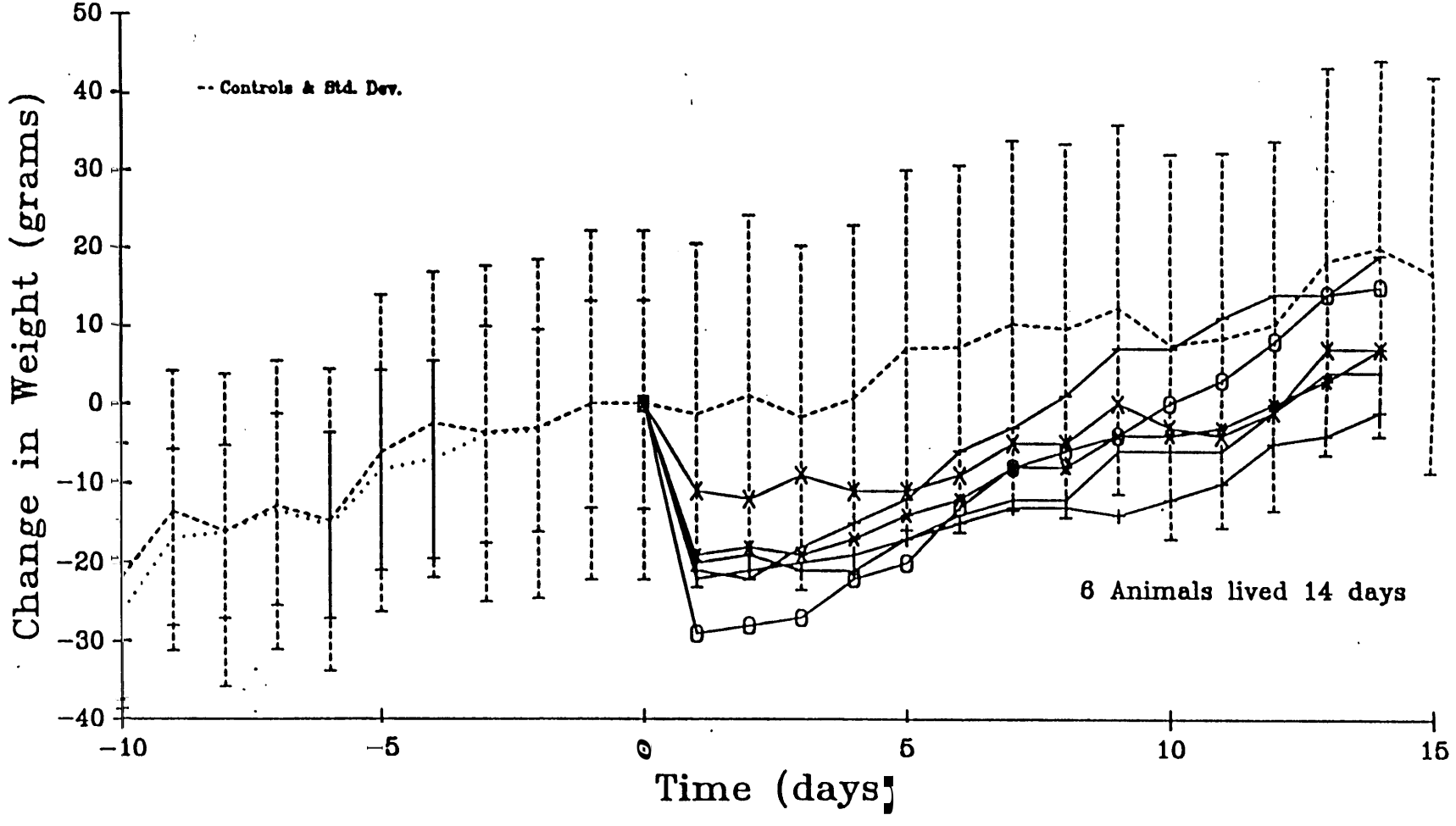

Figure 51. Individual animal weights following 30 minute exposure to 26 mg/ℓ CMHR Foam (F_3)

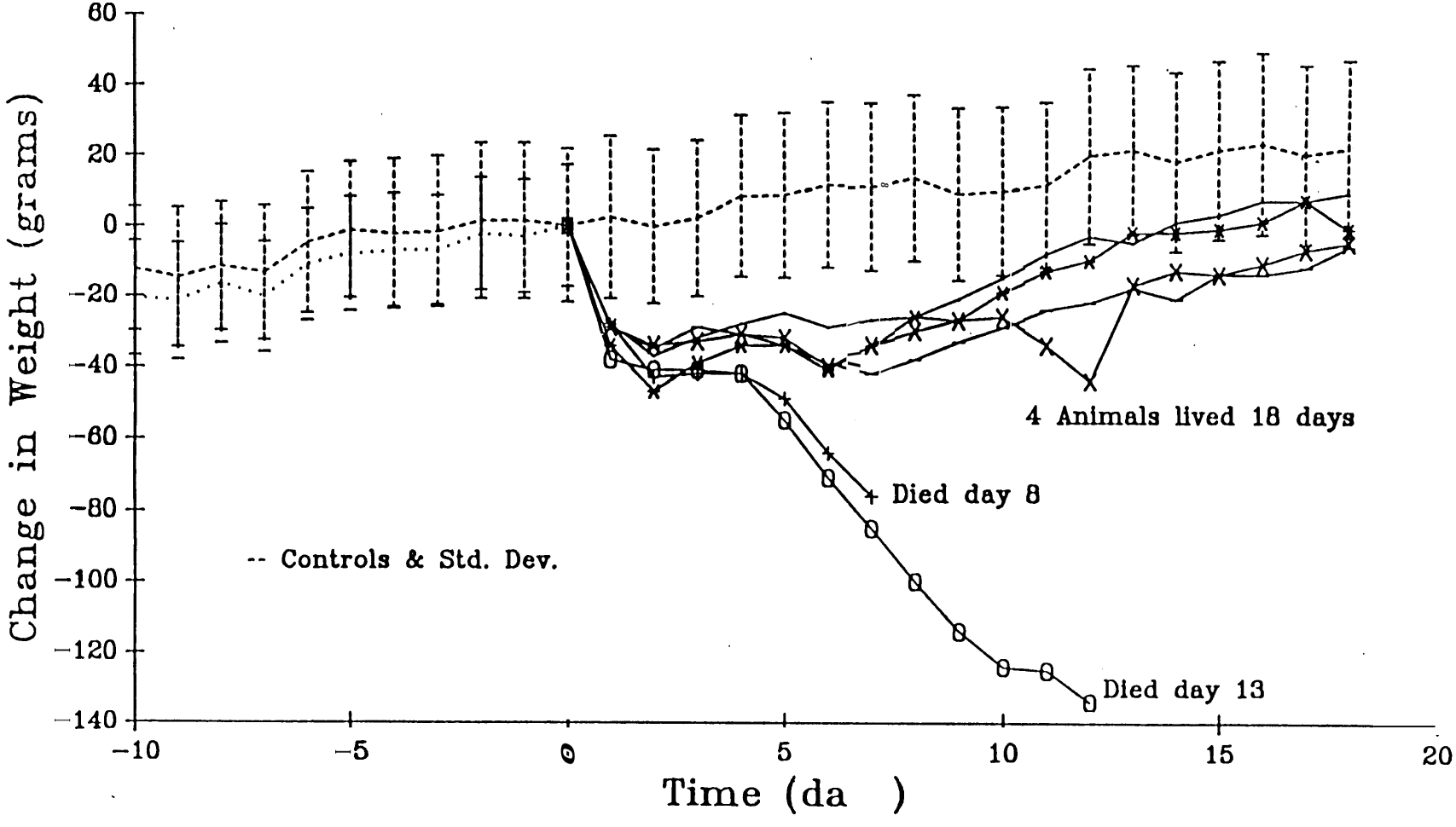

Figure 52 Individual animal weights following 30 minute exposure to 30 mg/ℓ CMHR Foam (F_3).

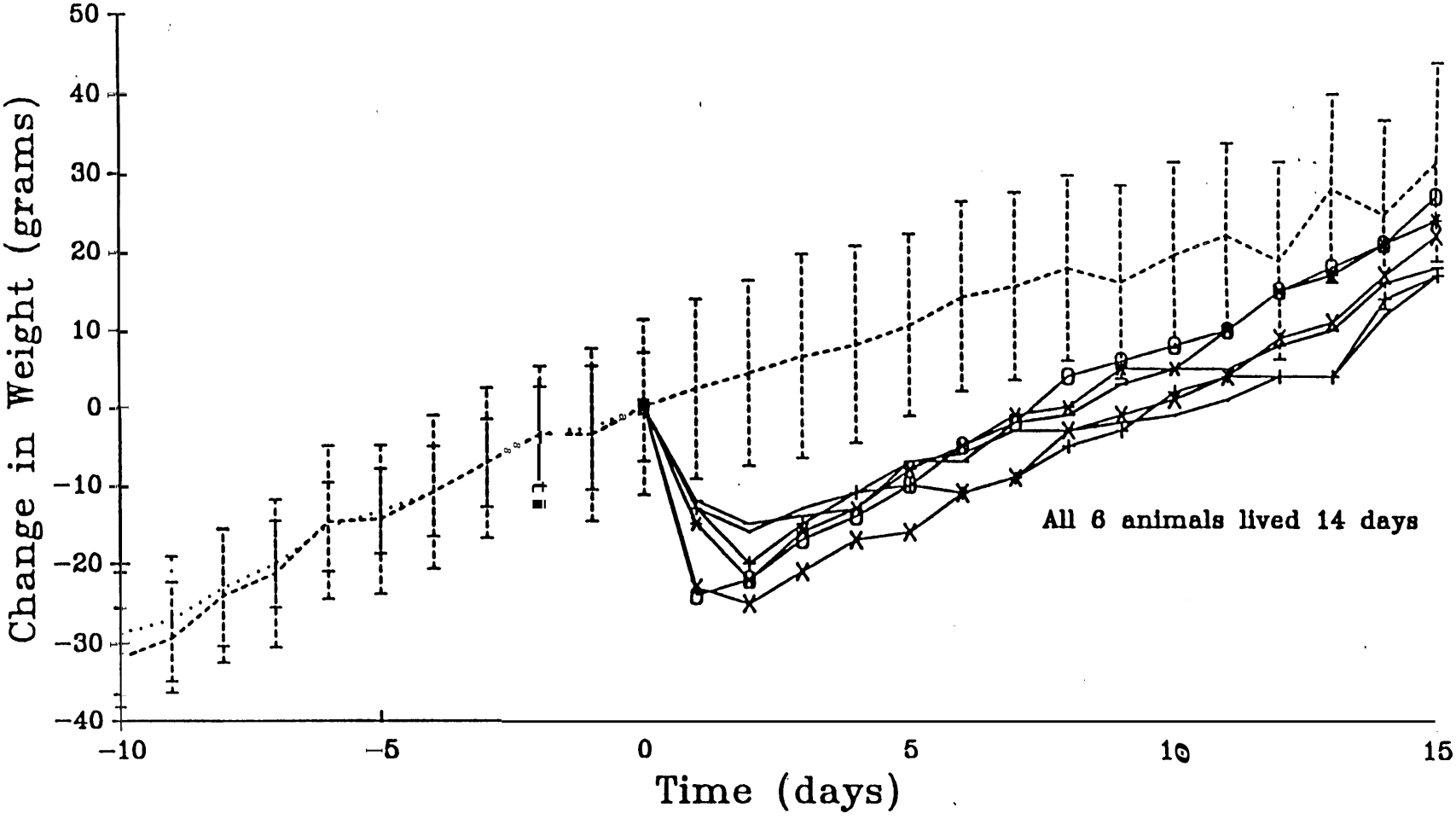

Figure 53. Individual animal weights following 30 minute exposure to 40 mg/ℓ Neoprene Foam (F_4)

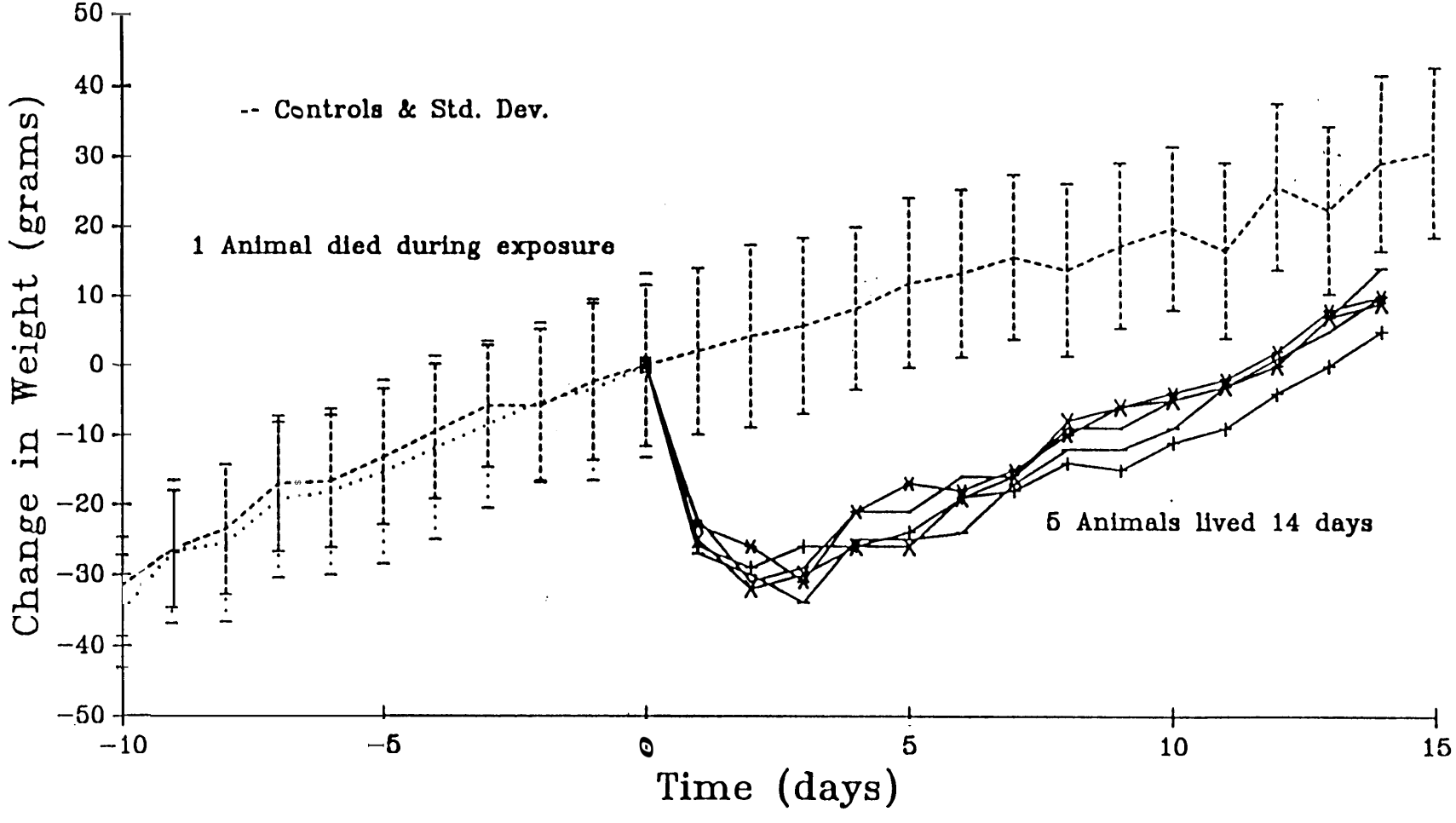

Figure 54. Individual animal weights following 30 minute exposure to 80 mg/ℓ Neoprene Foam (F_4)

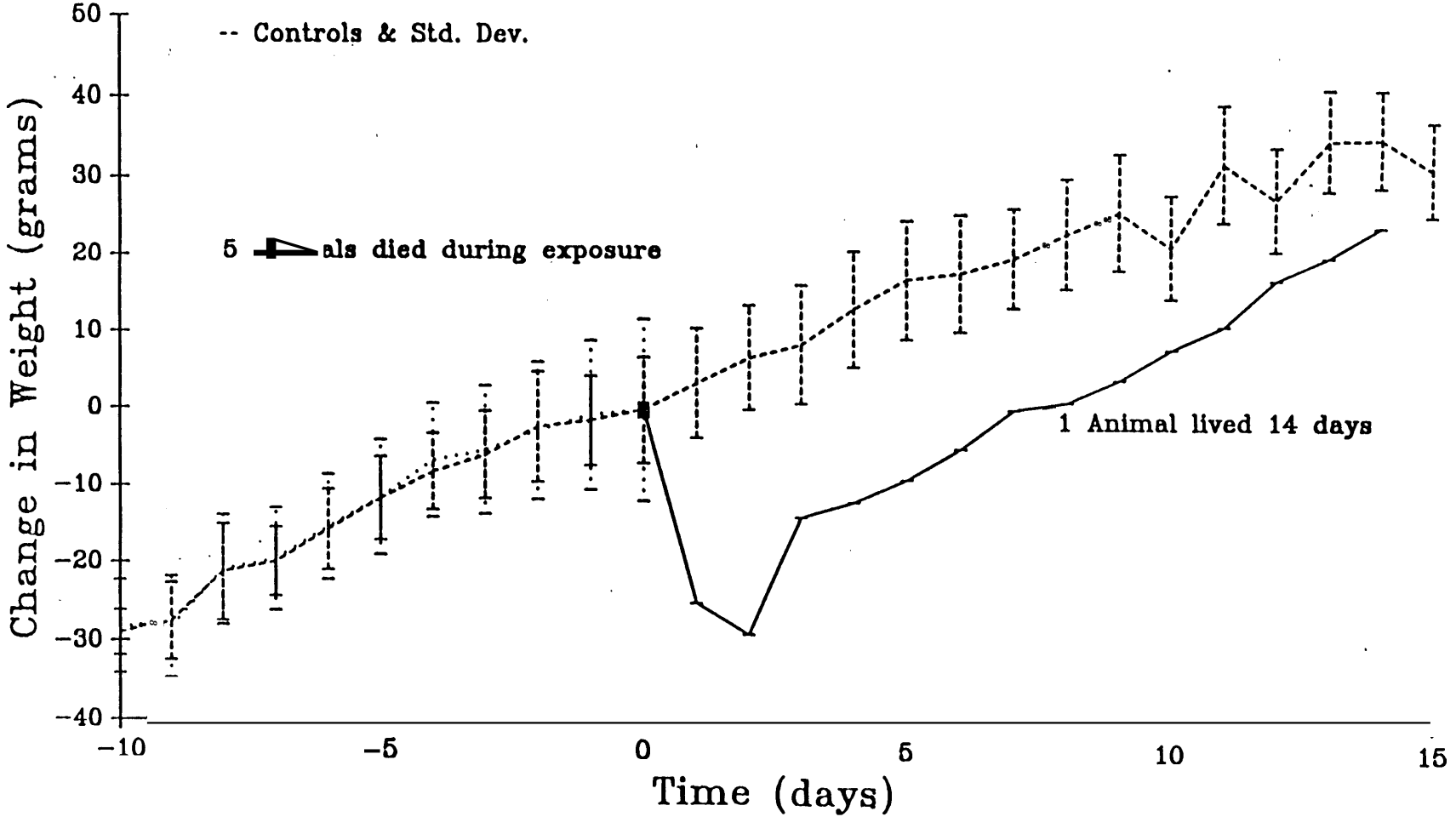

Figure 55. Individual animal weights following 30 minute exposure to 85 mg/ℓ Neoprene Foam (F_4)

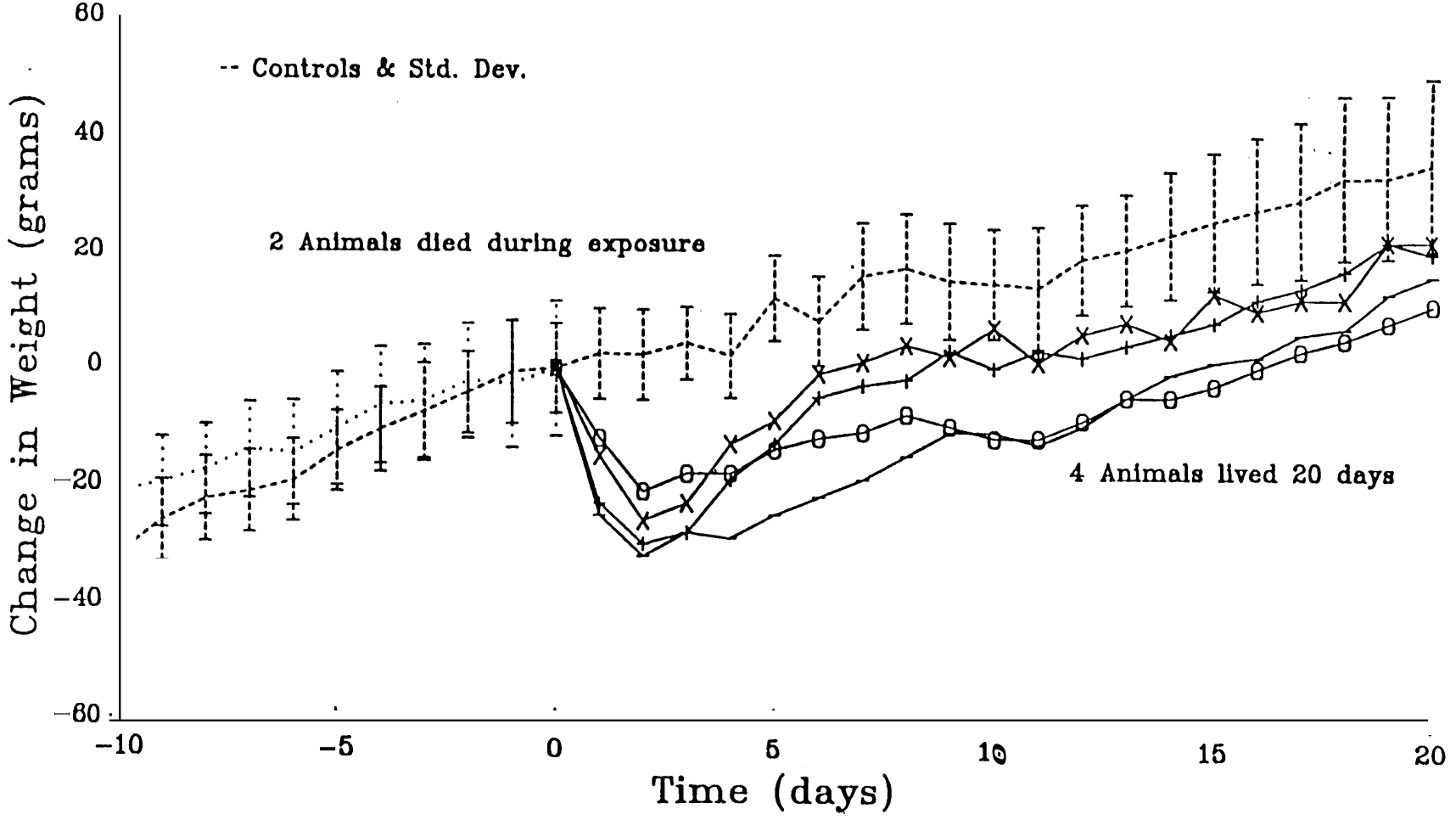

Figure 58. Individual animal weights following 30 minute exposure to 25 mg/ℓ Kevlar-Backed Vinyl (C_2)

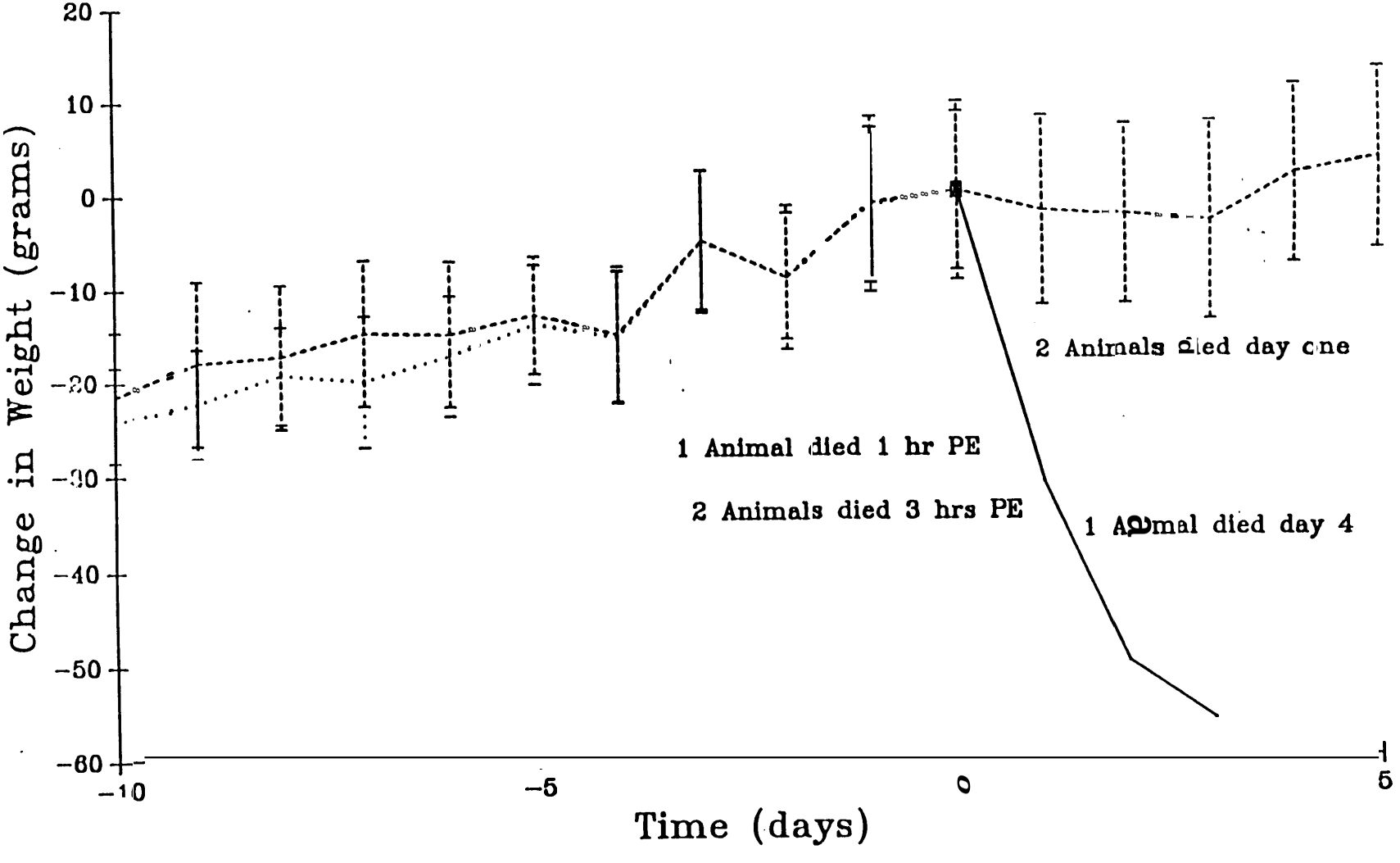

Figure 59. Individual animal weights following 30 minute exposure to 40 mg/ℓ UMTA-Type Vinyl (C_3)

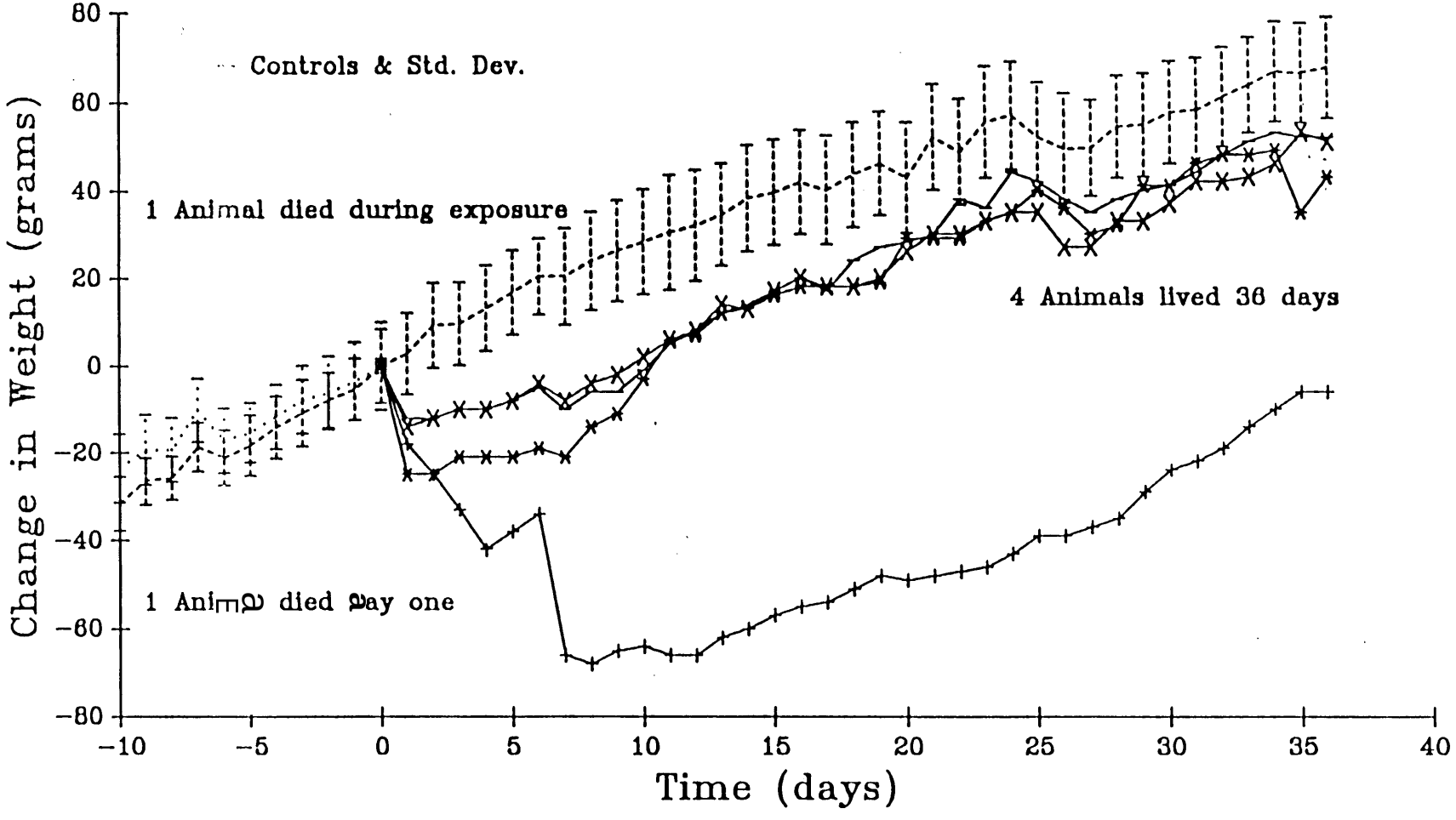

Figure 56. Individual animal weights following 30 minute exposure to 33 mg/ℓ IMPAK Foam (F_5)

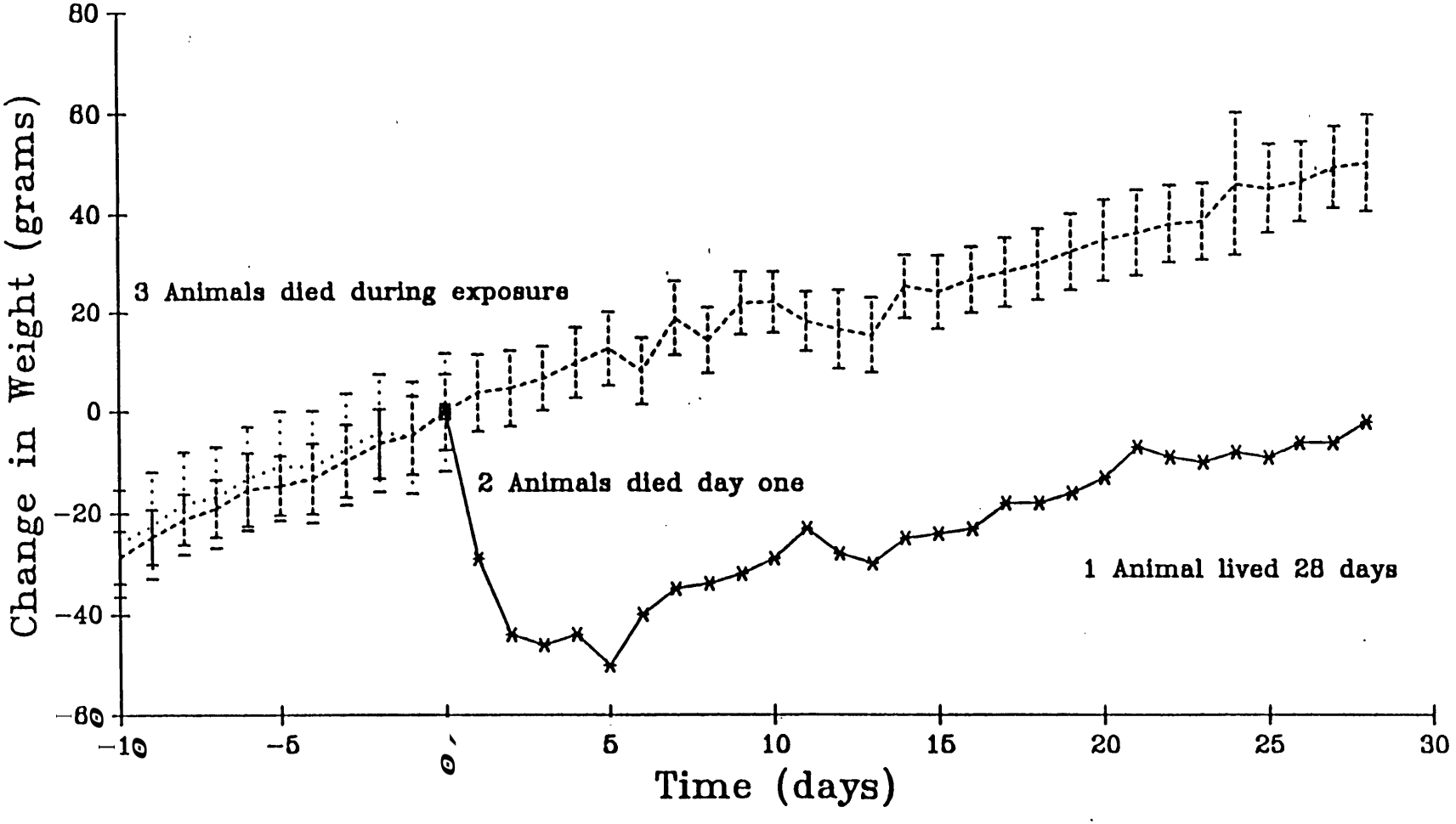

Figure 57. Individual animal weights following 30 minute exposure to 55.9 mg/ℓ Standard Vinyl (C_1)

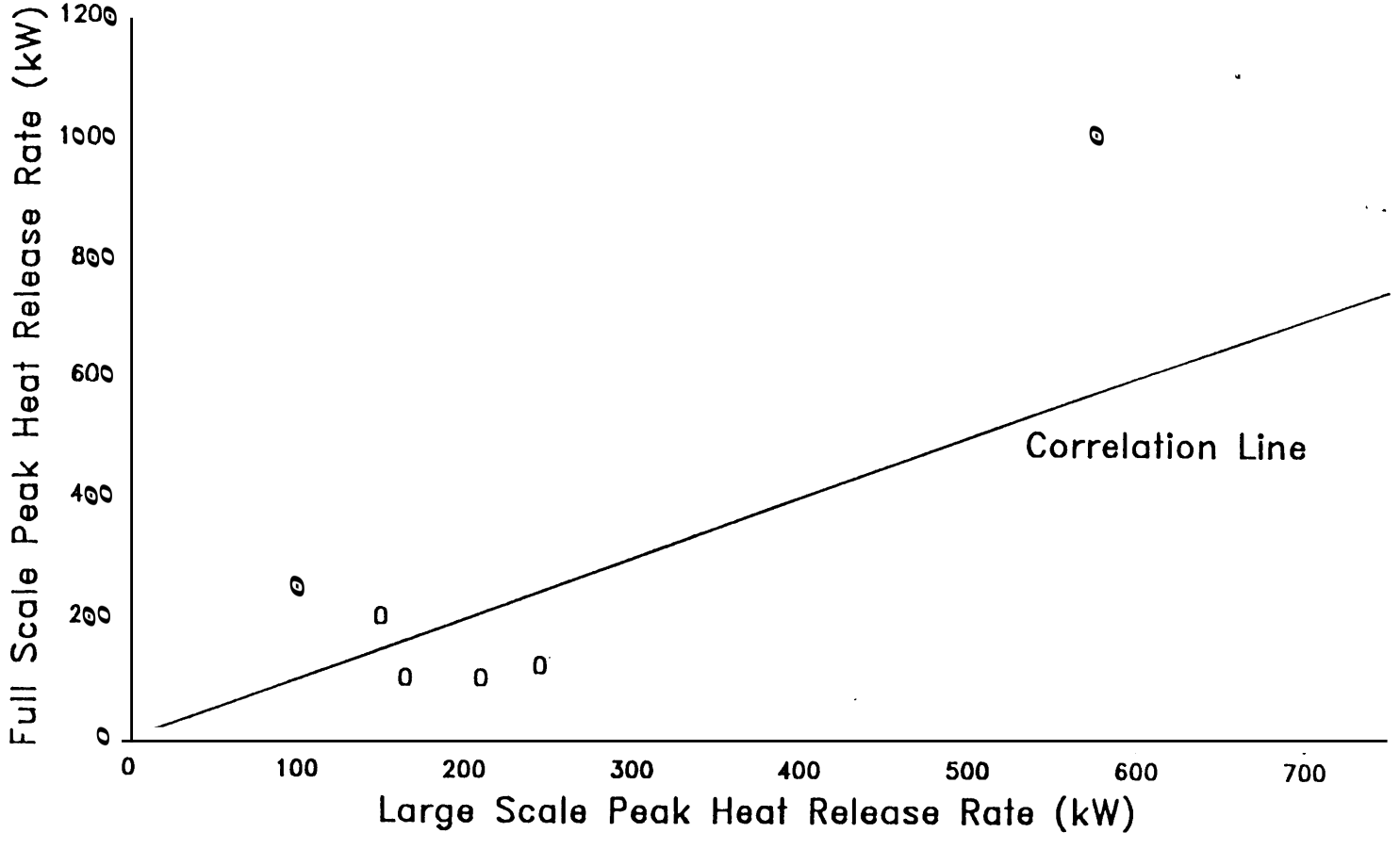

Figure 60. Comparison of large-scale and full-scale peak heat release rates

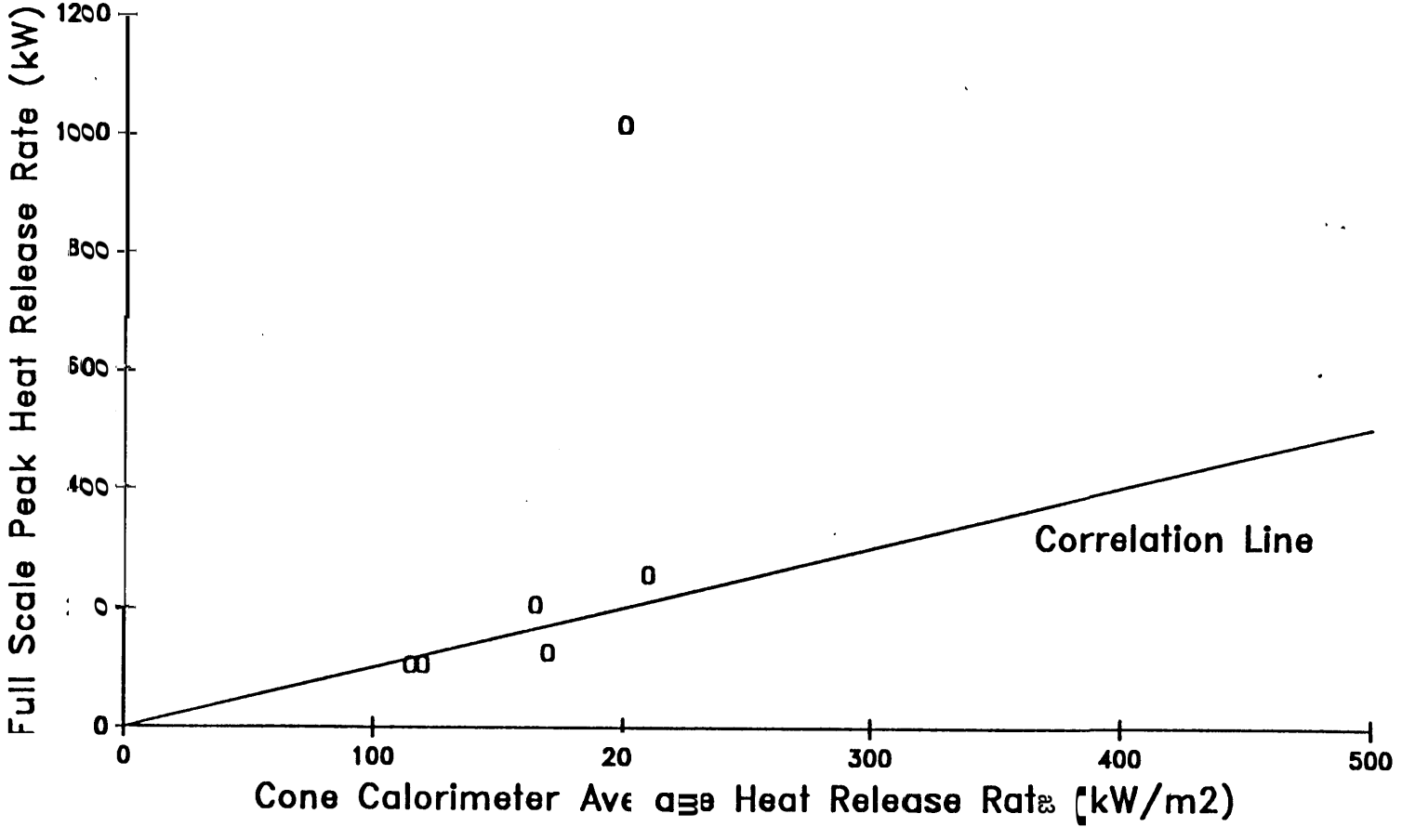

Figure 61. Comparison of 60 s average heat release rate and full-scale peak heat release rate

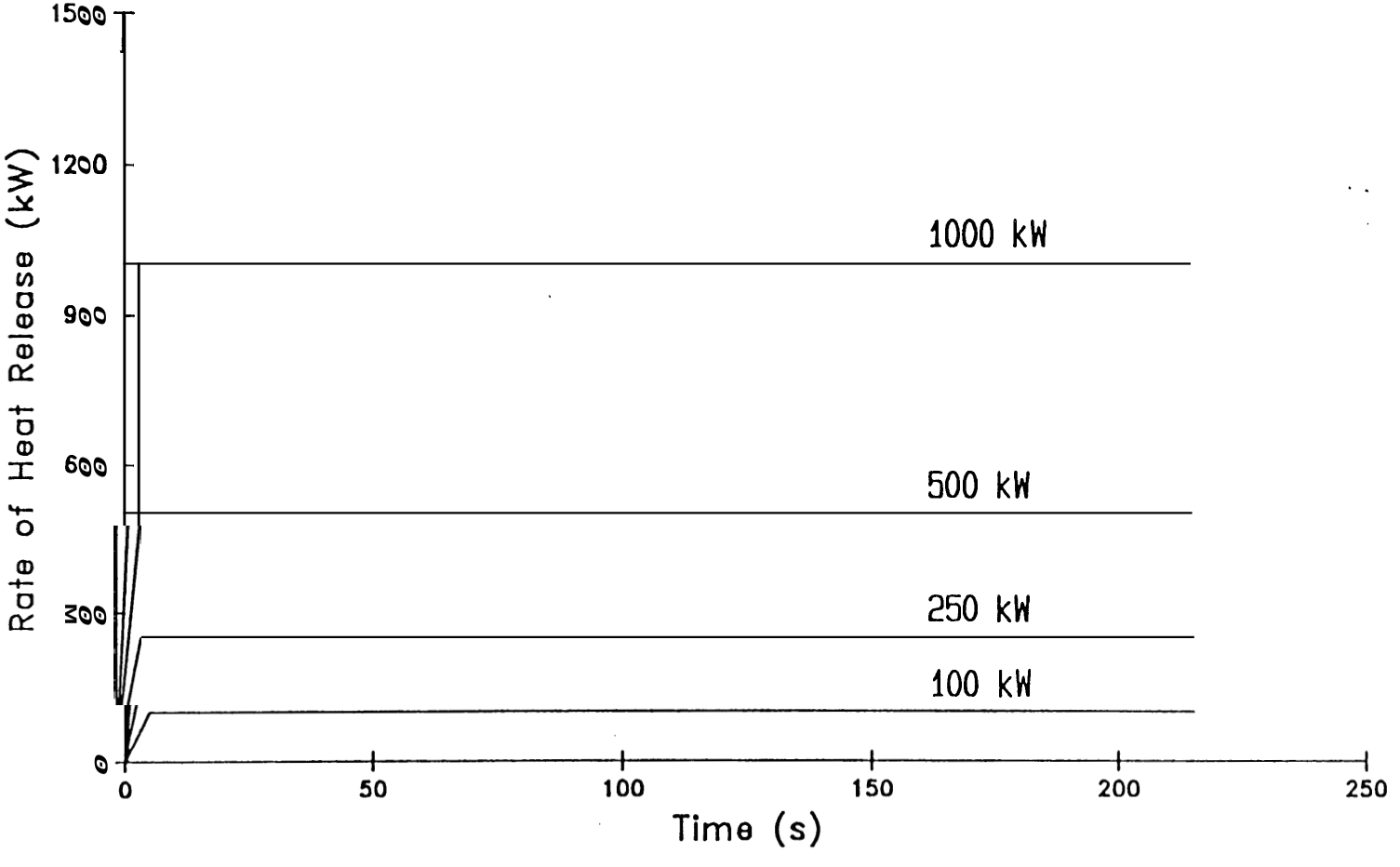

Figure 62. Heat release rates for four test cases used in HAZARD I

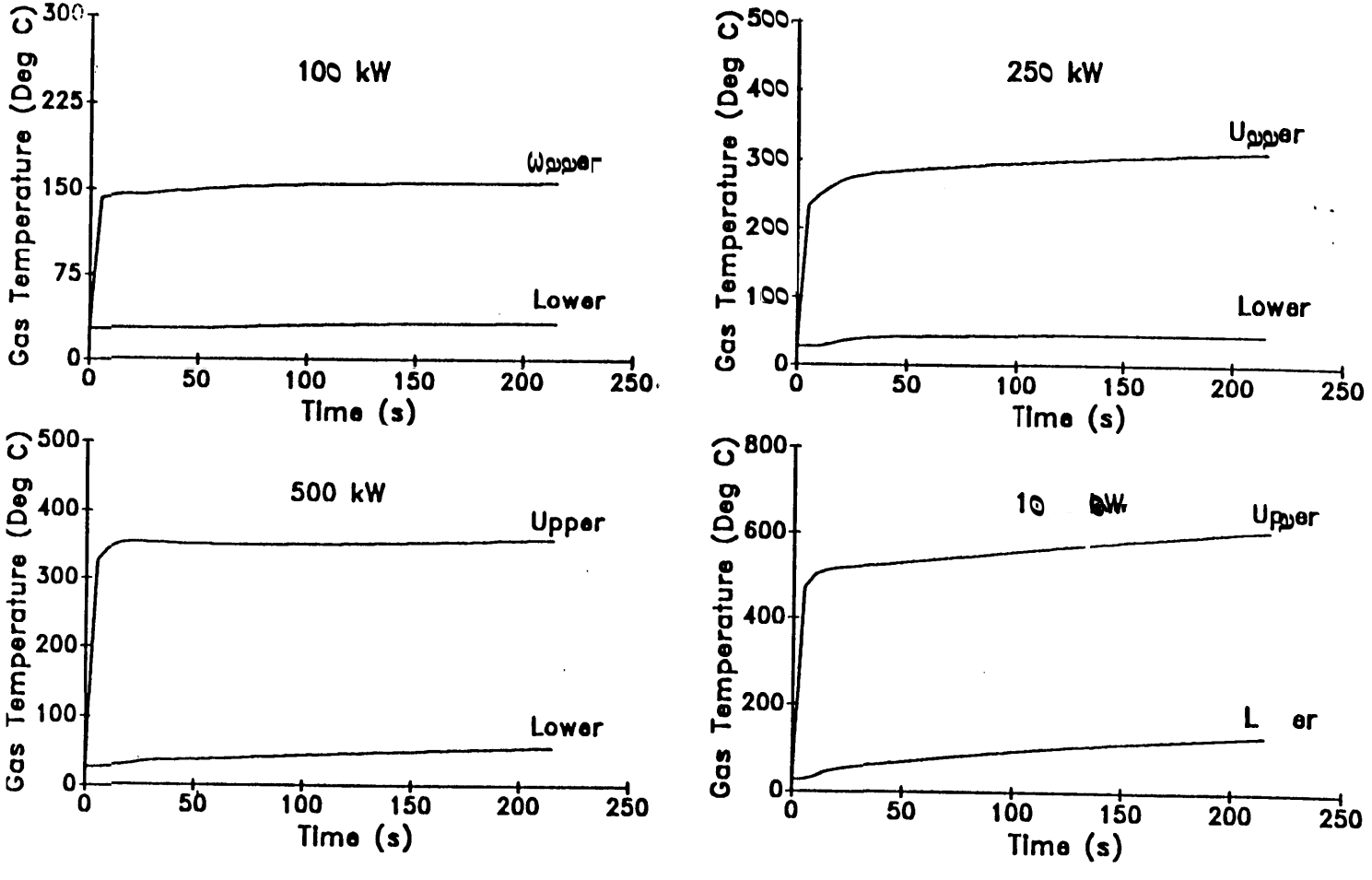

Figure 63. Calculated upper and lower temperatures in compartment simulating a bus enclosure for four heat release rates

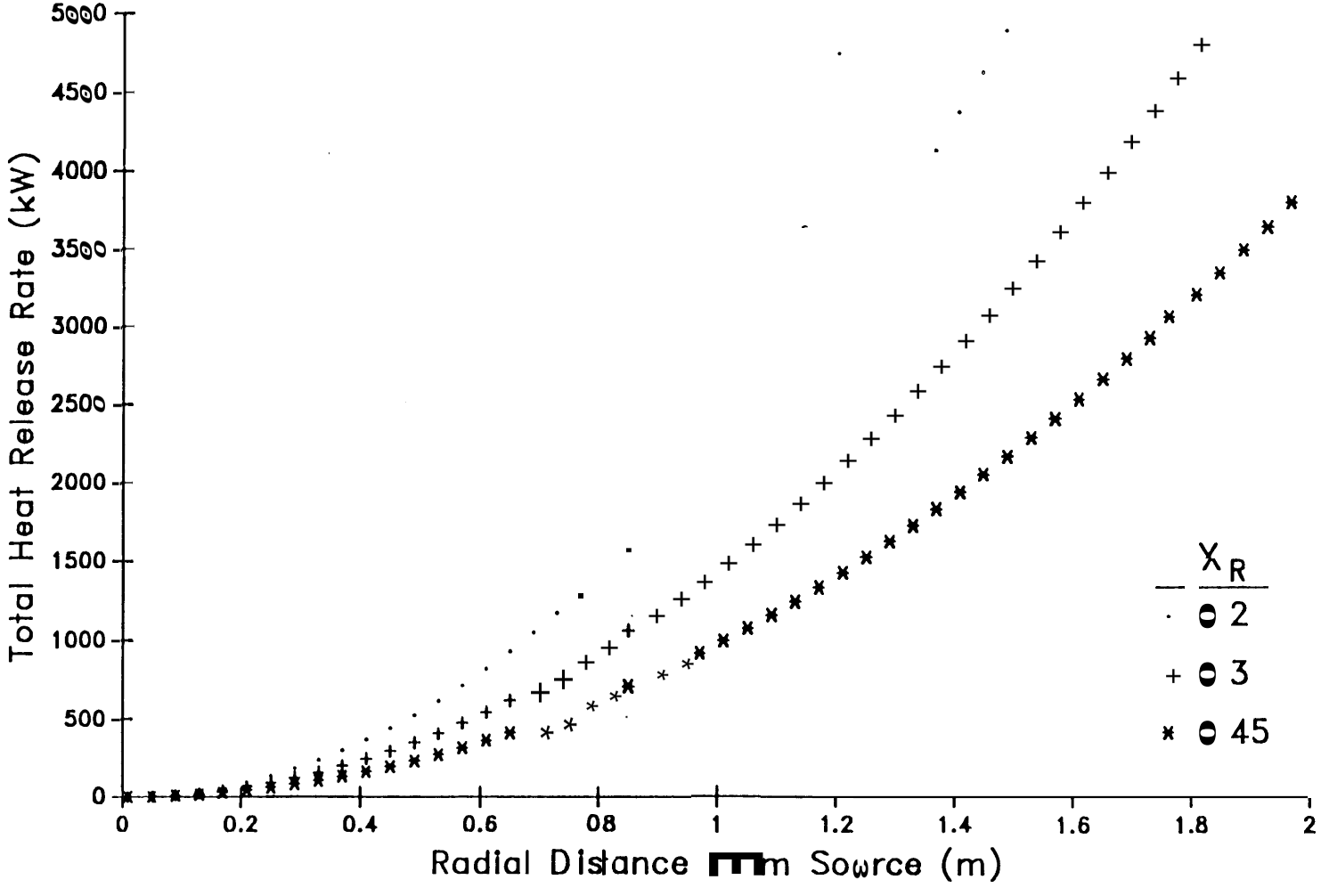

Figure 64. Total heat release for a source producing an incident irradiance of 35 kW/m^2

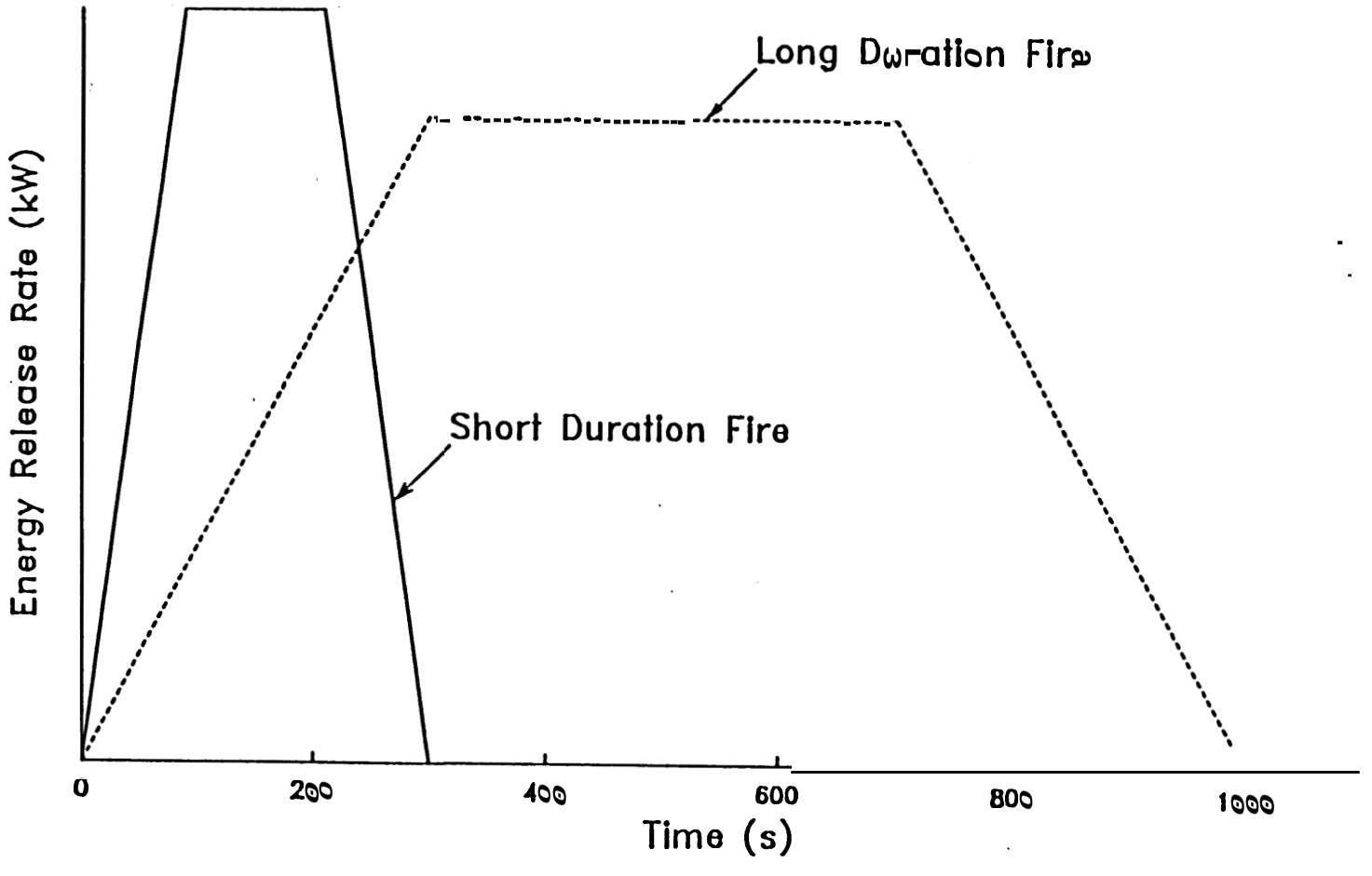

Figure 65. Representative energy release curves for bus seat assemblies

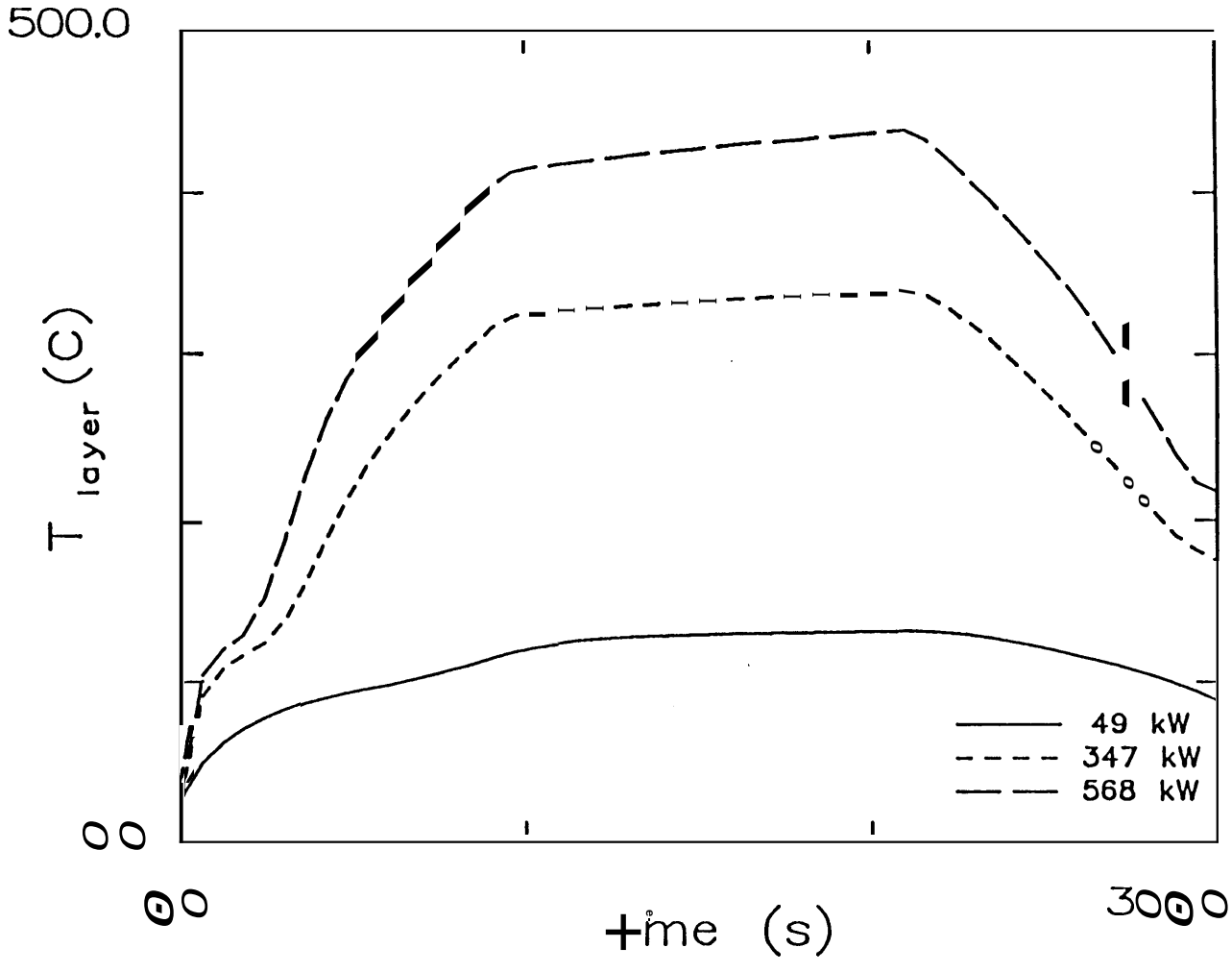

Figure 66. Calculated upper layer temperatures for 300 s duration fire

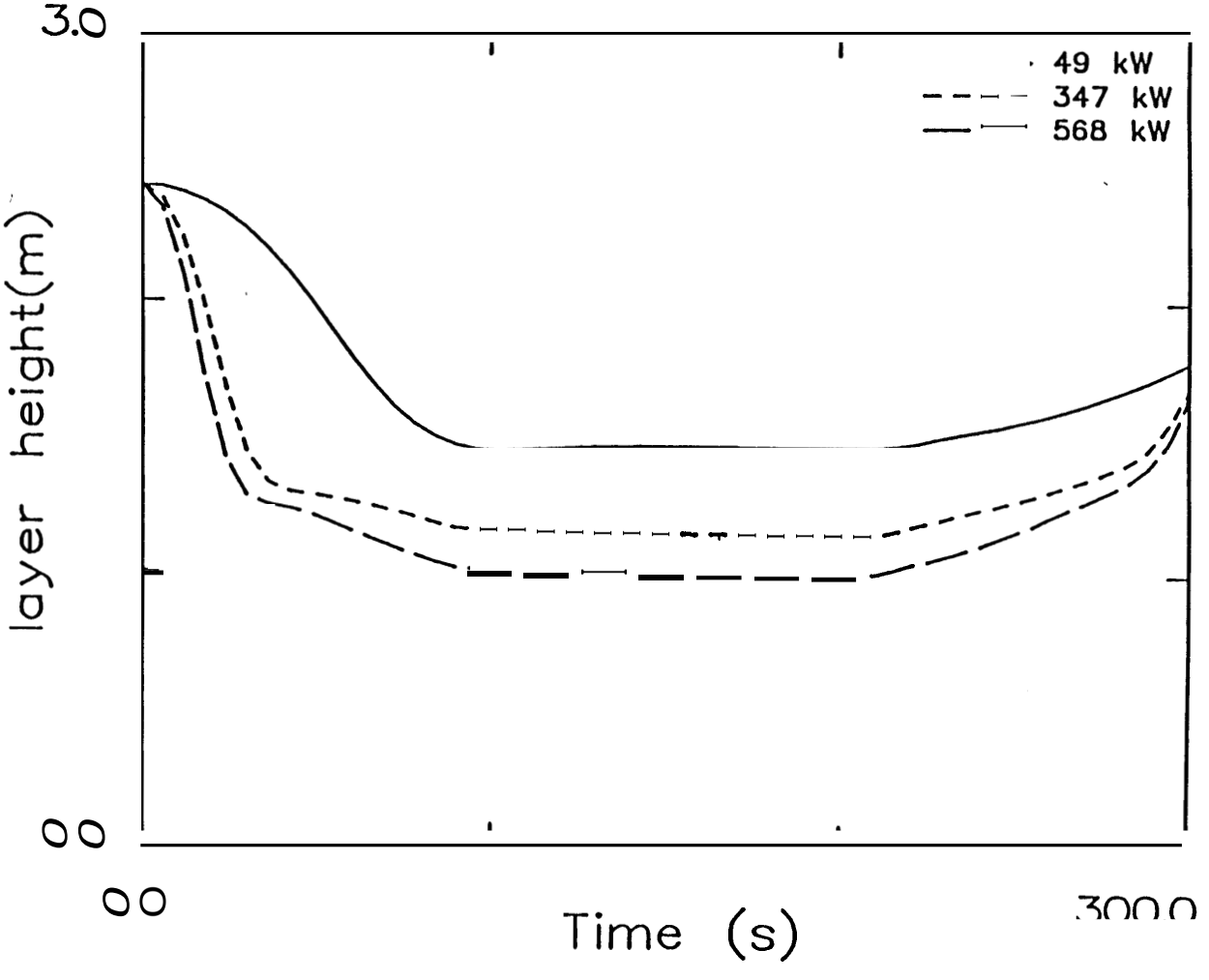

Figure 67. Calculated interface height for 300 s duration fires

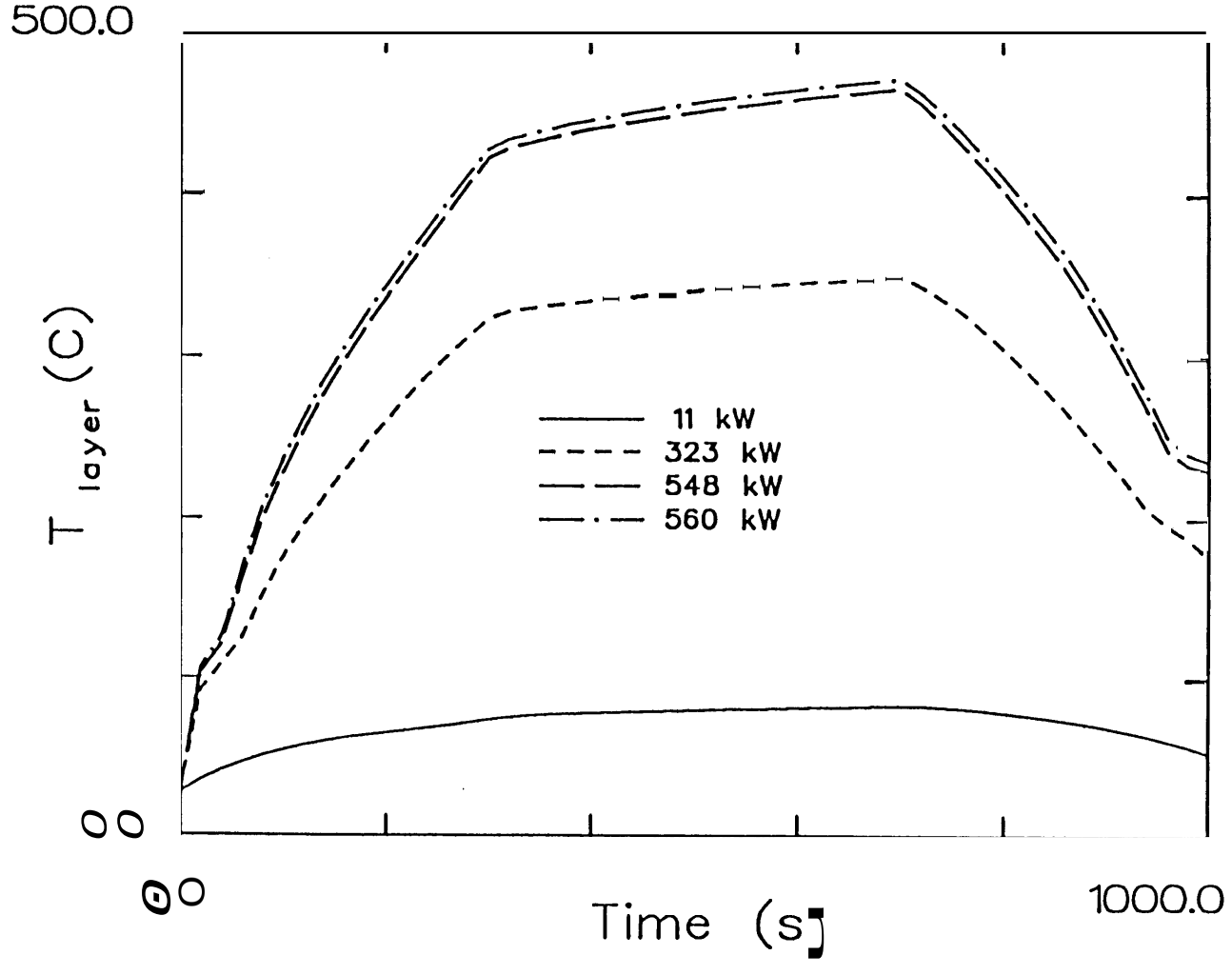

Figure 68. Calculated upper layer temperatures for 1000 s duration fires

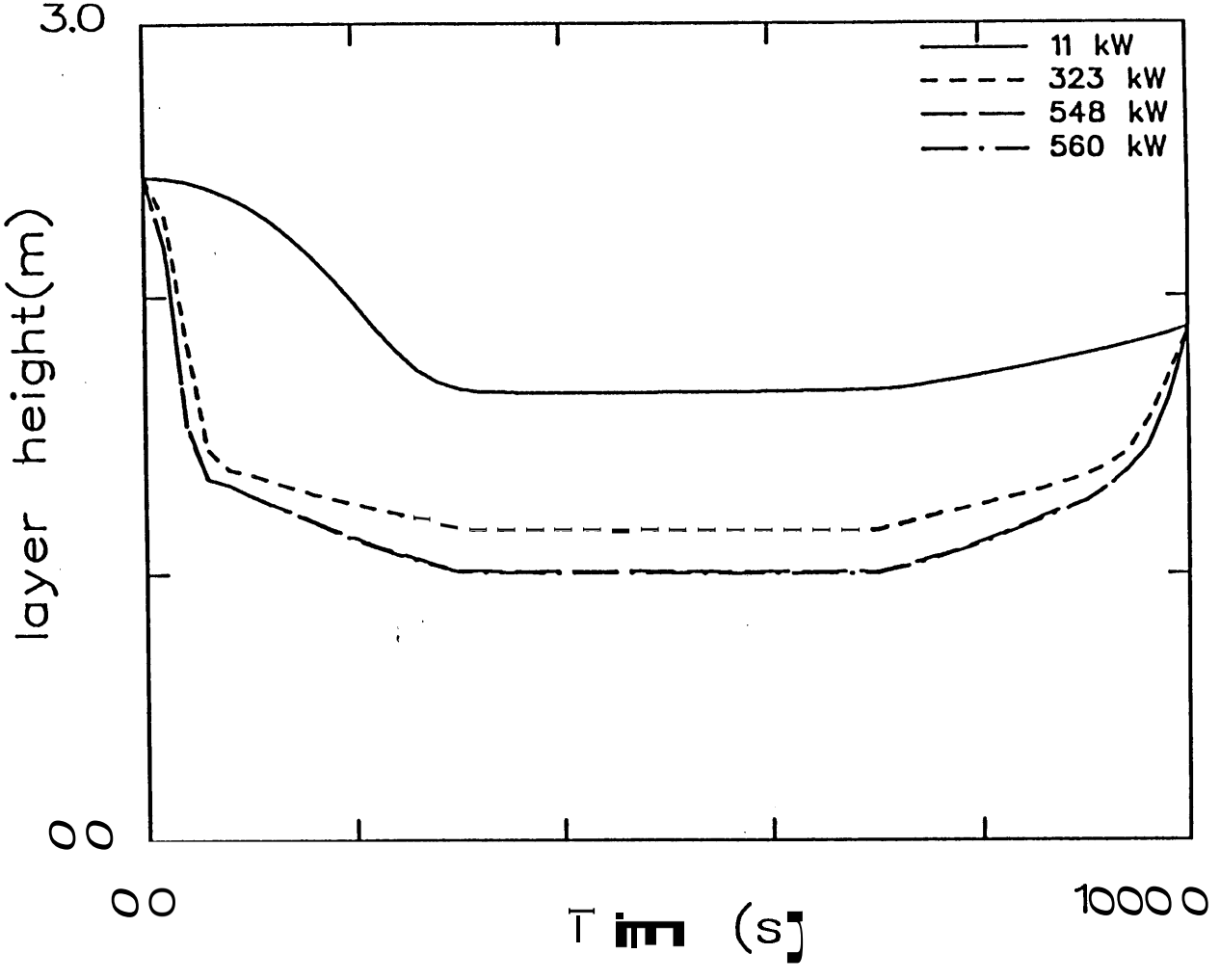

Figure 69. Calculated interface height for 1000 s duration fires

Appendix A

FMVSS No. 302 Testing of Six Seat Assemblies

Report of Test

FMVSS No. 302 Tests of Selected School Bus Seat Assemblies

by

Richard Harris

I. Introduction

Federal Motor Vehicle Safety Standard (FMVSS) No. 302 applies to all polymeric (i.e., non metallic) components used on the interior of passenger cars, multipurpose passenger vehicles, trucks, and buses. Seat assemblies must meet the requirements of FMVSS No. 302 before they can be used as school bus seats. The basic requirement of FMVSS No. 302 is that a horizontally mounted sample of material not propagate a flame faster than 4 inches per minute.

Eight seat assembly components (three cover fabrics and 5 foams) are listed in table 1. These were combined into six seat assemblies evaluated in this test method. These seat assemblies are listed in table 2. The composite seat assemblies were tested in FMVSS No. 302.

II. Test Procedure

Sampler were conditioned prior to testing at a relative humidity of 54 percent and at a temperature of 22°C (71°F).

Test samples were cut to a size of 356 mm by 102 mm (14 in by 4 in). Overall test sample thickness is limited to 12.7 mm (0.5 in). The foam cushions were cut to a nominal 12.7 mm (0.5 in) thickness. The test sample was assembled in the sample holder by placing the cover fabric and foam such that the exposed surface of the cover fabric faced downward with the foam material on top of the fabric. The exposed surface was 343 mm by 51mm (13.5 in by 2 in).

The test sample was then exposed horizontally, for 15 s to a 38 mm (1.5 in) natural gas diffusion flame. The flame was applied to the fabric surface at one end of the sample. After the flame was removed, the time for the flame to spread to 254 mm (10 in) was recorded.

III. Results

None of the composites tested would support a flame after the burner was removed. Therefore, no flame spread rate was recorded. All seat assemblies met the requirments of FMVSS No. 302.

Table 1. Physical Measurements of School Bus Seat Materials

Material Designation	Foams	Density kg/m³	Density lb/ft³
F_1	Rebonded PUR	73	4.6
F_2	Melamine-treated PUR	85	5.3
F_3	CMHR PUR	49	3.1
F_4	Polychloroprene	145	9.0
F_5	Rebonded FR PUR	90	5.6

	Cover Materials	Areal Density g/m²	Areal Density oz/yd²	Thickness mm	Thickness in
C_1	Standard	870	25.6	0.76	0.030
C_2	Kevlar-backed	830	24.6	1.2	0.047
C_3	UMTA-type	770	22.6	1.1	0.043

Table 2. Cover Fabric and Foam Combinations, Fraction and Initial Mass for a Single Seat Assembly

Seat Assembly	Initial Mass[a] kg	Fraction[b]	
		Fabric	Foam
F_1/C_1	12.0	0.25	0.75
F_1/C_2	11.5	0.23	0.77
F_2/C_3	9.9	0.20	0.80
F_3/C_3	12.6	0.30	0.70
F_4/C_3	16.4	0.13	0.87
F_5/C_3	17.3	0.19	0.81

[a] Includes cover, foam, and plywood.
[b] Excludes the mass of wood used in seat bottom and seat back.

NIST-114A
(REV. 3-89)

NATIONAL INSTITUTE OF STANDARDS AND TECHNOLOGY

NUMBER

2. PERFORMING ORGANIZATION REPORT NUMBER

6. PERFORMING ORGANIZATION (IF JOINT OR OTHER THAN NIST, SEE INSTRUCTIONS)

U.S. DEPARTMENT OF COMMERCE
NATIONAL INSTITUTE OF STANDARDS AND TECHNOLOGY
GAITHERSBURG, MD 20899

7. CONTRACT/GRANT NUMBER

8. TYPE OF REPORT AND PERIOD COVERED
Final Report

9. SPONSORING ORGANIZATION NAME AND COMPLETE ADDRESS (STREET, CITY, STATE, UP)
Office of Vehicle Safety Standards
National Highway Traffic Safety Administration
Department of Transportation
Washington, DC 20590

10. SUPPLEMENTARY NOTES

[ ] DOCUMENT DESCRIBES A COMPUTER PROGRAM; SF-185, FIPS SOFTWARE SUMMARY, IS ATTACHED.

11. ABSTRACT (A 200-WORD OR LESS FACTUAL SUMMARY OF MOST SIGNIFICANT INFORMATION. IF DOCUMENT INCLUDES A SIGNIFICANT BIBLIOGRAPHY OR LITERATURE SURVEY, MENTION IT HERE.)

Since seat assemblies represent the single largest type of combustible fuel in a school bus interior, this study is limited to currently used and state-of-the-art material assemblies. Six different seat assemblies having a range of fire performance were examined. Small-scale tests (Cone Calorimeter, LIFT, and NBS Toxicity Protocol) were performed on these materials. Large-scale tests (Furniture Calorimeter) were conducted on single seat assemblies. Full-scale tests were performed using a simulated bus enclosure measuring 2.44 m wide by 2.13 m high by 8.23 m long and three seat assemblies. The impact of ignition source size was determined by computer simulation. It was found that a 500 kW ignition source could produce untenable conditions in the simulated bus enclosure. Seat assemblies were exposed to 50 kW and 100 kW ignition sources in the large-scale tests and 100 kW ignition source in the full-scale tests. It was found that the small-scale tests were unable to provide a simple method for material selection that was consistent with the full-scale test results. At the present time, small-scale tests of materials cannot be depended upon to predict the fire behavior in the real world. Therefore, based on the full-scale test results, a generalized full-scale test protocol for seat assembly evaluation was developed that combines full-scale testing in an enclosure with an analysis protocol that detemines the time-to-untenable conditions. The procedure defines the conditions under which toxicity testing would be necessary. Full-scale test instrumentation and material orientation are also described.

12. KEY WORDS (6 TO 12 ENTRIES; ALPHABETICAL ORDER; CAPITALIZE ONLY PROPER NAMES; AND SEPARATE KEY WORDS BY SEMICOLONS)

Cone calorimeter; fire performance; flame spread; foams; furniture calorimeter; combustion products; hazard; ignitability; rate of heat release; school buses; smoke; tenability; toxicity.

13. AVAILABILITY

[XXX] UNLIMITED

[ ] FOR OFFICIAL DISTRIBUTION. DO NOT RELEASE TO NATIONAL TECHNICAL INFORMATION SERVICE (NTIS).

[ ] ORDER FROM SUPERINTENDENT OF DOCUMENTS, U.S. GOVERNMENT PRINTING OFFICE, WASHINGTON, DC 20402.

[XXX] ORDER FROM NATIONAL TECHNICAL INFORMATION SERVICE (NTIS), SPRINGFIELD, VA 22161.

14. NUMBER OF PRINTED PAGES
177

15. PRICE
A09

ELECTRONIC FORM